





This is to certify that the

dissertation entitled

AN ANALYSIS OF THE DIGITALLY ENHANCED HIGH RESOLUTION INFRARED SPECTRA OF CD₃Br AND CH₃CN

presented by

Dale Edward Bardin

has been accepted towards fulfillment of the requirements for

Ph.D. degree in Physics

Major professor

Date Sept 16, 1983



RETURNING MATERIALS:
Place in book drop to remove this checkout from your record. FINES will be charged if book is returned after the date stamped below.

AN ANALYSIS OF THE DIGITALLY ENHANCED HIGH RESOLUTION INFRARED SPECTRA OF CD₃Br AND CH₃CN

Ву

Dale Edward Bardin

A DISSERTATION

Submitted to
Michigan State University
in partial fulfillment of the requirements
for the degree of

DOCTOR OF PHILOSOPHY

Department of Physics and Astronomy

1983

ABSTRACT

AN ANALYSIS OF THE DIGITALLY ENHANCED HIGH RESOLUTION INFRARED SPECTRA OF CD₃Br AND CH₃CN

Bv

Dale Edward Bardin

A signal averaging procedure has been developed to make short segments of digital high resolution infrared grating spectra linear in frequency and to sum the segments in phase. Signal averaging can be used to increase the signal to noise ratio, to increase the resolution limit, or a combination of the two.

Combining signal averaging with other signal processing techniques, the resolution limit of the ν_4 band of CD₃Br was increased enough to warrant a reanalysis that included an x-y Coriolis interaction. The final resolution limit for the ν_4 band was approximately 0.025 cm⁻¹.

Signal averaging also increased the "signal strength" of the weakly absorbing $2\nu_5(\bot)$ band of CH₃CN enough to analyze it simultaneously with the ν_5 band. Analysis of eighty (80) lines from the $2\nu_5(\bot)$ band and one hundred sixty (160) lines from the ν_5 band improved the values of several molecular constants.

To my wife, Linda

ACKNOWLEDGMENTS

I wish to express my appreciation and gratitude to Professor T. H. Edwards for his guidance, encouragement, and patience during the years of my graduate education.

Fellow graduate students James R. Gillis and William C.

Lane provided much help and many useful discussions. I would like to give special thanks to Professor Paul Parker for teaching an excellent Molecular Spectroscopy course, taught in addition to his normal teaching load.

I would like to thank the Michigan State University

Physics Department for providing me with a teaching assistantship. I am grateful to The Timken Company for providing unlimited computer services during the final stages of my dissertation. Mrs. Delores Sullivan was very helpful with both the typing and the format of this dissertation.

I especially wish to express my love and appreciation to my wife, Linda, for her support and patience throughout the course of this endeavor.

TABLE OF CONTENTS

List	of	Tab	les	•	•		•	•	•	•	•	•	•	•	•	•	•	vi
List	of	Fig	ures	•				•			•	•				•	•	vii
List	of	App	endi	ces	•	•	•	•	•	•	•	•	•	•	•	•	•	ix
Chap	ter																	
I		Intr	oduc	tion	1	•		•		•	•	•	•	•	•	•	•	1
II	7	The	Symm	etri	ic '	Top	Hai	milt	toni	lan				•	•	•	•	6
III]	Digi	tal	Sign	nal	Av	era	ging	3	•	•		•	•	•	•		24
		Ту	pes (of N	loi	se	to 1	be I	Proc	cess	sed	•	•	•	•	•		25
		Sp	ectr	al I	in	ear	iza	tion	ı			•	•	•	•	•	•	32
		Ch	oice	of	A1	ign	men	t Tı	rigg	ger			•	•	•	•	•	34
		A1	.ignm	ent	Pr	oce	dur	е	•				•	•	•	•	•	35
		Ef	fect	iver	ies	s o	f S	igna	al A	lvei	ragi	ing	•	•		•		38
IV	1	Ехре	rime	ntal	L C	onf	igu	rati	ion	and	i Pı	oce	edui	re			•	42
		Ex	peri	ment	tal	Co	nfi	gura	atio	on			•	•				42
			Infr	arec	ı s	pec	tro	phot	tome	etei	r Co	nfi	igu	rat	ion			42
			In	frai	red	Pa	thw	ay	•		•		•	•		•		43
			Vi	sibl	le	Pat:	hwa	У	•					•				44
			Conf	iguı	rat	ion	Ch	ange	es				•					45
		Ex	peri	ment	tal	Pr	oce	dure	es	•		•	•	•		•		47
			Expe	rime	ent	al :	Pro	cedi	ure	for	r a	Ca	lib	rate	ed 1	Run		47
			Expe Run	rime	ent	al :	Pro •	cedi	ure	for	ra	Sig	gna:	1 A	ver	agi:	ng •	51
		D÷	gita	1 S	ign	al	Pro	ces	sins	z z	•	•				•		55

Chapter

V	The Analysis of the v_5 Band of CH_3CN	63
	Analysis	64
	Weighting Scheme	73
	Results	82
VI	The Analysis of the $2v_5$ Band of CH_3CN	84
	Introduction	84
	Procedures	85
	Calibration	90
	Analysis	91
	Parallel Component of $2v_5$ of CH_3CN	100
	Results	105
VII	A Review of Our Analysis of the v_4 Band of CD_3 Br	108
VIII	Conclusion	111
•		
Apper	101X	
I	A Listing of the Focal-12 Programs used to Signal Average Spectra	113
II	A Copy of the Publication of Our Analysis of v.	
	of CD ₃ Br	138
III	The Frequencies and Assignments of the v_4 Band of CD_3Br	148
IV	The Frequencies and Assignments of the v_5 Band of CH_3CN	152
V	5	162
List	of References	171

LIST OF TABLES

Table	2.1	The Darling-Dennison Hamiltonian
Table	2.2	Upper state energy levels (matrix) and ground state energies
Table	2.3	Symmetric top selection rules 15
Table	2.4	Axially symmetric energy expression 16
Table	2.5	Generalized frequency expression (transitions from the ground vibrational state) 19
Table	2.6	Simultaneous frequency expression for ν_5 , $2\nu_5\bot$, and $2\nu_5\parallel$ of CH ₃ CN
Table	3.1	Summary of signal averaged N_20 (120) data versus single scan N_20 (120) data 41
Table	5.1	Experimental conditions used for the v_5 band of CH ₃ CN data 65
Table	5.2	Single band Fit of v_5 of CH_3CN 83
Table	6.1	Experimental conditions used for the $2v_5$ band of CH_3CN data
Table	6.2	Single band fit of $2v_5(1)$ of CH_3CN 102
Table	6.3	Comparison of the K = 2 and K = 3 assignments of the $2v_5(\parallel)$ band of CH_3CN 104
Table	6.4	Simultaneous fit of v_5 and $2v_5(\bot)$ of CH_3CN 107

LIST OF FIGURES

Figure 1.1	The v_4 vibrational normal mode of CH ₃ X type molecule is an unsymmetric C-H stretch	2
Figure 3.1	Deconvolution of two independent "noisy" scans of the same region of the (120) band of N_2 0 (deconvoluted in the same manner)	26
Figure 3.2	Spectrophotometer noise at various stages of processing. Real spectral lines, raw and deconvoluted, at the same scale are provided in G and H respectively for comparison	30
Figure 3.3	Two independent deconvoluted spectra, each an average of eight scans, of the same region of the (120) band of N_2^0 (deconvoluted in the same manner)	39
Figure 4.1	Illustration of data recorded on magnetic tape and on chart paper during a typical calibrated run, not to scale	49
Figure 4.2	Data near the band center of the (120) band of N_2^0 , shown with fringes	50
Figure 4.3	Original, smoothed, and deconvoluted spectra from the ν_4 band of ${\rm CD_3Br.}$	52
Figure 5.1	Survey spectra of the v_5 band of CH_3CN	66
Figure 5.2	Q branch positions of ν_5 of CH_3CN versus K Δ K	68
Figure 5.3	Residuals (Q branches minus quadratic fit) for v_5 of CH_3CN	69
Figure 5.4	α_5^B versus KAK for ν_5 subband fits of CH3CN.	71
Figure 5.5	Residuals (calculated - quadratic fit) of subband origins versus KAK	72

Figure	5.6	$^{R}Q_{3}(J)$ of v_{5} of $CH_{3}CN$ calculated from P	75
Figure	5.7	$^{R}R_{3}(J)$ and $^{R}P_{3}(J)$ versus J for v_{5} of CH ₃ CN.	77
Figure	5.8	Residuals from linear fits of $^RR_3(J)$ and $^Rp_3(J)$ versus J for ν_5 of CH_3CN	78
Figure	5.9	${}^{R}R_{6}(\text{J})$ versus J for ν_{5} of CH ₃ CN	80
Figure	5.10	Residuals from linear fit of ${}^RR_6(J)$ versus J for v_5 of CH_3CN	81
Figure	6.1	Survey spectra of the $2v_5$ band of CH_3CN .	87
Figure	6.2	Q branches of $2v_5$ of CH_3CN versus $\text{K}\Delta\text{K}$	92
Figure	6.3	Residuals from a linear fit of low Q branches of $2v_5$ of CH_3CN	93
Figure	6.4	α_5^B versus KAK for $2\nu_5$ of CH $_3$ CN	94
Figure	6.5	Calculated subband origins of $2\nu_5$ of CH ₃ CN versus K $\!$	95
Figure	6.6	Hot band frequencies near $2v_5$ of CH $_3$ CN Q branches minus quadratic fit	97
Figure	6.7	Hot band frequencies minus Q branch frequencies of $2v_5$ of CH ₃ CN superimposed on Figure 6.6	98
Figure	6.8	$^{R}Q_{3}^{}(J)$ of $2v_{5}$ of $CH_{3}^{}CN$ versus $J(J+1)$	99
Figure	6.9	Residuals ($^{R}Q_{3}(J)$ of $2v_{5}$ of $CH_{3}CN$ minus linear fit) versus $J(J+1)$	101

LIST OF APPENDICES

Appendix	Ι	A Listing of the Focal Programs used to Signal Average Spectra
Appendix	II	A Copy of the Publication of Our Analysis of ν_4 of CD_3Br
Appendix	III	The Frequencies and Assignments of the ν_4 Band of CD_3Br
Appendix	IV	The Frequencies and Assignments of the ν_5 Band of CH_3CN
Appendix	V	The Frequencies of the $2\nu_5(\downarrow)$ Band and the $2\nu_5(\parallel)$ Band of CH_3CN 162

CHAPTER I

INTRODUCTION

With the development of quantum mechanics during the 1920's came rapid advances in many fields, including molecular spectroscopy. Treating molecules as rigid rotors and uncoupled harmonic oscillators, theorists were able to model the spectra of many molecules. As the size of the molecules studied increased and the experimental resolution and precision improved, so did the complexity of the required theory.

The basic theory of molecular spectroscopy has been refined over the years to match experimental and computational advances. Calculations of perturbed bands have been particularly difficult. Only relatively recently have Coriolis perturbed bands been analyzed with more than marginal success.

All three bands studied in this dissertation, the ν_4 band of ${\rm CD_3Br}$, and the ν_5 and $2\nu_5$ bands of ${\rm CH_3CN}$, belong to the same vibrational normal mode (an unsymmetrical C-H stretching mode, see Figure 1.1), and are Coriolis perturbed by nearby levels. To analyze the data, we adopted the basic theoretical approach used by P. M. Wilt of Centre College, Kentucky. Wilt calculates the frequencies of the

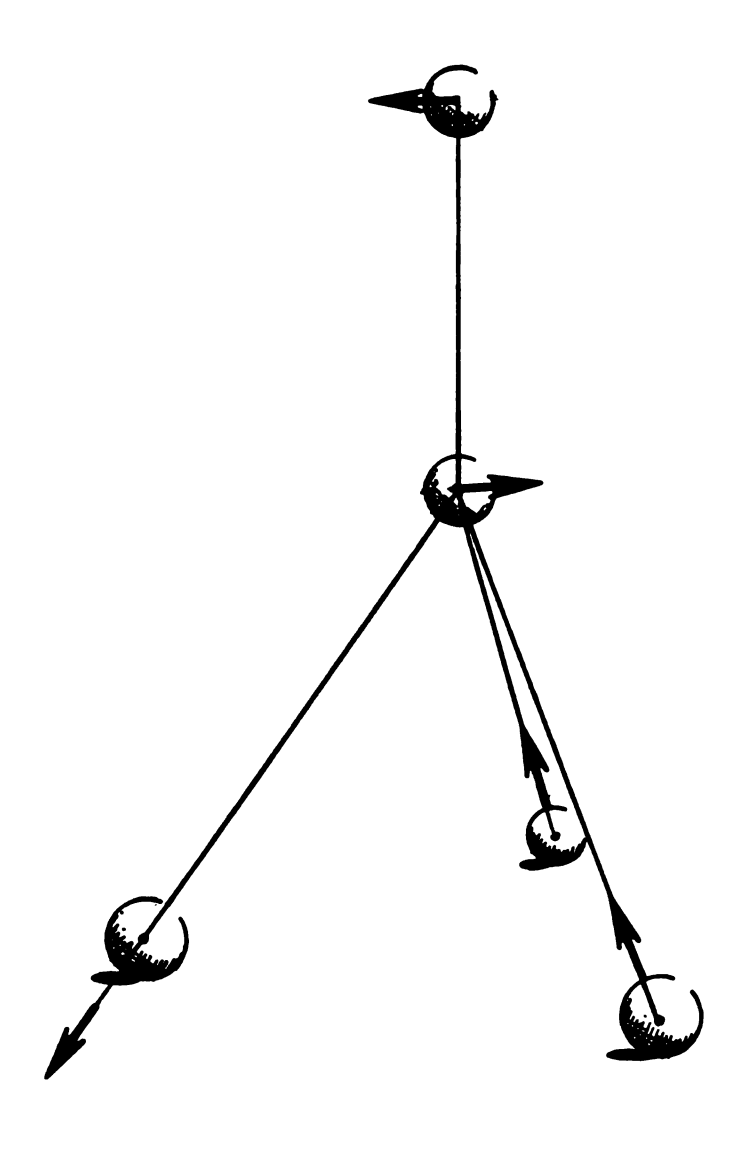


Figure 1.1 The ν_4 vibrational normal mode of CH₃X type molecule is an unsymmetric C-H stretch.

transitions with the DiLauro and Mills Hamiltonian (1), together with the Fermi matrix elements of Matsuura et al. (2), if needed.

Chapter II presents a brief development of the Hamiltonian used to analyze the ν_4 band of ${\rm CD_3Br}$, and lists the upper and lower state energies for ν_4 of ${\rm CD_3Br}$. Chapter II also gives the single band and simultaneous frequency expressions applied to ν_5 and $2\nu_5$ of ${\rm CH_3CN}$, as well as the selection rules for infrared transitions.

Progress in theory inevitably requires progress in experiment, and vice versa. Technological improvements led to probably the two most important experimental developments in molecular spectroscopy in recent years, tunable lasers and Fourier transform spectrometers. The application of tunable lasers to molecular spectroscopy vastly improved resolution, while the development of the ultra high resolution Fourier transform spectrometer, by Connes (3) of France, enabled experimentalists to obtain a whole band with a resolution limit almost comparable to that of the tunable laser. Unfortunately, tunable lasers are not able to obtain spectra over a very large range and high resolution Fourier transform spectrometers are very expensive (≥\$200,000). Because of these limitations, grating spectrometers continue to be the mainstay for much of high resolution infrared spectroscopy, despite an order of magnitude lower resolution.

During the past two decades, computers have become very sophisticated and relatively inexpensive. This has led to

the development of digital data processing methods by several investigators. The techniques for use with high resolution grating spectrometers include an improved means of measuring line positions (4), sampling and smoothing (5) to improve the signal-to-noise ratio (S/N), and deconvolution (6-8) to improve the resolution limit by as much as a factor of three. However, one of the limitations of deconvolution has been that the spectra must have a high S/N initially (≈ 50).

Chapter III discusses a signal averaging procedure whereby spectra, having a S/N of 10-15 initially, can be processed and then deconvoluted successfully. The signal averaging procedure that we have developed makes short segments (12 to 20 cm⁻¹) of a run linear in frequency, then sums several linearized segments (scans) of the same region of the spectrum. Ideally, the signal will add coherently and the noise incoherently, improving the S/N by approximately n^{1/2}, where n is the number of scans summed. We normally sum sixteen scans, improving the S/N by approximately a factor of four. The new spectrum may be normalized to a desired amplitude and then deconvoluted.

The results of signal averaging are impressive, but many hours were spent determining the best procedure for signal averaging. For this reason, our step by step recipe to obtain and process the data is presented in Chapter IV. The FOCAL programs used to process the data are included in the appendices.

Peterson and Edwards (9) had previously analyzed the v_4 band of CD_3Br , with the exception of the portion perturbed by a Coriolis resonance. Signal averaging enabled us to run the band at higher resolution and to resolve previously unresolved transitions. This permitted an improved analysis that, when coupled with an analysis of the perturbed portion, improved the values of the constants for this band. Chapter VII contains the new analysis of the v_4 band of CD_3Br .

Barnett and Edwards (10) believed that they had developed a method to calculate A_0 for symmetric tops by simultaneously analyzing a degenerate fundamental and its first overtone. This particular rotational constant is difficult to isolate. Peterson and Edwards (11) later showed that the coefficient isolated was actually $A_0 = \frac{1}{3} n_{tt}$. Both of the above groups applied the simultaneous band analysis method to various methyl halides (9,12-14). Until the development of the signal averaging technique (in this instance, signal adding would be a more descriptive name), the $2\nu_5$ band of CH₃CN was too weak to measure and assign a sufficient number of transitions to be analyzed simultaneously with the ν_5 band. The ν_5 and $2\nu_5$ simultaneous band analysis is the subject of Chapters V and VI respectively.

Chapter VIII summarizes the results and offers suggestions for future research.

CHAPTER II

THE SYMMETRIC TOP HAMILTONIAN

This chapter briefly outlines the development of the Hamiltonian used for the analysis of the v_4 band of CD_3Br and of the v_5 and $2v_5$ bands of CH_3CN .

Historically, using the Schrodinger equation in other than Cartesian coordinates was a non-trivial task. In 1928, Podolsky (15) formulated a Hamiltonian in generalized coordinates for a conservative system as:

$$H = (2\mu)^{-1} \sum_{r,s=1}^{n} g^{-\frac{1}{4}} p_r g^{\frac{1}{2}} g^{rs} p_s g^{-\frac{1}{4}} + U$$

where μ is the reduced mass, $\{g_{rs}^{}\}$ is the coordinate system metric, g is the determinant of $\{g_{rs}^{}\}$, and the p_{α} (where α is either r or s) are the conjugate momenta of the particles. This Hamiltonian was specialized to a semi-rigid rotating polyatomic molecule by Wilson and Howard (16). Darling and Dennison (17) reformulated the Wilson-Howard Hamiltonian into a Hermitian operator, which is usually more convenient to apply. The Darling-Dennison Hamiltonian is listed in Table 2.1.

Table 2.1 The Darling-Dennison Hamiltonian

$$H = \frac{1}{2} \sum_{\alpha,\beta} \mu^{\frac{1}{4}} (P_{\alpha} - p_{\alpha}) \mu_{\alpha\beta} \mu^{-\frac{1}{2}} (P_{\beta} - p_{\beta}) \mu^{\frac{1}{4}}$$
$$+ \frac{1}{2} \sum_{s\sigma} \mu^{\frac{1}{4}} p_{s\sigma}^* \mu^{-\frac{1}{2}} p_{s\sigma}^* \mu^{\frac{1}{4}} + V(Q_{s\sigma})$$

where, using the notation of H. H. Nielson (4),

α and β range over x, y, and z, the equilibrium principal axes of inertia of the molecule,

 P_{α} and p_{α} are the components of total and internal angular momentum, respectively,

 $p_{S\sigma}^{*}$ are the momenta conjugate to the normal coordinates $Q_{S\sigma}^{}$, i.e. $p_{S\sigma}^{*}=-i\hbar\frac{\partial}{\partial \hat{Q}_{S\sigma}^{}}$, (s enumerates the normal mode and σ enumerates the degenerate mode)

 $\mu_{\alpha\beta}$ are the inverse moments and products of inertia

 μ is the determinant of $\{\mu_{\alpha\beta}\}$

and

 $V(Q_{S^{\sigma}})$ is the potential energy of the molecule as a function of the normal coordinates $Q_{S^{\sigma}}$.

Also note that $p_{\alpha} = \sum_{\substack{s\sigma \\ s'\sigma'}} \zeta_{s\sigma,s'\sigma'}^{\alpha} Q_{s\sigma}^{p}_{s'\sigma'}^{s}$, where $\zeta_{s\sigma,s'\sigma'}$

are the Coriolis constants for a given molecule.

An exact solution to the Schrodinger wave equation for a rotating vibrating polyatomic molecule using the Darling-Dennison Hamiltonian has not been found. Perturbation theory through the fourth order provides sufficient accuracy for the cases presented here, however, the algebraic complexities involved are formidable.

The Darling-Dennison Hamiltonian has been transformed (18) to a form more convenient for perturbation theory by first expanding H, $V(Q_{SG})$, and $\mu_{\alpha\beta}$ in orders of magnitude:

$$\begin{split} \mathbf{H} &= \mathbf{H}_{0} \; + \; \lambda \mathbf{H}_{1} \; + \; \lambda^{2} \mathbf{H}_{2} \; + \; \cdots \\ \mathbf{V}(\mathbf{Q}_{s\sigma}) \; &= \; \mathbf{V}_{0} \; + \; \mathbf{V}_{1} \; + \; \mathbf{V}_{2} \; + \; \cdots \; = \; \frac{1}{2} \; \sum_{s\sigma} \lambda_{s} \mathbf{Q}_{s}^{2} \\ &+ \; \sum_{s\sigma} \; ^{\mathbf{k}} _{s\sigma} , s' \sigma' , s'' \sigma'' ^{\mathbf{Q}} _{s\sigma} ^{\mathbf{Q}} _{s' \sigma} , ^{\mathbf{Q}} _{s'' \sigma''} \; + \; \cdots \\ &= \; s' \sigma' \\ s'' \sigma'' \end{split}$$

and

$$\mu_{\alpha\beta} = (I_{\alpha}^{e}I_{\beta}^{e})^{-1} [\Omega^{(0)\alpha\beta} + \sum_{s\sigma} \Omega_{s\sigma}^{(1)\alpha\beta} Q_{s\sigma} + \sum_{s\sigma} \Omega_{s\sigma,s'\sigma'}^{(2)\alpha\beta} Q_{s\sigma} Q_{s'\sigma'} + \cdots]$$

where

$$\begin{split} &\Omega^{(0)\alpha\beta} = I^{e}_{\alpha\beta}\delta_{\alpha\beta} \\ &\Omega^{(1)\alpha\alpha}_{s\sigma} = -a^{\alpha\alpha}_{s\sigma} = -2\sum_{i}m^{\frac{1}{2}}_{i}(\beta^{0}_{i}\ell^{\beta}_{is\sigma} + \gamma^{0}_{i}\ell^{\gamma}_{is\sigma}), \\ &\Omega^{(1)\alpha\beta}_{s\sigma} = -a^{\alpha\beta}_{s\sigma} = \sum_{i}m^{\frac{1}{2}}_{i}(\alpha^{0}_{i}\ell^{\beta}_{is\sigma} + \beta_{i}\ell^{\alpha}_{is\sigma}), \ \alpha \neq \beta, \end{split}$$

and α , β , γ are cyclic,

and

$$\Omega_{S\sigma,S'\sigma'}^{(2)\alpha\beta} = \sum_{i} \ell_{iS\sigma}^{\alpha} \ell_{iS'\sigma'}^{\beta} + \sum_{s''\sigma''} \zeta_{s\sigma,S''\sigma''}^{\alpha} \zeta_{s'\sigma',S''\sigma''}^{\beta} + \sum_{i} \left(\frac{a_{s\sigma}^{\alpha\delta} a_{s'\sigma'}^{\beta\delta}}{I_{ss}} \right)$$

After expansion, a contact transformation of the form $e^{i\lambda S^{(1)}}H e^{-i\lambda S^{(1)}} = H' = H'_0 + \lambda H'_1 + \lambda^2 H'_2 + \cdots \text{ is made.}$

This similarity transformation, first performed on the Hamiltonian for polyatomic molecules by Shaffer, Nielsen and Thomas (18), will generate expressions for the allowed energies to second order by choosing the function $S^{(1)}$ such that the operator $H_0^{'} + \lambda H_1^{'}$ will have only diagonal matrix elements, with respect to v_s , in the representation that diagonalizes H_0 .

During the mid 1950's, experimentalists improved resolution sufficiently to require better than a second order analysis. To obtain vibration-rotation energies to fourth order, Goldsmith, Amat, and Nielsen (19-20) and Amat and Nielsen (21-23) applied a second contact transformation to the once transformed Darling-Dennison Hamiltonian such that $e^{i\lambda^2S^{(2)}}H' e^{-i\lambda^2S^{(2)}} = H'' = H''_0 + \lambda H''_1 + \lambda^2 H''_2 + \lambda^3 H''_3 + \cdots$

where $S^{(2)}$ is chosen to diagonalize $H_0'' + \lambda H_1'' + \lambda^2 H_2''$ with respect to the quantum number v_s in the representation that diagonalizes H_0 . Amat and Nielsen (21-22) list the

::e: .; ; .. ; 1.11 :::: 1.3 3 ... ::: ::; ;; ;; 7 ::-Ŗ. coefficients of the S function as well as the explicit form of the twice transformed Hamiltonian.

Usually nondegenerate perturbation theory can be used with both contact transformations. There are, however, denominators in the coefficients of $S^{(1)}$ and $S^{(2)}$ of the form $a\omega_s + b\omega_{s'} - c\omega_{s''}$. These terms arise when the first order anharmonic term in the potential energy of the Hamiltonian is transformed. But when two frequencies such as $a\omega_s + b\omega_{s'}$ and $c\omega_{s''}$ are nearly equal, i.e., accidentally degenerate, nondegenerate perturbation theory is no longer valid and degenerate perturbation theory must be used (24).

The approach of DiLauro and Mills (11) was adopted to apply the Darling-Dennison Hamiltonian to the ν_4 band of ${\rm CD_3Br}$ and the ν_5 and $2\nu_5$ bands of ${\rm CH_3CN}$, both molecules are of the ${\rm C_{3v}}$ point group. DiLauro and Mills approximate the molecular Hamiltonian as a rigid rotor, ${\rm H_r}$, a collection of simple harmonic vibrators, ${\rm H_v}$, and the appropriate cross terms to take into account the Coriolis interaction, ${\rm H'}$:

$$H = H_r + H_v + H'$$

Where

$$H_{r} = B(J_{x}^{2} + J_{y}^{2}) + AJ_{z}^{2}$$

$$H_{v} = \sum_{r} \frac{1}{2} (P_{r}^{2} + \lambda_{r}Q_{r}^{2})$$

$$H' = -2B(p_{x}J_{x} + p_{y}J_{y}) - 2Ap_{z}J_{z}$$

and where J_{α} and P_{α} (a ranges over x, y, and z of the appropriate molecular axes) are the components of total and vibrational angular momenta respectively, A and B are the

... :::6 . : Ľŧ .. : <u>::</u> --: 12. æ 7.: ... 11. į

prolate symmetric top rotational constants, $P_r = -i\hbar \frac{\partial}{\partial Q_r}$ is the momentum conjugate to the normal coordinate Q_r , and $\lambda_r = 4\pi^2 c^2 v_r^2$ is the force constant in that coordinate.

When two vibrational normal modes of the same symmetry are degenerate, or nearly so, the resulting motion consists of both vibration and rotation. This Coriolis coupling manifests itself in the Hamiltonian as H', which mixes the vibrational and total angular momentum operators. The matrix elements are obtained from degenerate perturbation theory and are of the form, $W_{xy}[J,k]$,

where

and

$$W_{xy} = \frac{1}{\sqrt{2}} B' \zeta_{rs}^{y} [(v_r/v_s)^{\frac{1}{2}} + (v_s/v_r)^{\frac{1}{2}}]$$

 $[J,k] = [J(J+1)-k(k+1)]^{\frac{1}{2}}$

Another term was added to the DiLauro and Mills
Hamiltonian to allow for a coupling of vibrational states
through the first anharmonic term in the potential energy
(a Fermi Resonance). Following Matsuura et. al. (2), J
dependent Fermi matrix elements of the form

$$W = \frac{k_{s,s'}}{2\sqrt{2}} + \alpha J(J+1) \text{ were used.}$$

A third resonance that should be considered is that due to ℓ -type doubling. Grenier-Besson (25) showed that the $|\mathbf{v}_t,\ell_t+1;\mathbf{J},\mathbf{k}+1\rangle$ and $|\mathbf{v}_t,\ell_t-1;\mathbf{J},\mathbf{k}-1\rangle$ states are coupled by the h'22 term in the second order contact transformed Hamiltonian. Non-zero matrix elements occur when $\Delta \ell_t = \pm 2$ and $\Delta \mathbf{k} = \pm 2$ and have the form (26):

$$\langle v_t, \ell_t+1; J, k+1 | H' | v_t, \ell_t-1; J, k-1 \rangle =$$

$$\left[\frac{\rho}{4} \right] q_t^{(+)} \big[(v_t^{+1})^2 - \ell_t^2 \big]^{\frac{1}{2}} \{ \big[J(J+1) - k(k+1) \big] \big[J(J+1) - k(k-1) \big] \}^{\frac{1}{2}}$$

These terms are usually negligible because of the size of $q_t^{(+)}$. The exception occurs when the two coupled states are degenerate, i.e. for the K=1, $|\ell|=1$ states. However, for C_{3v} molecules, only one subband of the perpendicular band is affected, as shown by Anderson and Overend (27). If the affected subband is excluded from the analysis, the matrix that must be diagonalized is greatly simplified.

With this model, i.e., the Hamiltonian used by DiLauro and Mills plus allowance for a Fermi interaction, F. W. Hecker and P. M. Wilt wrote a computer program to predict the spectrum, given the molecular constants. The upper state energy levels were calculated by diagonalizing a 4X4 matrix for each value of J', with k = J', J' - 1, ..., -J'. Table 2.2 lists the 4X4 matrix and the expression for the spectrum of the ν_4 band of CD_3Br . The requisite symmetric top selection rules are listed in Table 2.3

The same Hamiltonian was applied to the v_5 and $2v_5$ bands of $\mathrm{CH_3CN}$. To simplify the analysis and allow a simultaneous fit of the two bands, transitions that were perturbed were excluded, leaving only diagonal matrix elements. The generalized energy expression in Table 2.4 is obtained by replacing the equilibrium rotational constants with the corresponding effective rotational constants as follows:

Upper state energy levels (4x4 matrix) and ground state energies. Table 2.2

$$| v_4' = 1^{+1}, J, k \rangle | v_2 = 1, v_3' = 1^{+1}, v_4' = 1^{+1}, J, k \rangle | v_4' = 1^{-1}, J, k + 1 \rangle | v_2 = 1, v_3' = 1^{-1}, v_4' = 1^{-1}, J, k + 1 \rangle$$

$$0 \qquad W_{xy} \cdot F(J, k + 1)$$

$$E(v_3 = 1, v_3' = 1^{+1}, v_4' = 1^{+1}, J, k) \qquad -W_{xy} \cdot F(J, k + 1) \qquad 0$$

$$(Hermitian) \qquad E(v_3 = 1, v_3' = 1^{-1}, v_4' = 1^{-1}, J, k + 1) \qquad W$$

$$\frac{E(v_4^{\ell_4}, J, k)}{hc} = v_4^0 + B_4^J(J+1) + (A_4^4 - B_4^1)k^2 - 2A_e\zeta_4k \ell_4^4 + n_4^J(J+1)k\ell_4^4 + n_4^k\ell_4k^3$$

 $- \ D_{4J}^{'} J^{2} (J+1)^{2} \ - \ D_{4Jk}^{'} (J(J+1)k^{2} \ - \ D_{4k}^{'} k^{4}$

 $= v_{356}^0 + B_{356}^{i}J(J+1) + (A_{356}^i - B_{356}^i)k^2 \pm 2A_e^{\zeta}_{eff}^{i}k^{\pm}\eta_{356}^{J}(J+1)k^{\pm}\eta_{356}^{k}$ $- \ \, {\rm D_{356J}^{}J^{}^{}}{\rm (J+1)^{}^{2}} - \ \, {\rm D_{356Jk}^{}J(J+1)k^{}^{2}} - \ \, {\rm D_{356k}^{}k^{}^{4}}$ $E(v_3, v_5^{\ell_5}, v_6^{\ell_6}, J, k)$ and

(upper signs taken when $\ell_s = \ell_b = 1$, lower when $\ell_s = \ell_b = -1$), $\zeta_{\rm eff} = -(\zeta_5 + \zeta_6)$, $W = W_0 + J(J+1)$,

where $^{W}_{
m O}$ is the usual J independent Fermi resonance element.

(cont. on next page)



Table 2.2 (cont.)

$$W_{xy} = B^{\dagger} \zeta_{rs}^{y} [(v_r/v_s)^{\frac{1}{2}} + (v_s/v_r)^{\frac{1}{2}}], [J,k] = [J(J+L) - k(k+1)]$$

The ground while transitions to $|k\rangle$ are allowed when $\Delta k = \pm 1$ and to $|k+1\rangle$ when $\Delta k = 1$. state energy is given by the expression:

$$\frac{E_{gnd}(J,k)}{hc} = B''J(J+1) + (A''-B'')k^2 - D_J'J^2(J+1)^2 - D_J''J(J+1)k^2 - D_J''k^4$$

Table 2.3

Symmetric Top Selection Rules

Parallel band: $\Delta K = 0$

 $\Delta J = 0, \pm 1$

 $\Delta J \neq 0 \text{ if } K = 0$

Perpendicular band: $\Delta K = \pm 1$

 $\Delta J = 0, \pm 1$

for v_t : $\Delta \ell = \pm 1$

for $2v_t$: $\Delta \ell = 0$, ± 1

r Ke

Table 2.4*

Axially Symmetric Energy Expression

$$\begin{split} \mathbf{E}_{0} &= \mathbf{B}_{e}\mathbf{J}(\mathbf{J}+\mathbf{1}) + (\mathbf{A}_{e}-\mathbf{B}_{e})\mathbf{K}^{2} + \mathbf{\Sigma}_{s}\mathbf{w}_{s}(\mathbf{v}_{s}+\mathbf{g}_{s}/2) \\ \mathbf{E}_{1} &= -2\mathbf{A}_{e}\mathbf{\Sigma}_{t}\zeta_{t}^{2}\mathbf{L}_{t}\mathbf{K} \\ \mathbf{E}_{21} &= -\mathbf{D}_{e}^{\mathbf{J}_{s}^{2}}(\mathbf{J}+\mathbf{1})^{2} - \mathbf{D}_{e}^{\mathbf{J}_{s}}\mathbf{K}^{2}\mathbf{J}(\mathbf{J}+\mathbf{1}) - \mathbf{D}_{e}^{\mathbf{K}_{s}^{4}} \\ \mathbf{E}_{22} &= -\mathbf{\Sigma}_{s}\mathbf{a}^{\mathbf{B}}(\mathbf{v}_{s}+\mathbf{g}_{s}/2)\mathbf{J}(\mathbf{J}+\mathbf{1}) - \mathbf{\Sigma}_{s}(\mathbf{a}^{\mathbf{A}}_{s}-\mathbf{a}^{\mathbf{B}}_{s})(\mathbf{v}_{s}+\mathbf{g}_{s}/2)\mathbf{K}^{2} \\ \mathbf{E}_{23} &= \mathbf{\Sigma}_{ss}, \mathbf{v}_{ss}, (\mathbf{v}_{s}+\mathbf{g}_{s}/2)\mathbf{J}(\mathbf{v}_{s}+\mathbf{g}_{s})^{2} + \mathbf{\Sigma}_{tt}, \mathbf{v}_{tt}^{2}\mathbf{L}_{t}^{2}\mathbf{L}_{t}^{2}\mathbf{L}_{t}^{2}\mathbf{L}_{t}^{2} \\ \mathbf{E}_{31} &= \mathbf{\Sigma}_{t}\mathbf{h}_{t}^{\mathbf{J}_{t}}\mathbf{L}_{t}\mathbf{J}(\mathbf{J}+\mathbf{1})\mathbf{K} \\ \mathbf{E}_{32} &= \mathbf{\Sigma}_{t}\mathbf{h}_{t}^{\mathbf{K}_{t}}\mathbf{L}_{t}\mathbf{K}^{3} + \mathbf{\Sigma}_{t}(\mathbf{h}_{t}+\mathbf{\Sigma}_{s}\mathbf{h}_{t,s}(\mathbf{v}_{s}+\mathbf{g}_{s}/2))\mathbf{L}_{t}\mathbf{K} \\ \mathbf{E}_{41} &= \mathbf{\Sigma}_{s}\mathbf{\beta}_{s}^{\mathbf{J}}(\mathbf{v}_{s}+\mathbf{g}_{s}/2)\mathbf{J}^{2}(\mathbf{J}+\mathbf{1})^{2} + \mathbf{\Sigma}_{s}\mathbf{g}^{\mathbf{J}}\mathbf{K}(\mathbf{v}_{s}+\mathbf{g}_{s}/2)\mathbf{K}^{2}\mathbf{J}(\mathbf{J}+\mathbf{1}) \\ + \mathbf{\Sigma}_{s}\mathbf{\beta}_{s}^{\mathbf{K}}(\mathbf{v}_{s}+\mathbf{g}_{s}/2)\mathbf{L}^{4} \\ \mathbf{E}_{42} &= (\mathbf{\Sigma}_{ss}, \mathbf{v}_{ss}^{\mathbf{K}_{s}}, (\mathbf{v}_{s}+\mathbf{g}_{s}/2)(\mathbf{v}_{s}, +\mathbf{g}_{s}, (\mathbf{v}_{s}+\mathbf{g}_{s}/2))\mathbf{L}_{t}\mathbf{L}_{t}, \mathbf{v}_{t}^{\mathbf{L}_{t}}\mathbf{L}_{t}^{\mathbf{L}_{t$$

Table 2.4 (cont.)

Description of Energy Parameters

Quantity Description s,n,t s is an index of a given vibrational mode. n will refer to a specifically non-degenerate mode; t, the degenerate modes. $B_e = \frac{h}{4\pi c I^e}$ $A_e = \frac{\hbar}{4\pi c I_e^e}$ B , A where $I_{\nu}^{e} = I_{\nu}^{e}$ where z is the axis of symmetry w, g designate a purely harmonic frequency w of a normal mode s having degeneracy §. coriolis coupling constant about the symmetry axis. $\alpha_{\mathbf{a}}^{\mathbf{B}}, \alpha_{\mathbf{a}}^{\mathbf{A}}$ coefficients of vibrational corrections to B and A D_e^J , D_e^{JK} , D_e^K corrections due to centrifugal distortion of equilibrium configuration. Xss', Xl, L, first-anharmonic corrections yss', yst,t, second-anharmonic corrections β_{s}^{J} , β_{s}^{JK} , β_{s}^{K} third-order changes in centrifugal terms due to vibration. η_{t}^{J} , η_{t}^{K} third-order corrections to ζ_{+}^{z} Yas', A fourth-order corrections to A Yss', Ylli fourth-order corrections to B HJ, HK, HKJ, HK fourth-order corrections due to centrifugal distortion. Δωs fourth-order correction to $\left. \omega \right._{s}$ having the same quantum dependence as $\left. \omega \right._{s}^{s}$ ΔB_e , ΔA_e fourth order corrections to A and B , having same quantum dependence at A and B $_{\mbox{\scriptsize a}}$

$$A_{v} = A_{e} - \sum_{s} \alpha_{s}^{A}(v_{s} + g_{s}/2) + \sum_{\substack{s,s'\\s \leqslant s'}} \gamma_{ss'}^{A}(v_{s} + g_{s}/2)(v_{s'} + g_{s'}/2)$$

+
$$\sum_{\substack{\text{tt'}\\ \text{t} \leqslant \text{t'}}} \gamma_{\text{tt'}}^{\text{A}}, \ \ell_{\text{t}} \ell_{\text{t'}} + \Delta A_{\text{e}}$$

$$B_{\mathbf{v}} = B_{e} - \sum_{s} \alpha_{s}^{B} (v_{s} + g_{s}/2) + \sum_{\substack{s,s'\\s \leqslant s'}} \gamma_{ss}^{B} (v_{s} + g_{s}/2) (v_{s} + g_{s}/2)$$

+
$$\sum_{\substack{\text{tt'} \\ \text{t} \leqslant \text{t'}}} \gamma_{\text{tt}}^{\text{B}}, \ \ell_{\text{t}} \ell_{\text{t}}, + \Delta B_{\text{e}}$$

and

$$D_{\mathbf{v}}^{\mathbf{m}} = D_{\mathbf{e}}^{\mathbf{m}} - \sum_{\mathbf{s}} \beta_{\mathbf{s}}^{\mathbf{m}} (\mathbf{v}_{\mathbf{s}} + \mathbf{g}_{\mathbf{s}}/2)$$
 where $\mathbf{m} = \mathbf{J}, \mathbf{k}, \text{ or } \mathbf{J}\mathbf{k}$.

The frequency of a particular transition may be calculated from $\frac{E(\nu_5^{\ell_5},J,k)}{hc} = \frac{E_{gnd}(J,k)}{hc} \ .$ The generalized single band

frequency expression is given in Table 2.5. The simultaneous frequency expression may be obtained by inserting the appropriate selection rules into the generalized single band frequency expression. Peterson and Edwards (11) give the correct expression for the ν_4 , the $2\nu_4$ (||), and the $2\nu_4$ (||) bands of CD_3I . Since the ν_5 and $2\nu_5$ perpendicular and parallel bands of CH_3CN are the same normal modes as the ν_4 and $2\nu_4$ perpendicular and parallel bands of CD_3I , a simple substitution of 5 for 4 in the subscripts will yield the correct simultaneous frequency expression for CH_3CN

::3:

· . \$5'5' \$\$\$'

:::: :s:'

\$25' \$25'

. . 2_s3

TABLE 2.5

Generalized Frequency Expression (cm⁻¹)

(transitions from the ground vibrational state)

$$(v_{n}, v_{n+1}, \dots, v_{t}, \Delta l_{t}, v_{t+1}, \Delta l_{t+1}, \dots)^{\Delta K} \Delta J_{K}(J) = \Sigma_{s} (\omega_{s} + \Delta \omega_{s}) v_{s} + \Sigma_{s} \Sigma_{s} x_{ss} (v_{s} + g_{s}/2) (v_{s} + g_{s}/2) - g_{s} g_{s}/4] + S \leq s'$$

$$\Sigma_{s} \Sigma_{s} x_{ss} (v_{s} + g_{s}/2) (v_{s} + g_{s}/2) - g_{s} g_{s}/4] + S \leq s'$$

$$\Sigma_{\mathsf{t}}\Sigma_{\mathsf{t}}^{\mathsf{x}}{}_{\mathsf{t}}{}_{\mathsf$$

$$\Sigma_s \Sigma_t \Sigma_t y_{sl_t l_t} (v_s + g_s/2) \omega_t \omega_t$$
 +

$$A_0[(K+\Delta K)^2-K^2] +$$

$$B_0[(J+\Delta J)(J+1+\Delta J)-J(J+1) - (K+\Delta K)^2+K^2] +$$

$$[-2A_{\rm e}\Sigma_{\rm t}\zeta_{\rm t}^{\rm z}\Delta t_{\rm t} + \Sigma_{\rm t}\{\eta_{\rm t} + \Sigma_{\rm s}\eta_{\rm ts}(v_{\rm s} + g_{\rm s}/2)\}\Delta t_{\rm t}][K + \Delta K] +$$

$$-D_0^J[(J+\Delta J)^2(J+1+\Delta J)^2-J^2(J+1)^2] +$$

$$^{-D}_{O}^{JK}[(\kappa+\Delta\kappa)^{2}(J+\Delta J)(J+1+\Delta J)-\kappa^{2}J(J+1)] +$$

$$-D_0^K[(K+\Delta K)^4-K^4] +$$

$$[-\Sigma_{s}\alpha_{s}^{A}v_{s}+\Sigma_{s}\Sigma_{s},\gamma_{ss}^{A},(v_{s}v_{s}+v_{s}g_{s},2+v_{s}g_{s}/2)$$

$$s \leq s'$$

$$+\sum_{t \leq t} \sum_{t \neq \ell} A_{t} \Delta \ell_{t} = \sum_{t \leq t} (K + \Delta K)^{2} + \sum_{t \leq t} \sum_{t = \ell} A_{t} \Delta \ell_{t} = \sum_{t \leq t} (K + \Delta K)^{2}$$

(cont. on next page)

^{*}Taken from reference (28).

TABLE 2.5 (cont.)

Generalized Frequency Expression

$$\begin{bmatrix} -\Sigma_{s}\alpha_{s}^{B}v_{s}^{+}\Sigma_{s}\Sigma_{s}, \gamma_{s}^{B}, (v_{s}v_{s}, +v_{s}g_{s}, /2+v_{s}, g_{s}/2) \\ & +\Sigma_{t}\Sigma_{t}, \gamma_{t}^{B}, \Delta t_{t}\Delta t_{t}, \end{bmatrix} [(J+\Delta J)(J+1+\Delta J) - (K+\Delta K)^{2}] + \\ & +\Sigma_{t}^{T}U_{t}^{J}\Delta t_{t}^{T}(K+\Delta K)(J+\Delta J)(J+1+\Delta J)] + \\ & +\Sigma_{t}^{T}U_{t}^{K}\Delta t_{t}^{T}(K+\Delta K)(J+\Delta J)(J+1+\Delta J)] + \\ & +\Sigma_{t}^{T}U_{t}^{K}\Delta t_{t}^{T}(K+\Delta K)^{2}(J+1+\Delta J)^{2}] + \\ & +\Sigma_{s}^{T}U_{s}^{J}V_{s}^{T}(K+\Delta K)^{2}(J+\Delta J)(J+1+\Delta J)] + \\ & +\Sigma_{s}^{T}U_{s}^{J}V_{s}^{T}(K+\Delta K)^{2}(J+\Delta J)^{2}(J+1+\Delta J)^{2} + \\ & +U_{0}^{J}U_{s}^{T}(J+\Delta J)^{3}(J+1+\Delta J)^{3}U_{s}^{T}(J+1)^{3} + \\ & +U_{0}^{J}U_{s}^{T}(K+\Delta K)^{2}(J+\Delta J)^{2}(J+1+\Delta J)^{2}U_{s}^{T}(J+1)^{2} + \\ & +U_{0}^{T}U_{s}^{T}(K+\Delta K)^{4}(J+\Delta J)(J+1+\Delta J)^{2}U_{s}^{T}(J+1)^{2}U_{$$

(Table 2.6). The program SYMFIT (28) uses the simultaneous requency expression to determine the molecular constants.

Table 2.6

Simultaneous Frequency Expression for $\nu_5,~2\nu_5{}^{\parallel},~and~2\nu_5{}^{\perp}$ of CH3CN *

$${}^{K}\Delta J_{K}(J) - \{B_{o}[(J+\Delta J)(J+1+\Delta J) - J(J+1) - (K+\Delta K)^{2} + K^{2} - D_{o}^{J}[(J+\Delta J)^{2}(J+1+\Delta J)^{2} - J^{2}(J+1)^{2}] - D_{o}^{JK}[(K+\Delta K)^{2}(J+\Delta J)(J+1+\Delta J) - K^{2}J(J+1)] =$$

$${}^{J}O(V_{5}) \text{ or } + [A_{o} - \frac{1}{3}\eta_{5s}][(K+\Delta K)^{2} - K^{2}]$$

$${}^{J}O(2V_{5}^{\perp}) \text{ or } + [A_{o} - \frac{1}{3}\eta_{5s}][(K+\Delta K)^{2} - K^{2}]$$

$${}^{J}O(2V_{5}^{\perp})$$

(cont. on next page)

Table 2.6 (cont.)

$$\begin{array}{l} {\rm H}_{o}^{J} \big[\left({\rm J} \! + \! \Delta {\rm J} \right)^{3} \left({\rm J} \! + \! 1 \! + \! \Delta {\rm J} \right)^{3} - {\rm J}^{3} \left({\rm J} \! + \! 1 \right)^{3} \big] \\ \\ \frac{1}{2} \; {\rm q}_{5} \delta_{o}^{k} \delta_{1}^{\Delta \nu_{5}} \left({\rm J} \! + \! \Delta {\rm J} \right) \left({\rm J} \! + \! 1 \! + \! \Delta {\rm J} \right) \left(2 \; {\rm J}^{2} \! - \! 1 \right) \\ \end{array}$$

'aken from reference (11).

CHAPTER III

DIGITAL SIGNAL AVERAGING

The averaging of repeated scans, or signal averaging, has long been recognized and routinely used as a powerful technique to enhance the signal-to-noise ratio (S/N) in many areas of the physical sciences. To our knowledge, signal averaging has not been applied routinely to high resolution infrared spectra obtained on grating spectrophotometers because of the special difficulties, which will be discussed below.

Peter Jansson briefly mentioned the possibility of Signal averaging high resolution infrared data in his Ph.D. dissertation at Florida State University in 1968, but he did not discuss procedures or applications.

Paul D. Willson stated in his 1973 Ph.D. dissertation at Michigan State University that "... averaging of repeated runs has not been possible because our monochromator is not driven sufficiently linearly and reproducibly," i.e., the frequency spectrum is neither linear nor reproducible. These have been the major obstacles to signal averaging with grating spectrophotometers.

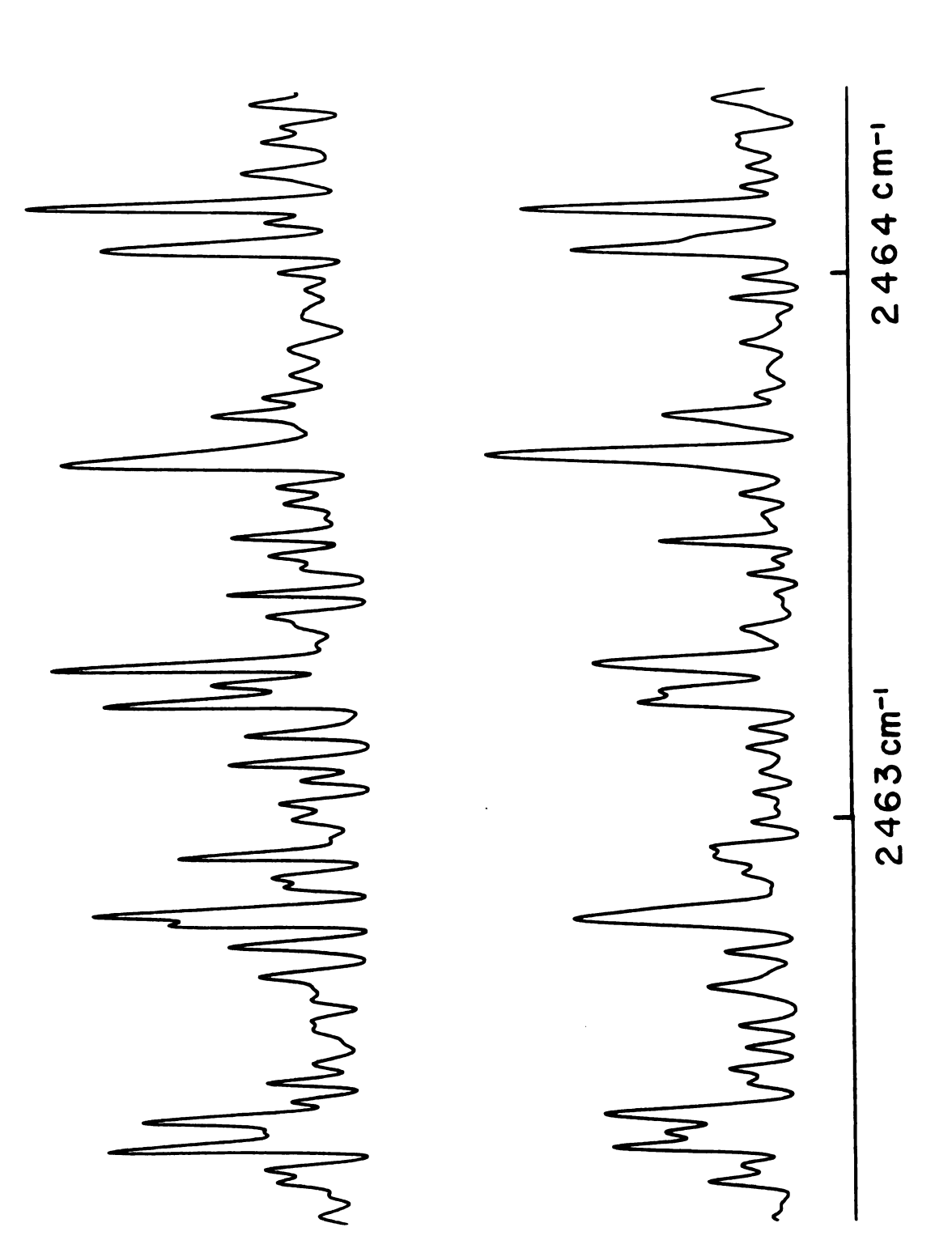
This chapter will describe an algorithm to render linear in frequency a short section (scan) of digitally recorded spectra obtained on our high resolution grating spectrophotometer. Several trigger mechanisms to align scans for averaging will also be discussed.

Types of Noise to be Processed

Developments of digital signal processing techniques, such as multiple sampling (5), followed by smoothing (5), and deconvolution (7), make possible an increase in the resolution limit by a factor of from 2.5 to 3.0 for digitally recorded high resolution infrared spectra, assuming a sufficiently high initial S/N (e.g., S/N ~ 50). A S/N of 50, however, is not always possible, such as when increasing the resolution limit by decreasing the slit width in an effort to resolve closely spaced lines.

Figure 3.1 demonstrates the inconsistencies that Occurred when an attempt was made to deconvolute two individual "noisy" scans of the same region of the spectrum Of N₂0. We believe these unsatisfactory results are due primarily to low and medium frequency noise, low frequency noise being noise with features having a "full width at half height" (FWHH) comparable to that of a single line. In all of our spectra, high frequency noise has been reduced effectively by RC smoothing, multiple sampling, and digital smoothing (5).

Deconvolution of two independent "noisy" scans of the same region of the (120) band of $\rm N_2O$ (deconvoluted in the same manner). Figure 3.1



In principle, there are two possible solutions to the problem of low and medium frequency noise. The first is to scan at a slower rate and change the RC constant, sampling rate, etc., appropriately. Scanning at a lower rate is effective for noise with a white power spectrum, is completely ineffective for f⁻¹ noise, and is somewhat effective for other types of noise (29). Unfortunately, we normally scan our grating spectrophotometer at as slow a rate as can be tolerated without introducing nonuniform frictional problems, associated with rotating the grating, that cannot be solved with our present equipment.

The second possible solution is to average repeated scans of the spectrum, i.e., to signal average. Although signal averaging is ineffective for some kinds of noise, such as noise that is correlated with the signal, the najority of noise power distributions can be signal averaged effectively. Ernst (29) has shown that for several kinds of noise (such as white noise, certain types of low pass RC littered white noise, and f⁻¹ noise) the signal-to-noise ratio increases approximately as the square root of the number of scans averaged together. Furthermore, for noise from non-recurring events, such as transients due to the opening or closing of a switch, the S/N increases even faster, viz., directly as the number of scans averaged together.

The effectiveness of signal averaging for improving the S/N in a given situation can be tested experimentally. To

test the effectiveness of signal averaging for our spectrophotometer and procedure, we evacuated the sample cell after
a typical run and continued recording the output of the
system. Since there was no absorption of the signal by a
sample, the recording consisted only of real spectrophotometer noise on top of a presumed fairly steady signal, as
processed with our normal RC and sampling settings.

Figure 3.2 shows scans of our spectrophotometer noise at various stages of processing. The top row shows a single scan (3.2a), an average of four scans (3.2b), and an average of sixteen scans (3.2c). The noise for the average of four scans (3.2b) has a measured root mean square (RMS) deviation from the baseline (2.10⁻¹) times that of a single scan, whereas, the noise for the average of sixteen scans (3.2c) has an RMS deviation (3.94⁻¹) times that of a single scan. Figures 3.2d, 3.2e, and 3.2f are the results of digitally smoothing Figures 3.2a, 3.2b, and 3.2c respectively. Figure 3.2g shows a short section of a signal averaged spectrum; 3.2h shows the same section after digital deconvolution. Some actual spectral lines are shown at the bottom to provide both vertical and horizontal scales for comparison.

A visual comparison of parts 3.2a and 3.2d reveals that digital smoothing significantly reduces high frequency noise, but is not very effective on low and medium frequency noise. In contrast, signal averaging not only reduces low frequency noise (compare f with d), but also reduces high frequency noise (compare c with a). We both digitally smooth and signal average to reduce noise on our spectra.

Spectrophotometer noise at various stages of processing. Real spectral lines, raw and deconvoluted, at the same scale are provided in G and H respectively for comparison. Figure 3.2

Inspection reveals that there are several noise features in the single scan (3.2a and 3.2d) whose height and width are comparable to the weakest real spectral lines shown in 3.2g. Such noise features would be enhanced by the deconvolution program in the same manner as the weak real spectral lines (compare 3.2g and 3.2h). Thus, the average of sixteen scans may be deconvoluted more reliably than the single scan because the low frequency noise features are much reduced.

Spectral Linearization

To signal average effectively, the noise must add incoherently but the signal must add coherently. To add the signal coherently, the scans must be reproducible (excepting noise) and must have a reliable trigger to align the scans. The more reproducible the scans are, and the more reliable the trigger is, the better the results from signal averaging. Our original data are not accurately reproducible and often do not have an obvious, reliable trigger.

Our data are sampled linearly in time and calibrated as a function of frequency in cm⁻¹. Our data are not linear in frequency, however, because of grating dispersion, which varies monotonically with grating angle, and nonlinearities in the grating drive. The nonreproducible grating drive nonlinearities have two basic causes, cyclical errors in the grating drive train gears, and a drive system that is not perfectly rigid. The undesirable effects of the grating drive nonlinearities must be counteracted in some way to achieve reproducibility.

In our spectrophotometer, visible light interference fringes are sampled digitally and recorded on magnetic tape alternately with the infrared data. The fringes provide a coordinate system to measure infrared frequencies as described in Rao, Humphreys and Rank (30). This process intimately couples the two signal records such that any nonlinearity that occurs in the infrared data also occurs in the fringe data in essentially the same way. Thus, should the fringe spectrum be made linear and reproducible, the infrared spectrum would also be made linear and reproducible by the same operation.

In principle, the interference fringes are equally spaced in frequency. The number of data points recorded between fringe peaks, however, varies due to the causes mentioned above by as much as four percent of the average number of points between fringes. Since the fringe peaks are equally spaced in frequency, the region between the fringes should be sufficiently linear in frequency. The data are nonlinear and not reproducible, because of the nonlinearities in sampling as a function of frequency. If all regions between fringes could be made to contain the same number of data points, the scans would be linear in frequency.

In practice, the fringes themselves need not actually

be reconstructed. The fringe spectrum is separated from the

infrared spectrum by the computer program SYSTEM (see

Chapter IV) so that a data point and its associated fringe

point would have the same magnetic tape coordinate, but on different tapes. The fringe positions are measured in tape coordinates and linear interpolation is then used on the infrared spectrum to construct the desired number of points between adjacent fringe positions. In this manner, the individual scans of infrared data are rendered both reproducible and linear in spectral frequency.

Choice of Alignment Trigger

In addition to linearity and reproducibility, successful signal averaging requires that the signal must have some consistent feature (a trigger) to align the scans, allowing the signal to add coherently.

Since our fringes generally have a high S/N, one logical Choice of trigger is a fringe (method A). Unfortunately, the etalon generating the fringes increases in temperature during operation so that in subsequent scans the position of each fringe changes slightly in frequency, relative to the infrared spectrum. Hence, when fringes are used to trigger the sum, the successive scan signals will add more and more Out of synchronization.

Another logical choice for a trigger is a single prominent line in the infrared spectrum (method B). Often, however, the S/N is not large enough to ensure the reliability of such a trigger, resulting in reduced resolution and a broadening of the signal averaged lines.



A trigger comprising many lines in the scan would statistically increase the reliability for triggering on lines (method C). A least squares fit of the line positions in one scan versus the line positions of another should provide a more reliable trigger.

Method C was not used until late in my analysis, but was then used very successfully on a region of the spectrum where every other method had failed. The region had many weak lines whose apparent shapes changed from scan to scan. This method was not applied to any other spectral regions and so remains incompletely tested. Based on this single application, however, I would use this triggering mechanism as my first choice in the future.

If the scans were sufficiently linear and reproducible, the entire scan could be used as the trigger by employing cross correlation (method D) or the method of least squares (method E). The time to process the data would probably be prohibitively long, however, if the processing were done on a microcomputer or a minicomputer. Hence, we selected only a portion of the linearized scan to trigger on. A suitable portion of the spectrum should have no incompletely resolved spectral lines and the lines should not be susceptible to large changes of intensity with small changes of pressure.

Alignment Procedure

Once the scans have been linearized and a suitable trigger chosen, the scans are ready to be summed.

As a first approximation, the position of a particular strong line is found for each scan and each scan is roughly aligned by compensating for any differences in the position of that line. This usually aligns the scans to better than ± 0.005 cm⁻¹, but the fit needs to be improved before summing. The method of refinement depends on the type of trigger.

If the actual spectrum is the trigger, in whole or in part, then either a cross correlation or the method of least squares can be used to determine the relative displacement that optimizes the fit between two scans. The discrete form of the cross correlation integral is given by:

$$G = \sum_{i} g_{i} = \sum_{i} \sum_{j} [f_{j} * h_{j+i}]$$

where f_j is the value of the ordinate at the jth point of scan f and h_{j+i} is the value of the ordinate at the $(j+i)^{th}$ point of scan h. The subscript i is varied to provide a relative displacement between the two scans. The two scans fit together best when the maximum value of g_i occurs.

The method of least squares, when applied to the spectrum (or a portion of the spectrum), determines the best fit by finding the smallest value of g_i , where now $g_i = \sum\limits_j \left[f_j - h_{j+i}\right]^2$, f_j , h_{j+i} , and i having the same definitions as given in the previous paragraph.

If the rough fit is refined using the position of many lines, the method of least squares is used. As usual with the method of least squares, the best fit occurs when $\mathbf{E}_{\mathbf{i}} = \sum_{j} \left[\mathbf{f}_{j} - \mathbf{h}_{j+i} \right]^{2} \text{ is a minimum, where } j \text{ identifies a}$

particular line position in scan f and scan h, and i is again an index to move the scans relative to each other. In all of our cases, the index i is moved about 0.02 cm^{-1} above and below the position of the rough fit by increments of 0.001 cm^{-1} .

When averaging more than two scans, the procedure is as follows:

- 1. A copy of the first scan is made in an empty file.
- 2. The best refined fit is found between the second scan and the first scan.
- The second scan is then added to the first scan, appropriately displaced.
- 4. The third scan is then compared to the normalized sum of the first two, assuming the trigger is a region of the spectrum. If the trigger is the position of several lines, all scans are compared to the first scan (the best choice would be to remeasure the position of all lines after adding in each scan, but this requires a prohibitively long time for our system). The third scan is then added to the sum of the first two, appropriately displaced.
- 5. Step 4 is repeated for each remaining scan.
- 6. The sum is then normalized to the desired signal strength for further signal processing.

Effectiveness of Signal Averaging

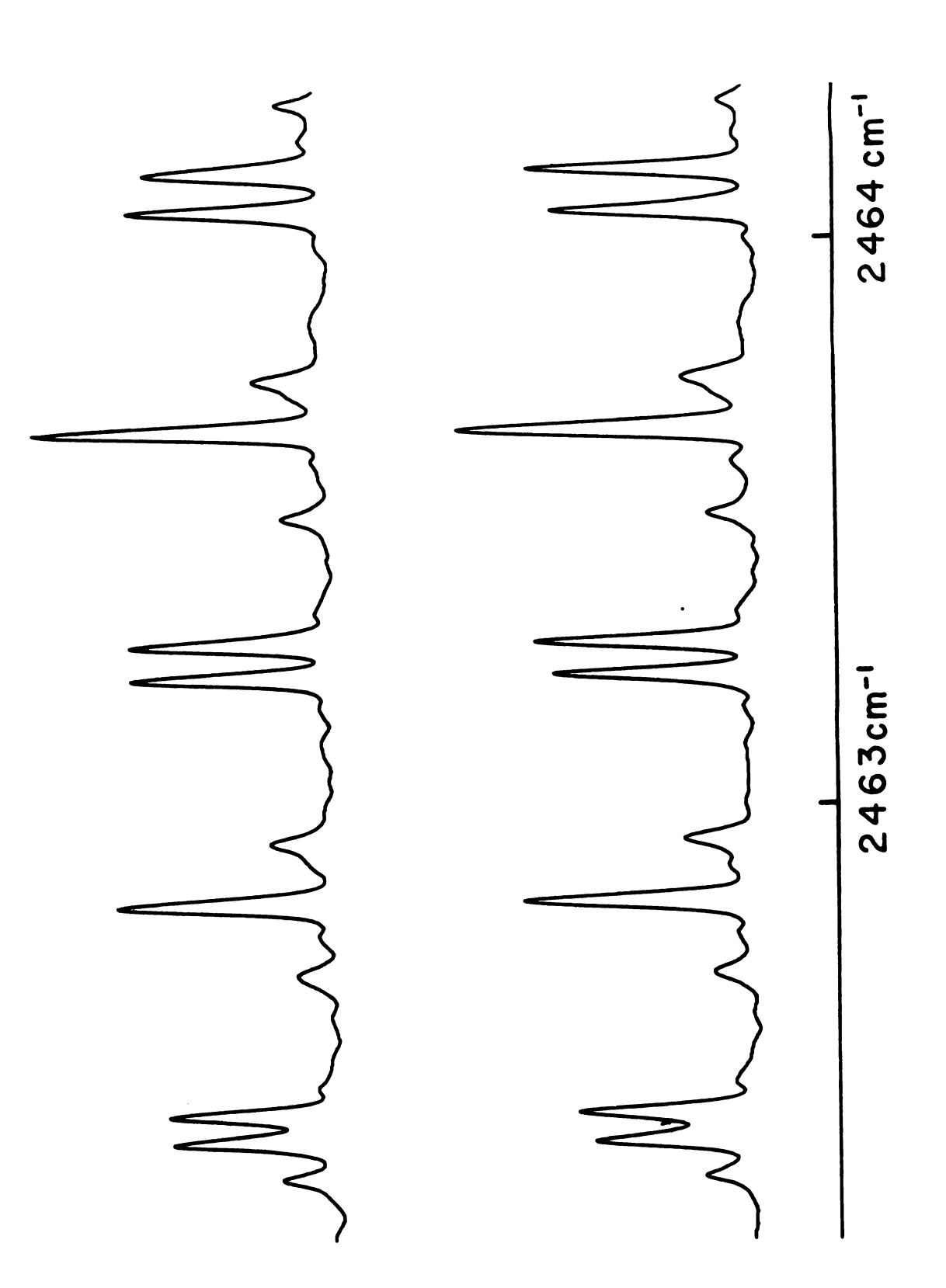
To examine the effectiveness of signal averaging, the region near the band center of the (1,2,0) band of N_2^0 was studied. Two single scans and two averages of eight scans were deconvoluted identically and compared.

Figure 3.1 compares two single scans of N_2 0 that have been deconvoluted. Even though each scan was deconvoluted in an identical manner, there are considerable differences in the appearance of the two scans. Figure 3.3 also shows two scans that have been deconvoluted in an identical manner, except each scan is an average of eight independent scans (sixteen total). It is clear that a factor of approximately $\sqrt{8}$ higher S/N in the two averaged scans, deconvoluted, led to a substantial improvement in consistency and apparent line shapes.

The reliability of these results was also examined by comparing them with higher resolution interferometer measurements (31). Seventy-two spectral lines of N_2 0 were measured in the 2462-2476 cm⁻¹ region of the spectrum for four cases: a single smoothed scan, a single deconvoluted scan, an average of sixteen scans smoothed, and an average of sixteen scans deconvoluted.

The seventy-two lines were compared to the higher resolution data for each of the four cases. A comparison of the signal averaged data to the higher resolution data yields a fit with a standard deviation of $\sigma = 0.0013$ cm⁻¹. Table 3.1 summarizes the results. Column 1 lists the four cases and

Two independent deconvoluted spectra, each an average of eight scans, of the same region of the (120) band of $\rm N_2O$ (deconvoluted in the same manner). Figure 3.3



column 2 lists the number of lines of the original seventy-two that lie within 0.0039 cm⁻¹ (3 σ) of the higher data. It should also be noted that σ for sixty-three lines of the single scans was calculated to be approximately 0.0040 cm⁻¹.

We conclude from these comparisons that the averaged scans yield appreciably better results. Furthermore, the averaged scan may be deconvoluted to enhance the resolution with assurance that the frequencies measured are reasonably accurate.

Cable 3.1 Summary of signal averaged N_2O (120) data versus single scan N_2O (120) data.

Case	Number of Lines Out of 72 within 0.0039 cm ⁻¹ of Reference 31
Single scan, smooth	46
Single scan, deconvoluted	46
Average of 16, smooth	63
Average of 16, deconvoluted	63

CHAPTER IV

EXPERIMENTAL CONFIGURATION AND PROCEDURE

Procedure. Part one briefly describes the configuration of the spectrophotometer and changes in the configuration.

Ore detailed descriptions of the spectrometer can be found in the dissertations of J. L. Aubel (32), D. B. Keck (33), and J. R. Gillis (35). The experimental procedure used to record the high resolution spectra on the Michigan State University near infrared spectrophotometer is discussed in part two. Part three describes the algorithms used to process the infrared data digitally.

Chapter IV is divided into three parts, experimental

Experimental Configuration

Infrared Spectrophotometer Configuration

The Michigan State University high resolution infrared Spectrometer (references 28, 32-35) is composed of eight main Subsystems categorized by function: the infrared and visible Sources, pre- and post-optics of each, the White type multiple traverse cell, the Littrow-Pfund monochromator, the fringe System, the detectors, the electronics, the PDP-12

minicomputer. All mirrors in the discussion that follows are front surface mirrors.

Infrared Pathway

An electrical current of approximately 350 amps is sent through a carbon rod with a small wedge shaped cavity that acts as a blackbody radiator in the infrared region of the spectrum. The carbon rod is mounted in a pure argon atmosphere and surrounded with a water-cooled housing (28, 33). A series of four mirrors reflects the infrared radiation into the White type multiple traverse cell and changes the f/# From f/5 to f/20. Several mirrors focus the radiation not absorbed by the sample in the multiple traverse cell onto the entrance slit of the monochromator and change the f/# back to f/10. A mechanical chopper located between the multiple traverse cell and the monochromator chops the infrared at 450 Hertz. The 1.08 meter focal length Littrow-Pfund monochromator contains three plane mirrors, a parabolic mirror, and two diffraction gratings (a 300 line/mm grating blazed for 5 microns, and a 600 line/mm grating blazed for 1.6 microns) mounted back to back on a turntable. design allows either a single pass or a double pass configuration. The monochromator was used only in the single pass Configuration for this work. The infrared post-optics focuses the radiation onto the detector housed in a small evacuated chamber with a CaF, window. The v, band of CD, Br Occurred in a region where our liquid nitrogen cooled

... ... : ·. -100 2

photovoltaic indium antimonide detector was the most sensitive, while the ν_5 and $2\nu_5$ bands of CH₃CN occurred in a region where our dry ice cooled photoconductive lead sulphide detector was most sensitive.

Visible Pathway

The visible light foreoptics focused the output for a 100 Watt zirconium arc lamp, mechanically chopped at 90 Hertz, onto the entrance slit of the monochromator slightly above the infrared. The visible ran "downhill" through the monochromator slightly below the infrared. Appropriately placed mirrors and lenses directed the light to an etalon to produce Edser-Butler band "fringes". A Littrow prism order sorting spectrometer selected the desired order to be detected by the dry ice cooled RCA 7265 photomultiplier tube (PMT).

A general description of the electronics can be found in the dissertation of James R. Gillis (35); a summary is **Provided** here.

A Princeton Applied Research HR-8 lock-in amplifier first suppresses most frequencies output from the infrared detector, except those near 90 Hertz, then amplifies the remaining signal. An adjustable gain amplifier further amplifies the signal into the voltage range of an analog-to-digital converter (ADC) for a PDP-12 minicomputer.

The visible light fringes were processed in a similar manner. The PMT converted fringe intensities into electrical Voltages. A Keithley 822 phase sensitive detector and a

Keithley 823 amplifier passed only those frequencies near 450 Hertz and amplified that signal. An adjustable gain amplifier made the signal suitable for an ADC.

An interactive program named SYSTEM (36) samples and stores the data on magnetic tape to await further processing. The SYSTEM data sampling rate is adjusted to sample between 30 to 60 magnetic tape data points per full width at half height of a single spectral line (5). Each of these magnetic tape data points is a multiple sample, averaging 32 consecutive data readings. Multiple sampling is the digital analog of electronic integration in that it sums data points to improve the signal to noise ratio and to help to prevent the aliasing of higher frequencies.

Configuration Changes

The configuration of the spectrophotometer as described above was used to collect the ${\rm CD_3Br}$ data. The $2\nu_5$ band of ${\rm CH_3CN}$, however, is weakly absorbing. In preparation for recording the $2\nu_5$ band of ${\rm CH_3CN}$, we realigned the spectrophotometer to optimize the signal strength, and corrected some minor problems before running the spectra.

The multiple traverse cell (MTC) was disassembled and the mirrors replaced with a spare set. The old set was then sent to be resurfaced. An extra mirror was installed at the end of the MTC nearest the foreoptics to allow observation of the intensity distribution on the other two mirrors. At some point during the reassembly of the MTC, stress caused a

flake to break away from the CaF₂ entrance window. Realignment of the foreoptics to avoid the flake was very difficult, and probably not optimum. All mirrors in the foreoptics were cleaned with non-flexible collodion (37) prior to realignment.

The entrance and exit slits to the monochromator required cleaning and recalibration. Minor physical changes were then made to permit the slits to open dependably and reproducibly. When reinstalled, however, the previous optic axis could not be recovered for some unknown reason. This changed the entire alignment of the system.

Unfortunately, at this stage of the realignment procedure,
the circuit breaker to the vacuum pump of the evacuated main
tank (i.e., the monochromator) tripped, turning the pump off.
This resulted in oil from an overfilled oil reservior in the
pump spraying back into the main tank, mostly onto the
300 line/mm grating, the large flat mirror, and the small
pickoff mirror. The mirrors were coated with several applications of non-flexible collodion to remove any oil. However,
the diffraction grating was not so easily cleaned. As
recommended by Bausch and Lomb, Xylene was dripped vertically
down the face of the grating with the grating remaining in
the mount. After treatment the grating appeared much cleaner,
but the effect on its efficiency is not known with certainty.

The small pickoff mirror at the center of the large flat had been dropped, necessitating replacement. The parabolic mirror had to be adjusted to accommodate the new optical axis.

The elliptical mirror in the post optics was cleaned and realigned to optimize the amount of energy leaving the monochromator and reaching the infrared detector.

It is not known how much the realignment process actually improved the performance of the spectrophotometer. When one compares CH₃CN data from 1967 with current data, the data from 1967 has a superior resolution limit and signal to noise ratio. The probable cause for the poorer performance is the deterioration of the spectrophotometer components. Contamination of the sample gas or basic changes to the configuration of the spectrophotometer could also be major contributors. The main advantage with the present CH₃CN data, however, is that signal processing techniques allow more information to be extracted. The data from 1967 cannot now be processed with digital techniques.

Experimental Procedures

Experimental Procedure for a Calibrated Run

The procedure for collecting the data of a calibrated run is well documented (28, 30, 34, 35). The following Section will briefly review that procedure.

Some lower resolution surveys of the region of interest are run to find the necessary experimental conditions, such as highest and lowest frequencies, grating angles, etc.

High resolution trials are also necessary to determine such parameters as gas pressure, slit width, signal to noise ratio, etc.

<u>in</u> ta
πιεθ
ii.er
2187
11189
teti
üi
3 1
118:
9119 gg 1 Marie
II
::
411 s 1944
£;ę
ie:
ilite
18 s
1.
130e
in in its
د ب اغآ
**\$

Suitable calibration gases (usually a simple linear molecule) whose frequencies are well known and bracket the region of interest are chosen, again performing preliminary tests to determine necessary parameters. The fringe order must be chosen and the fringes in the region of interest must be checked to ensure the S/N is large enough and that there are no anomalies.

To start a calibrated run, a calibration gas whose frequencies are well enough known to use as secondary standards is let into the multiple traverse cell. Several calibration 1 ines are then recorded. With the spectrophotometer still running continuously, i.e., with the diffraction grating turntable rotating and the output from both detectors being recorded, the multiple traverse cell is evacuated and then filled with the sample. The sample is removed from the cell after the region of interest has been recorded. In the manner described previously for the first calibration gas, several lines of second calibration gas are recorded. The entire run is simultaneously recorded on chart paper in real time to monitor the progress. Figure 4.1 is an illustration of the Output of the detectors and of what is recorded on magnetic tape. The upper trace consists of calibration gas 1, the Sample gas, and calibration gas 2; the lower trace is the fringes. Figure 4.2 shows actual N_2 0 data with fringes. Notes can be made on chart paper to mark noise spikes, angle Versus tape position, etc.

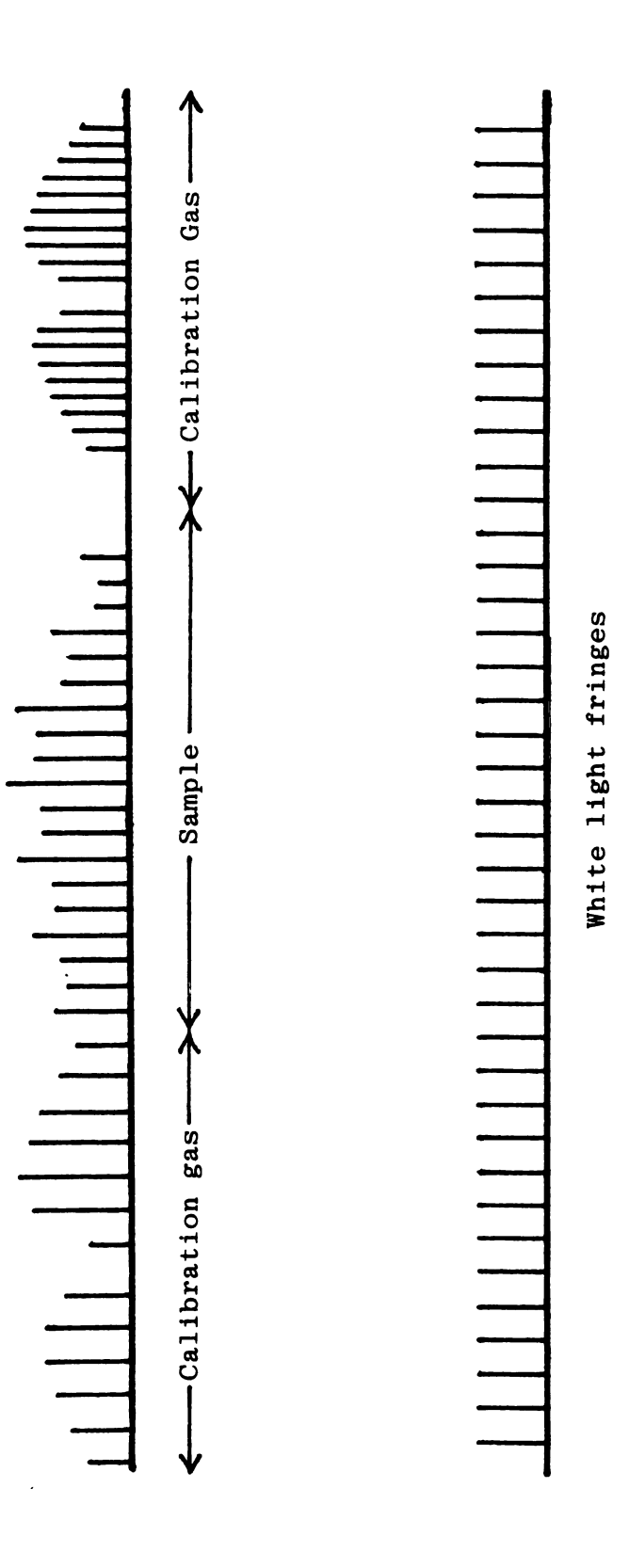
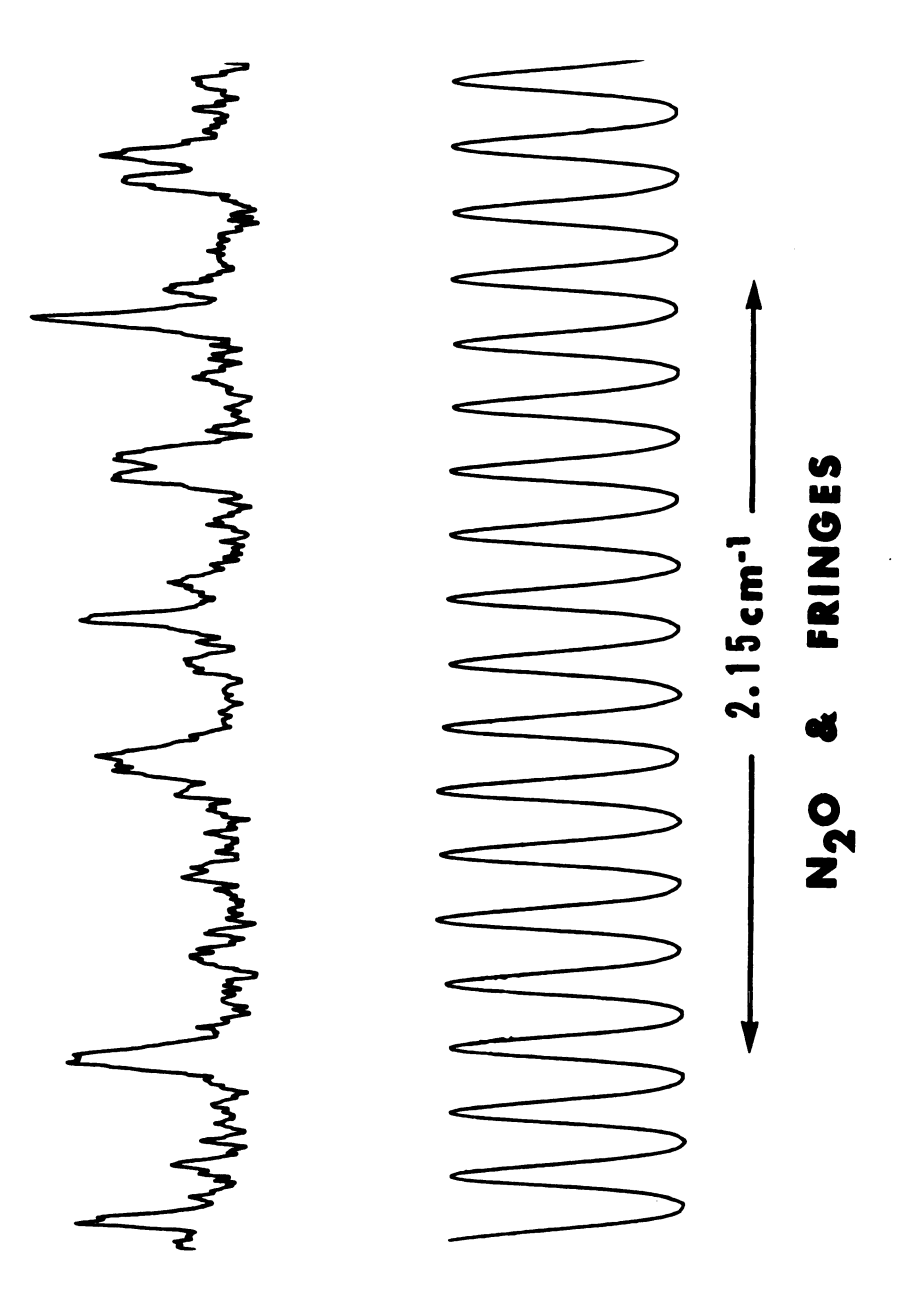


Illustration of data recorded on magnetic tape and on chart paper during a typical calibrated run, not to scale. Figure 4.1



Data near the band center of the (120) band of $\rm N_2^{} \rm O_{\rm s}$ shown with fringes. Figure 4.2

The

imige

man en

:: iete

izis a

Sta

igital

le uppe

ma as

milog c

Hilling

actbed

ts dat

`80. r

jes E

: ar

itegi Ite

:

tae

ite. U

allowing

atia III ca

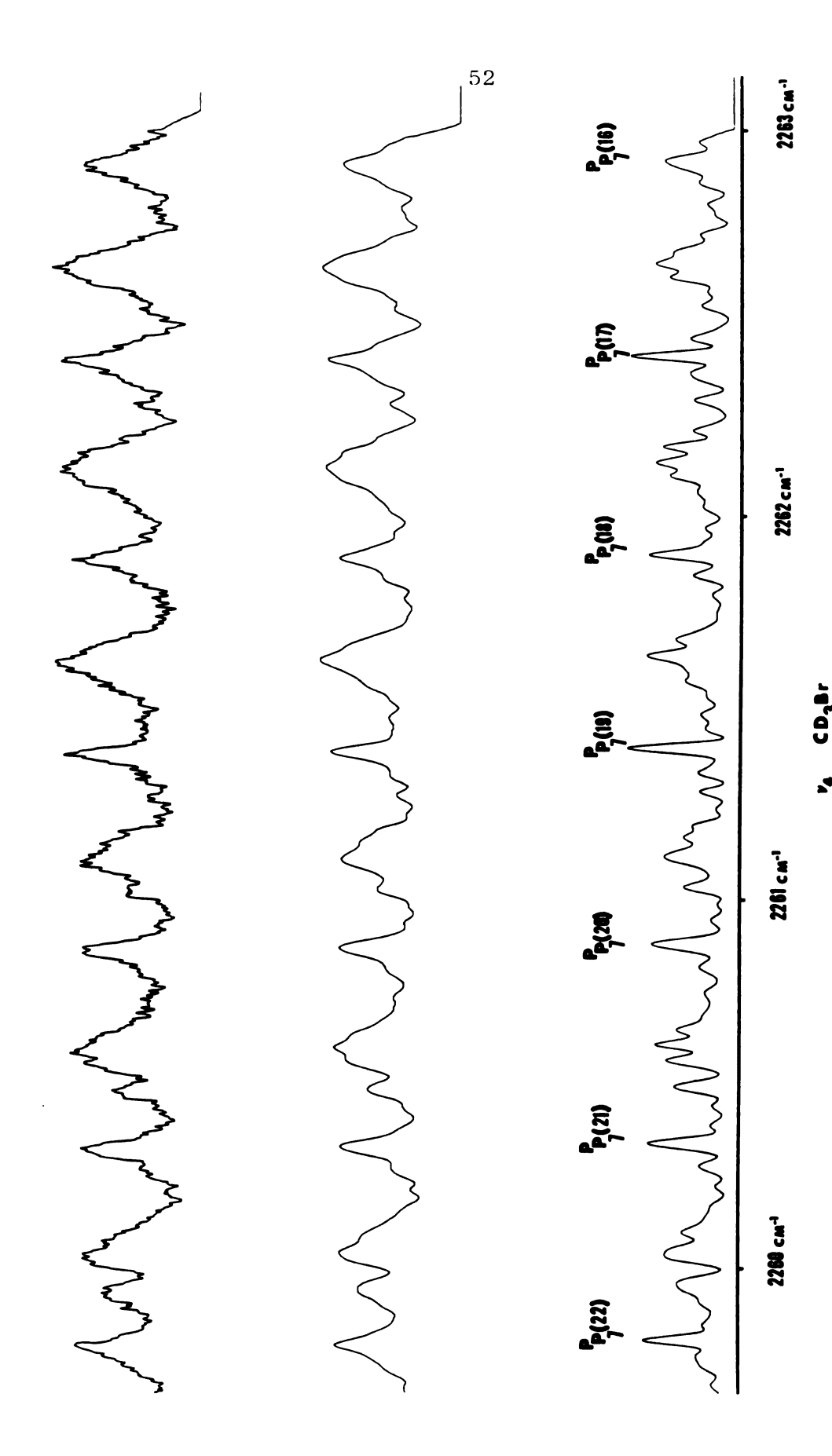
J. 37.31

The fringe spectrum is sampled alternately with the infrared spectrum and continuously recorded throughout. The fringe spectrum therefore provides a system of coordinates that enables interpolation between the calibration frequencies to determine the unknown frequencies because Edser-Butler bands are equally spaced in frequency.

Standard processing is performed on the data, viz., digital smoothing and, if necessary, digital deconvolution. The upper portion or trace of Figure 4.3 is original CD₃Br data as recorded on magnetic tape and then output to an analog chart recorder; the center trace shows the data corresponding to the data at the top after having been digitally smoothed; the bottom trace shows the data corresponding to the data at the center after having been digitally deconvoluted. The positions of the lines of the calibration gases are then measured in fringe numbers. A second order linear least squares fit of the measured fringe numbers to the calibration frequencies determines the scale of the coordinate system. The line positions of the sample gas under study are then measured in fringe numbers and converted to frequencies from the relationship determined by the least squares fit.

Experimental Procedures for a Signal Averaging Run

The process of collecting data to be signal averaged differs from collecting data for a calibration run. The following section describes our method for collecting the data in cases where the data is to be averaged to improve the signal to noise ratio (S/N) sufficiently for deconvolution.



Original, smoothed, and deconvoluted spectra from the $\mathbf{v_4}$ band of $\mathrm{CD_3Br.}$ Figure 4.3

"

11111

1112

fil na

pes t

æïle

676**21**1

i tes

izie

14712

ii:

0021

slit:

Sign Redn

1 fa 39j.

to h

Scan

\$1:

Numerous tests must be run on the spectra of interest to determine the best conditions for optimum resolution and S/N. To increase the amount of absorption of the "blackbody" radiation by the sample gas, the number of traversals in the MTC may be increased. However, as the number of traversals goes up, the signal loss due to multiple reflections with a reflection coefficient less than one also goes up, and eventually becomes larger than the "increase in absorption". A test on $\rm R_{\rm Q_{\rm O}}$ of $\rm 2\nu_{\rm 5}$ of $\rm CH_{\rm 3}CN$ determined that the optimum number of traversals for CH₃CN runs was between 20 and 24. The relative slit orientation must also be considered when trying to increase signal strength. Because the image is parabolic and the entrance slit is straight, the entrance slit must be continually rotated as the angle of the grating changes to maximize resolution. The resolution can also be controlled by varying the width of the entrance and exit slits: the narrower the slit widths the better the resolu-Unfortunately, as the slits become narrower, the signal gets weaker while the noise remains the same, thus reducing the S/N.

Finally, the resolution can be increased by as much as a factor of 3 by digitally deconvoluting the spectrum (7, 38, 39). To deconvolute reproducibly, however, it is necessary to have a S/N of approximately 50 or better. The S/N can be increased by approximately a factor of 4 by averaging 16 scans together. When the data is to be signal averaged, the slit width can be decreased until the S/N is approximately

12. 1 12.13

: is

171

.: s

218 34,1

10.0

8721 7821 2000

10 (

ii :

M

<u>27.</u>

19 155 155

ięg I. j

:Ç

12, without decreasing the final S/N necessary for effective deconvolution.

In principle, the S/N improves approximately as n^{1/2}, where n is the number of scans averaged. However, there is not much advantage to be gained by averaging more than approximately 16 scans. For example, the S/N can be improved by approximately a factor of 5 by averaging 25 scans, but the time required to obtain 25 scans is 25/16 times longer than the time required to obtain 16 scans. Thus, if 16 scans require approximately 8 hours, 25 scans would require approximately 12.5 hours. Furthermore, the minimum S/N that can be tolerated in a single scan for effective deconvolution is only reduced from 12 to 10. We have found that 16 scans is a good compromise between S/N enhancement and the time necessary to collect the data.

In principle, the interference fringes are equally spaced in frequency. In practice, however, the interference fringes are not quite equally spaced. For our purposes, scanning a range of no more than approximately 20 cm⁻¹ will assure a sufficiently linear scan.

Some overlap between scans to check the calibration of the two scans is desirable. For CH₃CN, each scan contained approximately 0.18 degrees (the grating turntable is rotated by 0.18 degrees) scanned at a rotational rate of 0.01 degrees/minute. This permitted an overlap of approximately 0.025 degrees at each end of the scan.

To ensure that each scan contains the same region of the spectrum and to minimize the actual run time, each scan

::: 5,1 26 ::: 500 81 ... ï <u>:-</u>; 1 3. :0 :: ŝę ÷ 3 , ; ,

should start at precisely the same angle. If one watches the computer monitor while moving to the starting point, one can start each scan at the same fringe, or at worst plus or minus one fringe from the nominal. The end point of the scan is not so critical, as long as one drives past the predetermined stopping point.

Adjustments to the system are to be avoided during a scan. The detector will need to have the coolant replenished periodically, but this should be done only between scans so as not to introduce unnecessary noise into the scan.

Amplifier and gain adjustments usually can be set so that adjustment during a scan is not necessary.

Exceptions do occur however. For $2v_5$ of CH₃CN, the S/N of the fringes was relatively low and minor adjustments had to be made continually to the order sorter.

With generally stable conditions the scans need not be recorded on chart paper. Should some of the controls be sensitive, the progress may need to be monitored over a long period of time. A simple means of doing this is to record the detector output on chart paper simultaneously, but at a very slow paper feed rate.

Digital Signal Process

The procedure for collecting data to be processed was described in the previous section. This section will describe our method of processing the digital data. The types of processing include frequency linearization, smoothing,

averaging (summing and then normalizing the signals to a desired amplitude), and deconvolution. Digital smoothing and digital deconvolution have been described elsewhere (references 5 and 7 respectively).

The digital infrared signal is intially recorded alternately with the digital fringe spectrum on magnetic tape. To do any kind of digital processing at all, the two signals must be separated.

The "Copy" option of the program SYSTEM is used to separate the data. Several questions must be answered interactively when this option (or any option) has been invoked. Two of the questions may require further clarification, viz., which points are to be copied and where to start copying. When separating the data and fringes, every second point is copied, since every other point belongs to the same data set. Usually the infrared data are the even numbered points and the fringes are the odd numbered. Thus to copy the infrared data, the first point to be copied would be point zero, the fringes would begin at point one.

The infrared data and the fringe data are copied onto corresponding blocks of separate tapes. For example, suppose the original data, both infrared and fringe, are on a tape named 8A. Each tape consists of 2000 octal blocks plus leaders on each end. If all 2000 blocks of tape 8A contained data, there would be 1000 blocks of infrared data and 1000 blocks of fringe data. The infrared data might, for example, be copied onto blocks 2 to 1001 of tape 8B. The fringe data,

1181 ::ce :: 1 eța 11:8 : 30 ::: 16 :<u>1</u>e 100-:1e 2: 112 **33**0 Ra 37 Sin

...

17

to

320

24

then, would also be copied onto blocks 2 to 1001, but on tape 8C.

After separating the data, it is desirable that the data be linearized in frequency. Over a 20 cm⁻¹ range, the fringe separation for our system varies from linearity by approximately 0.0003 cm⁻¹. Thus, if two fringes at the beginning of a scan are separated by 0.2000 cm⁻¹, two fringes at the end of the scan would be separated by 0.2003 cm⁻¹. Since the fringe peaks are theoretically equally spaced in frequency, the fringe spectrum may be linearized simply by constructing the same number of points between any two fringe peaks. Any non-linearities in the frequencies of the infrared data and the fringe data are closely correlated, hence, the infrared data are linearized by following the same steps used to linearize the fringes.

The fringe data and the infrared data are digitally smoothed using the "Smooth" option of SYSTEM. The four-times-quartic running average is applied over a length determined by the full width at half height (FWHH) of the narrowest single line of the spectrum. This is easy to determine for the fringe spectrum since all lines have nearly the same shape and FWHH. The infrared spectrum is a little more difficult to smooth because the FWHH of the best single line must be chosen.

After the fringes have been smoothed, a second order linear least squares fit of the intensity of the highest 2n+1 points (where n is usually 14) to their positions

determines the fringe position. The point at which the calculated slope is zero defines the fringe's position. Knowing the spacing of the fringes, the number of points between fringes is usually chosen to give either 0.001 cm⁻¹/point or 0.0005 cm⁻¹/point.

For example, suppose we have a set of fringes that are spaced 0.2000 cm⁻¹ apart. The sampling rate yields a range of from 140 to 170 data points recorded between fringes. To construct a spectrum in which each point represents 0.001 cm⁻¹ requires 200 points between fringes (400 points per fringe would represent 0.0005 cm⁻¹/point). Because the actual number of points between fringes is approximately 155, we would choose to construct 200 points between all fringes.

In practice, the interpolated fringe data points are not actually constructed. There is a one to one mapping between the fringe spectrum and the infrared spectrum so we linearize the infrared spectrum directly by linearly interpolating between points to construct 200 points per fringe. Let us suppose that the positions (measured in tape coordinates) of two consecutive fringes relative to the start of the scan are points 451.623 and 609.488. The intensity of the fringe spectrum at these points is found by linear interpolation. The value at 453.202 is found by linear interpolation between the points at 453 and 454. The height at 453.202 [h(453.202)] is determined from:

[h(453.202) - h(453)]/[453.202 - 453] = [h(454) - h(453)]/[454 - 453]

The infrared data point corresponding to the fringe data point at location 453 also has the coordinate 453. Thus, there is no need to construct 200 data points per fringe and then perform the same operations on the infrared data, simply perform the construction directly on the infrared data.

To average n scans, each of the n scans must contain essentially the same portion of the spectrum. This can be accomplished by finding the largest portion of the spectrum that is common to all n scans, i.e., the largest subset of points contained in all n sets of data points. I did this visually by recording the position of the first few fringes in my notes and counting the number of fringes in the scan. I then sorted and assigned the first few fringes an absolute number corresponding to their position relative to the infrared spectrum. For example, say the first scan had ten fringes before the first Q branch. The first fringe would be given the label 1, the second 2, and so forth. Another scan might have eleven fringes before the same Q branch, in this case the first would be labeled 0, the second 1, etc. A third scan may have only nine fringes before the Q branch. The first fringe would be labeled 2, etc. If the largest labeled first fringe of all scans is labeled two, and if the smallest labeled last fringe of all scans is eighty-three, then the largest portion of the spectrum that each scan contains is the region beginning with the fringe labeled two and ending with the fringe labeled eighty-three. In this way, the largest spectral region contained by all n scans can be found.

The spectral regions are examined to find as many good peaks as possible, where "good" means those that are clearly peaks on all scans and a precise measurement can be made. Ideally, the peaks would be distributed throughout the scan. Run 11 of $2v_5$ of CH₃CN used 37 positions. Each of the positions are measured relative to the beginning of the scan. For perfect data, each peak would have the same position within each scan, e.g., peak 1 located at point 82 in scan 1 would also be located at point 82 in every other scan. real data, these positions change because of noise. the distribution of noise is essentially gaussian in nature, an approximation to the true position of a particular peak can be found by measuring that position many times. Alternatively, it is hoped that by measuring many peaks at one time, as opposed to one peak many times, a good approximation to the "true" offset can be determined. Thus, using the method of least squares to fit the peak positions of each scan to the average of all of the preceding scans, an offset can be determined for the individual scan and that scan averaged into the total.

To illustrate, assume the average contains 3 peaks (y1, y2, y3) at 182, 324, and 646, while the single scan registers these peaks (x1, x2, x3) at 194, 320, and 641. What is the constant, k, necessary to add to all points in the single scan to obtain the best fit to the average? We wish to minimize:

$$R = \sum_{i=1}^{3} [y_i - x_i - k]^2$$

t:
:
æ
<u>:</u>
::
7
::
<i>S.</i>
<u> </u>
ù
\$
S S
:
٥
:
;
:
ŭ
ì
•

with respect to k, i.e. dR/dk = 0. This implies that

$$[y_i = [x_i + kn, or k = [[y_i - [x_i]/n = \frac{[1152-1155]}{3} = -1]]$$

To optimize the fit, each point in the scan should be moved to the left by one point, i.e., the peak at 194 should become the peak at 193, etc. After the scan has been displaced appropriately, it is added to the sum of the previous scans.

My summing method is to take the first scan and place it directly into an empty sum file. The chosen peaks of scan two are compared to those of scan one, then scan two is added to the sum file appropriately displaced. Scan three, and each succeeding scan, is then compared to scan one and added to the sum file appropriately displaced.

An improvement to this approximation is to remeasure the chosen peaks of the sum file after each new scan is added into the sum file, then compared each new scan to the remeasured values.

Finally, the sum of n scans is normalized to some desired signal strength and deconvoluted. The lines in the deconvoluted spectrum are then measured in terms of tape coordinates or points relative to the beginning of the scan.

To convert these positions to frequencies, a method similar to the one used for averaging is employed. A number of prominent lines are chosen to compare the averaged deconvoluted spectrum (line positions in tape coordinates) with the calibrated spectrum (same line positions in frequency units of cm⁻¹). The positions of these lines are compared with a linear least squares fit to determine a conversion from position to frequency.

The procedures described in this chapter should not be considered as "cast in concrete", but rather considered as guidelines. Considerable flexibility exists to customize the procedures to a particular problem. Improvements are possible, as well as desirable. Probably the most significant improvement would be to transmit data to and from the M.S.U. mainframe. The result would be a significant reduction in the real time required to perform the signal processing. Hours and days would be reduced to minutes or seconds, limited primarily by baud rates for data transmittal. Using the mainframe also permits usage of more sophisticated signal processing algorithms, such as a cubic spline interpolation instead of the simple linear interpolation.

In general, the procedures described in this chapter are not "user friendly", but the benefits far outweigh the associated problems when the user is trying to extract the most information from the available data.

CHAPTER V

THE ANALYSIS OF THE v_5 BAND OF CH_3CN

Most of the symmetric top molecules studied by the M.S.U. Infrared Lab were Methyl Halides (CH₃X), which belong to the C_{3v} point group. The axially symmetric molecule Methyl Cyanide (CH₃CN) also belongs to the C_{3v} point group, with the CN radical replacing the halogen (X) along the axis of symmetry. Because Methyl Cyanide has three more vibrational normal modes than the Methyl Halides (3N-6 total vibrational normal modes), the vibrational normal mode named ν_5 of Methyl Cyanide has essentially the same atomic motions as the vibrational normal mode name ν_4 of the Methyl Halides, viz. an unsymmetric C-H stretch, and occurs at a frequency near that of ν_4 .

With one exception, the infrared investigations of gaseous Methyl Cyanide prior to this study were of low to medium resolution. Venkateswarlu (41) used a prism spectrometer to find the band centers of the vibrational normal modes of CH₃CN and to assign and measure the Q branch positions of ν_5 of CH₃CN. Parker et. al. (42) measured the Q branch positions of ν_5 and also determined ζ , ζ_5^z , ν_0 , [(A'-A")-(B'-B")], and 2[A'(1- ζ_5)-B'] with a combination prism-grating spectrometer. Duncan et. al. (43) determined fundamental vibrational

frequencies with heavy isotopic substitution, identified Fermi resonances, and measured harmonic potential constants.

T. L. Barnett (34) investigated ν_5 of CH₃CN at a resolution limit of approximately 0.04 cm⁻¹. The results of the present study will be compared to Barnett's investigation, the only known study at high resolution prior to this one.

This chapter will present the single band analysis of the ν_5 band of CH₃CN, detail a technique to adjust relative weights of spectral lines, and compare the results of the analysis with the results Barnett obtained. Appendix IV contains the frequencies and assignments for ν_5 of CH₃CN.

Analysis

The M.S.U. high resolution grating spectrophotometer system was used to record the spectra of the ν_5 band of CH₃CN under the experimental conditions listed in Table 5.1. Survey spectra of the region are shown in Figure 5.1. It was not necessary to signal average the ν_5 band, although it could have been done.

Barnett had previously analyzed this band, hence many of the spectral lines already had their quantum dependencies assigned. His assignments were carefully checked and some additional assignments made. Several features characteristic of symmetric top molecules helped in determining the assignments. For any particular subband (i.e., for any particular value of $K\Delta K$) $J \geqslant K$, in both the upper and lower states. Thus, for $K\Delta K = 5$, the J = 0 through J = 4 transitions are absent

Table 5.1 Experimental conditions used for the ν_5 band of $\mathrm{CH}_3\mathrm{CN}$ data.

Region: 2973-3149 cm⁻¹

Pressure: 2 - 4 torr

Path Length: 15 meters

Detector: PbS @ 77K

Grating: 300 lines/mm

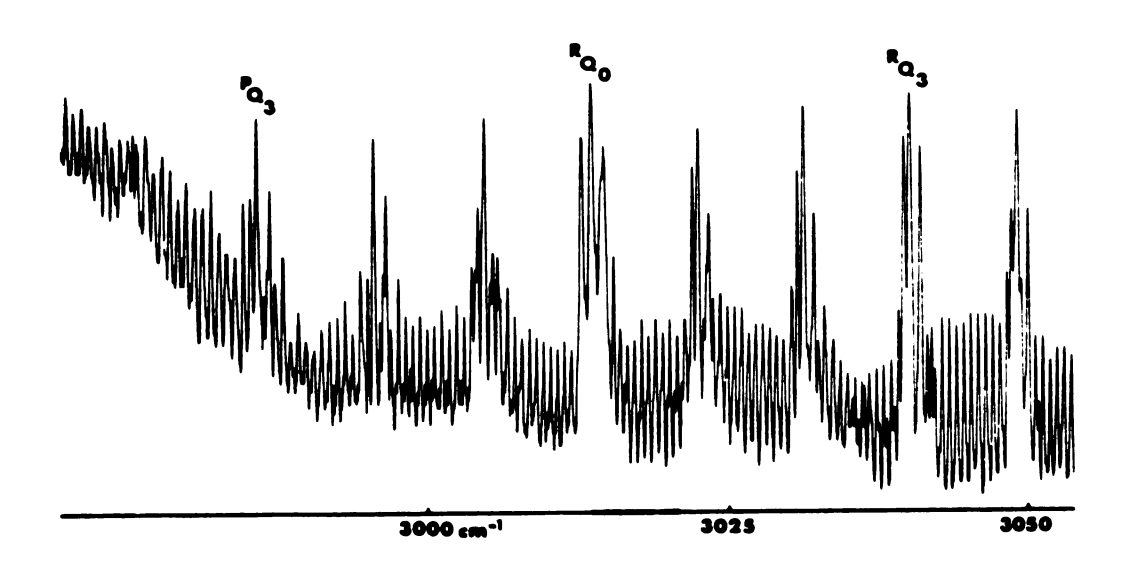
Calibrated Gases: HC1(1-0)

HCN(001)

Standard Deviation

of Calibration: 0.0055 cm⁻¹

Resolution Limit: ~0.032 cm⁻¹



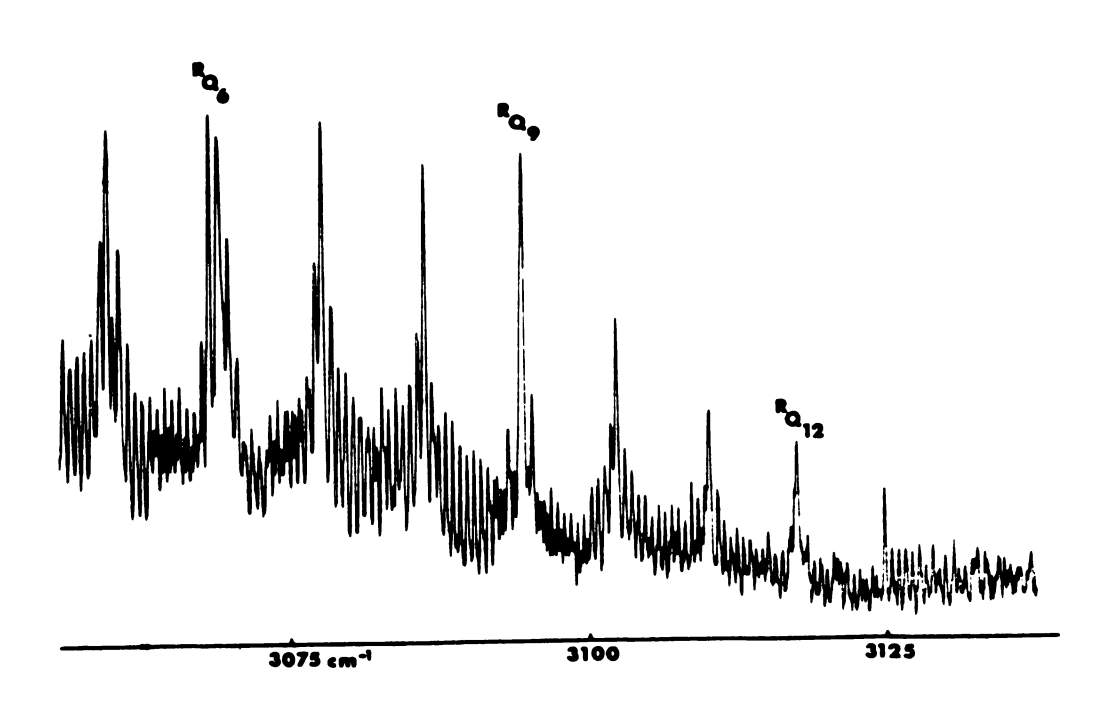


Figure 5.1 Survey spectra of the $\nu_{5}^{}$ band of $\mathrm{CH_{3}CN}_{.}$

for abse

1712

teit tric

itae subl

111

18 °

313

Sub

ii:

03

of in

ii

li (z

97

t

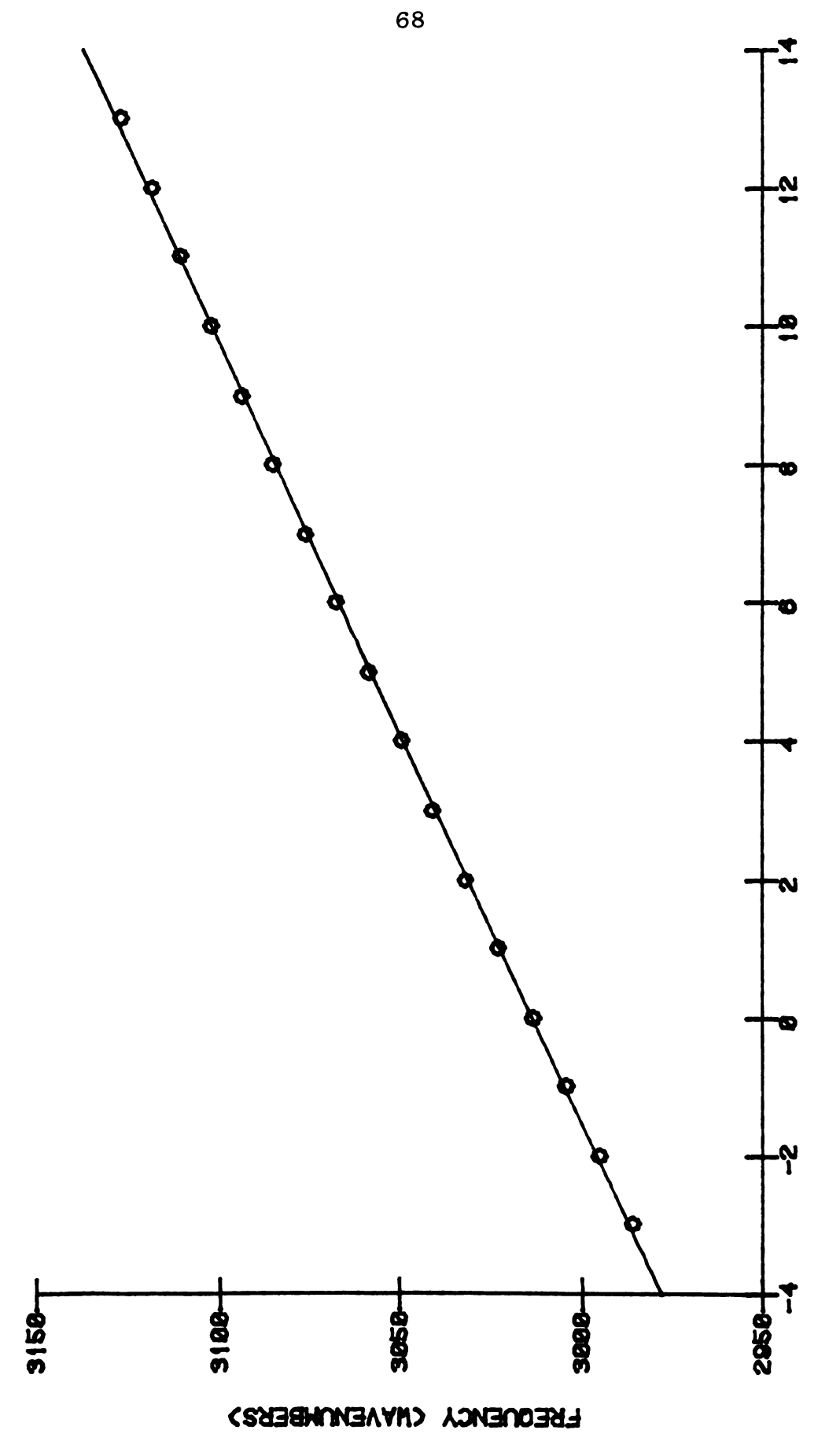
ì

-2

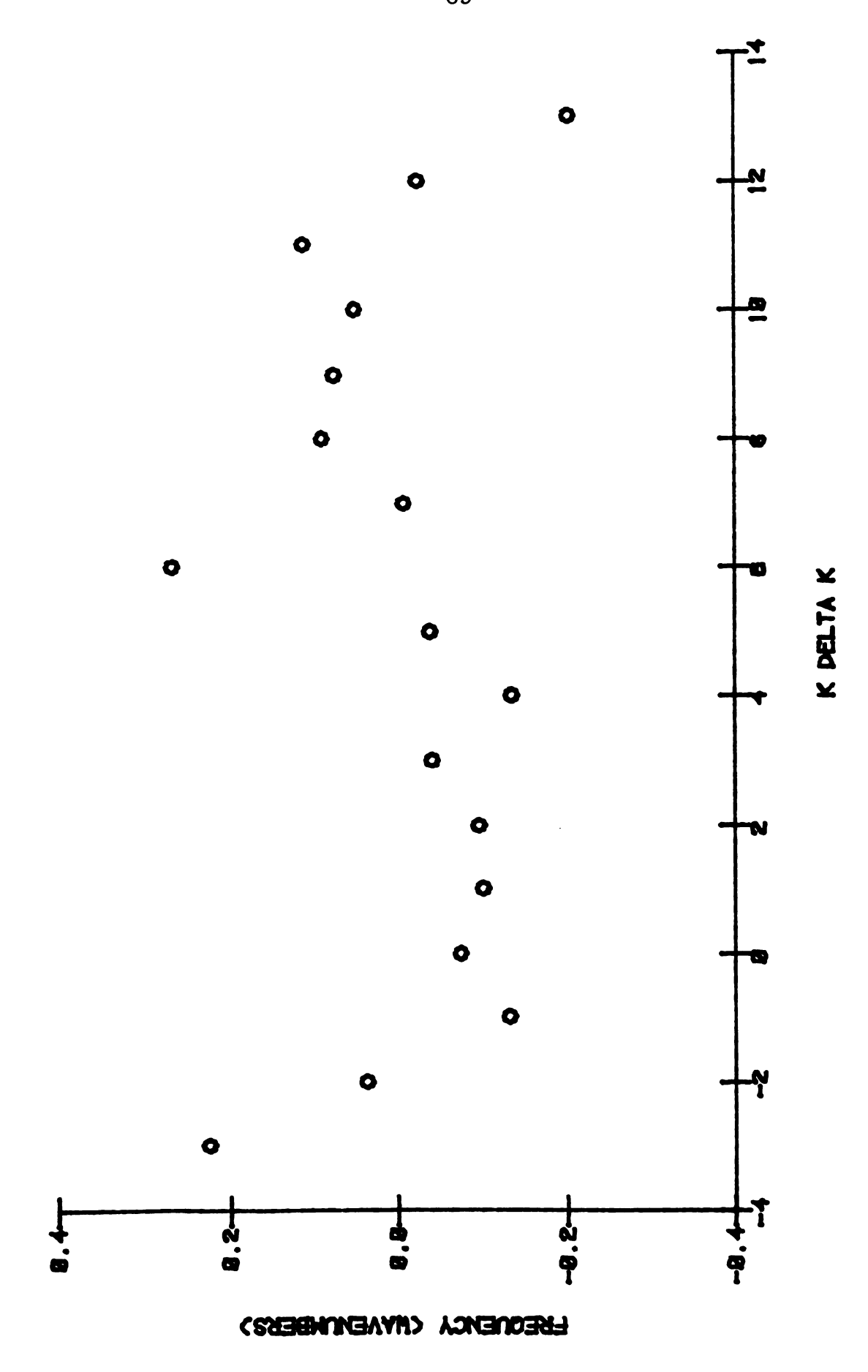
for $\Delta J=1$, while the J=1 through J=4 transitions are absent for $\Delta J=-1$. These criteria provide a check on Q branch assignments as well as on the P and R branch assignments. Subbands with K a multiple of three are theoretically twice as intense as subbands with K not equal to 3n for CH₃CN due to C_{3v} symmetry and nuclear spin statistics. Within a subband, the transitions having $\Delta K=\Delta J=\pm 1$ are more intense than those having $\Delta K=-\Delta J=\pm -1$; this advantage becomes greater as K increases. Herzberg (44) gives an excellent illustration of the relative positions and intensities of the transitions in a perpendicular band of a symmetric top molecule, both by subbands and the whole band.

The fitting routine SYMFIT (28) only fits the unperturbed subbands of symmetric top molecules. Thus to obtain a good fit, all subbands that are perturbed must be excluded from the whole band fit.

There are several aids to help recognize perturbed subbands or misassigned lines. A plot of the approximate position of the Q branches (I used the sharp high frequency side of the Q branch whenever possible) versus KAK provided an initial approximate indicator of perturbed subbands (Fig. 5.2). If the Q branches are fit to a quadratic in K, the residuals (measured - calculated) can be plotted (Figure 5.3) to show the Q branch plot on a more sensitive scale. It seems evident from the Q branch fit that the subbands $K\Delta K = -3$, -2, 6, 12, and 13 should be regarded with some suspicion. The single band frequency expression (Table 2.5) with the



O BRANCH POSITIONS OF NUS OF CHOCN VERSUS K DELTA K Figure 5.2



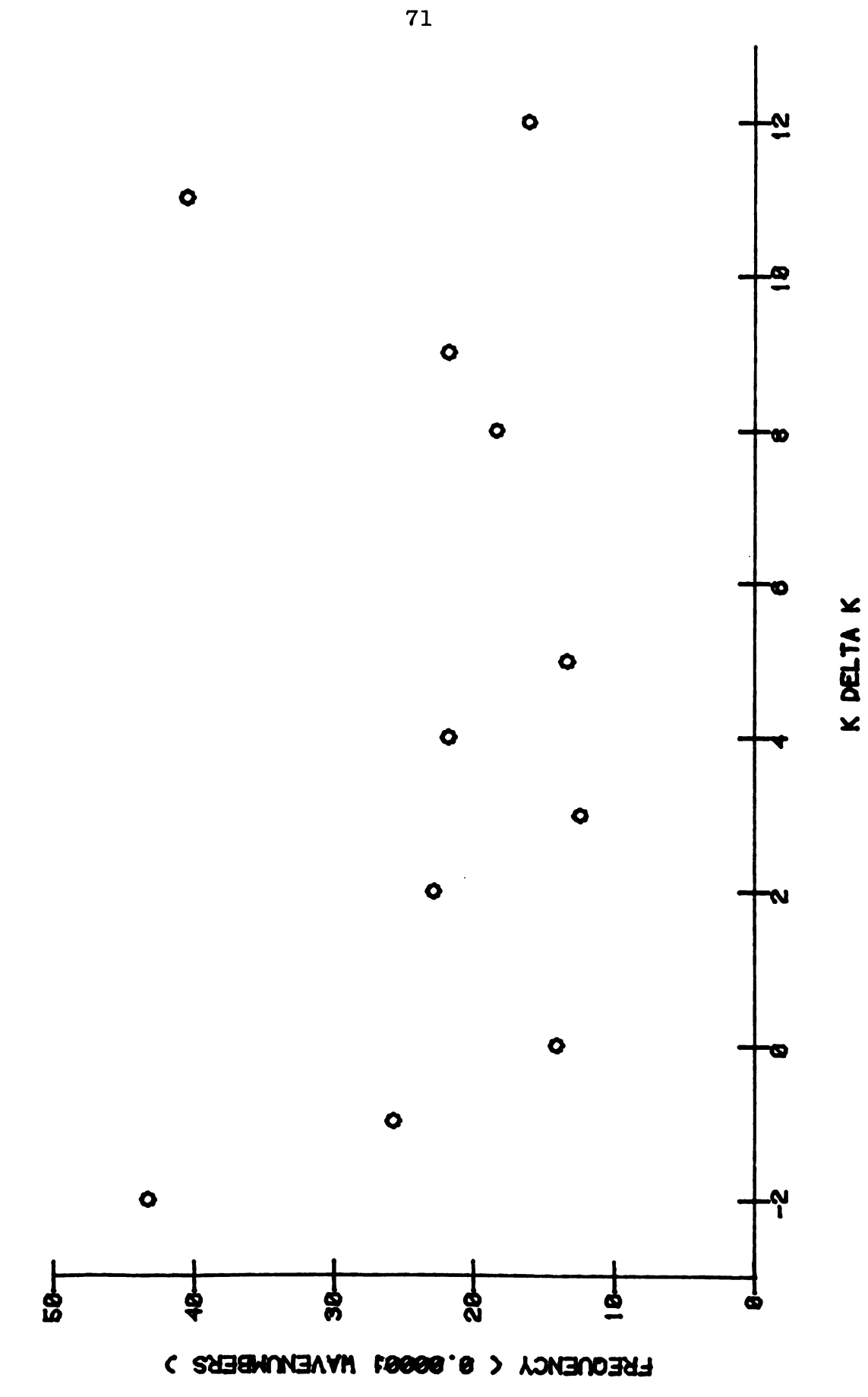
RESIDUALS to BRANCHES MINUS QUADRATIC FITS FOR NUS OF CHSCN Figure 5.3

appropriate quantum dependencies can be used to fit the Q branches. The Q branch fit of ν_5 of CH₃CN was also useful as an approximate indicator of which subbands might be perturbed and to calculate an approximate value for α_5^B . Unfortunately, most of the Q branches for K Δ K < 0 are obscured by the strongly absorbing parallel band ν_1 , so this method was of limited use.

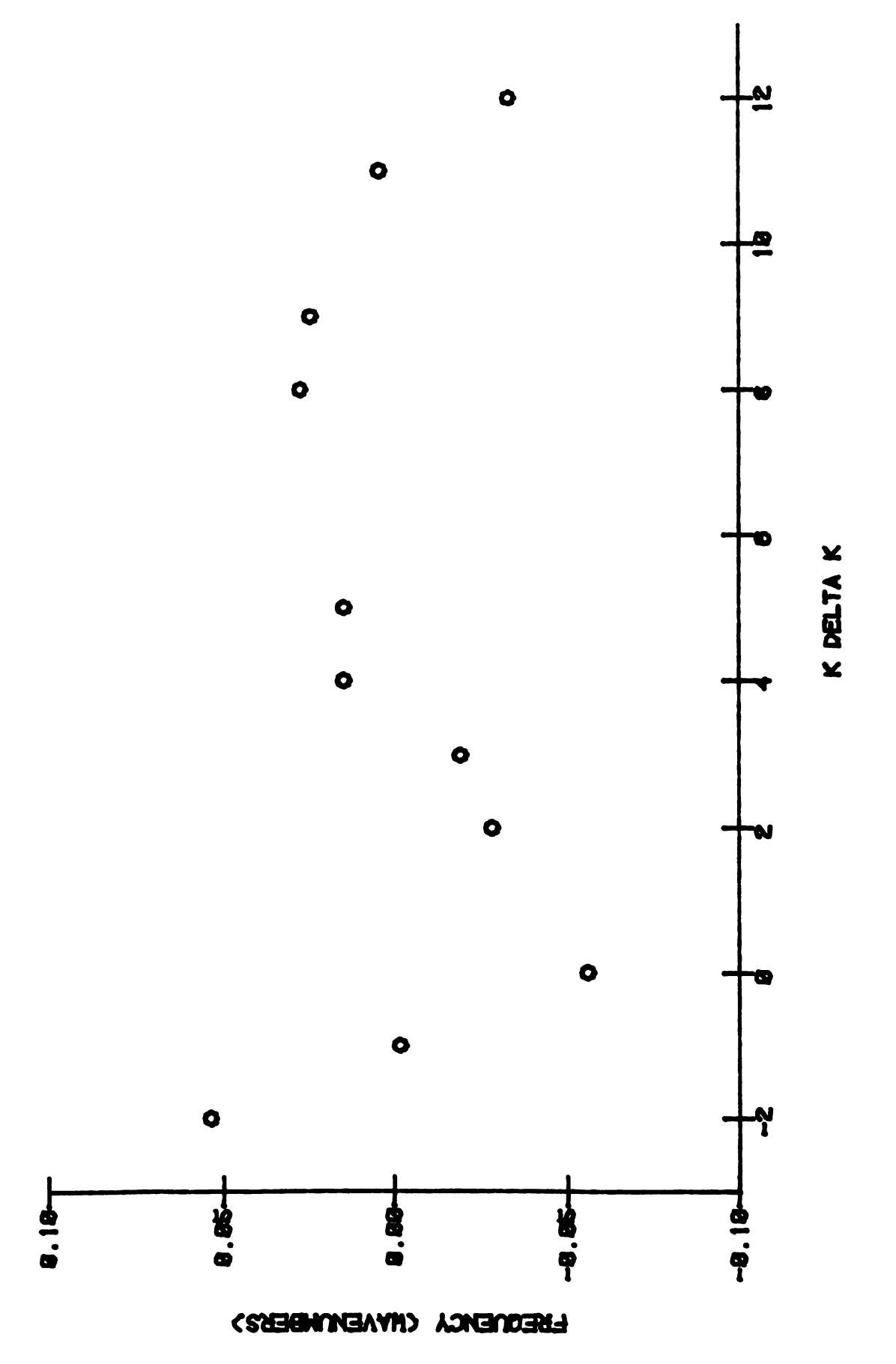
Subband fits can also reveal perturbed subbands and poorly fitting lines. A subband fit provides a calculated value for α_5^B and the subband origin for each subband, which are plotted versus $K\Delta K$ to provide a more sensitive indicator of perturbed subbands (Figures 5.4 and 5.5 respectively). These plots add $K\Delta K$ = 11 to the list of subbands to carefully consider before including in the final fit to determine constants.

Comparing the calculated frequency of a line with the measured frequency also gives some indication of the fit of the line as well as the assignment. This comparison can be done with either a subband fit or a whole band fit. The better the Hamiltonian parameters are known, the more confidence one has in the assignments and the fit. Thus, the subband and whole band fits are done in an iterative fashion, using the results from a previous fit to guide the new fit.

In a manner similar to that of the subband fit, the whole band fit can also be used to reveal perturbed subbands. Q branch positions and subband origins can be calculated, then compared to the measured values of Q branch positions and subband origin positions to reveal any perturbations.



ALPHA-B YERSUS K DELTA K FOR NUS SUBBAND FITS OF CHSCN Figure 5.4



RESIDUALS (CALCULATED - QUADRATIC FIT) OF SUBBAND ORIGINS VERSUS K DELTA K Figure 5.5

		:
		:
		:
		!
		26

Determining perturbed subbands and poorly fitting lines is an iterative process, as previously stated. SYMFIT was run 40 to 50 times before obtaining satisfactory values for the parameters of v_5 of CH₃CN. Even then, some parameters like A_0 - $A_e \zeta$, D_0^k , and α_5^A for v_5 of CH₃CN can remain highly correlated. More data, better data, or an alternate method must be used to better separate the effects of these parameters. For the aforementioned example, α_5^A was determined from a fit of the Q branches of $2v_5$. Decoupled parameters, such as α_5^A , are not varied in SYMFIT, then, until the final fit, if at all.

The results of the whole band fit were disappointing, however. The subband fit showed that the subbands fit very nicely individually, but the whole band fit was poor.

Weighting Scheme

Examining the outputs from whole band fits suggested a possible means of improvement in the analysis, viz., by using a revised method of assigning relative weights to the transitions. The primary criteria for assigning initial weights were the line shape and intensity, admittedly qualitative criteria. Some additional criteria were needed to better quantify the weighting scheme.

Ground state combination differences had been used to check line assignments and to make further assignments.

This suggested a modified weighting scheme, in particular, weight the transitions according to the reasonableness of

the measured frequency. To check the reasonableness of the measured frequency, the customary ground state combination differences for CH₃CN were used, viz.,

$${}^{\Delta K} R_{K}(J) - {}^{\Delta K} Q_{K}(J+1) = {}^{\Delta K} Q_{K}(J) - {}^{\Delta K} P_{K}(J+1) =$$

$$2(B_{O} - K^{2} D_{O}^{JK})(J+1) - 4D_{O}^{J}(J+1)^{3}$$

where B_0 , D_0^{JK} , and D_0^{J} are microwave constants (45). Given a measured value of the P or R branch lines of a particular subband, the expected locations of Q branch lines can be calculated without much loss of accuracy since the values for ground state microwave constants are orders of magnitude more accurate than our frequency measurements. branch lines are then plotted versus J(J+1) and should fit a straight line with a slope of $-2\alpha_5^B$ and an intercept of v_0^{sub} (the subband origin), neglecting higher order terms. A reasonable line is drawn through these data points accompanied by a reasonable error region (±0.010 to 0.020 cm⁻¹, see Figure 5.6) such that any data points falling outside this region are excluded from the least squares fits. residuals (measured - calculated) are then put into bins and assigned weights according to the magnitude of the residual. The following scheme was used in this study:

ROSCUS OF NUE OF CHECK CALCULATED FROM P AND R BRANCH LINES Figure 5.6

`

Fo ik

> re: by

7e Ch

it ex

p)

re ne

C)

b; Te

0;

$bin (cm^{-1})$	weight
.000002	8
.002004	4
.004006	2
.006008	1
.008012	. 5
.012016	. 25
.016024	.13
.024032	.06

For the most part, as the worst residual in the range doubles, the weight quarters. The weight of a spectral line whose residual lies on the border between two bins is determined by line shape and intensity.

One would argue that a plot of the P or R branch lines versus J would yield similar information. To some extent this argument is valid. Figure 5.7 shows a typical subband plot of $^RR_3(J)$ and $^RP_3(J)$ versus J. From Figure 5.7 only, it is not obvious that there are any lines that should be excluded from a fit to determine weights. To examine this in more detail, these data were fit to straight lines. The resulting calculated frequencies were subtracted from the measured frequencies and plotted versus J, as in Figure 5.8. Clearly, the poorly fitting lines are now easier to exclude by examining a plot of the residuals before determining line weights. The disadvantage to this method is that the plot of the measured frequencies versus J is not, in principle,

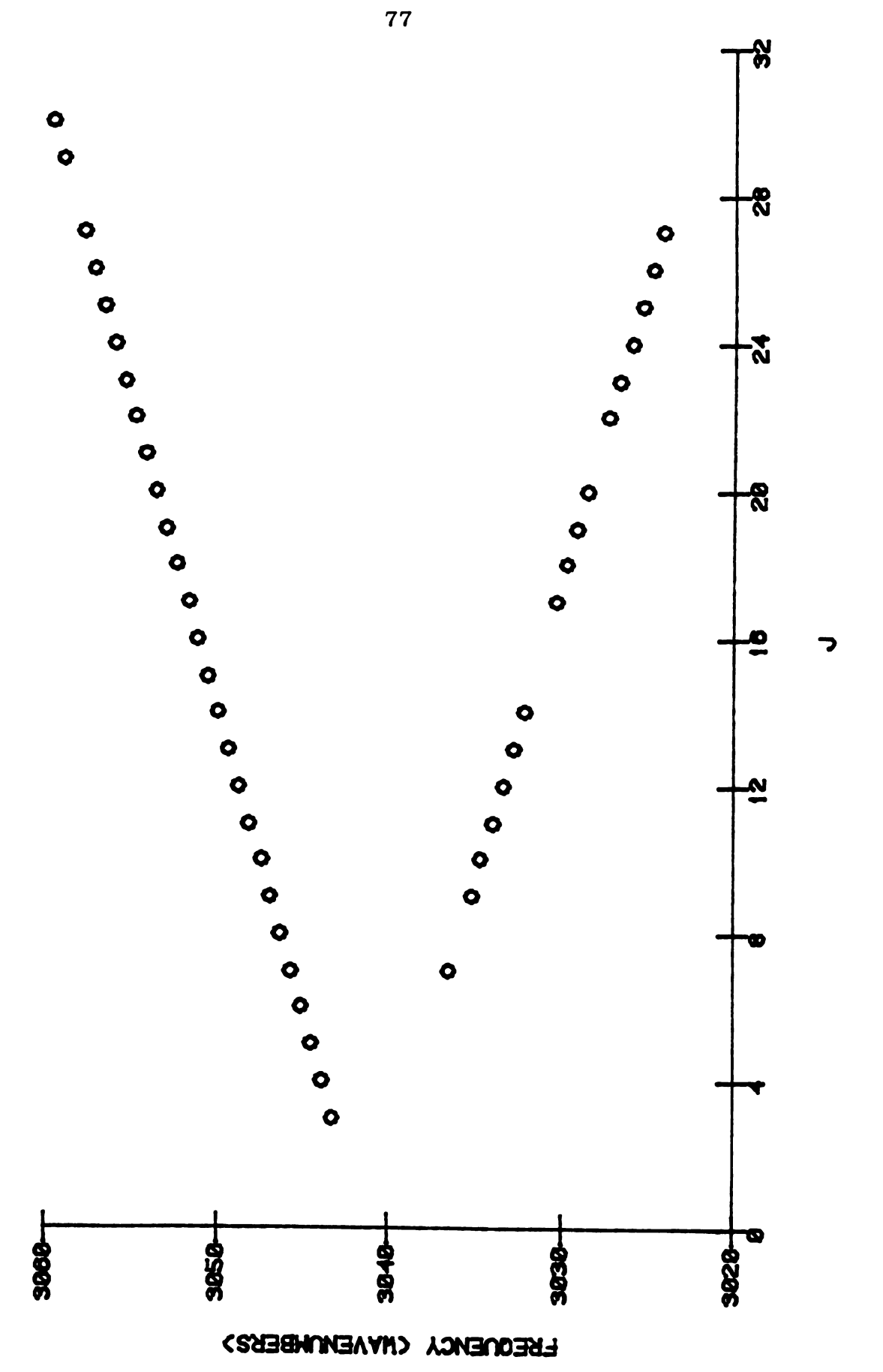
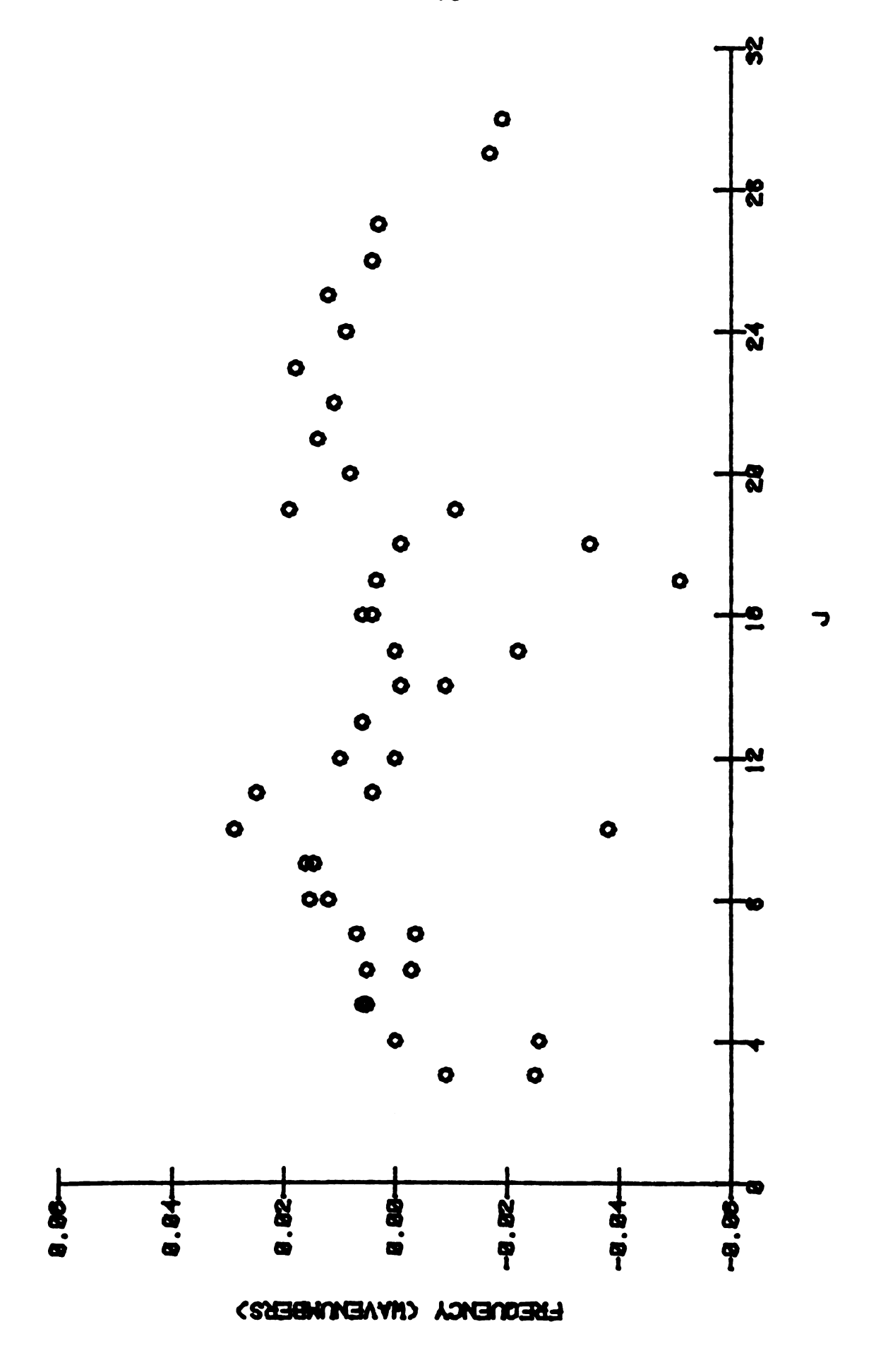


Figure 5.7 RR3(J) AND RP3(J) VERSUS J FOR NUS OF CH3CN



RESIDUALS FROM LINEAR FITS OF RRSCJJ AND RPSCJJ VERSUS J FOR NUS OF CHSCN Figure 5.8

a straight line. To discern anything but a straight horizontal line in the residuals is more difficult, making the task of assigning weights less accurate.

Futhermore, the perturbed subbands, such as the $K\Delta K=6$ subband, are more difficult to see from a plot of ${}^RR_K(J)$ or ${}^RP_K(J)$ versus J (Figure 5.9), than from a plot of the residuals (Figure 5.10) obtained by fitting a line to the data in Figure 5.9.

The residuals of either method are of comparable magnitude, however, and either method of calculating weights may be only of small benefit if the calculated weights are changed substantially. Some are of the opinion that weights should be changed to improve the fit until there is no longer an apparent change in the fit. The weights in this study were changed by no more than two bins to improve the fit, and then only if justified by the line shape and intensity. The justification for a change in weight at all is that there is some uncertainty involved in measuring the line position, especially for incompletely resolved lines. For bins having a small range (near zero residuals), any error at all can easily change a weight by two bins. For bins having a large range, there is so much uncertainty already that if line shape and intensity warrant, changing the weight by a relatively small amount can easily be justified. These guides have been strictly adhered to in this study.

It should also be noted that ground state combination differences work best for unperturbed subbands and some

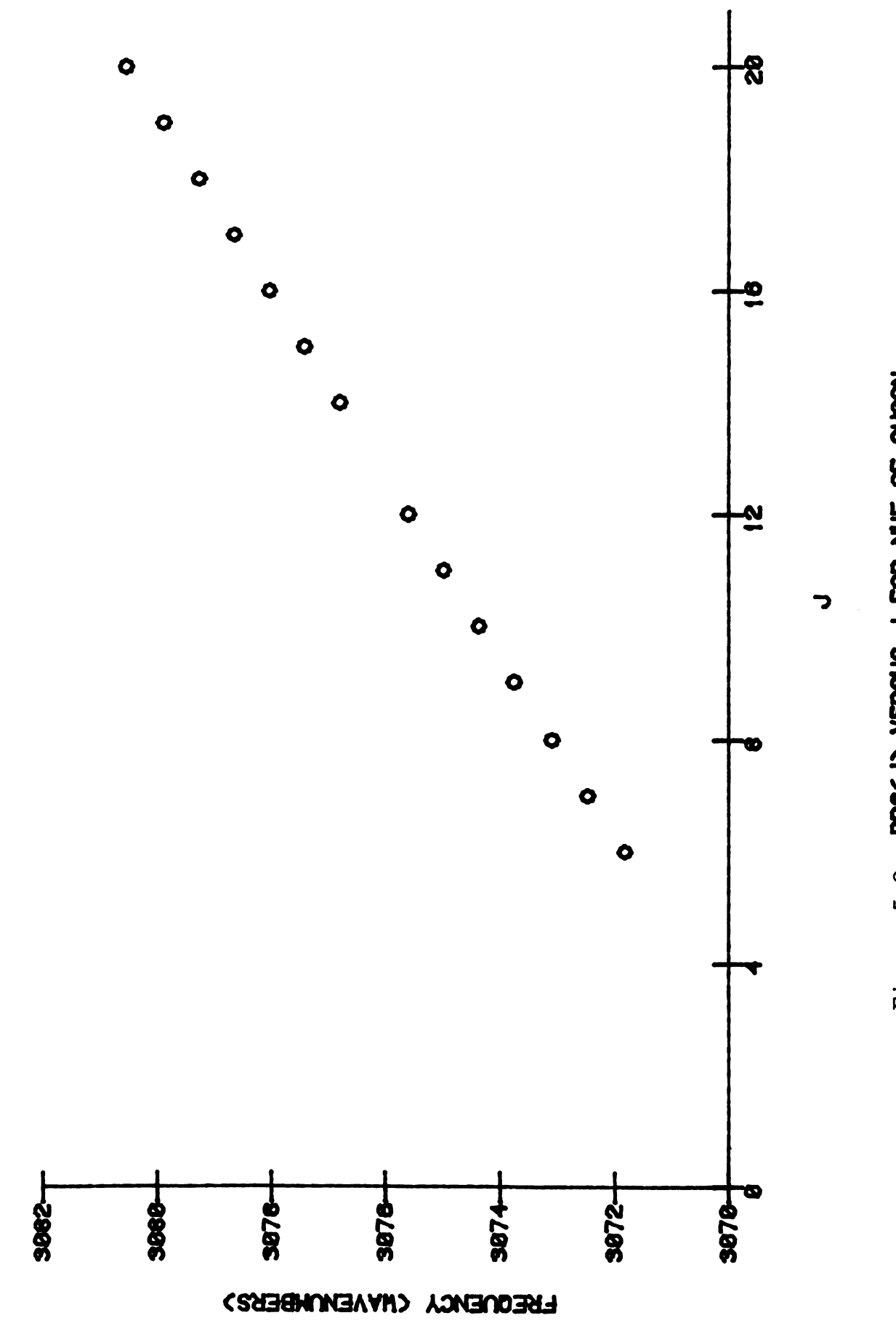
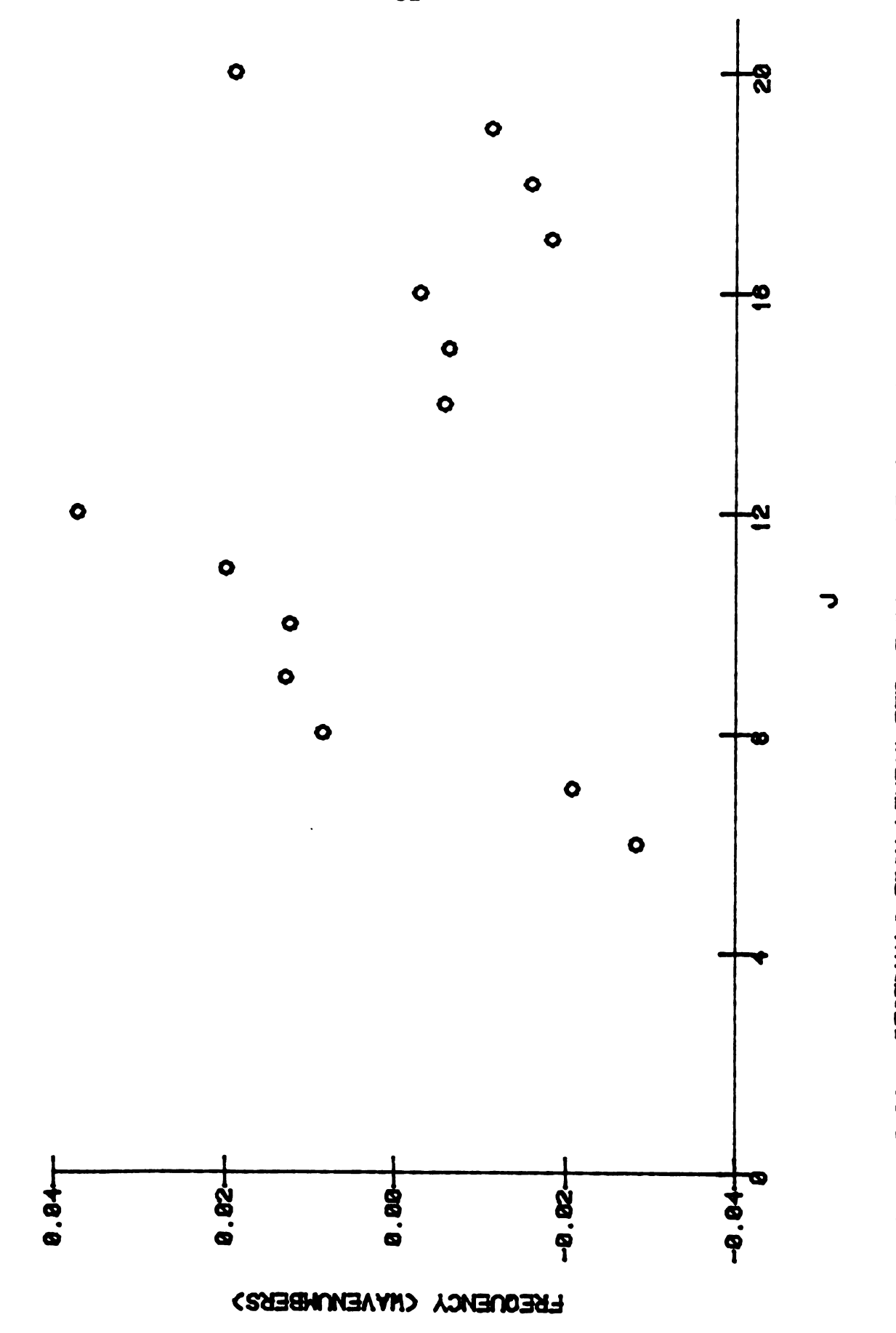


Figure 5.9 RR6CJ) VERSUS J FOR NUS OF CHSCN



RESIDUALS FROM LINEAR FIT OF RROCJO VERSUS J FOR NUS OF CHSCN Figure 5.10

perturbed subbands. Should a perturbation transform the Q branch plot into a smoothly varying line, for example, the ground state combination difference method could still be used.

Results

Utilizing the methods described in this chapter, the molecular constants for v_5 of CH_3CN were determined from a single band fit of 160 lines from the $K\Delta K = 0,2,3,4,5,8$, and 9 subbands. These constants are compared in Table 5.2 with the constants obtained from a single band fit by Barnett (34). Most of the uncertainties in the present study are smaller than those given by Barnett. In addition, two more parameters were determined in the present study.

The 95% simultaneous confidence interval (95% SCI) given in Table 5.2 can be found in many statistics texts. John Boyd (46) has a nicely written section that describes the method used at the M.S.U. I.R. lab. Boyd describes the 95% SCI as approximately $\sqrt{2p}^{7}\sigma$, where p is the number of parameters varied to obtain the standard deviation of the fit, σ is the standard deviation of the parameter, and 2 is an approximation to $F_{0.975}(p,n-p)$, F being the F distribution of reference (46) and n the number of data points.

The analysis of the parallel and perpendicular components of $2\nu_5$ and the simultaneous fit of ν_5 and $2\nu_5$ of CH₂CN will be presented in Chapter VI.

Table 5.2 Single Band Fit of v_5 of CH_3CN

(A) All parameters allowed to vary

Parameter	Barnett	Bardin
ν _o	3008.697(15)	3008.7183(59)
$A_o - A_e^{\zeta}$	4.96707(67)	4.9606(18)
$\alpha_5^A + \dots$	0.0323(22)	0.0301(10)
$\alpha_{5}^{\mathbf{B}}$	0.54(32)E-4	1.93(56)E-4
$eta_{f 5}^{f K}$	-0.27(11)E-4	-0.52(21)E-4
$\mathbf{H}_{\mathbf{O}}^{\mathbf{k}}$		0.77(41)E-8
Std. Dev. of Fit	0.009	0.0052

(B) α_5^A and α_5^B constrained to values consistent with simultaneous fit of ν_5 and $2\nu_5$, Q branch fit, and parallel component fit.

Parameter	Barnett	Bardin
ν _o	3008.697(15)	3008.7142(61)
$^{A}o^{-A}e^{\zeta}$	4.9607(67)	4.9606(18)
$D_{\mathbf{O}}^{\mathbf{k}}$		1.04(57)E-4
$\alpha_5^A + \dots$	0.0323(22)	0.02891(63)*
$\alpha_{5}^{\mathbf{B}}$	0.54(32)E-4	1.27(10)E-4*
$eta_{f 5}^{ m K}$	-0.27(11)E-4	-0.49(18)E-4
${\tt H}_{{\sf O}}^{f k}$		0.77(41)E-8
Std. Dev. of Fit	0.009	0.0056

^{*}These were known from two independent fits and thus held constant here.

CHAPTER VI

THE ANALYSIS OF THE 2v5 BAND OF CH3CN

Introduction

The $2\nu_5$ band of CH₃CN is the first overtone of the vibrational normal mode of ν_5 . The ideal model of $2\nu_5$ would vibrate at twice the rate of ν_5 , and in practice this is nearly so. The vibrational angular momentum for ν_5 is $\ell_{\nu_5} = 1$ or $\Delta \ell_{\nu_5} = \pm 1$, while for $2\nu_5$, $\ell_{2\nu_5} = 2$, or $\Delta \ell_{2\nu_5} = \pm 2$. This not only allows for a perpendicular component $\Delta \ell = \pm 2$, but also for a parallel component, $\Delta \ell = 0$.

To date, the previous work on $2v_5$ has been sparse. Venkateswarlu (41) determined that $2v_5$ (parallel and perpendicular) occurred near 5972 cm⁻¹. Parker et.al. (42) were able to obtain $v_0 = 6006.99$ cm⁻¹, $\zeta_5 = 0.042$, $\zeta_{55} = -0.084$, $[(A'-A'')-(B'-B')] = -0.055\pm0.006$ cm⁻¹, and the g_{55} , X_{55}^0 , and ω_5^0 force constants. Parker et.al. also identified the parallel component of $2v_5$. T. L. Barnett (34) was able to study $2v_5$ at a resolution limit of about 0.2 cm⁻¹ and determined several rotational constants. Unfortunately, there were too few unperturbed subbands to obtain a good single band fit.

The $2\nu_5$ band is a weakly absorbing band, which probably accounts for the sparseness of literature. To obtain a sufficient number of unperturbed subbands, and thus avoid the problems Barnett had to contend with, the $2\nu_5$ band was signal averaged. Signal averaging had been effective on "dense" spectra and extending the averaging technique to include weak spectra seemed feasible.

Details of how the signal averaging technique was specifically applied to $2\nu_5$ will be presented in this chapter, as well as the analysis of the parallel and perpendicular components of the $2\nu_5$ band. Both components presented problems that will be addressed in this chapter. The results from a single band fit and a simultaneous fit of ν_5 and $2\nu_5$ will be compared to the results Barnett obtained. Appendix V contains the frequencies and assignments of the $2\nu_5$ band of CH_2CN .

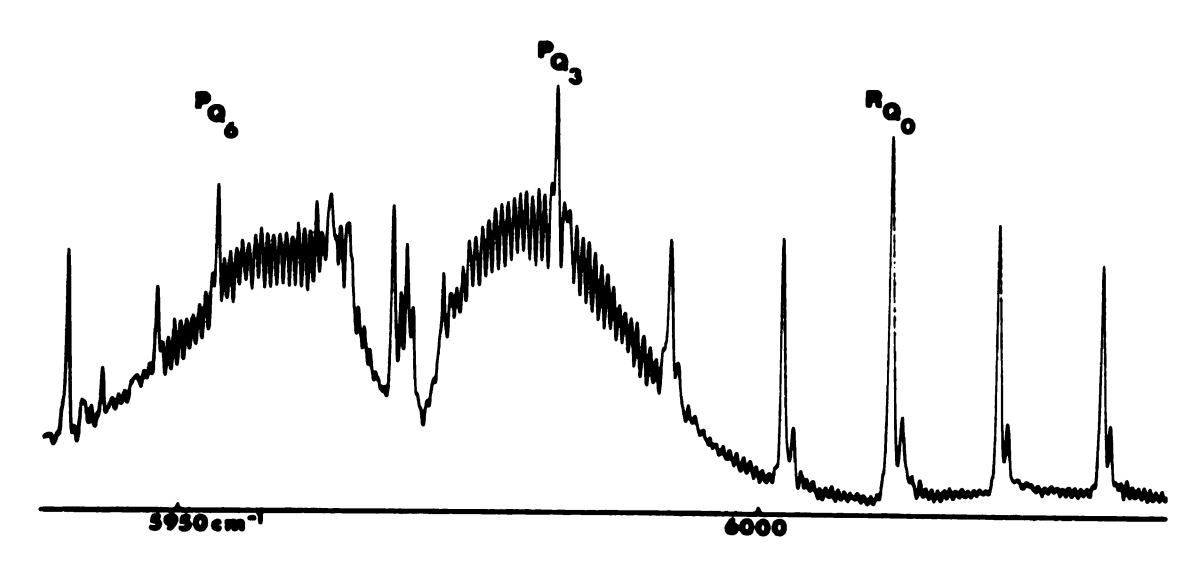
Procedures

The spectra of $2v_5$ of CH_3CN were recorded on the Michigan State University high resolution grating spectrophotometer under the experimental conditions listed in Table 6.1. Survey spectra of the region are shown in Figure 6.1.

The perpendicular component of $2v_5$ from 5988 cm⁻¹ to 6153 cm⁻¹ (P_{Q_2} to $R_{Q_{13}}$) was divided into about six equal regions. Each region was signal averaged, independent of the other regions. Each scan of a particular region was

Table 6.1 Experimental conditions used for the $2\nu_5$ band of ${\rm CH_3CN}$ data.

Region	5988-6153 cm ⁻¹
Pressure	10 - 15 torr
Path Length	15 meters
Detector	PbS @ 193K
Grating	600 lines/mm
Calibrated Gases	N ₂ 0(3,0,1)
	HCN(0,0,2)
Standard Deviation of Calibration	0.0059 cm ⁻¹
Resolution Limit	~0.055 cm ⁻¹



parallel component

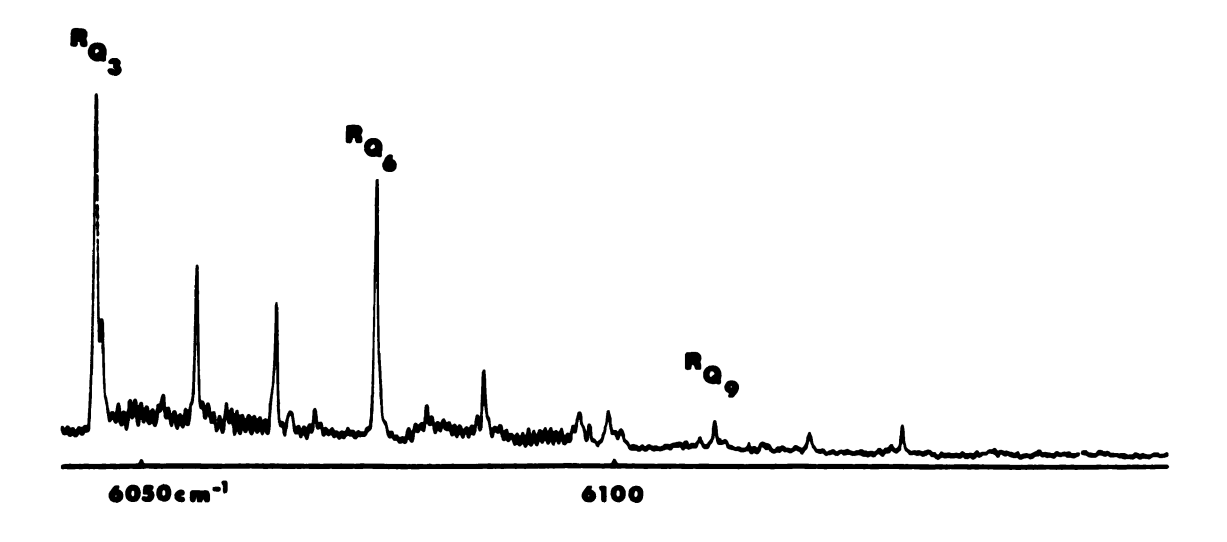


Figure 6.1 Survey spectra of the $2v_5$ band of CH_3CN .

linearized in the manner described in Chapter IV. To average effectively the scans must be properly aligned. To align the scans, the first scan was carefully examined and a suitable short segment was chosen as a trigger for other scans. The corresponding segment of each successive scan was then fit to this trigger using a least squares method to best align the scans. The scans were then summed and normalized appropriately for deconvolution.

The alignment method described above was not effective through R_Q. for the region that includes R_{Ω} single scan was compared to the average, there were many differences. Consequently, no assignments could be made. In an attempt to improve the results, an alignment scheme that had been previously considered was tried with great Several positions of peaks and valleys (for well resolved lines) distributed approximately evenly throughout the scan were selected from the first scan to serve as the triggering mechanism to align the remaining scans with the These same line positions from each successive scan were compared to the positions in the first scan, using the method of least squares, to determine the relative offset. In principle, several measurements of a line that changes its apparent position because of noise should give a good approximation to the "true" position of that line. Similarly, as the number of line positions (measurements) in a comparison of two scans increases, the error associated with measuring the relative offset between the two scans should

decrease. Based on the success of this one trial, this error assumption appears to be valid. There is an additional assumption implicit in all line measurement schemes; any systematic errors that are present in one region, are also present in all other regions, including the calibration run, and thus do not affect the frequency measurements. After aligning the scans, they were summed and normalized appropriately.

Assignments were subsequently made for $K\Delta K=10$ and 11. Unfortunately, none of the assignments were used in the final fit; either these subbands were perturbed or the triggering method was not successful. Barnett's data seems to support the argument that the subbands above $K\Delta K=8$ are perturbed. An analysis that includes perturbations would hopefully remove any doubts.

After signal averaging, the regions were deconvoluted to try to rid the spectra of the broadening effects of the instrument function. Although convolution is unique, deconvolution is not, and, at times the spectra were excessively deconvoluted. When this occurred, the original spectra were later deconvoluted in a slightly different manner in an attempt to acquire a more meaningful spectrum.

The parallel component frequencies and the Q branch frequencies were taken directly from the calibration run and were neither signal averaged nor deconvoluted.

Calibration

A secondary calibration method was necessary to calibrate the averaged spectra. The $2\nu_5$ calibration run consisted of two well known bands bracketing the $2\nu_5$ band of CH₃CN. The frequencies of $2\nu_5$ were obtained by interpolation between lines from N₂O(3,0,1) and HCN (0,0,2). These interpolated frequencies then calibrate the averaged spectra in a manner similar to that used in averaging the weak region of the spectrum (R_{Q10} to R_{Q13}).

For each region, a number of well resolved lines were selected, distributed approximately evenly throughout that particular region. The positions (in tape coordinates) of these well resolved lines were matched to their counter parts in the calibrated run via a weighted least squares fit. Once the relationship between the calibrated run and the uncalibrated averaged region had been determined, the remaining frequencies of the averaged region could be calculated.

Most of the region fit the calibrated run to between 0.002 and 0.006 cm⁻¹.

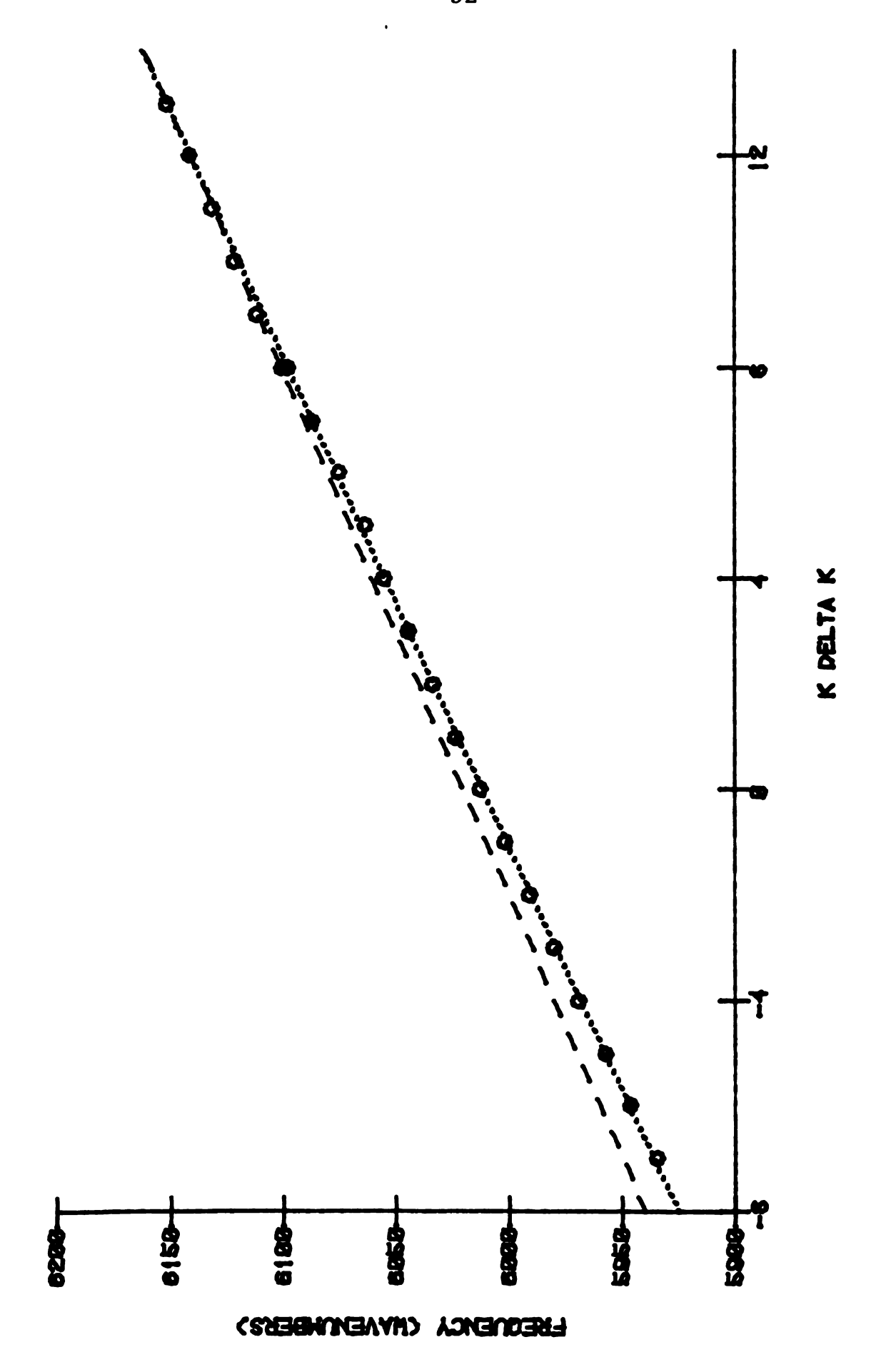
To provide some check of calibration between regions, each region overlapped neighboring regions by from three to four wavenumbers. Although it was thought at the time that this overlap would be sufficiently long, frequently there were not enough clearly resolved lines of high enough intensity to unambiguously provide this check.

Analysis

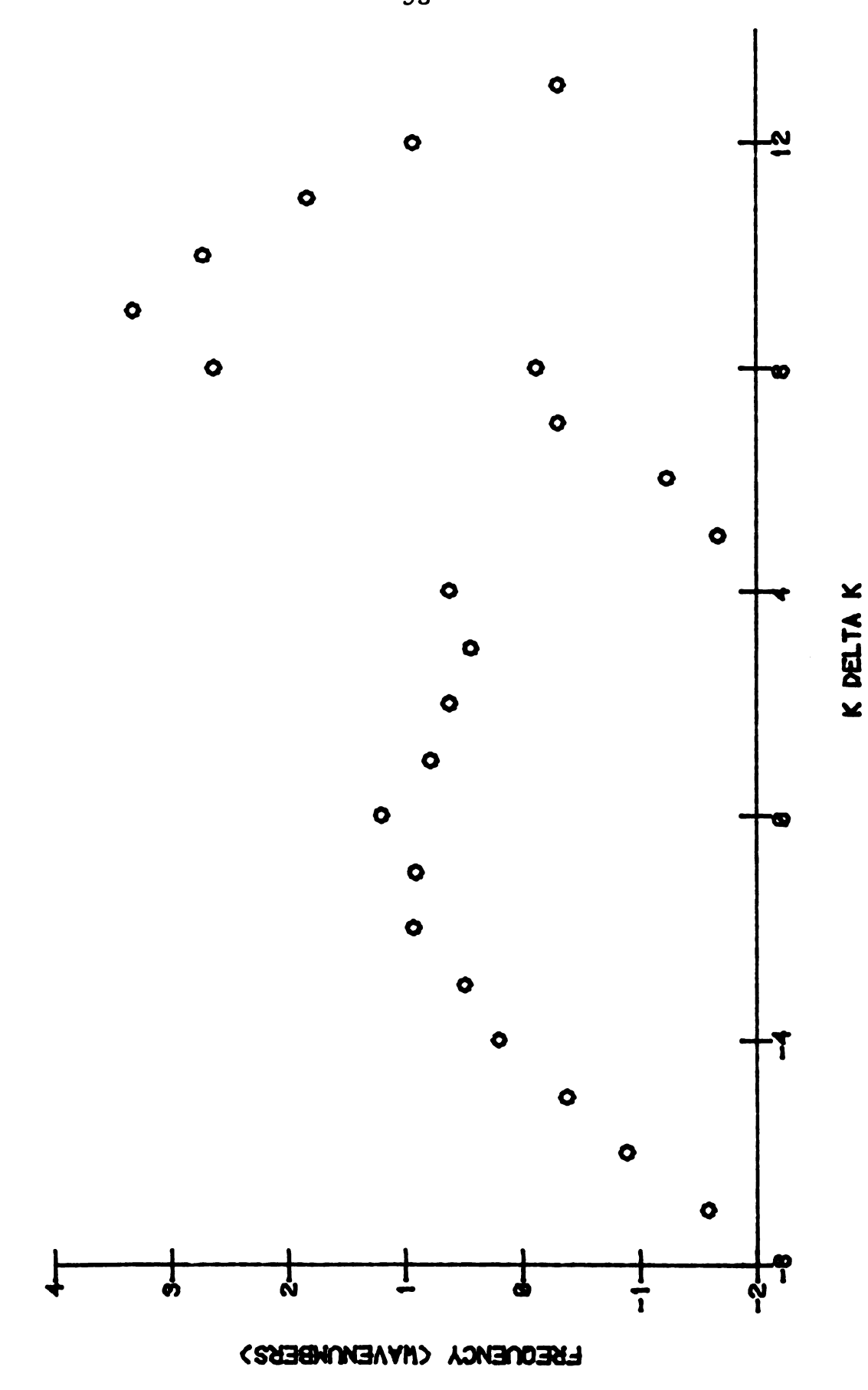
Barnett had made many transition assignments in the region $K\Delta K$ = -2 to 7 of $2\nu_5$ of CH_3CN , and, as with ν_5 , these were carefully checked. In addition to his assignments, this study enabled assignments to extend through $K\Delta K$ = 11, enabled Q branch assignments from -7 to 13, and to some extent facilitated the parallel component assignment.

The $2\nu_5$ band was analyzed in the manner described in Chapter V. Figure 6.2 shows the approximate Q branch positions plotted versus KAK, including both parts of R_{Q_8} . The effects of the pertubation near R_{Q_8} are shown by the splitting of the Q branch, illustrated by the two points at R_{Q_8} . Also shown in Figure 6.2 is a fit of the frequencies of the Q branches P_{Q_7} through P_{Q_8} versus KAK and a fit of P_{Q_8} through P_{Q_8} versus KAK. The two lines obtained from these fits are not parallel, but intersect at approximately KAK = 13 and illustrate the effects of the perturbation on the rest of the band. A plot of the residuals obtained from fitting all of the Q branches to a line (Figure 6.3) illustrates the perturbation even more dramatically, and further suggests another perturbation near P_{Q_8} .

A good guess at α_5^A can be obtained if only the unperturbed Q branches are included in a Q branch fit using SYMFIT. To determine which subbands were perturbed, plots of α_5^A versus KAK (Figure 6.4), subband origins versus KAK (Figure 6.5), and subband fits were used in addition to the information in Figures 6.2 and 6.3. The subband fits showed



O BRANCHES OF ENUS OF CHSCN VERSUS K DELTA K Figure 6.2



RESIDUALS FROM LINEAR FIT OF LOW K Q BRANCHES OF 2NUS OF CHSCN Figure 6.3

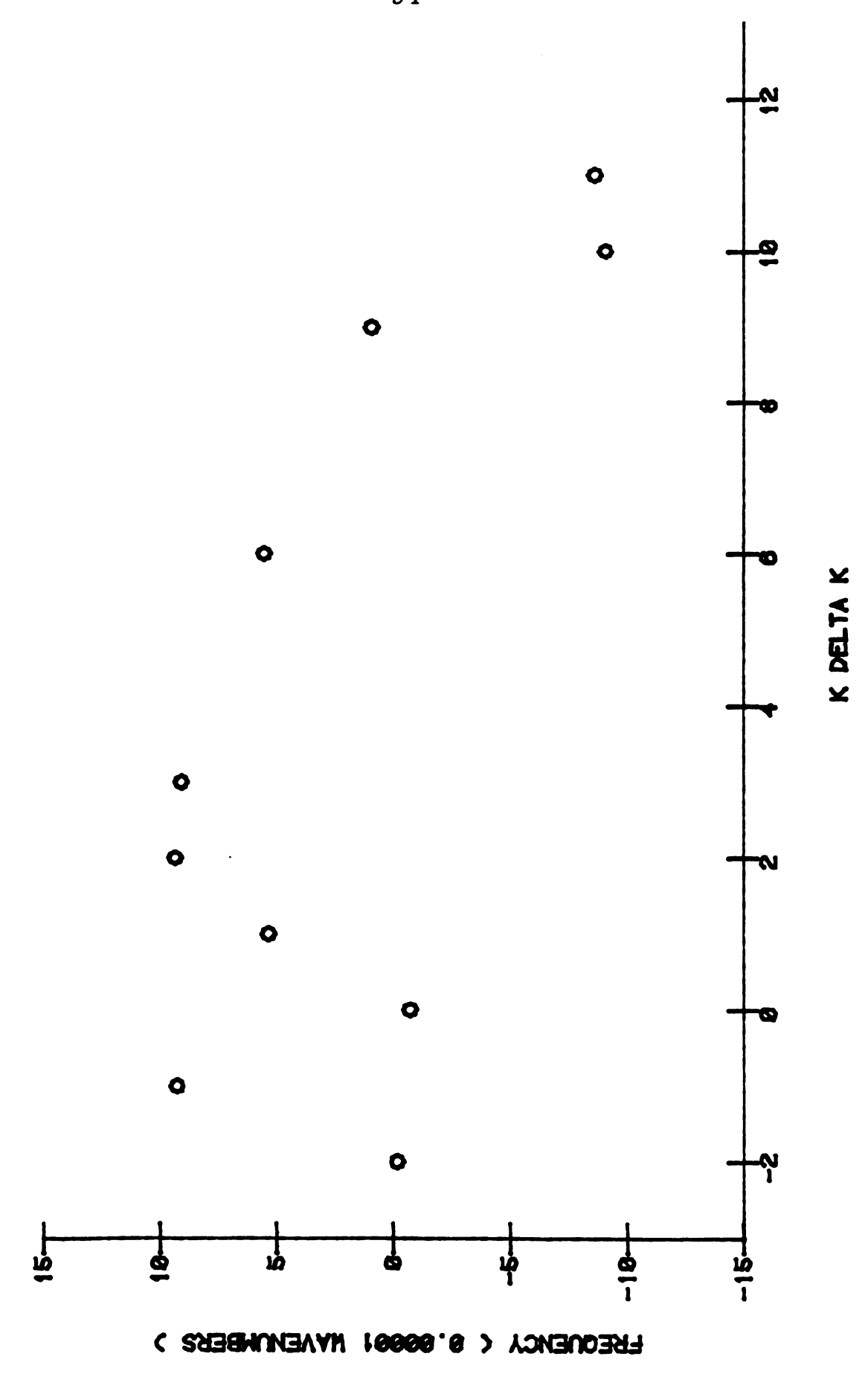


Figure 6.4 ALPHA-B VERSUS K DELTA K FOR 2NUS OF CH9CN

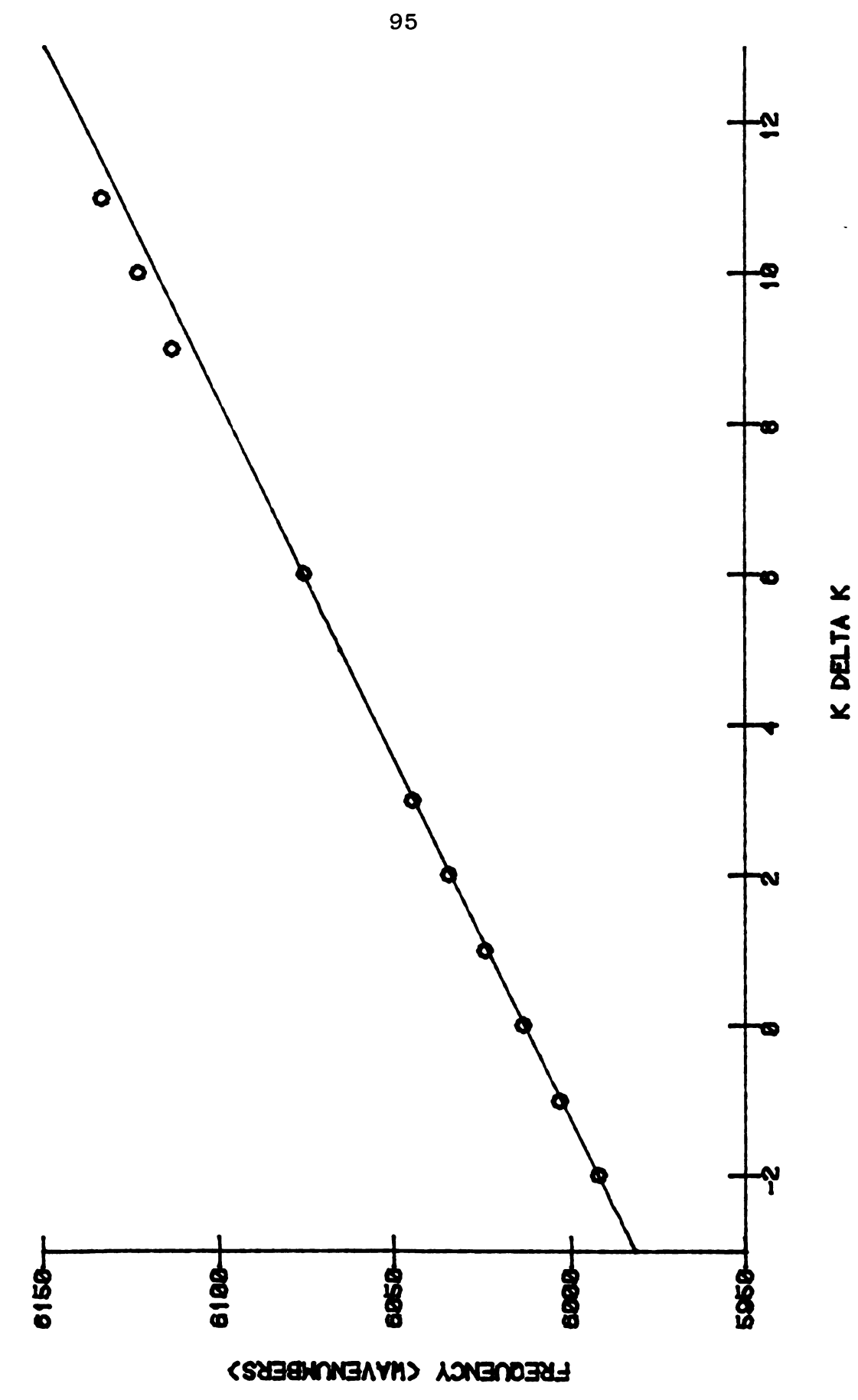
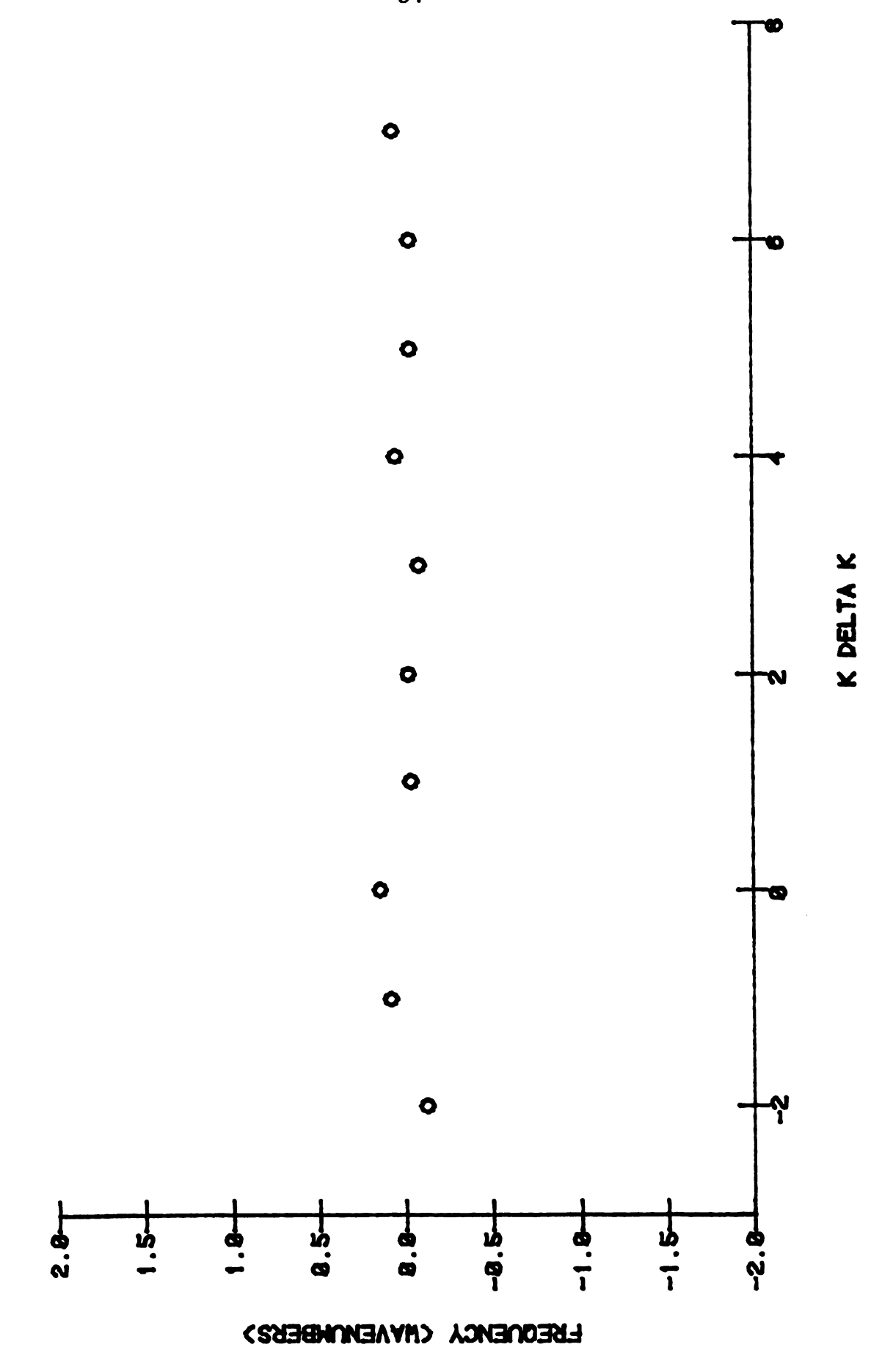


Figure 6.5 CALCULATED SUBBAND ORIGINS OF 2NUS OF CHECK VERSUS K DELTA K

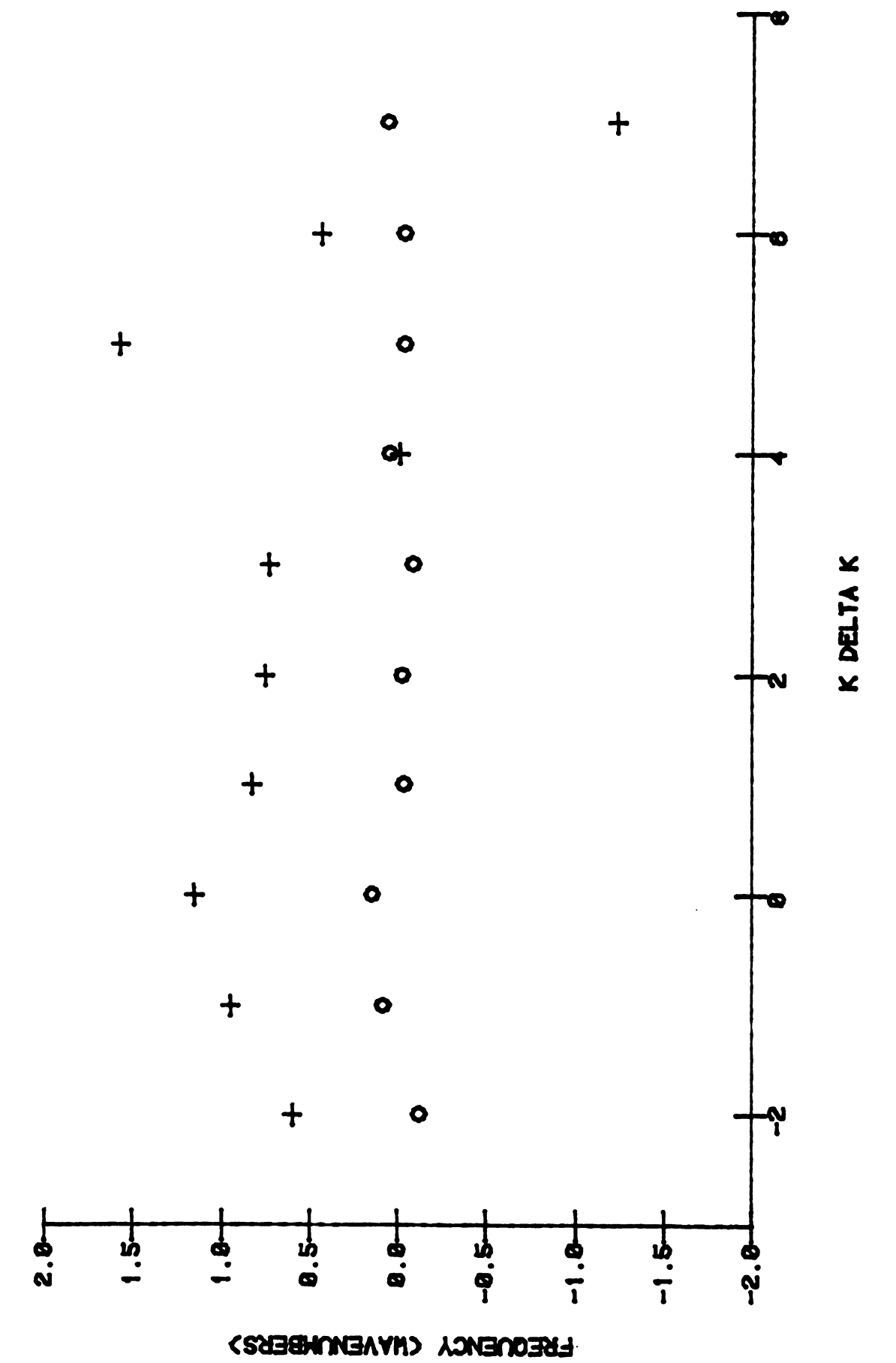
that each of the subbands were good fits and self-consistent. The α_5^B 's generated in these fits were plotted versus KAK but were not too helpful, probably because good values for $A_O + 2A_e\zeta$, D_O^K , and α_5^A were not yet available. The subband origins served to confirm the Q branch plots. When all subbands were included in the whole band fit, the fit was poor. Each subband suspected of being perturbed was excluded from the fit, one at a time, to see how the fit changed. Several possible combinations were tried, but still difficulties remained and the expected good fit did not occur.

In an effort to help determine perturbed subbands, we tried comparing the hot band line positions that occurred as a neighbor to the Q branches with the Q branches positions themselves to see how the relative positions changed. Figure 6.6 shows the hot band positions (minus a quadratic fit) versus $K\Delta K$ and indicates that the hot band in that region is less perturbed. Figure 6.7 shows the hot band position minus the nearest neighbor Q branch position. Notice that a straight line can be drawn through the subbands $K\Delta K = -1,1,2,3$, and 6, these are the subbands that were eventually chosen to comprise the "whole band" fit.

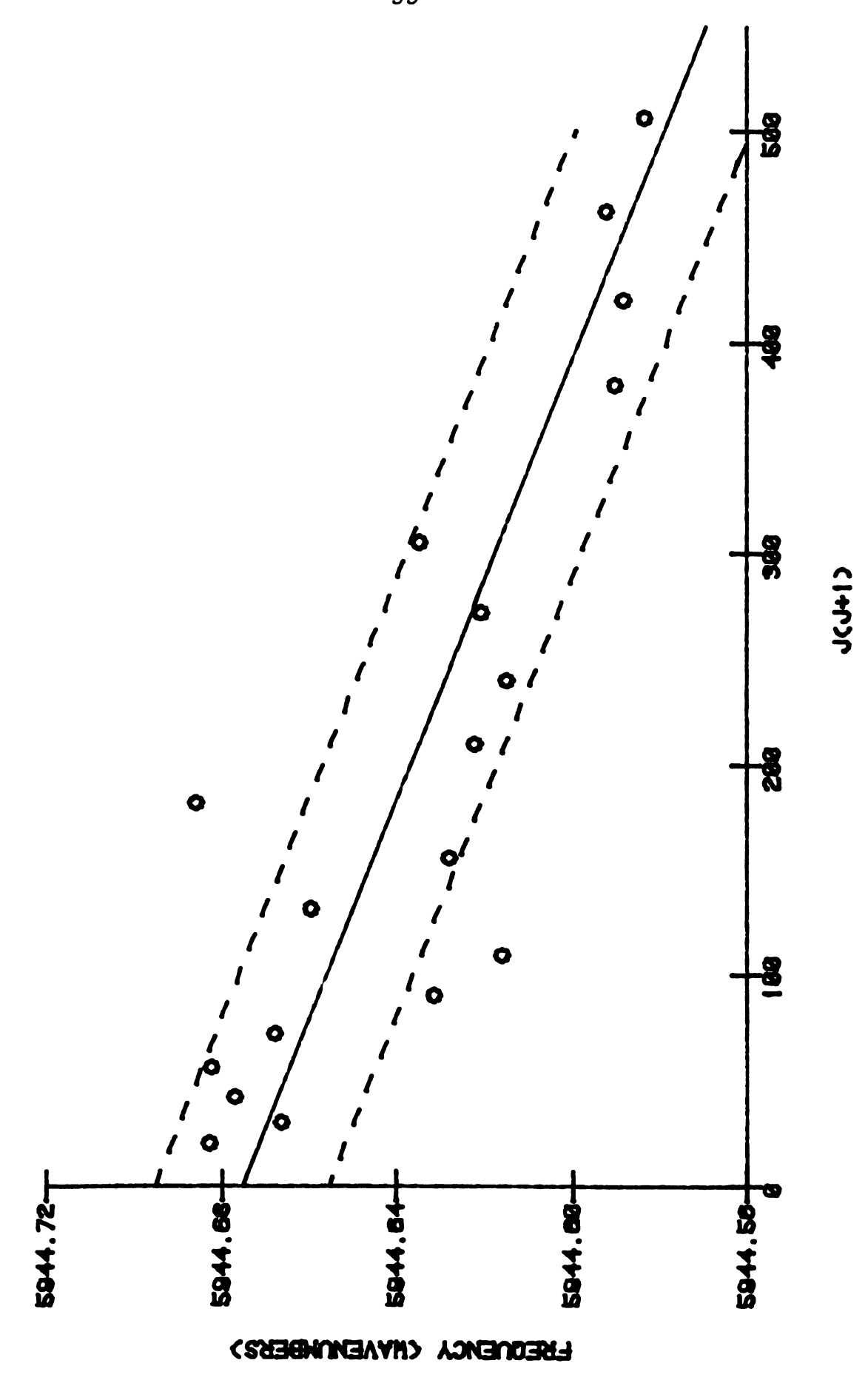
As with ν_5 , ground state combination differences (GSCD's) were used to assign weights to line positions for the whole band fit and were somewhat helpful for determining new transition assignments. Figure 6.8 illustrates a typical subband plot of calculated $R_{Q_3(J)}$ verus J(J+1) where the $R_{Q_3(J)}$ were calculated from the $R_{Q_3(J)}$ using GSCD's.



HOT BAND FREQUENCIES NEAR 2NUS OF CHOCK O BRANCHES MINUS QUADRATIC FIT Figure 6.6



HOT BAND FREQUENCIES MINUS Q BRANCH FREQUENCIES OF ZNUS OF CH3CN SUPERINFOSED ON FIBURE 6.6 Figure 6.7



ROSCUS OF ENUS OF CHECK VERSUS JOUR 13 Figure 6.8

Excluding the obviously non-fitting lines, fitting the remainder to a straight line, and then plotting the residuals verus J(J+1) (Figure 6.9) allows a quantitative weight assignment to the line position using the method described in Chapter V.

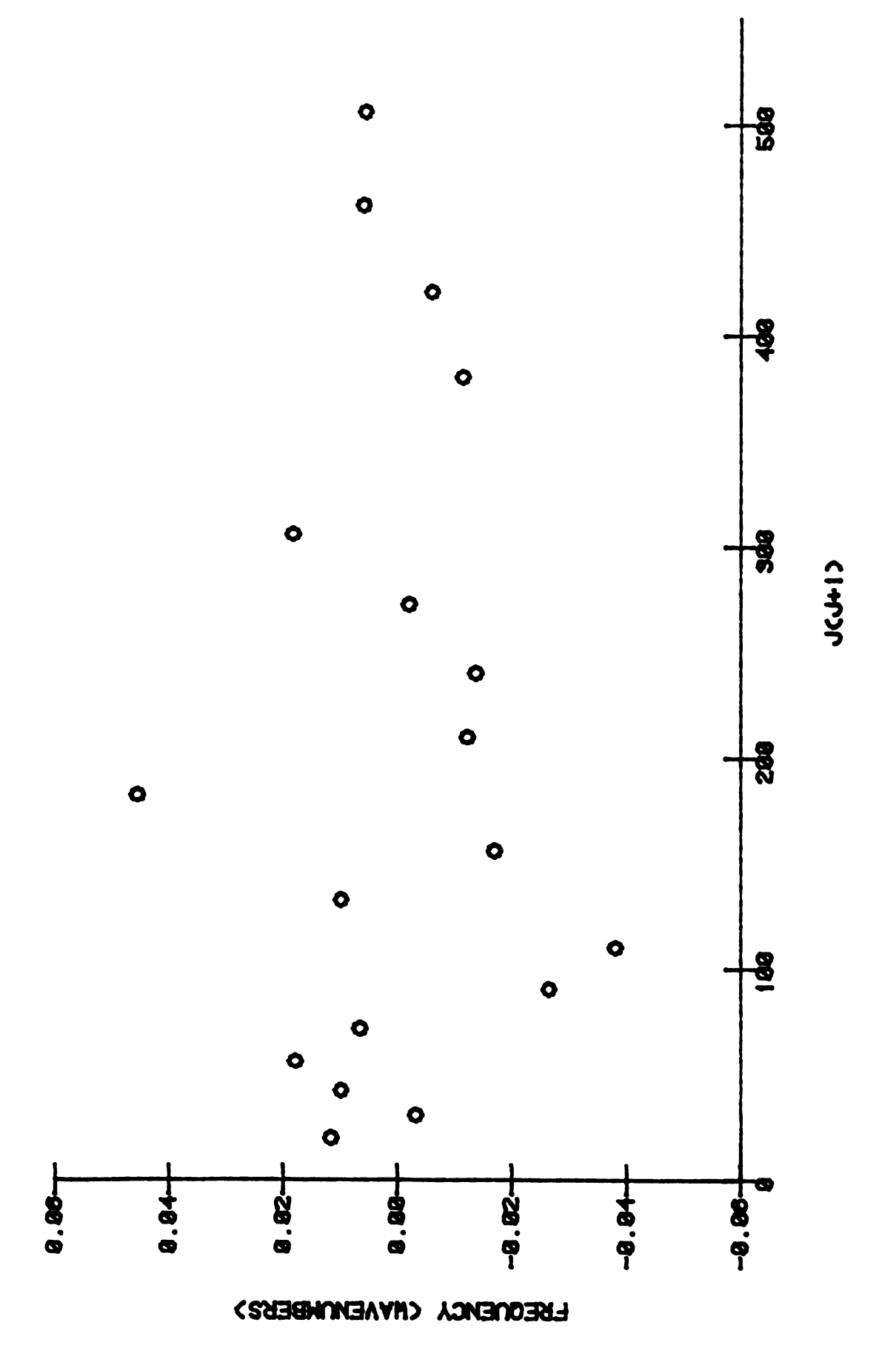
A single "whole band" fit was performed on 79 lines with the results given in Table 6.2. These results were then compared to the results of the single band fit of ν_5 to test somewhat for internal consistency of the two sets of data. Barnett's single band fit of $2\nu_5$ was not available for comparison.

The ν_5 and $2\nu_5$ bands were then combined to provide a simultaneous fit. The simultaneous fit gave fairly good results when compared to Barnett's results.

Parallel Component of $2v_5$ of CH_3CN

If the parallel component could be analyzed, SYMFIT would provide a value for the band origin of the parallel component and a value for α_5^B . The parallel component was very difficult to analyze, however, as the R and P branches were not resolved and the Q branch was only partially resolved.

As a first approximation one might guess that the two strongest lines in the center would correspond to K = 3 and K = 6 of the Q branch (~5965 cm⁻¹ of Figure 6.1), K = 6 being the lower of the two in frequency. Thus, the parallel component band origin might be taken to be at the high frequency



RESIDUALS (ROSCJ) OF ZNUS OF CHSCN HINUS LINEAR FIT > VERSUS JCJ+1> Figure 6.9

Table 6.2 Single Band Fit of $2v_5(\downarrow)$ of CH_3CN

Parameter	Calculated Value (cm ⁻¹)
ν _o	6007.700(23)
$A_o - A_e^{\zeta}$	5.790(14)
$\alpha_5^A + \dots$	0.0643(20)
${}^{lpha}_{f 5}^{f B}$	7.63(13.72)E-5
$H_{\mathbf{O}}^{\mathbf{K}}$	-7.47(17)E-5
$\mathtt{D}_{\mathbf{O}}^{\mathbf{k}}$	-0.60(39)E-3
$eta_{f 5}^{f k}$	0.001543(12)
Std. Dev. of Fit	0.0083

edge of the central portion. If the parallel component band origin was provided for SYMFIT, the simultaneous fit would calculate parallel component frequencies. This was, in fact, attempted, with poor results, indicating a need for more or better information.

It has been noted from studies of other molecules that one value of K is usually stronger than the other for a particular value of J. Thus, it was assumed in this analysis that the measured line positions all belonged to the same K value. A better model would be to assume that the measured line position is a combination of two or three neighboring K values.

To determine which K fit best, GSCD's were computed from measured line positions assuming K to be 1, 2, 3, ..., 9 and compared to the calculated GSCD's using microwave constants. The "true" K value would be expected to yield the best fit to the GSCD's calculated from microwave constants. Once K is determined, the $Q_{K}(J)$ are calculated using GSCD's and plotted versus J(J+1). The weights were again assigned according to the size of the residual. The weighted lines and appropriate constants were input to SYMFIT to obtain α_5^B and $\nu_O(\parallel)$

When these calculations were performed, all K except K=2 and K=3 were eliminated. The results of a fit of the parallel component tend to support setting K=3 (Table 6.3). α_5^B obtained in the fit using K=3 was closer to the value obtained the simultaneous fit than the value obtained

Table 6.3 Comparison of the K=2 and K=3 assignments of the $2v_5(\parallel)$ band of CH_3CN .

	α <mark>B</mark> 5	Standard Deviation of Fit
K = 2	1.350(51)E-4	0.0224 cm ⁻¹
K = 3	1.289(42)E-4	0.0133 cm^{-1}
Simultaneous Fit of v_5 and $2v_5(1)$	1.268(23)E-4	0.0083 cm ⁻¹

in the fit using K=2. The variation in α_5^B 's from the subband fits, however, reduces the reliability of using α_5^B as an indicator. Finally, the standard deviation of the fit using K=2 was about 60% larger than when K=3 was used, and since the K=3 lines would be expected to have more intensity, the natural choice is for K=3.

On the other hand, several circumstances recommend K = 2:

on the high frequency edge of the central portion identified as the Q branch, the expected position.

The fit for K = 3 predicts the band origin 0.25 cm⁻¹ lower than for K = 2, and to the low frequency side of the Q branch line at that edge, and unexpected position. Changing the J assignments only changes the band origin, by approximately 0.61 cm⁻¹, and thus does not remove the 0.25 cm⁻¹ difference.

- 2. The simultaneous band fit predicts the $2v_5$ (perpendicular) Q branch positions to approximately 0.1 cm⁻¹ of the measured positions, thus indicating a capability of predicting to 0.1 cm⁻¹. When the simultaneous band fit is used to predict the $Q_{Q_K}(0)$ lines, the results match the results obtained assuming K=2 to better than 0.02 cm⁻¹, but only to 0.34 cm⁻¹ when K=3 is assumed.
- 3. Prediction of $Q_{K}(0)$ line positions using K=2 gives reasonable assignments for the two highest intensity lines, i.e., K=3 and K=6. The fit assuming K=3 gives less reasonable assignments for these two lines.

It should also be mentioned that predicting the perpendicular component Q branches from the parallel component fit did not discriminate between K = 2 and K = 3, primarily because α_5^B is not significantly different for the two cases.

Results

Because of the uncertainty as to whether K = 2 dominates the R and P branches or whether K = 3 dominates, the parallel component was not included in the final simultaneous band fit. The final fit contained approximately 240 lines, about 2/3 of which were from the ν_5 band and the remainder from $2\nu_5$. Consideration was given, however, to the Q branch fit of $2\nu_5$ in the determination of α_5^A and to the parallel component fit of $2\nu_5$ in the determination of the parallel component band origin.

The results of this analysis are compared to Barnett's results in Table 6.4. Most of the constants are similar to Barnett's values, while every 95% SCI improved relative to that given by Barnett. Where there were disagreements in the values of the constants, the values were checked against values obtained on a similar molecule, under the presumption that similar molecules should have similar values for constants. The values of constants obtained in this study are comparable in magnitude to the values of constants obtained by Barnett for the simultaneous fit of ν_4 and $2\nu_4$ of CH₃Br (34), whereas the values obtained by Barnett for CH₃CN for those constants that differed were farther from the CH₃Br values.

Table 6.4 Simultaneous Fit of v_5 and $2v_5(\bot)$ of CH_3CN

Parameter (cm ⁻¹)	Barnett	Bardin	CH ₃ Br
^V 5	3009.111(15)	3008.9721(58)	3056.3525(40)
2v ₅ (₁)	6005.96(23)	6007.143(12)	6095.3793(88)
A _O	5.026(64)	5.2125(10)	5.12909(97)
A _e ζ +	0.328(21)	0.25311(45)	0.30493(71)
D_{O}^{K}	0.0238(16)	-9.42(54)E-5	0.37(33)E-4
α_5^A +	-0.143(27)	0.02891(63)	0.02849(39)
$\alpha_{\bf 5}^{\bf B}$	0.79(14)E-4	1.27(10)E-4	-1.844(62)E-4
n	0.0248(15)	-6.04(30)E-4	-0.83(37)E-4
β <mark>k</mark> 5	0.00656(28)	-63(19)E-6	-1.62(93)E-5
$\mathtt{H}^{\mathtt{O}}_{\mathbf{F}}$	-4.54(19)E-5	77(34)E-8	11(9)E-8
$\mathfrak{s}_5^{\mathbf{J}}$		68(49)E-9	
2v ₅ ()		5966.366(12)	
Std. Dev. of Fit	0.008	0.0075	0.006

CHAPTER VII

A REVIEW OF OUR ANALYSIS OF THE v_4 BAND OF CD_3Br

Our study and analysis of an x-y Coriolis interaction between v_4 and $v_3 + v_5^{\pm 1} + v_6^{\pm 1}$ of CD_3Br was published in 1981 in the Journal of Molecular Spectroscopy (40). A copy of this paper appears in Appendix IV. The measured frequencies and assignments for v_4 of CD_3Br appear in Appendix V. This chapter will review our contributions to this publication.

Professor Marshall Wilt, F. W. Hecker, and J. D. Fehribach of Centre College, Kentucky, wrote a computer program (CORIFERM) to calculate the intensities and frequencies of transitions in axially symmetric C_{3v} molecules. The diagonal part of the Hamiltonian is the Hamiltonian for axially symmetric molecules as described in Chapter II. Additional terms are added to this Hamiltonian to allow for an x-y Coriolis interaction and a Fermi interaction between vibrational states. These additional terms connect different vibrational states and thus are off-diagonal. An iterative technique (similar to a force constant calculation) is used to solve this system for the parameters. A parameter is changed slightly to determine how the frequency of each transition changes. This is repeated for each parameter.

the most recent values of the parameters for the previous values. The iterations are stopped when the calculated residuals are smaller than the experimental error. Wilt used this iterative technique to analyze the Fermi and x-y Coriolis interacting bands for CH₃I and for CH₃Br.

These successes suggested that analyses of other $\mathrm{CH_3X}$ type molecules would also be successful. From the literature, Marshall Wilt picked $\mathrm{CD_3Br}$ as a good candidate. The experimental work done by Peterson and Edward (9), however, did not quite resolve the transitions necessary for the analysis of $\mathrm{v_4}$ of $\mathrm{CD_3Br}$ using Wilt's procedure. Hence, Wilt asked T. H. Edwards, one of the original authors, if $\mathrm{CD_3Br}$ could be run at higher resolution using the M.S.U. high resolution infrared spectrophotometer. Deconvolution had recently been developed, so it was thought that the $\mathrm{CD_3Br}$ spectrum could be deconvoluted to improve the resolution limit.

We reran the v_4 spectrum of CD_3Br under conditions optimum for deconvolution, which requires a high signal to noise ratio ($\gtrsim 50$). To improve resolution, the spectrophotometer slits must be narrowed, which lowers the signal to noise ratio. When the slits were widened to improve the signal to noise ratio enough to deconvolute effectively, there was not sufficient gain in the final resolution limit to be helpful to Marshall Wilt.

The insufficient gain in resolution prompted an examination of possible means to signal average spectra. Signal averaging spectra permits a higher initial noise level and hence a higher initial resolution limit. Although signal averaging had not been successful for high resolution infrared spectroscopists in the past, a successful technique was eventually developed at the M.S.U. high resolution infrared lab.

The signal processing techniques described in previous chapters were originally developed for this application to ${\rm CD_3Br.}$ Much time was spent trying various ideas and then testing thoroughly before applying the final procedure to ${\rm CD_3Br.}$ Deconvoluting the spectrum then produced a more resolved spectrum for ν_4 of ${\rm CD_3Br.}$ especially in the region of interest to Marshall Wilt. We assigned as many transitions as we could, then gave the data and intermediate results to M. Wilt. Wilt confirmed our assignments and made many more. He then extended the analysis to include an x-y Coriolis interaction and the possibility of a Fermi interaction, although no Fermi interaction was found.

The extension of the usual method to include x-y Coriolis and Fermi interactions resulted in the publication given in Appendix IV.

CHAPTER VIII

CONCLUSION

A technique has been developed to signal average high resolution infrared spectra. The band under study is run in segments approximately 20 wavenumbers in length. Each segment is scanned and recorded approximately 16 times. These scans are linearized in frequency and summed using a least squares fit of each scan to the first scan as an alignment trigger. The averaged segments are calibrated by fitting to a calibrated run using a least squares fit.

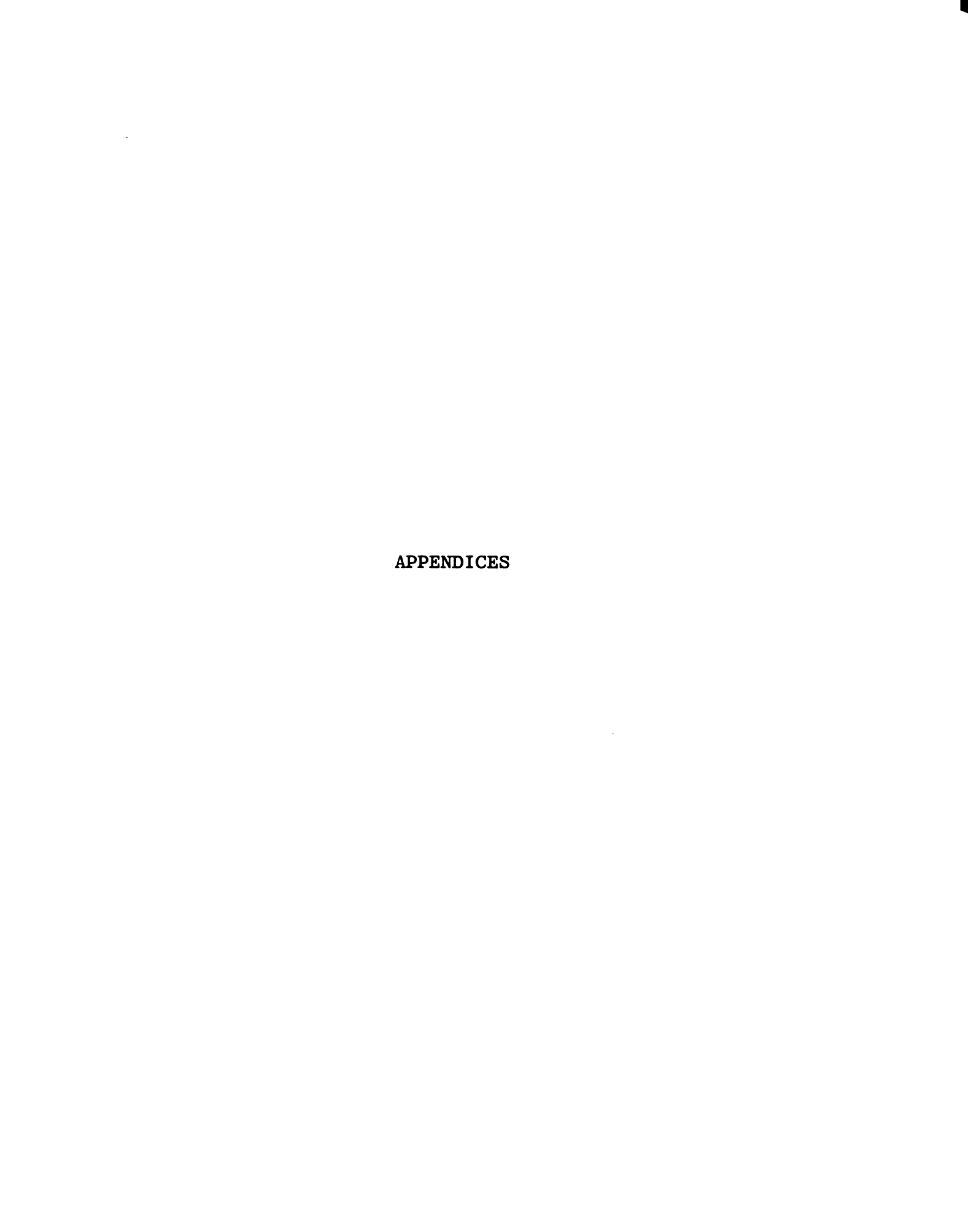
The signal averaging technique was successfully applied to the ν_4 band of ${\rm CD_3Br}$ and the $2\nu_5$ band of ${\rm CH_3CN}$. Each band represents a different application. The ν_4 band of ${\rm CD_3Br}$ is a dense band where the transitions appear to be many incompletely resolved lines. The $2\nu_5$ band of ${\rm CH_3CN}$ is a weak band in that the intensities of the individual transitions are relatively small.

Signal averaging allowed us to obtain a higher resolution limit for ν_4 of CD₃Br than had been obtained previously. As a result, Marshall Wilt was able to extend the analysis to include an x-y Coriolis interaction between ν_4 and $\nu_3 + \nu_5^{\pm 1} + \nu_6^{\pm 1}$. The analysis resulted in improved values of the molecular constants not held constant in the calculation.

The v_5 and $2v_5$ bands of CH₃CN were rerun at a higher resolution limit. The $2v_5$ band had to be signal averaged to obtain sufficient signal strength for some parts of the band. A Q branch fit of the $2v_5$ (perpendicular) band gave a significant improvement in the value of α_5^A . A simultaneous fit of v_5 and $2v_5$ (perpendicular) resulted in improved values of most constants and significantly improved values of the remaining constants. Although the P and R branches were unresolved, and the Q branch only partially resolved, assignment of the parallel component of $2v_5$ and the subsequent fit yielded values for the band origin and α_5^B . The parallel component was not included in the simultaneous fit, however, because of the uncertainties in the assignments.

Signal processing and numerical techniques were necessary for us to improve upon the work done in the past. In the future, signal processing and numerical techniques will become more and more useful, and general, as the limits of instrumentation are reached. Signal processing can extract information from spectra normally not subject to analysis.

Numerical techniques can bring computers to bear on problems, such as resonances, where other techniques fail. With these tools, the future will bring improved values of molecular constants, and, in addition, allow analysis of larger and more complicated molecules.



APPENDIX I

A LISTING OF THE FOCAL-12 PROGRAMS USED

TO SIGNAL AVERAGE SPECTRA

APPENDIX I

A LISTING OF THE FOCAL-12 PROGRAMS USED TO SIGNAL AVERAGE SPECTRA

LINQ

This program was last revised on March 12, 1982. LINQ ensures that each point of a run, or a portion of a run, represents the same interval of frequency, i.e., to make the run linear in frequency. The program was written in the PDP-12 minicomputer interpretive language FOCAL-12. Availability of three tapes drives is assumed, units one, two and three:

- UNIT 1: Tape 424 blocks 2 through 23 contain the fringe positions necessary for file "Fl"
- UNIT 2: Tape 423 blocks 2 through 744 contain the original data necessary for file "F2"
- UNIT 3: Tape 82-1 blocks 2 through approximately 1371 contain the data after it has been linearized (i.e., the output) necessary for file "F3"

Following is a list of symbols and their meanings:

A ratio of the number of points between fringes in original scan to the number of points between fringes in the linearized scan

- B the coefficient to the linear term in CALFIT, an M.S.U. I.R. lab program
- B used in "FOR" loop as a temporary storage for truncated D
- Bl value of B (B in "FOR" loop) in original scan
- C the coefficient of the quadratic term in CALFIT.

 2 * C gives the change in B for an increase in fringe number of one.
- D pointer to mark point in original scan that corresponds to the point being operated on in linear scan
- D2 first point of present fringe for the linear scan
- D3 position of the Rth fringe from the beginning of the scan
- D5 position of the (R+1)st fringe from the beginning of the scan
- Fl integer array containing fringe positions
- F2 integer array containing original data
- F3 integer array containing linearized data
- K pointer marking present point in linear scan
- K1 first point in the original scan
- K2 last point in the original scan
- PC desired number of points per wavenumber
- R pointer marking present fringe (of either scan)

RIN first fringe of the portion to be linearized (i.e., first fringe preceding K1). Note that only the first two letters in name count for variable name)

RMAX last fringe of the portion to be linearized (i.e., first fringe beyond K2).

X number of points between fringes (not constant)

Y floating point value of F3(K)

The following code is stored on my tape under name "LINQ". Spaces are added to improve clarity, they are not present in actual code.

C...

C... OPEN FILES

C...

1.1. L 0,F1,F,#2,1

1.20 L 0,F2,I,#2,2

1.30 L 0,F3,I,#2,3

C...

C... INITIALIZE VARIABLES

C...

1.40 S RMAX = 1436; S PC = 500; S RIN = 0; S K2 = 67000

C...

C... DETERMINE LAST FRINGE

C...

1.42 S RMAX = RMAX - 1

1.44 IF < F1(RMAX) - K2 > 1.46, 1.46, 1.42

1.46 S RMAX = RMAX + 1

C...

C... SUBROUTINE TO CALCULATE LINEAR

C... POINT BY LINEAR INTERPOLATION

C... BETWEEN POINTS IN ORIGINAL SCAN

C...

8.10 S D3 = F1(R); S D5 = F1(R+1)

8.20 S X = X + 2 * C * PC

8.25 S A = (D5 - D3) / X; S D2 = D2 + X

8.30 S D = D3 + (K - D2) * A

8.40 S B = FITR(D); S B1 = F2(B)

 $8.50 S Y = \langle F2(B+1) - B1 \rangle * (D - B) + B1$

8.70 S K = K + 1

8.80 IF (K - D2 - X) 8.3

8.90 CONTINUE

FIND

This program was last revised on August 9, 1981. FIND finds fringe positions by fitting a quadratic to the uppermost 29 points using a least squares fit. The program is written in the PDP-12 minicomputer interpretive language FOCAL-12. Accessibility to two tape drives is assumed.

- UNIT 0: Tape containing fringes
- UNIT 2: Tape on which to store fringe positions

Following is a list of symbols and their definitions:

- A constant coefficient in quadratic for least squares fit
- B linear coefficient in quadratic for least squares fit
- C quadratic coefficient in quadratic for least squares
- DB constant determined from least squares fit necessary to determine point where slope is zero
- DC constant determined from least squares fit necessary to determine where slope is zero
- FO file containing original fringe data
- F2 file that will contain fringe positions

- I index for least squares fit
- K data point index
- L number of points between first point of scan n and first point of scan n+1
- Q marks first point of scan; increments by L after each scan
- QQ counts number of scans completed
- Ql counter that increments by 85 thus allowing fringe positions from each scan to be stored on a separate block
- R fringe counter
- SC number of points in data scan

The following code is stored on my tape and named "FIND". Spaces are added to improve clarity, actual code does not have these spaces.

C...

C... INITIALIZE VARIABLES AND OPEN FILES

C...

1.10 S Q = 0; S QQ = 0; S Q1 = 0; S SC = 12032; S L = 12288

1.20 L O, FO, I, #2, O; L O, F2, F, #2, 2

1.30 S K = Q; S R = Q1

C...

C... FIND OUT WHERE POSITION K IS

C... RELATIVE TO PEAK OF FRINGE, THEN

C... FIND PEAK OF FRINGE.

```
1.40 IF < FO(K) - FO(K+1) > 1.6
C...
C...
                           CHECK TO SEE IF MUST GO TO NEXT SCAN
C...
1.50 \text{ S K} = \text{K} + 25; IF < \text{SC} + \text{Q} - \text{K} > 2.5, 2.5, 1.4
C...
C...
                              THE FRINGES ARE MANUALLY ADJUSTED
                              DURING THE RUN TO MAINTAIN AN AP-
C...
C...
                              PROXIMATE HEIGHT OF 1200 (OCTAL)
C...
                              HENCE THERE SHOULD NOT BE ANY
C...
                              FRINGES WITH HEIGHT LESS THAN 400,
C...
                              SO GO TO GREATER THAN 400 BEFORE
                              CHECKING FOR TOP POINT
C...
C...
1.60 \text{ IF} < FO(K) - 400 > 1.7, 1.7, 1.8
C...
                              CHECK TO SEE IF MUST GO TO NEXT SCAN
C...
C...
1.70 \text{ S K} = \text{K} + 5; IF < \text{SC} + \text{Q} - \text{K} > 2.5, 2.5, 1.6
1.80 S K = K + 1; IF < FO(K) - FO(K+1) > 1.8
C...
                              TOP POINT WAS FOUND IN 1.80 AND IS
C...
                              POINT K. NOW INITIALIZE CONSTANTS
C...
                              FOR LEAST SQUARES FIT OF 14 POINTS
C...
                              TO LEFT AND 14 TO RIGHT OF TOP
C...
C...
                              POINT TO A QUADRATIC
C...
```

```
1.85 S A = FO(K); S B = 0; S C = 0
1.90 \text{ F I} = 1, 14; D 9
C...
C...
                            A QUADRATIC HAS THE FORM Y=A+BX+CX^2
C...
                            THE POINT WHERE THE SLOPE IS ZERO,
C...
                            OR THE PEAK OF THE QUADRATIC, IS AT
C...
                            dY/dX = 0 = B + 2 C X(PEAK) OR
                            X(PEAK) = -B/2C, WHERE HERE "B" = DB,
C...
C...
                            "C" = DC, AND X(PEAK)=F2(R).
C...
2.20 S DB = 32849.46 * B
2.25 \text{ S DC} = -41209 * A + 588.7 * C
2.35 \text{ S } F2(R) = -DB / (2 * DC) + K - Q; S R = R + 1; S K = K + 5
C...
C...
                            IF NOT AT LAST POINT OF SCAN, REPEAT
C...
                            PROCESS UNTIL LAST POINT EXCEEDED
C...
2.40 \text{ IF} < K - SC - Q > 1.4
C...
C...
                             IF BEYOND LAST POINT OF SCAN, TYPE
C...
                            OUT NUMBER OF FRINGES IN SCAN, GO
C...
                            TO NEXT SCAN, CHECK TO SEE IF DONE.
C...
                             IF NOT, REPEAT PROCESS FOR NEW SCAN,
C...
                            ELSE QUIT. FRINGES FOR SCAN 1 ARE
C...
                             STORED ON BLOCK 2, FRINGES FOR SCAN
C...
                             2 ARE STORED ON BLOCK 3, ETC.
```

```
2.50 T R - Q1 - 1
```

$$3.10 S Q = Q + L; S Q1 = Q1 + 85$$

3.20 S
$$QQ = QQ + 10$$
; IF $\leq QQ - 16 > 1.3$

3.30 L C, FO; L C, F2; QUIT

C...

C... SUBROUTINE TO COMPUTE MATRIX

C... ELEMENTS IN LEAST SQUARES FIT

C...

$$9.10 S A = A + FO(K+I) + FO(K-I)$$

$$9.20 S B = B + < FO(K+I) > * I$$

9.30 S B = C + < FO(K+I) > * I ** 2

LIN2

This program was last revised on August 17, 1981. LIN2 linearizes several (usually 16 for our applications) scans of data. The program is written in the PDP-12 minicomputer interpretive language FOCAL-12. Accessibility to three tape drives is necessary.

UNIT 1: Tape containing original data

UNIT 3: Tape containing fringe positions

UNIT 4: Tape containing linear data

Following is a list of symbols and their definitions:

- A number of original points per new point (a combination of constants to save momory)
- B truncated "D"
- Bl function "Fl" at "B"
- D interpolated data point
- D2 counter to count fringe points
- D3 the "Rth" fringe
- D5 the "(R+1)st" fringe
- Fl array containing original data

F3	array	containing	fringe	positions	(previously	measured
	with '	"FIND")				

- F4 array containing linearized data
- K counter to mark present original data point
- Kl counter to mark present linear data point
- L number of points between scans of original data
- L3 number of points between scans of linear data
- M flag to allow file containing data to change tapes
- Q original data point counter
- Ql fringe counter
- Q3 linear data point counter
- R counter to mark present fringe
- RMAX number of fringes minus 1 (only RM counts in variable name)
- X number of points between fringes
- Y new linearized data point, still in floating point format

The following code is stored on my tape and named "LIN2". Spaces are added to the code here to improve clarity.

C...

C... INITIALIZE VARIABLES AND OPEN FILES

```
1.10 S RMAX = 63; S X = 267.958; S Q = 0; S Q1 = 0
1.20 S Q3 = 0; S L = 12288; S L3 = 16896; S M = 0
1.30 L O, F1, I, #2, 1; L O, F4, I, #22, 4
1.35 L O, F3, F, #2, 2
1.40 S K = Q; S R = Q1; S D2 = Q; S K1 = Q3
C...
C...
                               CALCULATE NUMBER OF ORIGINAL POINTS
C...
                              PER NEW POINT
C...
2.16 \text{ S D3} = \text{F3(R)}; \text{ S D5} = \text{F3(R+1)}
2.17 S A = < D5 - D3 > / X
C...
C...
                               CALCULATE POSITION OF NEW POINT
C...
                               RELATIVE TO ORIGINAL POINTS, THEN
C...
                               CALCULATE HEIGHT AT THAT POINT BY
C...
                               LINEARLY INTERPOLATING BETWEEN
                              HEIGHTS OF ORIGINAL POINTS
C...
C...
                               \{ F4(K1) \}
~c:..
2.20 S D = D3 + (K - D2) * A
2.25 S B = FITR(D); S B1 = F1(B)
2.30 S Y = \langle F1(B+1) - B1 \rangle * (D - B) + B1
2.35 \text{ S } \text{F4}(\text{K1}) = \text{FITR} < \text{Y} + .5 >
C...
                               INCREMENT COUNTERS, AND CHECK TO
C...
C...
                               SEE IF NEW FRINGE
C...
```

```
2.40 \text{ S K} = \text{K} + 1; \text{S Kl} = \text{Kl} + 1; \text{IF} < \text{K} - \text{D2} - \text{X} > 2.20
2.50 \text{ S R} = \text{R} + 1; S D2 = D2 + X; IF < R - RMAX - Q1 > 2.16
C...
C...
                                  CHECK TO SEE IF NEW SCAN
C...
3.10 S Q = Q + 1; S Q1 = Q1 + 85; S Q3 = Q3 + L3
3.20 \text{ IF} < Q3 + 10 - 8 * L3 > 1.40
C...
C...
                                  CHECK TO SEE IF CHANGE TAPES
C...
3.30 \text{ S M} = \text{M} + 10; \text{ IF} < 15 - \text{M} > 3.80
C...
C...
                                  CHANGE TAPES
C...
3.40 L C, F4; L O, F4, I, #22, 2
3.50 L C, F3; L O, F3, F, #2, 4
3.60 S Q3 = 0; G 1.4
C...
C...
                                  CLOSE LIBRARIES AND GO HOME
C...
```

3.80 L C, F1; L C, F3; L C, F4

LSF

This program was last revised on August 14, 1981. LSF performs a least squares fit between a particular region of the average of scans (initially just scan number 1) and the same region of a remaining scan. The program is written in the PDP-12 minicomputer interpretive language FOCAL-12. Accessiblity to minimum of two tape drives is necessary:

- UNIT 1: Tape containing scans of uniformly separated data
- UNIT 2: Tape on which to store averaged data (floating point)

Following is a list of symbols with definitions:

- A Number of points between beginning of first scan and the beginning of the trigger region (i.e., the region on which the least squares fit will be performed, hereafter referred to as "the LSF region")
- B A constant used to skip a number of blocks after opening a file
- FO Averaged data (in floating point format)
- Fl Original data, first point of each scan is separated from the first point of its neighboring scan by a constant number of points

- F3 Final averaged data (in integer format)
- F7 File contains the offset of each scan from the "average" position of the scans (a rough offset usually determined from some significant feature in the scan)
- I Index for data points
- N Counter to count scans, used to find "average" height of LSF region and to access offset for the scan being fitted
- P Calculated number of points needed to add to all points of a scan for the "average" height of scan to match that of the average of all scans
- P6 "Average" height for the LSF region of average of scans
- Q Index used to change tapes when data is on two tapes
- R Sum of residuals squared
- RA Number of points in the LSF region
- RB Number of points in total scan
- T Trial offset between scan and average (used to fine tune the fit of scan and average of scans)
- U Smallest sum of residuals squared
- W Offset position of smallest sum of residuals squared
- X Index to locate the LSF region of the scans
- Xl Approximate number of points needed to add to the position of a scan to move to "average" position of all scans

```
Index used to access all scans on the same tape
Y
      Number of points between successive scans
Yl
The following code is stored on my tape and named "LSF".
Spaces are added to improve clarity, actual code does not
have these spaces.
C...
                              INITIALIZE VARIABLES AND OPEN FILES
C...
C...
1.05 \pm 0, F7, I, #22, 0; S X1 = F7(1); S A = 10193; S Q = 0
1.07 \text{ S RA} = 1834; \text{ S RB} = 15810; \text{ S Y1} = 16384; \text{ S Y} = \text{Y1}
1.10 \text{ S N} = 1; S B = 256 * 21; S A = A + X1; S X = Y + A
1.20 L O, F1, I, #2, 1; L O, F0, F, #777, 2
C...
C...
                              READ FIRST SCAN INTO FILE CONTAINING
C...
                              AVERAGED DATA, INITIALLY EMPTY
C...
1.30 F I = 0, RB; S FO( I+E+X1 ) = F1( I )
C...
C...
                              DETERMINE AVERAGE HEIGHT OF AVERAGED
C...
                              DATA
C...
2.10 \text{ S P6} = 0; \text{ S X1} = \text{F7} (\text{N+1})
2.20 \text{ F I} = A, A+RA; S P6 = P6 + F0(I+B) / N
C...
                              DETERMINE AVERAGE HEIGHT OF NEXT SCAN
C...
```

```
2.30 S P = 0
2.40 F I = X, X+RA; S P = P + F1( I-X1 )
C...
C...
                           CALCULATE AMOUNT NEEDED TO COMPEN-
C...
                           SATE FOR ANY DIFFERENCE BETWEEEN
C...
                           AVERAGE HEIGHTS OF AVERAGED DATA
C...
                           AND NEXT SCAN
C...
2.50 S P = (P - P6) / (RA + 1)
C...
C...
                           CALCULATE THE SUM OF SQUARES OF
                           RESIDUALS BETWEEN THE AVERAGE AND
C...
C...
                           THE NEXT SCAN DISPLACED T POINTS.
C...
                           THEN REPEAT FOR A DISPLACEMENT OF
                           T+1 POINTS, ETC., FOR -16<T<16.
C...
                           KEEP THE DISPLACEMENT THAT GIVES
C...
C...
                           THE SMALLEST SUM OF RESIDUALS
C...
                           SQUARES
C...
3.10 S T = -15: S U = 9 E 99
3.20 S R = 0
3.30 F I = X-X1, X-X1+RA; S R = R
              < FO (I+B+X1-Y) / N - FL(I+T) + P > ** 2
3.40 IF ( R-U ) 3.5; ST = T + 1; G 3.6
3.50 S U = R; S W = T; S T = T + 1
3.60 IF ( T-16 ) 3.2
```

```
C...
C...
                                ADD SCAN (APPROPRIATELY DISPLACED)
C...
                                INTO SUM OF PREVIOUSLY FITTED SCANS
C...
4.10 \text{ F I} = Y + 15, Y + RB - 15;
         S FO(I+B-Y) = RO(I+B-Y) + F1(I+W+X1)
C...
C...
                                INCREMENT INDICES AND CONSTANTS.
C...
                                CHECK TO SEE IF GO TO NEXT SCAN,
C...
                                NEXT TAPE, OR IF DONE
C...
4.20 \text{ S } \text{X} = \text{X} + \text{Y1}; \text{ S } \text{Y} = \text{Y} + \text{Y1}; \text{ S } \text{N} = \text{N} + \text{1}
4.25 IF ( Y + 10 - Y1 * 8 ) 2.1
4.27 S Q = Q + 10; IF (Q - 15) 5.1
C...
C...
                                CLOSE TWO FILES, OPEN FINAL
C...
                                AVERAGED DATA FILE (INTEGER FORMAT),
C...
                                CLOSE THE REST OF THE FILES, AND
C...
                                QUIT
C...
4.30 L C, F1; L C, F7; L O, F3, I, #777, 2
4.40 \text{ F I} = 15, \text{ RB} - 15; \text{ S F3( I+B )} =
                   FITR< FO( I+B) * .4 - 400.5 >
4.50 L C, FO; L C, F3; QUIT
C...
                                SUBROUTINE TO SWITCH F1 and F0
C...
C...
                                FILES, I.E., PUT ON OPPOSITE TAPES
C...
```

```
5.10 L C, F1; L O, F1, F, #777, 1
```

5.20 F I = 0, RB; S F1(I+B) = R0(I+B)

5.30 L C, F0; L C, F1; L O, F0, F, #777, 1

5.40 L 0, F1, I, #2, 2; S Y = 0; S X = A; G 2.1

C...

C... NOTE: I+W+X1 FROM STATEMENT 4.10

C... MAY BE A PROBLEM ON FIRST SCAN OF

C... SECOND HALF; IF SO, SET Y = 256 IN

C... LINE 5.40 AND OPEN FILE ONE BLOCK

C... SOONER

PTLSF

This program was last revised on August 7, 1982. PTLSF performs a least squares fit on line peaks between the first scan and each succeeding scan, then sums the scans appropriately displaced in a separate file. The program is written in the PDP-12 minicomputer interpretive language FOCAL-12. Accessibility to a minimum of three tape drives is necessary:

- UNIT 0: Contains approximate offsets for each scan. Also contains the least squares fit calculation positions.
- UNIT 1: Contains the original data.
- UNIT 2: Contains the averaged data.

Following is a list of symbols with definitions:

- D1 Trial index used with the least squares fit
- D2 Flag indicating when to change tape and when to quit
- D3 Constant containing number of scans on each tape
- D9 Best relative displacement for scan being tested
- FO Array containing averaged data (floating point format)
- Fl Array containing original data

- F7 Block 21, positions 1 through 16 contain approximate offset for each scan relative to the position of a strong line in scan 1; positions 17 through 53 contain the positions at which the least squares fit will be calculated (scan 1 positions).
- I Data point index
- Ml Average difference in intensities between scan to be tested and the first scan (from S5 and S6)
- N Counter to count scans
- Nl Number of positions at which least squares fit is to be calculated (LSF points)
- P Counter to count scans on a particular tape; manually reset to zero when tape is changed.
- Q Counter to count scans
- RB Total number of points per scan
- S5 Average intensity of averaged data at LSF points
- S6 Average intensity of trial data at LSF points
- S8 Minimum sum of residuals squared (residuals are the difference between averaged data at LSF points and trial data at LSF points)
- W Marks first point of scan after accounting for offset
- Wl Index to locate first point of trial scan
- X Position of a least squares fit line (temporary)

- Xl Approximate number of points trial scan must move to left (+) or right (-) to match first scan
- X2 Position of a least squares fit line (temporary)
- X3 Position of a least squares fit line (temporary)
- X4 Position of a least squares fit line (temporary)
- Yl Number of points between first points of successive scans (scan separation)
- Z Sum of squares of residuals between first scans and trial scan

The following code is stored on my tape and named "PTLSF". Spaces are added to improve clarity, actual code does not have these spaces.

C...

C... INITIALIZE VARIABLES AND OPEN FILES

C...

- 1.10 LO, F7, #21, O; L O, F1, I, #22, 1
- 1.20 L O, FO, F, #700, 2
- 1.30 S X1 = 0; S N1 = 36; S D2 = 1; S D3 = 8
- 1.40 S RB = 18944; S Y1 = 20480.
- 1.50 S N = 1

C...

C... PUT FIRST SCAN INTO "AVERAGED" FILE

C...

1.60 F I = 0, RB; S FO(I) = F1(I)

```
C...
C...
                                  DETERMINE AVERAGE INTENSITY OF POINTS
C...
                                  WHERE LEAST SQUARES FIT WILL BE
C...
                                  CALCULATED, FIRST FOR FIRST SCAN
C...
                                  THEN FOR TRIAL SCAN
C...
2.10 S S5 = 0
2.20 \text{ F I} = 17, \text{ N1+16}, 4; D 7
2.30 S P = N - ( D2 - 1 ) * 8; S N = N + 1; S D1 = -30
2.40 \text{ S X1} = \text{F7}(\text{ N}); \text{ S S8} = 9 \text{ E } 30
2.45 S W1 = Y1 * P; S W = W1 + X1
2.50 \text{ S S6} = 0
2.60 \text{ F I} = 17, \text{ N1+16}, 4; D 9
2.70 \text{ S M1} = ( \text{S6} - \text{S5} ) / \text{N1}
C...
C...
                                  DO LEAST SQUARES FIT OF TRIAL SCAN
                                  TO AVERAGE OF SCANS THAT HAVE BEEN
C...
                                  SUMMED TO FIND THE OFFSET FOR TRIAL
C...
C...
                                  SCAN, BASED ON PRESELECTED LINE
C...
                                  POSITIONS
C...
3.10 S Z = 0
3.20 \text{ F I} = 17, \text{ N1+16}, 2; \text{ D 8}
 3.40 \text{ IF} < Z - S8 > 3.5, 3.6, 3.6
 3.50 S D9 = D1; S S8 = Z
 3.60 \text{ S D1} = \text{D1} + 2; IF < \text{D1} - 30 > 2.5
```

```
C...
C...
                             ADD TRIAL SCAN INTO AVERAGE OF SCANS
C...
                             APPROPRIATELY DISPLACED. GO TO NEW
C...
                             TRIAL SCAN, CHECK FOR NEW TAPE OR END
C...
4.10 \text{ F I} = 0, RB-30; S FO(I) = FO(I) + F1( I + W + D9 )
4.20 \text{ IF } (N - D2 * D3) 2.1
5.10 IF ( 1 - D2 ) 6.1
C...
C...
                             GET REST OF DATA FROM OTHER TAPE
C...
5.20 \text{ S } D2 = D2 + 1; L C, F7; L C, F1
5.30 L O, F7, F, #21, 1; L O, F1, I, #22, O
C...
C...
                             CLOSE FILES AND QUIT
C...
6.10 L C, F7; L C, F1; L C, F0; QUIT
C...
C...
                             SUBROUTINE TO FIND AVERAGE
C...
                             INTENSITY OF AVERAGED DATA
C...
7.10 \text{ S X} = \text{F7(I)}: S X2 = F7(I+1); S X3 = F7(I+2); S X4 = F7(I+3)
7.20 S S5 = S5 + < F0(X) + F0(X2) + F0(X3) + F0(X4) > / N
C...
C...
                             SUBROUTINE TO CALCULATE SUM OF
C...
                             RESIDUALS SQUARED, WHERE RESIDUALS
C...
                             ARE DIFFERENCE BETWEEN AVERAGED
```

```
DATA AND TRIAL DATA AT LEAST
C...
C...
                            SQUARES FIT POINTS
C...
8.10 S X = F7(I); S X2 = F7(I+1); S Q = P + (D2 - 1) * 8
8.20 S Z = Z + < FO( X ) / Q - F1( X+W+D1 ) + M1 > ** 2 +
                 < FO(X2) / Q - F1(X2+W+D1) + M1 > ** 2
C...
C...
                            SUBROUTINE TO FIND AVERAGE DENSITY
C...
                            OF TRIAL SCAN
C...
9.10 S X = F7(I); S X2 = F7(I+1); S X3 = F7(I+2);
             S X4 = F7(I+3)
9.20 S S6 = S6 + F1( X+W+D1 ) + F1( X2+W+D1 ) + F1 ( X3+W+D1 )
             + F1( X4+W+D1 )
```

APPENDIX II

APPENDIX II

A COPY OF THE PUBLICATION OF OUR ANALYSIS OF v_4 of CD_3^Br

JOURNAL OF MOLECULAR SPECTROSCOPY 90, 33-42 (1981)

An X-Y Coriolis Perturbation in ν_4 of CD₃Br

P. M. WILT, F. W. HECKER, AND J. D. FEHRIBACH
Department of Physics, Centre College, Danville, Kentucky 40422

AND

DALE E. BARDIN AND T. H. EDWARDS

Department of Physics, Michigan State University, East Lansing, Michigan 48824

The region 6242-2273 cm⁻¹ of the ν_4 band in CD₂Br was remeasured at a resolution limit of 0.025 cm⁻¹. Line assignments were extended up to J=50 in some subbands. Transitions in the $K\Delta K=-8$ subband were assigned, and the perturbation apparent in this region was attributed to the x-y Coriolis interaction with $\nu_3+\nu_5^{-1}+\nu_7^{-1}$. The x-y Coriolis coupling parameter W_{xy} and the $\nu_3+\nu_7^{-1}+\nu_7^{-1}$ band center (in cm⁻¹) are 0.01960 and 2339.17 for CD₂¹⁰Br, while the corresponding values for CD₂¹⁰Br are 0.01956 and 2337.95.

INTRODUCTION

For several years it has been known from the infrared study of Peterson and Edwards (1) and the Raman work of Edwards and Brodersen (2) that the k'l' = -7 energy levels in ν_4 of CD₃Br are perturbed. The effects of the perturbation are easily recognized from the appearance of ${}^{P}Q_{0}$ in Fig. 1 of (1), and of ${}^{R}Q_{-0}$ and ${}^{O}Q_{-0}$ in Fig. 2 of (2). A similar perturbation observed in the k'l' = +6 levels of ν_4 of CH₃Br has been identified by Betrencourt-Stirnemann et al. (3) as an x-y Coriolis interaction with the $l_5 = l_6 = \pm 1$ levels of $\nu_3 + \nu_5 + \nu_6$. Their analysis also showed that while the resulting effects were most pronounced in the $K\Delta K$ = 5 subband, the perturbation produced widespread effects that could not be neglected in neighboring subbands.

Figure 1 is a plot of residuals from Peterson and Edwards' (1) analysis of the $K\Delta K = -6, -7, -9$, and -10 subbands; they were unable to assign transitions in the $K\Delta K = -8$ subband. These residuals may be explained qualitatively by an x-y Coriolis interaction with a nearby vibrational level ν_x with rotational levels situated as shown in Fig. 2. From the fundamentals of CD₃Br (4), no binary combination, and only one ternary combination, $\nu_3 + \nu_5 + \nu_6$, provides a probable explanation for the perturbing vibrational state. Using $\zeta_{eff} = -(\zeta_3 + \zeta_6)$ we calculated the energy level pattern for $l_5 = l_6 = \pm 1$ and found that, with a downward anharmonicity shift of about 5 cm⁻¹ in the band center, the resulting levels of $\nu_3 + \nu_5$ fit the pattern in Fig. 2. It appeared from this evidence and the similar

We use k as the signed quantum number for the projection of angular momentum on the molecular symmetry axis, and K = |k|.

34 WILT ET AL.

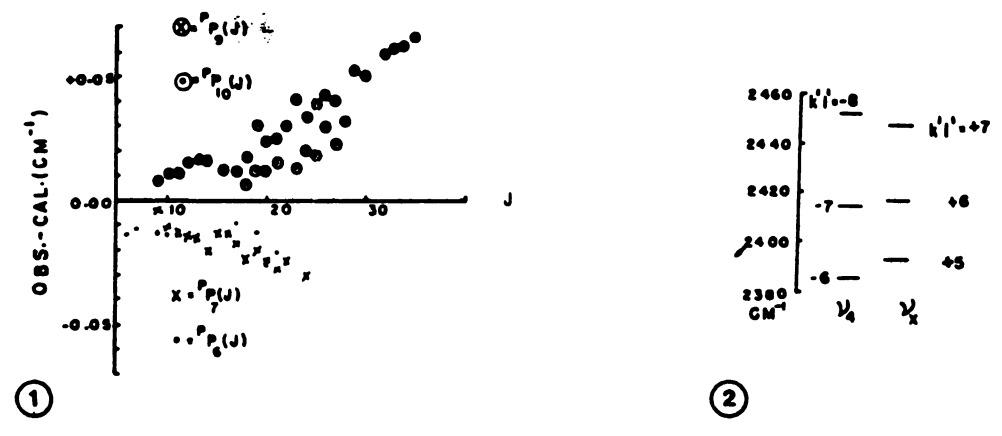


Fig. 1. Wavenumber residuals vs J^{μ} for the $K\Delta K = -6$, -7, -9, and -10 subbands of CD₃Br. Values are from the analysis of Peterson and Edwards (1).

Fig. 2. Relative positions of the levels of ν_4 and the perturbing level ν_2 necessary to explain the residuals plotted in Fig. 1. An x-y Coriolis interaction is assumed.

case of CH₃Br that the perturbing level in question for ν_4 of CD₃Br is most probably $\nu_3 + \nu_5^{\pm 1} + \nu_6^{\pm 1}$.

We present below new experimental data and a quantitative analysis supporting this conclusion. During the final stages of our work we learned that Graner (5) has also suggested that the perturbing vibrational state is $\nu_2 + \nu_3^{\pm 1} + \nu^{\pm 1}$.

EXPERIMENTAL DETAILS

The spectrum of ν_4 of CD₃Br was obtained using the Michigan State University near-infrared grating spectrophotometer interfaced with a PDP-12 minicomputer.

The experimental conditions are listed in Table I. The spectrum was run in segments approximately 12 cm^{-1} long. Each segment was scanned 16 times using an appropriate time constant, then multiply sampled in the manner recommended by Willson and Edwards (6). Following this, each scan was baseline adjusted and made linear in frequency. The 16 scans were subsequently averaged, improving signal-to-noise ratio (S/N) by a factor of \sim 4. The averaged spectrum was then digitally smoothed (6) and deconvoluted, improving the resolution limit by a factor of \sim 2.5 to 0.025 cm⁻¹.

The signal-averaged spectrum was calibrated via a complete run of the CD₃Br spectrum plus calibration gases, using Edser-Butler interference fringes as described by Rao et al. (7).

The portion of the spectrum from 2255 to 2263 cm⁻¹ is shown in Fig. 3.

A table listing the observed frequencies and transition assignments will be included in the Ph.D. thesis of Bardin (8). These data have also been deposited in the Editorial Office of the *Journal of Molecular Spectroscopy*. Please contact the authors first for these data.

DESCRIPTION OF THE SPECTRUM

The ν_4 region from 2242 to 2273 cm $^{-1}$ contains the Q branches $^{\mu}Q_7$ through $^{\mu}Q_{14}$, and $^{\mu}P_{\kappa}(J)$ lines for the $K\Delta K=-3$ to -12 subbands. In general, the

PERTURBATION IN v4 OF CD2Br

TABLE I Experimental Conditions

Region:	2242-2273 cm ⁻
Pressure:	3-6 torr
Path Length:	12.6 m
Detector:	InSb ● 77 K
Grating:	300 1/mm
Calibration Gases:	CO (1-0)ª
	N ₂ O (1,2,0) ^b
Standard Deviation of Calibration fit:	0.0026 cm ⁻¹
Resolution Limit:	0.02-0.03 cm

⁸Line frequencies taken from Ref. (15).

appearance of the spectrum is that of a normal perpendicular band composed of two isotopic components ($CD_3^{79}Br$, $CD_3^{81}Br$) of approximately equal abundance, almost coincident band centers, and slightly different B values. The Q branches degrade slightly to lower wavenumber except for ${}^{P}Q_8$ which is much more strongly red-degraded. The ${}^{79}Br-{}^{81}Br$ isotopic splitting of ${}^{P}P_K(J)$ lines in our spectrum begins to be resolved around J=20 for $K\Delta K=-3$, -4, at which point the doublet spacing of $\simeq 0.025$ cm⁻¹ can be predicted by the different B_0 values (5), an effective α_4^B for each species (1), and an isotopic shift in the ν_4 band center of less that 0.010 cm⁻¹. Figure 3 shows a typical portion of the spectrum and gives many line assignments. We observed no isotopic splittings for $K\Delta K=-7$, -9, -10, -11, or -12 transitions.

The $K\Delta K=-6$ and -8 transitions overlap for low J, and are first resolved beginning at 2261.6 cm⁻¹. The ${}^{p}P_{6}(J)$ series then appears as a well-resolved isotopic doublet which can be followed to about J=50. The ${}^{p}P_{8}(J)$ isotopic doublets have anomalously large separations for $J\geq 12$, and the ${}^{81}\mathrm{Br}$ component, in contrast to the situation in other subbands, is the lower-wavenumber member. The reason for this inversion is discussed below. The wavenumber separation of lines in the ${}^{p}P_{8}(J)$ series is anomalously large and is larger for the ${}^{81}\mathrm{Br}$ component than for the ${}^{79}\mathrm{Br}$ component. The series ${}^{p}P_{8}(J)$ for ${}^{81}\mathrm{Br}$ was assigned through J=20, above which point it merges with ${}^{p}P_{7}(J)$, while the corresponding ${}^{79}\mathrm{Br}$ series was assigned through J=24, above which it merges with the ${}^{p}P_{10}(J)$ series. No convincing assignments could be made for the extensions of the ${}^{p}P_{8}(J)$ series. The line ${}^{p}P_{8}(17)$ for ${}^{81}\mathrm{Br}$ may be split into a doublet by an unidentified, localized perturbation. No lines attributable to $\nu_{3}+\nu_{5}+\nu_{6}$ were observed.

bLine frequencies taken from Ref. (16).

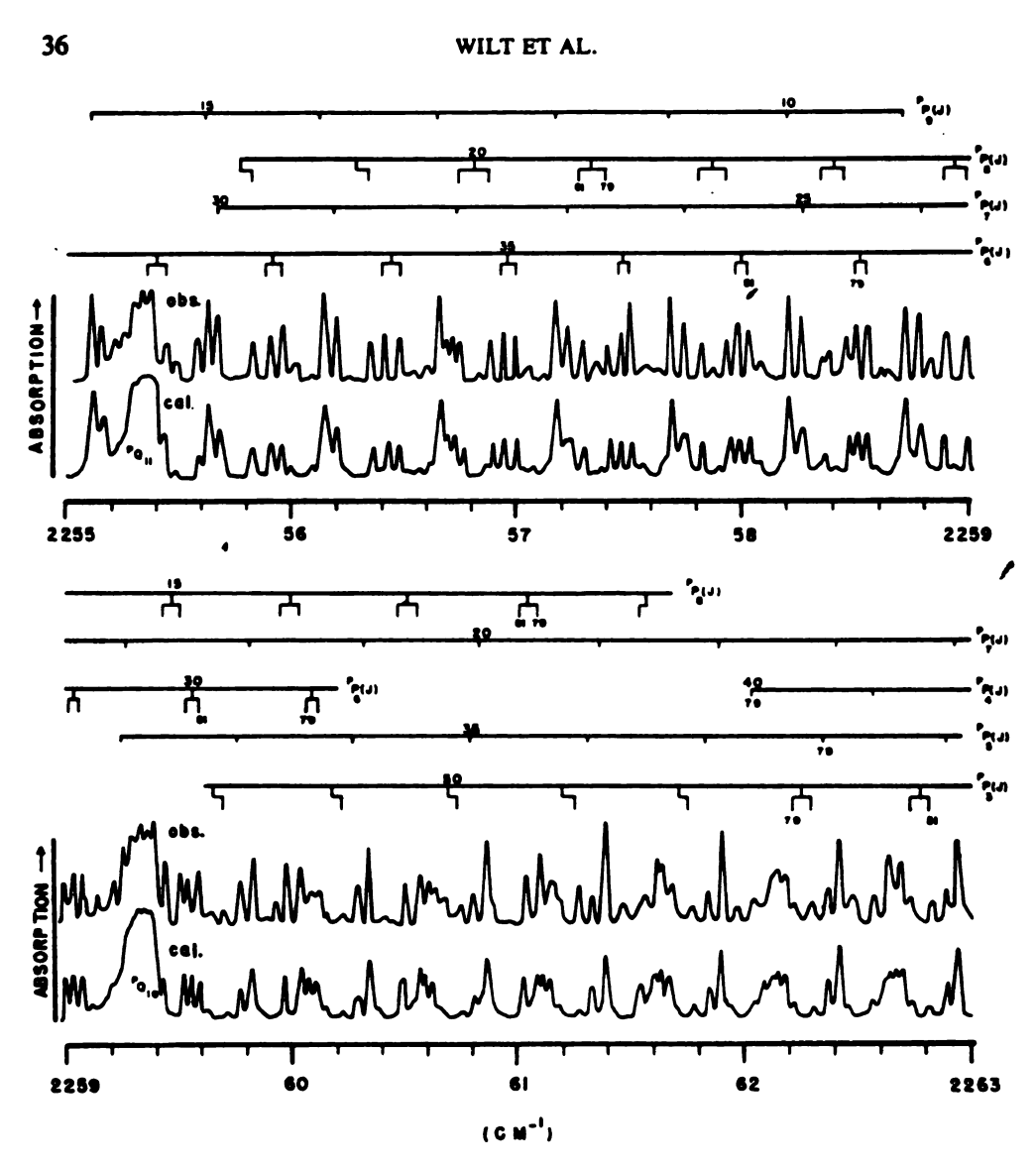


Fig. 3. Experimental and computer-calculated spectra of ν_4 of CD₃Br from 2263 to 2255 cm⁻¹. The experimental conditions are as stated in the text, and the calculation utilizes the constants in Table II for ν_4 and $\nu_3 + \nu_5 + \nu_6$.

THEORETICAL MODEL

We have attributed the anomalies described above to an x-y Coriolis interaction between ν_4 and $\nu_3 + \nu_5^{\pm 1} + \nu_6^{\pm 1}$ in which the k'l' = -7 levels of the former state are nearly degenerate with the k'l' = +6 levels of the latter. We have allowed for the possibility of Fermi resonance between these vibrational states. For each value of J', the upper-state energy levels involved in the interaction may be calculated by diagonalizing, for an appropriate range of k values, the 4×4 matrix shown in Eq. (1).

				_
$ \nu_4^i = 1^{-1}, J, k + 1\rangle$ $ \nu_3 = 1, \nu_3^i = 1^{-1}, \nu_6^i = 1^{-1}, J, k + 1\rangle$	$W_{xy} \cdot F(J, k+1)$	0	¥	$T_{ij} = 1$, $i = 1$, $i = 1$
$ \nu_4^{l_4}=1^{-1}, J, k+1\rangle$	0	$-W_{xy}\cdot F(J,k+1)$	$E(\nu_k^1 = 1^{-1}, J, k+1)$	
= 1, $\nu_3^{l_3}$ = 1 ⁺¹ , $\nu_6^{l_3}$ = 1 ⁺¹ , J, k	ž	$E(\nu_3 = 1, \nu_5^{i_5} = 1^{+1}, \nu_6^{i_6} = 1^{+1}, J, k)$	(HERMITIAN)	-
$ \nu_4^{l_2} = 1^{+1}, J, k \rangle \nu_3 $	$E(\nu_4^t = 1^{+1}, J, k)$			

38

WILT ET AL.

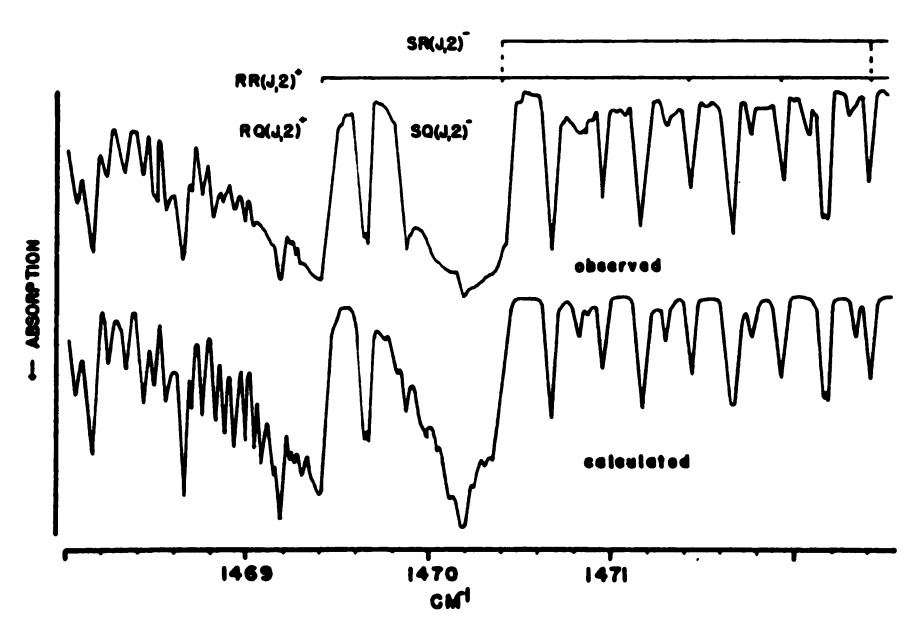


Fig. 4. Comparison of the experimental and computer-generated spectra for the ν_3 , $\nu_3 + \nu_6$ Fermi and x-y Coriolis interacting bands in CH₂I. Experimental data and constants are taken from Refs. (9) and (12).

In Eq. (1), the diagonal elements are defined as follows:

$$E(\nu_4^{\prime\prime}, J, k)/hc = \nu_4^{\prime\prime} + B_4^{\prime}J(J+1) + (A_4^{\prime} - B_4^{\prime})k^2 - 2A_e\zeta_4kl_4 + \eta_2^{\prime}J(J+1)kl_4 + \eta_4^{\prime\prime}l_4k^3 - D_{4J}^{\prime\prime}J^2(J+1)^2 - D_{4JK}^{\prime\prime}J(J+1)k^2 - D_{4K}^{\prime\prime}k^4, \quad (2)$$

$$E(\nu_3, \nu_5^{l_3}, \nu_6^{l_4}, J, k)/hc = \nu_{364}^9 + B_{366}'J(J+1) + (A_{366}' - B_{266}')k^2 \mp 2A_e\zeta_{eff}k$$

$$\pm \eta_{356}^{356}J(J+1)k \pm \eta_{356k^2}^{356k^2} - D_{356J}^{\prime}J^2(J+1)^2 - D_{356JK}^{\prime}J(J+1)k^2 - D_{356K}^{\prime}k^4, \quad (3)$$

where the upper signs are to be taken when $l_s = l_4 = +1$, and the lower when $l_s = l_4 = -1$, $\zeta_{eff} \simeq -(\zeta_s + \zeta_6)$, and the Fermi resonance element (9)

$$W = W_0 + \alpha J(J+1). \tag{4}$$

The x-y Coriolis matrix element (9, 12) is composed of a vibrational factor W_{xy} and a rotational factor

$$F(J, k \pm 1) = \{J(J+1) - k(k \pm 1)\}^{1/2}.$$
 (5)

The dependence of the vibrational factor W_{xy} on fundamental molecular constants may be derived using the phase conventions and procedure of Di Lauro and Mills (10) as extended by Anderson and Overend (11). For C_{3y} molecules we have performed these calculations for two interacting E fundamentals, and for the case studied here: ν_4 with $\nu_3 + \nu_5^{\pm 1} + \nu_6^{\pm 1}$ and, as cited below, ν_5 with $\nu_3 + \nu_6$. The results are available upon request; they agree with those quoted by Matsuura et al. (12) for the case of the fundamentals.

The above theoretical model is adequate to explain the details observed in our spectrum of ν_4 of CD₃Br in the region 2242-2273 cm⁻¹. The wavenumbers of the

observed transitions are calculated from the eigenvalues of the matrix in Eq. (1) and the ground-state energies which are calculated from the expression

$$E_{\text{ground}}(J, k)/hc = B''_J(J+1) + (A''-B'')k^2 - D''_J(J+1)^2 - D''_J(J+1)k^2 - D''_Jk^4.$$
 (6)

The intensities of the transitions are calculated from the eigenvectors of Eq. (1), the appropriate vibrational transition moments M_4 and M_{336} (10), rotational line strengths, nuclear spin statistical weights, and Boltzmann factors. Transitions to the states labeling the two left columns in Eq. (1) are allowed when $\Delta k = +1$, while transitions to the states labeling the two right columns are allowed when $\Delta k = -1$.

We have written a computer program to perform the calculations described above and to generate a computed spectrum composed of overlapping ⁷⁹Br and ⁸¹Br components, the ratio of whose intensities is equal to the ratio of the natural abundances of the isotopes. This program was tested carefully and was found to reproduce correctly the ν_s and $\nu_3 + \nu_6$ Fermi and x-y Coriolis-interacting bands in CH₃I (9) and the simpler case of ν_4 and $\nu_3 + \nu_5 + \nu_6$ in CH₃Br which does not involve a Fermi interaction (3). As an example of the agreement between observed and calculated spectra, we reproduce in Fig. 4 the region 1468–1472 cm⁻¹ in CH₃I (12), where the x-y Coriolis effects are strongest and are responsible for the doubled Q-branch. The calculation of Fig. 4 is based on values quoted in (9) and (12), and used a ratio of vibrational transition moments $|M_{36}/M_5| = 0.10 \pm 0.05$, which is somewhat lower than, but within the error limits previously determined by Maki and Hexter (13). We have also confirmed that the sense of the perturbation is negative, i.e., $W \cdot M_{36} \cdot M_5$ is negative.

We have carefully investigated the effects on line intensities produced by the signs of W, W_{xy} and the ratio of the vibrational transition moments. Our conclusion is that the intensity perturbation depends on the sign of the product of W and the vibrational transition moment ratio, and is independent of the sign of W_{xy} .

ANALYSIS OF THE SPECTRUM

The analysis of ν_4 of CD₃Br that we present here assumes that the x-y Coriolis perturbation is localized in the $K\Delta K=-6$ to -10 subbands and that the band constants of Peterson and Edwards (1), obtained by assigning 0 weights to the $K\Delta K=-7$, -8, and -9 subbands, can be used in Eq. (1) to explain the other transitions in the ν_4 spectrum from 2242 to 2273 cm⁻¹. This assumption was modified slightly as our analysis progressed, and will be discussed below.

We have confined our analysis to the $K\Delta K = -3$ to -10 subbands, for much of which we have improved data (8). However, it became desirable to include as many lines as possible in the $K\Delta K = -3$, -4, and -5 subbands, and many of these occur in the region 2273-2285 cm⁻¹. Hence, we have combined some data from (1) with the new measurements (8). Comparison of lines measured in the two experiments shows that the results are consistent to about $\pm 6 \times 10^{-3}$ cm⁻¹.

We have detected no experimental evidence for a Fermi resonance between ν_4 and $\nu_3 + \nu_5^{\pm 1} + \nu_6^{\pm 1}$; thus our analysis assumes W = 0. Equation (1) then factors

40 WILT ET AL.

TABLE II

Molecular Constants from the ν_4 , $\nu_3 + \nu_5^{\pm 1} + \nu_4^{\pm 1}$ Interaction in CD₃Br

	CD ₃ ⁷⁹ Br		CD ₃ ³¹ Br		
Parameter	٧4	⁴ 3 ⁺⁴ 5 ⁺⁴ 6	v ₄	v3+v5+v6	
v _o	2296.460(5)	2339.17	2296.453(5)	2337.95	
A.	2.58981 a	2.5963 (10)	2.58981 a	2.5963 (10)	
в'	0.257199 a	0.2556 (25)	0.256088 a	0.2561 (25)	
رٰم	1.87 (6)x10 ⁻⁷	₀ ງື	1.89 (6)x10 ⁻⁷	סי	
ס'י ס'זא ס'י	2.115 x10 ⁻⁶	DJK	2.45 (40)x10 ⁻⁶	DJK	
o _K '	0 _K "	o _K "	D _K "	o _K "	
Aζ	0.47422	0.31675	0.47422	0.36867	
W _{xy}	0.01960	(10)	0 .01956	(10)	
A _o	2.603	b	2.603	b	
	0.257328	З с	0.25621	7 с	
B _o DJ	1.945 x	10 ⁻⁷ b	1.945 x	10 ⁻⁷ b	
0 <mark>JK</mark>	2.115 x	10 ⁻⁶ ь	2.115 x	10 ⁻⁶ ь	
$D_{\mathbf{K}}^{\mathbf{o}}$	1.0 x 10) ⁻⁵ b	1.0 x 1	0 ⁻⁵ b	

All parameters quoted in cm⁻¹

The errors quoted in parentheses are estimated uncertainties of the last significant digits.

- a Constrained by either α_4^A or α_4^B from Ref. (1).
- b Constrained to values from Ref. (1).
- c Microwave values from Ref. (5).

into two 2 \times 2 matrices, one of which is the central 2 \times 2 block containing the (2, 2) and (3, 3) diagonal elements of Eq. (1). Furthermore, the third-order terms η_J and η_K of Maes (14) were neglected.

The perturbing level $\nu_3 + \nu_5^{\pm 1} + \nu_4^{\pm 1}$ involves ν_3 , for which the ⁷⁸Br-⁸¹Br isotopic shift (~1.3 cm⁻¹) is appreciable (5). Consequently, the quantitative effects of the perturbation on the ν_4 $^PP_8(J)$ series will be different for each Br isotopic species. The wavenumber separation between the (2, 2) and (3, 3) diagonal elements in Eq. (1) is smaller for CD₃⁸¹Br than for CD₃⁷⁹Br. Since the (2, 2) element is larger than the (3, 3) element, the effect in ν_4 of the perturbation will be a downward shift in the upper-state energy level for $^PP_8(J)$ transitions, the shift being significantly greater for CD₃⁸¹Br than for CD₃⁷⁹Br. These statements are valid for $J'' \leq 24$, the only values for which we have identified transitions. For $^PP_8(20)$ this downward shift is found to be ~0.22 cm⁻¹ for CD₃⁸¹Br and ~0.08 cm⁻¹ for CD₃⁷⁹Br. The result is a strongly red-degraded $K\Delta K = -8$ subband, and an inversion of the

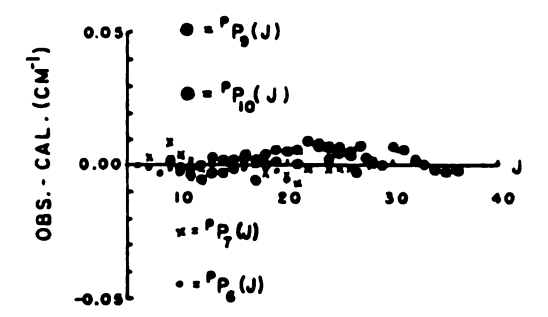


Fig. 5. Wavenumber residuals vs J^{**} for the $K\Delta K = -6$, -7, -9, and -10 subbands of CD₂Br. Values are from the present analysis.

isotopic components in the isotopic doublets from the normal situation where the $CD_3^{a_1}Br$ component is higher in wavenumber.

Our analysis used the values from Ref. (1) for the ground-state constants, except that we allowed for the isotopic variation in $B_{\bullet}(5)$. We assumed no isotopic variation of α_4^A , α_5^B , and $A_0 - A_c \zeta_4$, but found that it was necessary to allow a small isotopic variation in ν_4^0 in order to reproduce the observed isotopic splitting. The distortion constants for $\nu_3 + \nu_5^{\pm 1} + \nu_6^{\pm 1}$ were constrained to ground-state values. The band centers for this state were originally estimated to be near 2338 and 2339.3 cm⁻¹ for the ⁸¹Br and ⁷⁸Br species, respectively. The remaining parameters in Eq. (1) were then varied in a least-squares fit of the assigned transitions.

The band parameters resulting from the least-squares fit are shown in Table II along with the values of constrained constants used in the analysis. These constants reproduce 277 lines in the $K\Delta K = -3$ to -10 subbands with a standard deviation of 6×10^{-3} cm⁻¹. The new residuals shown in Fig. 5 are much reduced compared to those in Fig. 1. Many of the parameters quoted here for $\nu_3 + \nu_i^{\pm 1} + \nu_i^{\pm 1}$ have large uncertainties and the values of ν_0 , $A\zeta$, α^4 , and α^8 are highly correlated. As for CH₃Br (3), $A\zeta$ and the isotopic shift in ν_0 differ somewhat from values predicted from measurements involving fundamentals (5). The uncertainty in ν_0 of $\nu_3 + \nu_3 + \nu_6$ is estimated to be at least 0.3 cm⁻¹. This situation may be attributed to the absence of assigned lines in $\nu_3 + \nu_3 + \nu_6$. It is gratifying to find that W_{xy} is essentially the same for both isotopic species.

In order to reproduce observed wavenumbers for $40 \le J \le 50$ it was found necessary to vary Peterson and Edwards' (1) values of D'_J and D'_{JR} in ν_4 . (The previous analysis was done for an average of the two isotopes and was limited to $J \le 35$.) In addition, observable effects of the x-y Coriolis interaction extend into the $K\Delta K = -3$ subband, e.g., ${}^{P}P_3(50)$ is shifted by about 0.03 cm⁻¹. Thus the assumptions upon which our initial analysis was based, while very useful, are not quite consistent with the observed data.

To improve matters significantly it would be necessary to remeasure the entire band, preferably with a resolution appreciably higher than presently available to us, and to reevaluate the ν_4 band constants using data from throughout the band.

Using the results of the least-squares fit, we have calculated the ν_4 spectrum and included part of the results in Fig. 3. The good agreement shown there is

42 WILT ET AL.

typical, and supports both the model used and the values of the molecular constants given in Table II. Since no transitions attributed to $\nu_3 + \nu_5^{\pm 1} + \nu_6^{\pm 1}$ were observed, we were unable to determine M_{356}/M_4 ; our calculation assumes 0 for this ratio.

ACKNOWLEDGMENTS

Wilt, Hecker, and Fehribach wish to make acknowledgment to the Donors of the Petroleum Research Fund, administered by the American Chemical Society, for the partial support of this research, and to acknowledge generous support from Research Corporation of America. We also thank Professor J. Overend for making available original spectra showing examples of x-y Coriolis perturbations.

RECEIVED: March 26, 1981

REFERENCES

- I. R. W. PETERSON AND T. H. EDWARDS, J. Mol. Spectrosc. 41, 137-142 (1972).
- 2. T. H. EDWARDS AND S. BRODERSON, J. Mol. Spectrosc. 54, 121-131 (1975).
- C. Betrencourt-Stirnemann, G. Graner, and G. Guelachvili, J. Mol. Spectrosc. 51, 216– 237 (1974).
- E. W. Jones, R. J. L. Popplewell, and H. W. Thompson, Spectrochim. Acta 22, 639–646 (1966).
- 5. G. GRANER, J. Mol. Spectrosc., in press.
- 6. P. D. WILLSON AND T. H. EDWARDS, Appl. Spectrosc. Rev. 12, 1-81 (1976).
- K. NARAHARI RAO, C. J. HUMPHREYS, AND D. H. RANK, "Wavelength Standards in the Infrared," pp. 160, 161, Academic Press, New York, 1966.
- DALE E. BARDIN, Ph.D. dissertation, Michigan State University, East Lansing, Michigan, to be submitted.
- 9. H. MATSUURA, T. NAKAGAWA, AND J. OVEREND, J. Chem. Phys. 59, 1449-1456 (1973).
- 10. C. DI LAURO AND I. M. MILLS, J. Mol. Spectrosc. 21, 386-413 (1966).
- 11. D. R. ANDERSON AND J. OVEREND, Spectrochim. Acta 28A, 1231-1251 (1972).
- 12. H. MATSUURA AND J. OVEREND, J. Chem. Phys. 55, 1787-1797 (1971).
- 13. A. MAKI AND R. HEXTER, J. Chem. Phys. 53, 453-454 (1970).
- 14. S. MAES, J. Mol. Spectrosc. 9, 204-215 (1962).
- 15. G. GUBLACHVILI, J. Mol. Spectrosc. 75, 251-269 (1979).
- 16. C. AMIOT AND G. GUELACHVILI, J. Mol. Spectrosc. 59, 171-190 (1976).

APPENDIX III

THE FREQUENCIES AND ASSIGNMENTS OF THE v_4 BAND OF CD_3Br

APPENDIX III THE REQUENCIES AND ASSIGNMENTS OF THE ν_4 BAND OF CD_3Br

CD₃⁷⁹Br-CD₃⁸¹Br v₄ Observed Vacuum Wavenumbers
(add 2200 cm⁻¹ to each value)

		P _{P5} (J)			P _{P6} (J)	
J	79 _{Br}	(unresolved)	81 _{Br}	79 _{Br}	(unresolved)	81 _{Br}
		76.379		•		
5 6		75.863			71.986	
7		75.345			71.471	
8		13.543			70.954	
9		74.308			70.440	
10		73.787			69.929	
ü		73.270			69.412	
12		72.751			68.894	
13		72.233			68.378	
14		71.717			67.857	
15		71.193			67.345	
16		70.684			66.826	
17		70.165			66.310	
18		69.648			65.792	
19		69.129			65.273	
20		68.612			64.751	
21		68.098			64 .240	
22					63.721	
23						
24						
25	65.997					
26	64.475					
27	64.959					
28	64.448			40.00 0		60.115
29	63.919			60.061		60.113
30	63.410			59.544		59.587
31	62.886			59.025		59.065
32	62.365			58.506		58.557
33	61.844			57.987		58.043
34	61.331			57.468		57.517
35	60.808			56.947		57.004
36	60.291			56.431		56.487 55.966
37	59.771			55.912		55.457
38	59.250			55.387		54.930
39				54.870		J4.730
40				54.352		54.411 53.895
41				53.828		53.381
42				53.314		52.863
43				52.792 52.280		52.341
44				34.2 5 U		
45				51.757		51.858
46				50 71P		50.792
47				50.718		50.792
48				50.195		20,213

(add 2200 cm⁻¹ to each value)

	P _{P3} (J)		P	P ₄ (J)	
J	79 Br (unresolved)	⁶¹ Br	78	esolved)	Br
3					
4	84.500			80.711	
5	84.012			80.206	
6	83.489			79.689	
7 8	82.974			79.168	
9	81.939			78.142	
10	81.426				
11	80.913			77.104	
12	80.400			76.592	
13	79.876			76.087	
14 15	79.368			75.569	
16	78.326			74.533	
17 18	. 77.815 77.294			74.012	
19	76.784			73.491 72.974	
20	76.268			72.456	
21	75,738			71.918	
22	75.224			71.401	
23	<u> </u>			70.880	
24	74.189		70.360		70.382
25	73.671			69.847	
26	73.131	73.182	69.319		69.357
27	72.604	72.661	68.807		
28	72.088	72.140	68.285		68.323
29 30	71.570	71.624	67.763 67.231		67.806 67.279
31	70.527	70.584	66.722		66.769
32	70.008	70.070	66.202		66.254
33 34	69.488 68.970	69.552 69.036	65.687 65.169		65.739 65.219
35	68.452	68.523	64.658		64.711
36	67.931	68,000	64.132		64.193
37	67.417	67.479	63.611		
38	66.894	66.963	63.091		
39	66.375	66.447	62.567		
40	65.859	65.923	62.051		
41	65.338	65.396			
42	64.818	64.890			
43 44	64.294 63.778	64.369 63.855			
45	93,110	43.633			
46	62.732	62,818			
47	62.222	62.302			
48		61.773			
49		61.271			
50		60.747			

 $\frac{\text{CD}_3^{79}\text{Br-CD}_3^{81}}{\text{(add 2200 cm}^{-1} \text{ to each value)}}$

P _{P7} (J)		P ₈ (J)		
J	(unresolved)	79 _{Br}	81 _{Br}	
7	67.585			
7 8 9				
9	66.548			
10	66.037			
11	65.520		61.565	
12	65.007	61.087	61.027	
13	64.491	60.568	60.503	
14	63.976	60.042	59.966	
15	63.459	59.511	59.438	
16	62.940	58.990	58.909	
17	62.422	58.466	58.365	
18	61.901	57.943	57.829	
19	61.388	57.413	57.303	
20	60.863	56.892	56.763	
21	60.342	56.363		
22	59.830	55.839		
23				
24	58.794	54.777		
25	58.271			
26	57.750			

CD₃⁷⁹Br-CD₃⁸¹ v₄ Observed Vacuum Wavenumbers

(add 2200 cm⁻¹ to each value)

	P _{Pg} (J)	P _{P10} (J)
J	(unresolved)	(unresolved)
9	58.725	
10	58.207	54.250
11	57.691	53.736
12	57.176	53.223
13	56.665	52.712
14	56.152	52.197
iš	55.640	51.682
16	55.132	51.169
17	54.609	50,653
18	54 . 108	50.140
19	53.589	49.628
20	53.080	49.105
21	52,568	48.592
22	52.057	48.086
23	51.543	47.571
24	51.023	47.055
25	50.515	46.538
26	49.999	46.024
27	49.478	45.511
28	48.971	44.990
29	48.456	44.481
30	47.949	43.958
31	47.435	43.453
32	46.918	42.927
33	46.403	42.429
34	45.888	
35	45.375	
36	44.863	

APPENDIX IV

THE FREQUENCIES AND ASSIGNMENTS OF THE ν_{5} BAND OF CH_{3}CN

APPENDIX IV

THE FREQUENCIES AND ASSIGNMENTS OF THE v_5 BAND OF $\mathrm{CH_3CN}$

The frequencies from v_5 of CH₃CN given in this appendix were part of the output from the program SYMFIT, a linear least squares fit of v_5 and $2v_5(\bot)$ of CH₃CN. The columns in the table are:

- 1. Assignment of each transition $(^{\Delta K} \Delta J_K(J) \equiv \Delta K \Delta J K, J)$
- 2. The weight assigned each transition.
- 3. The observed frequency of each transition.
- 4. The frequency calculated after the least squares fit.
- 5. The residuals, observed frequency minus calculated frequency.

K J	WI	OBS FREQ	CALC FREQ	OBS-CALC
PR 3, 6	0.00		2989.6281	
PR 3, 5	0.00		2989.0158	
PR 3, 4	0.00		2988.4034	
PR 3, 3	0.00		2987.7908	
PP 3, 3	0.00		2983.497 0	
PP 3, 4	0.00		2982.8829	
PP 3, 4	0.00		2982.2686	
PP 3, 6	0.00		2981.6542	
PP 2,22	0.00	2981.1620	2981.2016	-0.0396
	0.00	2981.7820	2981.8165	-0.0345
PP 2,21 PP 2,20	0.00	2982.3780	2982.4316	-0.0536
•	0.00	2983.0090	2983.0468	-0.0378
PP 2,19		2984.89 4 0	2984.8932	0.0008
PP 2,16	0.00	2986.1580	2986 .12 4 3	0.0337
PP 2,14	0.00			
PP 2,13	0.00	2986.7610	2986.7399	0.0211
PP 2,12	0.00	2987.4070	2987 .3554	0.0516
PP 2,11	0.00	2987.9930	2987.9708	0.0222
PP 2,10	0.00	2988.6330	2988.5862	0.0468
PP 2, 9	0.00	2989.1870	2989.2014	-0.0144
PP 2, 8	0.00	2989.8840	2989.8165	0.0675
PP 2, 7	0.00	2990.4880	2990.4315	0.0565
PP 2, 6	0.00	2991.1240	2991.0463	0.0777
PP 2, 5	0.00	2991.7400	2991.6609	0.0791
PP 2, 4	0.00	2992.3680	2992.2754	0.0926
PP 2, 3	0.00	2992.9930	2992.8897	0.1033
PP 2, 2	0.00	2993.6050	2993.5037	0.1013
PR 2, 2	0.00		2996.5709	
PR 2, 3	0.00		2997.1836	
PR 2, 4	0.00		2997.7962	
PR 2, 5	0.00		2998.4086	
PR 2, 6	0.00		2999.0207	
PR 2, 7	0.00		2999.6327	
PR 2, 8	0.00		3000.2445	
PR 2, 9	0.00		3000.8561	
PR 2,10	0.00		3001 .4 676	
PR 2,17	0.00	3005.7330	3005.7451	-0.0121
PR 2,18	0.00	3006.3600	3006.3561	0.0039
PR 2,19	0.00	3006.9710	3006.9671	0.0039
PR 2,20	0.00		3007.5781	
PR 2,21	0.00	3008.2060	3008.1893	0.0167
PR 2,22	0.00		3008.8006	
PR 2,23	0.00	3009.4450	3009.4121	0.0329
PR 2,24	0.00		3010.0237	
PR 2,25	0.00	3010.6980	3010.6357	0.0623
PP 1,25	0.00	2988.6330	2988.6842	-0.0512
PP 1,23	0.00	2989.8840	2989.9140	-0.0300
PP 1,22	0.00	2990.4880	2990.5292	-0.0412
PP 1,21	0.00	2991.1240	2991.1447	-0.0207
_,				/

1	K J	ı wi	OBS FREQ	CALC FREQ	OBS-CALC
PP	1,20	0.00	2991.7400	2991.7604	-0.0204
	1,1		2992.3680	2992.3761	-0.0081
	1,1		2992.9930	2992.9920	0.0010
	1,17		2993.6050	2993.6080	-0.0030
	1,10		2994.2540	2994.2240	0.0300
	1,1		2995.4790	2995.4559	0.0231
	1,13		2996.1030	2996.0719	0.0311
	1,1		2996.7390	2996.6877	0.0513
	1,1		2997.3420	2997.3035	0.0385
	1,10		2997.9500	2997.9192	0.0308
	1, 9		2998.5380	2998.5347	0.0033
	1,		2999.1560	2999.1500	0.0060
PP	1,	7 0.00	2999.8150	2999.7652	0.0498
PP	1, (0.00	3000.4270	3000.3802	0.0 4 68
PP	1, !	0.00	3001.0310	3000.9950	0.0360
PP	1,	0.00	3001.6430	3001.6096	0.0334
PP	1, 3	0.00	3002.2710	3002.2240	0.0470
PP	1, 3	2 0.00	3002.8920	3002.8381	0.0539
PP	1,	0.00	3003.4870	3003.4521	0.0349
PR	1, 3	0.00	3005.3310	3005.2924	0.0386
PR	1, 3	2 0.00	3005 .94 20	3005.9053	0.0367
	1, 3		3006.5720	3006.5180	0.0540
PR	1,	4 0.00	3007.1850	3007.1305	0.0545
PR	1, !	5 0.00	3007.8060	3007 . 7427	0.0633
PR	1, (0.00	3008.4120	3008.3548	0.0572
PR	1,	7 0.00		3008.9666	
PR	1,	0.00	3009.6430	3009.5782	0.0648
	1, 9			3010.1896	
PR	1,1	0.00		3010.8008	
RP	0,3	B 0.00	2989.7390	2989.9373	-0.1983
RP	0,3	7 0.00	2990.3840	2990.5479	-0.1639
RP	0,30	0.00	2990.9920	2991.1594	-0.1674
RP	0,2	9 0.00	2995.4790	2995.4588	0.0202
	0,2		2996.1030	2996. 0751	0.0279
	0,2		2996.7390	2996.6918	0.0472
	0,2		2997.3420	2997.3087	0.0333
	0,2		2997.9500	2997.9259	0.0241
	0,2		2998.5380	2998.5434	-0.0054
	0,2		2999.1560	2999. 1610	-0.0050
	0,2		2999.8150	2999.7788	0.0362
	0,2		3000.4270	3000.3966	0.0304
	0,2		3001.0310	3001.0145	0.0165
	0,1		3001.6430	3001.6325	0.0105
	0,1		3002.2710	3002.2504	0.0206
	0,17		3002.8920	3002.8683	0.0237
	0,10		3003.4870	3003.4861	0.0009
	0,1		3004.6930	3004.7214	-0.0284
RP	0,13	3 1.00	3005.3310	3005.3388	-0.0078

K J	WI	OBS FREQ	CALC FREQ	OBS-CALC
RP 0,12	0.25	3005.9420	3005.9560	-0.0140
RP 0,11	8.00	3006.5720	3006.5730	-0.0010
RP 0,10	2.00	3007.1850	3007.1898	-0.0048
RP 0, 9	8.00	3007.8060	3007.8064	-0.0004
RP 0, 8	1.00	3008.4120	3008.4226	-0.0106
RP 0, 7	8.00	3009.0410	3009.0386	0.0024
RP 0, 6	1.00	3009.6430	3009.6543	-0.0113
RP 0, 5	8.00	3010 .2680	3010.26 <i>9</i> 7	-0.0017
RP 0, 4	0.50	3010.8710	3010.8848	-0.0138
RP 0, 3	0.06	3011.4770	3011.4995	-0.0225
RP 0, 2	0.25	3012.1320	3012.1139	0.0181
RP 0, 1	0.13	3012.7100	3012.7279	-0.0179
RR 0, 0	8.00	3013 .954 0	3013.9549	-0.0009
RR 0, 1	0.00		3014.5679	
RR 0, 2	4.00	3015.1850	3015.1806	0.0044
RR 0, 3	0.00	2016 4120	3015.7928	0.000
RR 0, 4	1.00	3016.4130	3016.4047	0.0083
RR 0, 5	0.00	2017 6250	3017.0163	0.0074
RR 0, 6	2.00	3017.6350	3017.6276	0.0074
RR 0, 7	2.00	3018.2460	3018.2385	0.0075
RR 0, 8	1.00	3018.8600	3018.8491	0.0109
RR 0, 9	0.00		3019.4593	
RR 0,10	0.00		3020.0693	
RR 0,11	0.00		3020.6790	
RR 0,12	0.00	2021 0020	3021.2885	0.0157
RR 0,13	0.50	3021.8820	3021.8977	-0.0157
RR 0,14	0.13	3022.5340	3022.5067	0.0273
RR 0,15 RR 0,16	0.00	3023.0860	3023.1155	-0.0295
•	4.00	3023.7240	3023.7241	-0.0001
RR 0,17 RR 0,18	0.50 0.50	3024.3210 3024.9550	3024.3325 3024.9409	-0.0115 0.0141
RR 0,19	0.50	3025.5620	3025.5491	0.0129
RR 0,20	1.00	3025.5620	3026.1573	
RR 0,21	0.00	3026.8000	3026.7654	0.0107 0.03 4 6
RR 0,22	0.00	3027.4080	3027.3736	0.0344
RR 0,23	4.00	3027.9790	3027.9818	-0.0028
RR 0,24	0.00	3028.6300	3028.5900	0.0400
RR 0,25	0.00	3029 . 22 4 0	3029.1984	0.0256
RR 0,26	0.00	3029.8640	3029.8069	0.0571
RP 2,15	0.00	3022.4340	3022.4731	-0.0391
RP 2,14	1.00	3023.0810	3023.0903	-0.0093
RP 2,13	0.25	3023.7240	3023.7073	0.0167
RP 2,12	4.00	3024.3210	3024.3242	-0.0032
RP 2,11	0.50	3024.9550	3024.9409	0.0141
RP 2,10	4.00	3025.5620	3025.5574	0.0046
RP 2, 9	1.00	3026.1680	3026.1736	-0.0056
RP 2, 8	1.00	3026.8000	3026.7896	0.0104
RP 2, 7	8.00	3027.4080	3027.4054	0.0026
21 I	0 .00	JUL / 1 TUOU	JU4/ • 9UJ9	0.0020

	K	J	WI	OBS FREQ	CALC FREQ	OBS-CALC
RP	2.	6	0.00		3028.0209	
RP	-		1.00	3028.6300	3028.6361	-0.0061
RP			0.00	3029.2240	3029.2510	-0.0270
RP			2.00	3029.8640	3029.8656	-0.0016
RR			0.50	3033.5600	3033.5465	0.0135
RR			1.00	3034.1690	3034.1588	0.0102
RR	•		2.00	3034.7790	3034.7708	0.0082
RR			4.00	3035.3820	3035.3825	-0.0005
RR			2.00	3035.9890	3035.9938	-0.0048
RR			2.00	3036.6010	3036.6049	-0.0039
RR			8.00	3037.2150	3037.2157	-0.0007
	$\bar{2}$,		2.00	3037.8220	3037.8262	-0.0042
	2,		4.00	3038.4400	3038.4364	0.0036
	2,		0.25	3039.0300	3039.0464	-0.0164
	2,		0.13	3039.6750	3039.6561	0.0189
	2,		1.00	3042.0710	3042.0930	-0.0220
	2,		1.00	3042.6790	3042.7019	-0.0229
	3,		8.00	3024.1380	3024.1405	-0.0025
	3,		0.00	3024.7300	3024.7575	-0.0275
	3,		1.00	3025.3840	3025.3748	0.0092
	3,		2.00	3025.9970	3025.9923	0.0047
	3,		4.00	3026.6130	3026.6100	0.0030
	3,		1.00	3027.2200	3027.2278	-0.0078
	3,		4.00	3028.4670	3028.4637	0.0033
	3,		2.00	3029.0870	3029.0816	0.0054
	3,		0.25	3029.7180	3029.6996	0.0184
	3,		0.13	3030.3380	3030.3175	0.0205
	3,		0.00	3031.5640	3031.5530	0.0110
	3,		8.00	3032.1720	3032.1706	0.0014
	3,		8.00	3032.7890	3032.7880	0.0010
	3,		0.13	3033.3860	3033.4052	-0.0192
	3,		0.13	3034.0030	3034.0221	-0.0191
	3,		0.50	3034.6270	3034.6389	-0.0119
	3,		0.00	3035.2120	3035.2554	-0.0434
RP	3,	8	0.00		3035.8716	
RP			0.00		3036.4876	
RP			0.00		3037.1032	
RP			0.00		3037.7185	
RP			0.00		3038.3335	
RP			0.00		3038.9481	
RR	3,	3	1.00	3043.2310	3043.2406	-0.0096
RR	3,	4	4.00	3043.8490	3043.8524	-0.0034
RR	3,	5	4.00	3044.4640	3044.4638	0.0002
RR	•		4.00	3045.0720	3045.0749	-0.0029
RR			4.00	3045.6830	3045.6857	-0.0027
RR	3,	8	4.00	3046.2970	3046.2961	0.0009
RR	•		4.00	3046.9100	3046.9062	0.0038
RR	3,	10	0.00	3047.4650	3047.5160	-0.0510

K	J	WI	OBS FREQ	CALC FREQ	OBS-CALC
RR 3	.11	1.00	3048.1160	3048.1255	-0.0095
RR 3		0.25	3048.7210	3048.7348	-0.0138
RR 3	,13	1.00	3049.3360	3049.3438	-0.0078
RR 3		0.25	3049.9380	3049.9526	-0.0146
RR 3		0.00	3050.5260	3050.5611	-0.0351
RR 3		2.00	3051.1630	3051.1695	-0.0065
RR 3		0.00	3051.7150	3051.7778	-0.0628
RR 3		0.50	3052.3740	3052.3859	-0.0119
RR 3	3,19	1.00	3053.0030	3052.9939	0.0091
RR 3	3,20	4.00	3053.6010	3053.6018	-0.0008
RR 3		1.00	3054.2160	3054.2097	0.0063
RR 3	3,22	2.00	3054.8220	3054.8175	0.0045
RR 3	3,23	0.50	3055.4380	3055.4254	0.0126
RR 3	3,24	2.00	3056.0380	3056.0334	0.0046
RR 3	3,25	1.00	3056.6500	3056.6415	0.0085
RR 3		8.00	3057.2510	3057 .249 7	0.0013
RR 3	27,	8.00	3057.8590	3057.8581	0.0009
RR 3	3,29	0.25	3059.0570	3059.0757	-0.0187
RR 3	3,30	0.50	3059.6640	3059.6849	-0.0209
RR 3	3,31	0.00	3060.2660	3060.2945	-0.0285
RR 3	3,32	0.00	3060.8810	3060.9046	-0.0236
RP 4	1,19	0.50	3038.0870	3038.0871	-0.0001
RP 4	1,18	0.06	3038.6740	3038.7056	-0.0316
RP 4	1,17	0.25	3039.3360	3039.3239	0.0121
RP 4	1,16	0.00	3039.9450	3039.9422	0.0028
RP 4	1,15	0.00	3040.5640	3040.5603	0.0037
RP 4	1,14	0.50	3041.1870	3041.1783	0.0087
RP 4	1,13	8.00	3041.7980	3041.7960	0.0020
RP 4	-	0.00	3042.4470	3042.4135	0.0335
RP 4	1,11	0.00	3042.9990	3043.0308	-0.0318
RP 4	1,10	2.00	3043.6430	3043.6478	-0.0048
	1, 9		3044.2600	30 44.264 5	-0.0045
RP 4	•	0.06	3044.9120	3044.8810	0.0310
RP 4		0.00		3045.4970	
RP 4		0.25	3046.0990	3046.1128	-0.0138
RP 4	•	0.25	3046.7140	3046.7282	-0.0142
RP 4		1.00	3047.3340	3047.3432	-0.0092
RR 4	•	0.50	3052.8740	3052.8611	0.0129
RR 4		1.00	3053.4810	3053.4723	0.0087
RR 4	•	1.00	3054.0930	3054.0830	0.0100
RR 4		2.00	3054.6860	3054.6934	-0.0074
RR 4	•	8.00	3055.3060	3055.3035	0.0025
RR 4		8.00	3055.9130	3055.9131	-0.0001
RR 4		8.00	3056.5250	3056.5225	0.0025
RR 4	-	4.00	3057.1280	3057.1315	-0.0035
RR 4	-	1.00	3057.7 4 70	3057.7403	0.0067
RR 4	-	0.00	3058.3350	3058.3487	-0.0137
RR 4	,14	0.50	3058.9440	3058.9569	-0.0129

_	_			03.7.0 ED.EO	ODG. CAT C
K	J	WI	OBS FREQ	CALC FREQ	OBS-CALC
RR 4,	15	0.00	3059.5050	3059.5649	-0.0599
RR 4,		1.00	3060.1600	3060.1726	-0.0126
RR 4,		1.00	3060.7650	3060.7802	-0.0152
RR 4,		0.13	3061.4000	3061.3875	0.0125
RR 4,		0.06	3061.9530	3061.9948	-0.0418
RP 5,		0.50	3048.2560	3048.2539	0.0021
RP 5,		0.00		3052.5802	
RP 5,		0.00		3053.1971	
RP 5,		0.00		3053.8137	
RP 5,		0.00		3054.4299	
RP 5,		0.00		3055.0458	
RP 5,		0.00		3055.6613	
RR 5,		0.50	3062.4130	3062.4038	0.0092
RR 5,		1.00	3063.0000	3063.0142	-0.0142
RR 5,		0.25	3063.6060	3063.6242	-0.0182
RR 5,		8.00	3064.2300	3064.2338	-0.0038
RR 5,		0.13	3064.8200	3064.8431	-0.0231
RR 5,		0.13	3065.4300	3065.4519	-0.0219
RR 5,		0.13	3066.0380	3066.0604	-0.0224
RR 5,		2.00	3066.6730	3066.6686	0.0044
RR 5,		0.00	3067.2500	3067.2765	-0.0265
RR 5,		8.00	3068.4890	3068.4913	-0.0023
RR 5,		8.00	3069.1000	3069.0984	0.0016
RR 5,		0.25	3069.7190	3069.7052	0.0138
RR 5,		2.00	3070.3150	3070.3118	0.0032
RR 5,	19	1.00	3070.9240	3070.9182	0.0058
RR 5,		1.00	3071.5340	3071.5245	0.0095
RR 5,	21	0.00	3072.1230	3072.1307	-0.0077
RR 5,	22	0.00	3072.7610	3072.7368	0.0242
RR 5,	23	0.00	3073.3440	3073.3429	0.0011
RR 5,		0.00	3073.9490	3073.9490	
RR 5,	25	0.00	3074.5420	3074.5551	-0.0131
RR 5,		0.00	3075.1510	3075.1613	-0.0103
RR 5,		0.00	3075.7400	3075.7676	-0.0276
RP 6,	10	0.00		3061.4331	
RP 6,	9	0.00		3062.0502	
RP 6,	8	0.00		3062.6670	
RP 6,	7	0.00		3063.2833	
RP 6,	6	0.00		3063.8993	
RR 6,	6	0.00	3071.8360	3071.8655	-0.0295
RR 6,	7	0.00	3072.4630	3072.4751	-0.0121
RR 6,		0.00	3073.1100	3073.0843	0.0257
RR 6,		0.00	3073.7340	3073.6930	0.0410
RR 6,	10	0.00	3074.3510	3074.3013	0.0497
RR 6,		0.00	3074.9780	3074.9093	0.0687
RR 6,		0.00	3075.6140	3075.5169	0.0971
RR 6,		0.00		3076.1241	
RR 6,		0.00	3076.8080	3076.7310	0.0770
- •	-	· - -		= = : • • • • • • • • • • • • • • • • •	

K J	WI	OBS FREQ	CALC FREQ	OBS-CALC
RR 6,15	0.00	3077.4260	3077.3375	0.0885
RR 6,16	0.00	3078.0470	3077.9438	0.1032
RR 6,17	0.00	3078.6500	3078.5499	0.1001
RR 6,18	0.00	3079.2720	3079.1556	0.1164
RR 6,19	0.00	3079.8950	3079.7612	0.1338
RR 6,20	0.00	3080.5430	3080.3666	0.1764
RR 7, 7	0.00	3081.1530	3081.2447	-0.0917
RR 7, 8	0.00	3081.7690	3081.8534	-0.0844
RR 7, 9	0.00	3082.3750	3082.4616	-0.0866
RR 7,10	0.00	3082.9960	3083.0694	-0.0734
RR 7,11	0.00	3083.6630	3083.6767	-0.0137
RR 7,12	0.00	3084.2280	3084.2836	-0.0556
RR 7,14	0.00	3085.4500	3085.4963	-0.0463
RR 7,15	0.00	3086.0610	3086.1022	-0.0412
RR 7,16	0.00	3086.6450	3086.7077	-0.0627
RR 7,17	0.00	3087.2430	3087.3128	-0.0698
RR 7,18	0.00	3087.8900	3087.9178	-0.0278
RR 7,19	0.00	3088.4440	3088.5224	-0.0784
RR 7,20	0.00	3089.0410	3089.1269	-0.0859
RR 7,21	0.00	3089.6350	3089.7312	-0.0962
RR 7,22	0.00	3090.2110	3090.3353	-0.1243
RR 7,23	0.00	3090.8520	3090.9393	-0.0873
RR 7,24	0.00	3091.4840	3091.5433	-0.0593
RR 7,25	0.00	3092.1090	3092.1472	-0.0382
RR 7,26	0.00	3092.6540	3092.7511	-0.0971
RR 7,28	0.00	3093.9370	3093.9591	-0.0221
RR 7,29	0.00	3094.5470	3094.5632	-0.0162
RR 7,30	0.00	3095.1450	3095.1676	-0.0226
RR 7,31	0.00	3095.7150	3095,7722	-0.0572
RR 8, 8	1.00	3090.5320	3090.5420	-0.0100
RR 8, 9	0.50	3091.1390	3091.1496	-0.0106
RR 8,10	4.00	3091.7610	3091.7568	0.0042
RR 8,11	2.00 4.00	3092.3580	3092.3635 3092.9697	-0.0055
RR 8,12 RR 8,13	0.00	3092.9720	3093.5755	0.0023
RR 8,14	0.06	3094.2070	3094.1809	0.0261
RR 8,15	2.00	3094.7900	3094.7860	0.0040
RR 8,16	0.06	3095.3650	3095.3906	-0.0256
RR 8,17	0.06	3095.9690	3095.9949	-0.0259
RR 8,18	8.00	3096.5970	3096.5989	-0.0019
RR 8,19	0.25	3097.1870	3097.2026	-0.0156
RR 8,21	0.25	3098.4220	3098.4093	0.0127
RR 8,22	0.00	3098.9650	3099.0124	-0.0474
RR 8,23	0.06	3099.6390	3099.6153	0.0237
RR 8,24	0.00	3100.2440	3100.2181	0.0259
RR 8,25	0.00	3100.8520	3100.8208	0.0312
RR 8,28	0.25	3102.6120	3102.6288	-0.0168
RR 9, 9	2.00	3099.7670	3099.7606	0.0064
, -	-100	343311010	3033.7000	0.0004

K J	WI	OBS FREQ	CALC FREQ	OBS-CALC
RR 9,10	1.00	3100.3590	3100.3671	-0.0081
RR 9,11	4.00	3100.9760	3100.9731	0.0029
RR 9,12	2.00	3101.5730	3101.5786	-0.0056
RR 9,13	0.00		3102.1837	
RR 9,14	8.00	3102.7870	3102.7883	-0.0013
RR 9,15	8.00	3103.3920	3103.3924	-0.0004
RR 9,16	4.00	3103 . 9990	3103.9962	0.0028
RR 9,17	1.00	3104.6080	3104.5996	0.0084
RR 9,18	0.25	3105.1890	3105.2026	-0.0136
RR 9,19	4.00	3105.8070	3105.8053	0.0017
RR 9,20	8.00	3106.4090	3106.4077	0.0013
RR 9,21	0.00	3106.9750	3107.0098	-0.0348
RR 9,22	4.00	3107.6140	3107.6118	0.0022
RR 9,23	0.00	3108.2490	3108.2135	0.0355
RR 9,24	0.50	3108.8080	3108.8151	-0.0071
RR 9,25	0.06	3109.4360	3109.4165	0.0195
RR 9,26	0.50	3110.0270	3110.0179	0.0091
RR 9,28	0.00	3111.2410	3111.2206	0.0204
RR 9,29	0.25	3111.7900	3111.8220	-0.0320
RR 9,30	0.00	3112.4300	3112.4235	0.0065
RR 9,31	0.25	3113.0140	3113.0251	-0.0111
RR 9,32	0.25	3113.6110	3113.6270	-0.0160
RR10,10	0.00	3108.8080	3108.9070	-0.0990
RR10,11	0.00	3109.4340	3109.5123	-0.0783
RR10,12	0.00	3110.0260	3110.1171	-0.0911
RR10,13	0.00	2111 2400	3110.7213	_0 0050
RR10,14	0.00	3111.2400	3111.3250 3111.9283	-0.0850
RR10,15 RR10,16	0.00 0.00	3112.4290	3112.5311	-0.1021
RR10,17	0.00	3113.0140	3113.1335	-0.1195
RR10,17	0.00	3113.6110	3113.7355	-0.1245
RR11,11	0.00	3117.9360	3117.9918	-0.0558
RR11,12	0.00	3118.5560	3118.5957	-0.0397
RR11,13	0.00	3119.1310	3119.1991	-0.0681
RR11,14	0.00	3119.7350	3119.8019	-0.0669
RR11,15	0.00	3120.3540	3120.4043	-0.0503
RR11,16	0.00	3120.9300	3121.0061	-0.0761
RR11,17	0.00	3121.5060	3121.6075	-0.1015
RR11,18	0.00	3122.1450	3122.2084	-0.0634
RR11,19	0.00	3122.7090	3122.8089	-0.0999
RR11,20	0.00	3123.2930	3123.4091	-0.1161
RR11,21	0.00	3123.9190	3124.0089	-0.0899
RR11,22	0.00	3124.5180	3124.6084	-0.0904
RR11,23	0.00	3125.0650	3125.2076	-0.1426
RR11,24	0.00	3125.6330	3125.8065	-0.1735
RR11,25	0.00	3126.2660	3126.4053	-0.1393
RR12,12	0.00		3127.0297	
RR12,13	0.00	3127.4830	3127.6321	-0.1491

K J	WI	OBS FREQ	CALC FREQ	OBS-CALC
RR12,14	0.00		3128.2340	
RR12,15	0.00	3128.6920	3128.8354	-0.1434
RR12,16	0.00	3000000	3129.4362	7,000
RR12,17	0.00		3130.0365	
RR12,18	0.00		3130.6363	
•				
RR12,19	0.00	0101 6000	3131.2356	0.1516
RR12,20	0.00	3131.6830	3131.8346	-0.1516
RR12,23	0.00	3133.4500	3133.6292	-0.1792
RR12,25	0.00	3134.6150	3134.8241	-0.2091
RR13,13	0.00	3135.8890	3136.0405	-0.1515
RR13,14	0.00	3136.4600	3136.6414	-0.1814
RR13,15	0.00		3137.2417	
RR13,16	0.00	3137.6680	3137.8415	-0.1735
RR13,17	0.00	3138.2170	3138.4406	-0.2236
RR13,18	0.00	3138.8460	3139.0393	-0.1933
RR13,19	0.00	323010-00	3139.6374	012500
RR13,20	0.00		3140.2351	
		21.40 65.40		_0 1792
RR13,21	0.00	3140.6540	3140.8323	-0.1783
RR13,23	0.00	3141.8510	3142.0256	-0.1746
RR13,24	0.00	3142.4660	3142.6217	-0.1557
RR13,26	0.00	3143.6560	3143.8131	-0.1571
RR14,15	0.00	3145.4160	3145.6490	-0.2330
RR14,16	0.00	3146.0740	3146.2476	-0.1736
RR14,18	0.00	3147.2350	3147.4430	-0.2080
PQ 7, 0	0.00		2947.0904	
PQ 6, 0	0.00		2956.7719	
PQ 5, 0	0.00		2966.3657	
PQ 4, 0	0.00		2975.8849	
PQ 3, 0	0.00		2985.3383	
PQ 2, 0	0.00		2994.7312	
PQ 1, 0	0.00		3004.0657	
RQ 0,-1	0.00		3013.3416	
RQ 1,-1	0.00		3022.5567	
RQ 2,-1	0.00		3031.7075	
RQ 3,-1	0.00		30 40. 7899	
RQ 4,-1	0.00		30 49. 79 9 5	
RQ 5,-1	0.00		3058.7324	
RQ 6,-1	0.00		3067.5857	
RQ 7,-1	0.00		3076.3579	
RQ 8,-1	0.00		3085.0499	
RQ 9,-1	0.00		3093.6650	
RO10,-1	0.00		3102.2102	
RQ11,-1	0.00		3110.6961	
-				
RQ12,-1	0.00		3119.1376	
RQ13,-1	0.00		3127.5550	

APPENDIX V

THE FREQUENCIES OF THE $2v_5(\perp)$ BAND AND THE $2v_5(\parallel)$ BAND OF CH_3CN

APPENDIX V

THE FREQUENCIES OF THE $2v_5(\perp)$ BAND AND THE $2v_5(\parallel)$ BAND OF CH₃CN

The frequencies of $2\nu_5(\bot)$ of CH_3CN were part of the output of the program SYMFIT, a linear least squares fit of ν_5 and $2\nu_5(\bot)$ of CH_3CN . The $2\nu_5(\bot)$ frequencies were calculated from a single band fit using most of the constants determined by the simultaneous fit. The columns in the table are:

- 1. Assignment of each transition $(^{\Delta K} \Delta J_K(J) \equiv \Delta K \Delta J K, J)$
- 2. The weight assigned each transition.
- 3. The observed frequency of each transition.
- 4. The frequency calculated after the least squares fit.
- 5. The residuals, observed minus calculated frequency.

K S	ı wr	OBS FREQ	CALC FREQ	OBS-CALC
PQ 7, 0	0.00	5935.0150	5934.6315	0.3835
PQ 6,		5946.4820	5946.3604	0.1216
PQ 5,		5957.7530	5957.8685	-0.1155
PQ 4, (5969.1002	5969.1874	-0.0872
PQ 3, (5980.1569	5980.3424	-0.1855
PQ 2, (5991.3622	5991.3539	0.0083
PQ 1, (6002.0997	6002.2377	-0.1380
RQ 0,-1		6013.1600	6013.0054	0.1546
RQ 1,-1		6023.5059	6023.6651	-0.1592
RQ 2,-1		6034.1232	6034.2223	-0.0991
RQ 3,-1		6044.7000	6044.6797	0.0203
RQ 4,-1		6055.6386	6055.0387	0.5999
RQ 5,-1		6064.1299	6065.2993	-1.1694
RQ 6,-1		6075.3170	6075.4609	-0.1439
RQ 7,-1		6087.0215	6085.5228	1.4987
RQ 8,-1		0007.0213	6095.4852	1.4307
RQ 9,-1		6112.1833	6105.3489	6.8344
RQ10,-1		6122.3572	6115.1169	7.2403
RO11,-1		6132.2323	6124.7941	7.4382
RO12,-		6142.0919	6134.3884	7.7035
RO13,-1		6151.6197	6143.9112	7.7085
QQ_1 ,		0131.0137	5966.3305	7.700
$\overset{\circ}{0}\overset{\circ}{0}\overset{\circ}{2},\overset{\circ}{0}$			5966.1566	
QQ 3, (5965.8613	
QQ 4, (5965.4367	
QQ 5, (5964.8718	
QQ 6, (5964.1520	
QQ 7, (5963.2600	
OP 7, 7			5958,9565	
QP 6, 6			5960.4643	
OP 5, 5			5961.7995	
OP 4, 4			5962.9796	
QP 3, 3			5964.0190	
OP 2, 2			5964.9288	
œ 1, 1			5965.7169	
OR 7, 7			5968.1446	
QR 6,			5969.6470	
QR 5,			5970.9770	
QR 4,10			5972.1520	
QR 3,11			5973.1862	
OR 2,12			5974.0907	
OR 2, 2			5967.9944	
OR 1,13			5974.8734	
PP 2,10			5985.1975	
PP 2, 9			5985.8150	
PP 2, 8			5986.4320	
PP 2, 7			5987.0488	
PP 2, 6			5987.6651	
_, -,				

	K	J	WI	OBS	FREQ	CALC FREQ	OBS-CALC
PP	2,	5	0.00	5988	.5836	5988.2810	0.3026
	2,		0.00		.1659	5988.8965	
	2,		0.00		.8265	5989.5116	0.3149
	2,		0.00		.3882	5990.1262	0.2620
	2,		0.00			5993.1920	***************************************
	2,		0.00			5993.8037	
	2,		0.00			5994.4150	
	2,		0.00			5995.0258	
	2,		0.00			5995.6362	
	2,		0.00			5996.2462	
	2,		0.00	5997	.1101	5996.8559	0.2542
	2,		0.00		.7459	5997.4651	0.2808
	2,		0.00		.3223	5998.0741	0.2482
	2,		0.00		.8915	5998.6827	0.2088
	2,		0.00		.5547	5999.2911	0.2636
	2,		0.00		.1947	5999.8993	0.2954
	2,		0.00		.7884	6000.5073	0.2811
	2,		0.00		.3729	6001.1151	0.2578
	1,		0.50		.5924	5993.6071	
	1,		0.13		.1972	5994.2258	
	1,		4.00		.8360	5994.8442	-0.0082
	1,		1.00		.4454	5995.4624	-0.0170
	1,		0.50		.0597	5996.0803	-0.0206
	1,		0.13		.6728	5996.6979	
	ī,		0.00		.2435	5997.3151	-0.0716
	ī,		0.00		.8501	5997.9320	
	ī,		0.00			5998.5484	3,73,223
	ī,		0.00			5999.1645	
	ī,		0.00			5999.7801	
	ī,		0.00			6000.3952	
	ī,		0.00			6001.0099	
	1,		0.00			6001.6240	
	1,		0.06	6003	.4300	6003.4636	-0.0336
	1,		0.00	6004	.0240	6004.0758	-0.0518
	1,		0.06	6004	.6470	6004.6875	-0.0405
	1,		0.00			6005.2987	
	1,		0.00	6005	.8406	6005.9095	-0.0689
	1,		0.00	6006	.4674	6006.5198	-0.0524
	1,		1.00		.1289	6007.1298	-0.0009
	1,		0.00		.6805	6007.7393	-0.0588
	1,		0.00		.3715	6008.3484	0.0231
	1,		0.06	6008	.9158	6008.9572	-0.0414
	1,		1.00		.5615	6009.5657	-0.0042
	1,		0.13		.1432	6010.1739	-0.0307
	1,		0.00		.8140	6010.7819	0.0321
	0,		0.00		.4684	5994.4903	-0.0219
	0,		0.00		.0971	5995.1040	-0.0069
	0,		0.00		.7526	5995.7186	0.0340

K J	WI	OBS FREQ	CALC FREQ	OBS-CALC
RP 0,27	0.00	5996.3537	5996.3340	0.0197
RP 0,26	0.00	5996.9637	5996.9502	0.0135
RP 0,25	0.00	5997.5684	5997.5671	0.0013
RP 0,24	0.00	5998.2471	5998.1845	0.0626
RP 0,23	0.00	5999.7853	5998.8024	0.9829
RP 0,22	0.00	5999.4676	5999.4207	0.0469
RP 0,21	0.00	6000.0795	6000.0393	0.0402
RP 0,20	0.00	6000.6713	6000.6582	0.0131
RP 0,19	0.00	6001.2578	6001.2772	-0.0194
RP 0,15	0.00	6003.7660	6003.7540	0.0120
RP 0,14	0.00	6004.3695	6004.3730	-0.0035
RP 0,13	0.00	6004.9908	6004.9919	-0.0011
RP 0,12	0.00	6005.5740	6005.6105	-0.0365
RP 0,11	0.00	6006.2209	6006.2289	-0.0080
RP 0,10	0.00	6006.7827	6006.8470	-0.0643
RP 0, 9	0.00	6007.4162	6007.4648	-0.0486
RP 0, 8	0.00	6008.0614	6008.0822	-0.0208
RP 0, 7	0.00	6008.6646	6008.6992	-0.0346
RP 0, 6	0.00	6009.2456	6009.3158	-0.0702
RP 0, 5	0.00	6009.8514	6009.9319	-0.0805
RP 0, 4	0.00	6010.4957	6010.5476	-0.0519
RP 0, 3	0.00	6011.1220	6011.1628	-0.0408
RP 0, 2	0.00		6011.7775	
RP 0, 1	0.00		6012.3917	
RQ 0,-1	0.00		6013.0054	
RR 0, 0	0.00		6013.6185	
RR 0, 1	0.00	6014 0072	6014.2312	-0.0161
RR 0, 2	0.00	6014.8273	6014.8434 6015.4550	-0.0161 0.0239
RR 0, 3	0.00	6015.4789 6016.0429	6016.0662	-0.0233
RR 0, 4	0.00 0.00		6016.6769	-0.0017
RR 0, 5 RR 0, 6	0.00	6016.6752 6017.2844	6017.2871	-0.0027
RR 0, 7	0.00	6017.8697	6017.8969	-0.0272
RR 0, 8	0.00	6018.5152	6018.5062	0.0090
RR 0, 9	0.00	6019.0495	6019.1152	-0.0657
RR 0,10	0.00	6019.6650	6019.7238	-0.0588
RR 0,11	0.00	6020.3573	6020.3321	0.0252
RR 0,12	0.00	6020.9459	6020.9401	0.0058
RR 0,13	0.00	6021.5834	6021.5479	0.0355
RR 0,19	0.00	6025.2541	6025.1918	0.0623
RR 0,20	0.00	6025.8831	6025.7992	0.0839
RR 0,21	0.00	6026.4763	6026.4068	0.0695
RR 0,22	0.00	6027.0536	6027.0147	0.0389
RR 0,23	0.00	6027.6638	6027.6229	0.0409
RP 1,14	0.00	6015.1049	6015.0310	0.0739
RP 1,13	0.00	6015.7326	6015.6501	0.0825
RP 1,12	0.00	6016.3253	6016.2690	0.0563
RP 1,11	0.00	6016.9357	6016.8876	0.0481
		•		

RP 1,10	K J	WI	OBS FREQ	CALC FREQ	OBS-CALC
RP 1, 9 0.00 6018.1460 6018.1239 0.0221 RP 1, 8 0.00 6019.3980 6018.7414 0.0481 RP 1, 6 0.13 6019.9938 6019.9753 0.0185 RP 1, 5 0.50 6020.6272 6020.5915 0.0357 RP 1, 4 0.13 6021.2258 6021.2073 0.0185 RP 1, 2 0.00 6022.4372 RP 1, 1 0.00 6022.4372 RP 1, 1 0.00 6025.5303 6025.5030 0.0273 RR 1, 1 0.00 6026.1443 6026.1145 0.0298 RR 1, 2 1.00 6025.5303 6025.5030 0.0273 RR 1, 3 1.00 6026.1443 6026.1145 0.0298 RR 1, 4 0.00 6026.7186 6026.7256 -0.0070 RR 1, 5 0.50 6027.3756 6027.3361 0.0395 RR 1, 6 0.25 6027.9889 6027.9462 0.0427 RR 1, 7 0.00 6028.5584 6028.5558 0.0026 RR 1, 9 1.00 6029.2196 6029.1649 0.0547 RR 1, 9 1.00 6030.4347 6030.3321 0.0526 RR 1,11 0.00 6031.1312 6030.9901 0.1231 RR 1,12 1.00 6031.6370 6031.5978 0.0392 RR 1,13 0.50 6032.2498 6032.2052 0.0446 RR 1,14 0.00 6031.6370 6031.5978 0.0392 RR 1,13 0.50 6032.2498 6032.2052 0.0446 RR 1,14 0.00 6030.4347 6030.3901 0.1231 RR 1,12 1.00 6031.6370 6031.5978 0.0392 RR 1,13 0.50 6032.2498 6032.2052 0.0446 RR 1,14 0.00 6032.9345 6032.8125 0.1220 RP 2,15 0.25 6024.9751 6024.9669 0.0082 RP 2,10 0.06 6030.4347 6031.5978 0.0392 RR 2, 3 0.06 6029.2615 6029.2982 -0.0367 RP 2, 9 0.13 6028.6531 6028.6605 -0.0274 RR 2, 2 0.05 6036.6578 6032.3797 0.0258 RP 2, 6 0.00 6032.9345 6032.3797 0.0258 RP 2, 1 0.00 6031.7827 6031.7644 0.0183 RP 2, 3 0.00 6032.9530 6032.9982 -0.0367 RP 2, 6 0.00 6032.9530 6032.9984 -0.0414 RR 2, 2 0.25 6036.6578 6036.6598 -0.0133 RR 2, 3 0.25 6036.6578 6036.5998 -0.0133 RR 2, 4 0.25 6036.6578 6036.5994 -0.0138 RR 2, 7 1.00 6039.1064 6039.1118 -0.0054 RR 2, 8 0.00 6039.7390 6039.7207 0.0183 RR 2, 1 1.00 6040.3117 6040.3392 -0.0175 RR 2, 1 1.00 6040.9194 6040.3372 -0.0175 RR 2, 1 1.00 6040.317 6040.3292 -0.0175 RR 2, 1 1.00 6040.317 6040.3292 -0.0175 RR 2, 1 1.00 6040.317 6040.3292 -0.0175 RR 2, 1 1.00 6040.3176 6040.3772 -0.0184	RP 1.10	0.00	6017,5300	6017.5059	0.0241
RP 1, 8 0.00 6018.7895 6018.7414 0.0481 RP 1, 7 0.00 6019.3980 6019.3586 0.0394 RP 1, 6 0.13 6019.9938 6019.9753 0.0185 RP 1, 5 0.50 6020.6272 6020.5915 0.0357 RP 1, 4 0.13 6021.2258 6021.2073 0.0185 RP 1, 3 0.00 6022.4372 RP 1, 1 0.00 6022.4372 RR 1, 1 0.00 6024.8864 6024.8909 -0.0045 RR 1, 2 1.00 6025.5303 6025.5030 0.0273 RR 1, 3 1.00 6026.1443 6026.1145 0.0298 RR 1, 4 0.00 6026.7186 6026.7256 -0.0070 RR 1, 5 0.50 6027.3756 6027.3361 0.0395 RR 1, 6 0.25 6027.9889 6027.3361 0.0395 RR 1, 7 0.00 6028.5584 6028.5558 0.0026 RR 1, 8 0.00 6029.8102 6029.1649 0.0547 RR 1, 9 1.00 6029.8102 6029.7737 0.0365 RR 1,10 0.00 6030.4347 6030.3821 0.0526 RR 1,11 0.00 6031.1132 6030.9901 0.1231 RR 1,12 1.00 6031.1313 6030.9901 0.1231 RR 1,13 0.50 6032.2498 6032.2052 0.0446 RR 1,14 0.00 6032.9345 6032.8125 0.1220 RP 2,15 0.25 6024.9751 6024.9669 0.0057 RP 2, 9 0.13 6028.6531 6028.6605 -0.0274 RP 2, 8 0.06 6029.2615 6029.9155 RP 2, 9 0.13 6028.6531 6028.6605 -0.0274 RP 2, 9 0.13 6028.6531 6028.6605 -0.0274 RP 2, 9 0.00 6032.9345 6032.9155 RP 2, 0.00 6032.9345 6032.9155 RP 2, 0.00 6032.9345 6032.8125 0.1220 RP 2, 10 0.00 6032.9345 6032.8125 0.1220 RP 2, 10 0.00 6032.9345 6032.8125 0.0367 RP 2, 9 0.13 6028.6531 6028.6605 -0.0274 RP 2, 9 0.13 6028.6531 6028.6605 -0.0274 RP 2, 9 0.00 6032.9536 6032.9982 -0.0367 RP 2, 0 0.00 6032.9530 6032.9982 -0.0367 RP 2, 0 0.00 6032.9530 6032.9982 -0.0367 RP 2, 0 0.00 6032.9530 6032.9984 -0.0414 RR 2, 2 0.25 6036.6578 6036.6713 -0.0135 RR 2, 4 0.25 6036.6578 6036.6713 -0.0135 RR 2, 6 0.50 6038.4989 6038.5024 -0.0013 RR 2, 7 1.00 6039.1064 6039.1118 -0.0054 RR 2, 10 0.00 6040.3117 6040.3392 -0.0175 RR 2, 11 0.13 6041.5151 6041.5449 -0.0298 RR 2, 11 0.13 6041.5151 6042.7594 -0.0018 RR 2, 11 0.13 6042.7559 6042.7594 -0.00184 RR 2, 11 0.13 6042.7559 6042.7594 -0.00184					
RP 1, 7					
RP 1, 6					
RP 1, 5	•				
RP 1, 4	•				
RP 1, 3	•				
RP 1, 2 0.00 6022.4372 RP 1, 1 0.00 6024.8864 6023.0514 RR 1, 1 1.00 6025.5303 6025.5030 0.0273 RR 1, 3 1.00 6026.1443 6026.1145 0.0298 RR 1, 4 0.00 6026.7186 6026.7256 -0.0070 RR 1, 5 0.50 6027.3756 6027.3361 0.0395 RR 1, 6 0.25 6027.9889 6027.9462 0.0427 RR 1, 7 0.00 6028.5584 6028.5558 0.0026 RR 1, 8 0.00 6029.2196 6029.1649 0.0547 RR 1, 9 1.00 6029.8102 6029.7737 0.0365 RR 1, 10 0.00 6031.1132 6030.9901 0.1231 RR 1,11 0.00 6031.6370 6031.5978 0.0392 RR 1,11 0.00 6031.6370 6031.5978 0.0392 RR 1,14 0.00 6032.2498 6032.2052 0.0446 RR 1,14 0.00 6032.3345 6032.8125 0.1220 RP 2,15 0.25 6024.9751 6024.9669 0.0082 RP 2,12 1.00 6026.8193 6026.8250 -0.0057 RP 2, 9 0.13 6028.6531 6028.6805 -0.0274 RP 2, 8 0.06 6029.2615 6029.2982 -0.0367 RP 2, 7 0.00 6031.7827 6031.7644 0.0183 RP 2, 2 0.00 6032.9345 6032.3797 0.0258 RP 2, 2 0.00 6032.9530 6032.9944 -0.0414 RR 2, 2 0.25 6036.0455 6032.3797 0.0258 RP 2, 2 0.00 6032.9530 6032.9944 -0.0414 RR 2, 2 0.25 6036.0455 6032.3797 0.0258 RP 2, 5 0.06 6031.7827 6031.7644 0.0183 RP 2, 3 0.00 6032.9530 6032.9944 -0.0414 RR 2, 2 0.25 6036.0455 6036.598 -0.0133 RR 2, 3 0.25 6036.6578 6036.6713 -0.0155 RR 2, 5 1.00 6037.8745 6037.2822 -0.0291 RR 2, 6 0.50 6038.4989 6038.5024 -0.0035 RR 2, 7 1.00 6039.7390 6039.7207 0.0183 RR 2, 8 0.00 6039.7390 6039.7207 0.0183 RR 2, 8 0.00 6039.7390 6039.7207 0.0183 RR 2, 9 1.00 6040.3117 6040.3292 -0.0175 RR 2,11 0.13 6041.5151 6041.5449 -0.0298 RR 2,11 0.13 6042.7599 6042.7594 -0.0085 RR 2,11 0.05 6042.7599 6042.7594 -0.0085 RR 2,11 0.00 6043.3478 6043.3662 -0.0184			0021 (2200		0.0100
RP 1, 1 0.00 6024.8864 6024.8909 -0.0045 RR 1, 1 1 0.00 6025.5303 6025.5030 0.0273 RR 1, 3 1.00 6025.7186 6026.1145 0.0298 RR 1, 4 0.00 6026.7186 6026.7256 -0.0070 RR 1, 5 0.50 6027.3756 6027.3361 0.0395 RR 1, 6 0.25 6027.9889 6027.9462 0.0427 RR 1, 7 0.00 6028.5584 6028.5558 0.0026 RR 1, 8 0.00 6029.2196 6029.1649 0.0547 RR 1, 9 1.00 6029.8102 6029.7737 0.0365 RR 1,10 0.00 6031.4347 6030.3821 0.0526 RR 1,11 0.00 6031.6370 6031.5978 0.0392 RR 1,12 1.00 6031.6370 6031.5978 0.0392 RR 1,13 0.50 6032.2498 6032.2052 0.0446 RR 1,14 0.00 6032.9345 6032.8125 0.1220 RP 2,15 0.25 6024.9751 6024.9669 0.0082 RP 2,15 0.25 6024.9751 6024.9669 0.0082 RP 2,2 9 0.13 6028.6531 6028.6805 -0.0057 RP 2, 9 0.13 6028.6531 6028.6805 -0.0057 RP 2, 7 0.00 6032.9345 6031.1486 -0.0367 RP 2, 7 0.00 6032.9615 6029.2982 -0.0367 RP 2, 7 0.00 6032.935 6032.3797 0.0258 RP 2, 2 0.00 6032.9530 6032.3797 0.0258 RP 2, 2 0.00 6032.9530 6032.3797 0.0258 RP 2, 2 0.00 6032.9530 6032.9944 -0.0414 RR 2, 2 0.25 6036.6578 6036.6713 -0.0135 RR 2, 4 0.25 6037.2531 6037.2822 -0.0291 RR 2, 5 1.00 6037.8745 6036.6713 -0.0135 RR 2, 6 0.50 6038.4989 6038.5024 -0.0013 RR 2, 7 1.00 6039.1064 6039.1118 -0.0054 RR 2, 8 0.00 6039.7390 6039.7207 0.0183 RR 2, 9 1.00 6040.3117 6040.3292 -0.0175 RR 2, 9 1.00 6040.3117 6040.3292 -0.0175 RR 2, 10 1.00 6040.9194 6040.9372 -0.0178 RR 2, 11 0.13 6041.5151 6041.5449 -0.0298 RR 2, 12 1.00 6042.7509 6042.7594 -0.0085 RR 2, 14 1.00 6043.3478 6043.3662 -0.0184					
RR 1, 1 0.00 6024.8864 6024.8909 -0.0045 RR 1, 2 1.00 6025.5303 6025.5030 0.0273 RR 1, 3 1.00 6026.1443 6026.1145 0.0298 RR 1, 4 0.00 6026.7186 6026.7256 -0.0070 RR 1, 5 0.50 6027.3756 6027.3361 0.0395 RR 1, 6 0.25 6027.9889 6027.9462 0.0427 RR 1, 7 0.00 6028.5584 6028.5558 0.0026 RR 1, 8 0.00 6029.2196 6029.1649 0.0547 RR 1, 9 1.00 6029.8102 6029.7737 0.0365 RR 1,10 0.00 6031.1132 6030.9901 0.1231 RR 1,11 0.00 6031.6370 6031.5978 0.0392 RR 1,13 0.50 6032.2498 6032.2052 0.0446 RR 1,14 0.00 6032.9345 6032.8125 0.1220 RP 2,15 0.25 6024.9751 6024.9669 0.0082 RP 2,12 1.00 6036.8193 6026.8250 -0.0057 RP 2, 9 0.13 6028.6531 6028.6805 -0.0057 RP 2, 9 0.13 6028.6531 6028.6805 -0.0057 RP 2, 7 0.00 6031.1322 6031.1486 -0.0367 RP 2, 7 0.00 6031.1322 6031.7644 0.0183 RP 2, 3 0.06 6032.24055 6032.3797 0.0258 RP 2, 4 0.00 6031.7827 6031.7644 0.0183 RP 2, 3 0.00 6032.9530 6032.9944 -0.0414 RR 2, 2 0.25 6036.0465 6032.3797 0.0258 RP 2, 2 0.00 6032.9530 6032.9944 -0.0414 RR 2, 2 0.25 6036.6578 6036.6713 -0.0135 RR 2, 4 0.25 6037.2531 6037.2822 -0.0291 RR 2, 5 1.00 6037.8745 6037.2822 -0.0291 RR 2, 5 1.00 6037.8745 6037.2822 -0.0291 RR 2, 6 0.50 6038.4989 6038.5024 -0.0013 RR 2, 7 1.00 6039.1064 6039.1118 -0.0058 RR 2, 7 1.00 6039.1064 6039.1118 -0.0058 RR 2, 8 0.00 6039.7390 6039.7207 0.0183 RR 2, 9 1.00 6040.3117 6040.3292 -0.0175 RR 2, 10 1.00 6040.3117 6040.3292 -0.0175 RR 2, 11 0.13 6041.5151 6041.5449 -0.0298 RR 2, 12 0.06 6042.1210 6042.1523 -0.0313 RR 2, 11 0.05 6042.7509 6042.7594 -0.0085 RR 2, 14 0.00 6043.3478 6043.3662 -0.0184	-				
RR 1, 2	•		6024.8864		-0.0045
RR 1, 3	-				
RR 1, 4	•				
RR 1, 5					
RR 1, 6	· ·				
RR 1, 7 0.00 6028.5584 6028.5558 0.0026 RR 1, 8 0.00 6029.2196 6029.1649 0.0547 RR 1, 9 1.00 6029.8102 6029.7737 0.0365 RR 1,10 0.00 6030.4347 6030.3821 0.0526 RR 1,11 0.00 6031.1132 6030.9901 0.1231 RR 1,12 1.00 6031.6370 6031.5978 0.0392 RR 1,13 0.50 6032.2498 6032.2052 0.0446 RR 1,14 0.00 6032.9345 6032.8125 0.1220 RP 2,15 0.25 6024.9751 6024.9669 0.0082 RP 2,12 1.00 6026.8193 6026.8250 -0.0057 RP 2, 9 0.13 6028.6531 6028.6805 -0.0274 RP 2, 8 0.06 6029.2615 6029.2982 -0.0367 RP 2, 7 0.00 6031.1132 6031.1486 -0.0354 RP 2, 4 0.00 6031.1132 6031.1486 -0.0354 RP 2, 3 0.00 6032.4055 6032.3797 0.0258 RP 2, 2 0.00 6032.9530 6032.3797 0.0258 RP 2, 2 0.00 6032.9530 6032.9944 -0.0414 RR 2, 2 0.25 6036.0465 6036.6578 -0.0133 RR 2, 3 0.25 6036.6578 6036.6713 -0.0135 RR 2, 4 0.25 6037.2531 6037.2822 -0.0291 RR 2, 5 1.00 6037.8745 6037.8925 -0.0133 RR 2, 6 0.50 6038.4989 6038.5024 -0.0035 RR 2, 7 1.00 6039.1064 6039.1118 -0.0054 RR 2, 8 0.00 6039.7390 6039.7207 0.0183 RR 2, 9 1.00 6040.3117 6040.3292 -0.0175 RR 2, 9 1.00 6040.3117 6040.3292 -0.0178 RR 2, 9 1.00 6040.3117 6040.3292 -0.0178 RR 2, 11 0.13 6041.5151 6041.5449 -0.0298 RR 2,11 0.13 6041.5151 6041.5449 -0.0298 RR 2,11 0.13 6042.7509 6042.7594 -0.0085 RR 2,14 1.00 6043.3478 6043.3662 -0.0184					
RR 1, 8					
RR 1, 9					
RR 1,10 0.00 6030.4347 6030.3821 0.0526 RR 1,11 0.00 6031.1132 6030.9901 0.1231 RR 1,12 1.00 6031.6370 6031.5978 0.0392 RR 1,13 0.50 6032.2498 6032.2052 0.0446 RR 1,14 0.00 6032.9345 6032.8125 0.1220 RP 2,15 0.25 6024.9751 6024.9669 0.0082 RP 2,12 1.00 6026.8193 6026.8250 -0.0057 RP 2, 9 0.13 6028.6531 6028.6805 -0.0274 RP 2, 8 0.06 6029.2615 6029.2982 -0.0367 RP 2, 7 0.00 6030.5323 RP 2, 5 0.06 6031.1132 6031.1486 -0.0354 RP 2, 4 0.00 6031.7827 6031.7644 0.0183 RP 2, 3 0.00 6032.4055 6032.3797 0.0258 RP 2, 2 0.00 6032.9530 6032.9944 -0.0414 RR 2, 2 0.25 6036.0465 6036.0598 -0.0133 RR 2, 3 0.25 6036.0465 6036.0598 -0.0133 RR 2, 3 0.25 6036.6578 6036.6713 -0.0135 RR 2, 4 0.25 6037.2531 6037.2822 -0.0291 RR 2, 5 1.00 6037.8745 6037.8925 -0.0180 RR 2, 6 0.50 6038.4989 6038.5024 -0.0035 RR 2, 7 1.00 6039.1064 6039.1118 -0.0054 RR 2, 8 0.00 6039.7390 6039.7207 0.0183 RR 2, 9 1.00 6040.3117 6040.3292 -0.0175 RR 2, 10 1.00 6040.9194 6040.9372 -0.0178 RR 2, 11 0.13 6041.5151 6041.5449 -0.0298 RR 2, 12 0.06 6042.1210 6042.1523 -0.0313 RR 2, 13 0.50 6042.7509 6042.7594 -0.0085 RR 2, 14 1.00 6043.3478 6043.3662 -0.0184					
RR 1,11 0.00 6031.1132 6030.9901 0.1231 RR 1,12 1.00 6031.6370 6031.5978 0.0392 RR 1,13 0.50 6032.2498 6032.2052 0.0446 RR 1,14 0.00 6032.9345 6032.8125 0.1220 RP 2,15 0.25 6024.9751 6024.9669 0.0082 RP 2,12 1.00 6026.8193 6026.8250 -0.0057 RP 2, 9 0.13 6028.6531 6028.6805 -0.0274 RP 2, 8 0.06 6029.2615 6029.2982 -0.0367 RP 2, 7 0.00 6030.5323 RP 2, 5 0.06 6031.1132 6031.1486 -0.0354 RP 2, 4 0.00 6031.7827 6031.7644 0.0183 RP 2, 3 0.00 6032.4055 6032.3797 0.0258 RP 2, 2 0.00 6032.9530 6032.9944 -0.0414 RR 2, 2 0.25 6036.0465 6036.0598 -0.0133 RR 2, 3 0.25 6036.0465 6036.6578 -0.0135 RR 2, 4 0.25 6037.2531 6037.2822 -0.0291 RR 2, 5 1.00 6037.8745 6037.8925 -0.0180 RR 2, 6 0.50 6038.4989 6038.5024 -0.0035 RR 2, 7 1.00 6039.1064 6039.1118 -0.0054 RR 2, 8 0.00 6039.7390 6039.7207 0.0183 RR 2, 9 1.00 6040.3117 6040.3292 -0.0175 RR 2, 10 1.00 6040.3117 6040.3292 -0.0175 RR 2, 11 0.13 6041.5151 6041.5449 -0.0298 RR 2, 12 0.06 6042.1210 6042.1523 -0.0313 RR 2, 13 0.50 6042.7509 6042.7594 -0.0085 RR 2, 14 1.00 6043.3478 6043.3662 -0.0184					
RR 1,12					
RR 1,13					
RR 1,14 0.00 6032.9345 6032.8125 0.1220 RP 2,15 0.25 6024.9751 6024.9669 0.0082 RP 2,12 1.00 6026.8193 6026.8250 -0.0057 RP 2, 9 0.13 6028.6531 6028.6805 -0.0274 RP 2, 8 0.06 6029.2615 6029.2982 -0.0367 RP 2, 7 0.00 6030.5323 RP 2, 5 0.06 6031.1132 6031.1486 -0.0354 RP 2, 4 0.00 6031.7827 6031.7644 0.0183 RP 2, 3 0.00 6032.4055 6032.3797 0.0258 RP 2, 2 0.00 6032.9530 6032.9944 -0.0414 RR 2, 2 0.25 6036.0465 6036.0598 -0.0133 RR 2, 3 0.25 6036.6578 6036.6713 -0.0135 RR 2, 4 0.25 6037.2531 6037.2822 -0.0291 RR 2, 5 1.00 6037.8745 6037.8925 -0.0180 RR 2, 6 0.50 6038.4989 6038.5024 -0.0035 RR 2, 7 1.00 6039.1064 6039.1118 -0.0054 RR 2, 8 0.00 6039.7390 6039.7207 0.0183 RR 2, 9 1.00 6040.3117 6040.3292 -0.0175 RR 2,10 1.00 6040.3117 6040.3292 -0.0175 RR 2,11 0.13 6041.5151 6041.5449 -0.0298 RR 2,12 0.06 6042.1210 6042.1523 -0.0313 RR 2,13 0.50 6042.7509 6042.7594 -0.0085 RR 2,14 1.00 6043.3478 6043.3662 -0.0184					
RP 2,15					
RP 2,12					
RP 2, 9 0.13 6028.6531 6028.6805 -0.0274 RP 2, 8 0.06 6029.2615 6029.2982 -0.0367 RP 2, 7 0.00 6029.9155 RP 2, 6 0.00 6030.5323 RP 2, 5 0.06 6031.1132 6031.1486 -0.0354 RP 2, 4 0.00 6031.7827 6031.7644 0.0183 RP 2, 3 0.00 6032.4055 6032.3797 0.0258 RP 2, 2 0.00 6032.9530 6032.9944 -0.0414 RR 2, 2 0.25 6036.0465 6036.0598 -0.0133 RR 2, 3 0.25 6036.0465 6036.65713 -0.0135 RR 2, 4 0.25 6037.2531 6037.2822 -0.0291 RR 2, 5 1.00 6037.8745 6037.8925 -0.0180 RR 2, 6 0.50 6038.4989 6038.5024 -0.0035 RR 2, 7 1.00 6039.1064 6039.1118 -0.0054 RR 2, 8 0.00 6039.7390 6039.7207 0.0183 RR 2, 9 1.00 6040.3117 6040.3292 -0.0175 RR 2,10 1.00 6040.9194 6040.9372 -0.0178 RR 2,11 0.13 6041.5151 6041.5449 -0.0298 RR 2,12 0.06 6042.1210 6042.1523 -0.0313 RR 2,13 0.50 6042.7509 6042.7594 -0.0085 RR 2,14 1.00 6043.3478 6043.3662 -0.0184					
RP 2, 8 0.06 6029.2615 6029.2982 -0.0367 RP 2, 7 0.00 6029.9155 RP 2, 6 0.00 6030.5323 RP 2, 5 0.06 6031.1132 6031.1486 -0.0354 RP 2, 4 0.00 6031.7827 6031.7644 0.0183 RP 2, 3 0.00 6032.4055 6032.3797 0.0258 RP 2, 2 0.00 6032.9530 6032.9944 -0.0414 RR 2, 2 0.25 6036.0465 6036.0598 -0.0133 RR 2, 3 0.25 6036.6578 6036.6713 -0.0135 RR 2, 4 0.25 6037.2531 6037.2822 -0.0291 RR 2, 5 1.00 6037.8745 6037.8925 -0.0180 RR 2, 6 0.50 6038.4989 6038.5024 -0.0035 RR 2, 7 1.00 6039.1064 6039.1118 -0.0054 RR 2, 8 0.00 6039.7390 6039.7207 0.0183 RR 2, 9 1.00 6040.3117 6040.3292 -0.0175 RR 2,10 1.00 6040.3117 6040.3292 -0.0175 RR 2,11 0.13 6041.5151 6041.5449 -0.0298 RR 2,12 0.06 6042.1210 6042.1523 -0.0313 RR 2,13 0.50 6042.7509 6042.7594 -0.0085 RR 2,14 1.00 6043.3478 6043.3662 -0.0184					
RP 2, 7 0.00 6030.5323 RP 2, 6 0.00 6031.1132 6031.1486 -0.0354 RP 2, 4 0.00 6031.7827 6031.7644 0.0183 RP 2, 3 0.00 6032.4055 6032.3797 0.0258 RP 2, 2 0.00 6032.9530 6032.9944 -0.0414 RR 2, 2 0.25 6036.0465 6036.0598 -0.0133 RR 2, 3 0.25 6036.6578 6036.6713 -0.0135 RR 2, 4 0.25 6037.2531 6037.2822 -0.0291 RR 2, 5 1.00 6037.8745 6037.8925 -0.0180 RR 2, 6 0.50 6038.4989 6038.5024 -0.0035 RR 2, 7 1.00 6039.1064 6039.1118 -0.0054 RR 2, 8 0.00 6039.7390 6039.7207 0.0183 RR 2, 9 1.00 6040.3117 6040.3292 -0.0175 RR 2,10 1.00 6040.3117 6040.3292 -0.0175 RR 2,11 0.13 6041.5151 6041.5449 -0.0298 RR 2,12 0.06 6042.1210 6042.1523 -0.0313 RR 2,13 0.50 6042.7509 6042.7594 -0.0085 RR 2,14 1.00 6043.3478 6043.3662 -0.0184	•				
RP 2, 6 0.00 6031.1132 6031.1486 -0.0354 RP 2, 4 0.00 6031.7827 6031.7644 0.0183 RP 2, 3 0.00 6032.4055 6032.3797 0.0258 RP 2, 2 0.00 6032.9530 6032.9944 -0.0414 RR 2, 2 0.25 6036.0465 6036.0598 -0.0133 RR 2, 3 0.25 6036.6578 6036.6713 -0.0135 RR 2, 4 0.25 6037.2531 6037.2822 -0.0291 RR 2, 5 1.00 6037.8745 6037.8925 -0.0180 RR 2, 6 0.50 6038.4989 6038.5024 -0.0035 RR 2, 7 1.00 6039.1064 6039.1118 -0.0054 RR 2, 8 0.00 6039.7390 6039.7207 0.0183 RR 2, 9 1.00 6040.3117 6040.3292 -0.0175 RR 2,10 1.00 6040.9194 6040.9372 -0.0178 RR 2,11 0.13 6041.5151 6041.5449 -0.0298 RR 2,12 0.06 6042.1210 6042.1523 -0.0313 RR 2,13 0.50 6042.7509 6042.7594 -0.0085 RR 2,14 1.00 6043.3478 6043.3662 -0.0184	•				
RP 2, 5 0.06 6031.1132 6031.1486 -0.0354 RP 2, 4 0.00 6031.7827 6031.7644 0.0183 RP 2, 3 0.00 6032.4055 6032.3797 0.0258 RP 2, 2 0.00 6032.9530 6032.9944 -0.0414 RR 2, 2 0.25 6036.0465 6036.0598 -0.0133 RR 2, 3 0.25 6036.6578 6036.6713 -0.0135 RR 2, 4 0.25 6037.2531 6037.2822 -0.0291 RR 2, 5 1.00 6037.8745 6037.8925 -0.0180 RR 2, 6 0.50 6038.4989 6038.5024 -0.0035 RR 2, 7 1.00 6039.1064 6039.1118 -0.0054 RR 2, 8 0.00 6039.7390 6039.7207 0.0183 RR 2, 9 1.00 6040.3117 6040.3292 -0.0175 RR 2,10 1.00 6040.9194 6040.9372 -0.0178 RR 2,11 0.13 6041.5151 6041.5449 -0.0298 RR 2,12 0.06 6042.1210 6042.1523 -0.0313 RR 2,13 0.50 6042.7509 6042.7594 -0.0085 RR 2,14 1.00 6043.3478 6043.3662 -0.0184	•				
RP 2, 4 0.00 6031.7827 6031.7644 0.0183 RP 2, 3 0.00 6032.4055 6032.3797 0.0258 RP 2, 2 0.00 6032.9530 6032.9944 -0.0414 RR 2, 2 0.25 6036.0465 6036.0598 -0.0133 RR 2, 3 0.25 6036.6578 6036.6713 -0.0135 RR 2, 4 0.25 6037.2531 6037.2822 -0.0291 RR 2, 5 1.00 6037.8745 6037.8925 -0.0180 RR 2, 6 0.50 6038.4989 6038.5024 -0.0035 RR 2, 7 1.00 6039.1064 6039.1118 -0.0054 RR 2, 8 0.00 6039.7390 6039.7207 0.0183 RR 2, 9 1.00 6040.3117 6040.3292 -0.0175 RR 2,10 1.00 6040.9194 6040.9372 -0.0178 RR 2,11 0.13 6041.5151 6041.5449 -0.0298 RR 2,12 0.06 6042.1210 6042.1523 -0.0313 RR 2,13 0.50 6042.7509 6042.7594 -0.0085 RR 2,14 1.00 6043.3478 6043.3662 -0.0184	•		6031.1132		-0.0354
RP 2, 3 0.00 6032.4055 6032.3797 0.0258 RP 2, 2 0.00 6032.9530 6032.9944 -0.0414 RR 2, 2 0.25 6036.0465 6036.0598 -0.0133 RR 2, 3 0.25 6036.6578 6036.6713 -0.0135 RR 2, 4 0.25 6037.2531 6037.2822 -0.0291 RR 2, 5 1.00 6037.8745 6037.8925 -0.0180 RR 2, 6 0.50 6038.4989 6038.5024 -0.0035 RR 2, 7 1.00 6039.1064 6039.1118 -0.0054 RR 2, 8 0.00 6039.7390 6039.7207 0.0183 RR 2, 9 1.00 6040.3117 6040.3292 -0.0175 RR 2,10 1.00 6040.9194 6040.9372 -0.0178 RR 2,11 0.13 6041.5151 6041.5449 -0.0298 RR 2,12 0.06 6042.1210 6042.1523 -0.0313 RR 2,13 0.50 6042.7509 6042.7594 -0.0085 RR 2,14 1.00 6043.3478 6043.3662 -0.0184	· ·				
RP 2, 2 0.00 6032.9530 6032.9944 -0.0414 RR 2, 2 0.25 6036.0465 6036.0598 -0.0133 RR 2, 3 0.25 6036.6578 6036.6713 -0.0135 RR 2, 4 0.25 6037.2531 6037.2822 -0.0291 RR 2, 5 1.00 6037.8745 6037.8925 -0.0180 RR 2, 6 0.50 6038.4989 6038.5024 -0.0035 RR 2, 7 1.00 6039.1064 6039.1118 -0.0054 RR 2, 8 0.00 6039.7390 6039.7207 0.0183 RR 2, 9 1.00 6040.3117 6040.3292 -0.0175 RR 2,10 1.00 6040.9194 6040.9372 -0.0178 RR 2,11 0.13 6041.5151 6041.5449 -0.0298 RR 2,12 0.06 6042.1210 6042.1523 -0.0313 RR 2,13 0.50 6042.7509 6042.7594 -0.0085 RR 2,14 1.00 6043.3478 6043.3662 -0.0184	•				
RR 2, 2 0.25 6036.0465 6036.0598 -0.0133 RR 2, 3 0.25 6036.6578 6036.6713 -0.0135 RR 2, 4 0.25 6037.2531 6037.2822 -0.0291 RR 2, 5 1.00 6037.8745 6037.8925 -0.0180 RR 2, 6 0.50 6038.4989 6038.5024 -0.0035 RR 2, 7 1.00 6039.1064 6039.1118 -0.0054 RR 2, 8 0.00 6039.7390 6039.7207 0.0183 RR 2, 9 1.00 6040.3117 6040.3292 -0.0175 RR 2,10 1.00 6040.9194 6040.9372 -0.0178 RR 2,11 0.13 6041.5151 6041.5449 -0.0298 RR 2,12 0.06 6042.1210 6042.1523 -0.0313 RR 2,13 0.50 6042.7509 6042.7594 -0.0085 RR 2,14 1.00 6043.3478 6043.3662 -0.0184					
RR 2, 3 0.25 6036.6578 6036.6713 -0.0135 RR 2, 4 0.25 6037.2531 6037.2822 -0.0291 RR 2, 5 1.00 6037.8745 6037.8925 -0.0180 RR 2, 6 0.50 6038.4989 6038.5024 -0.0035 RR 2, 7 1.00 6039.1064 6039.1118 -0.0054 RR 2, 8 0.00 6039.7390 6039.7207 0.0183 RR 2, 9 1.00 6040.3117 6040.3292 -0.0175 RR 2,10 1.00 6040.9194 6040.9372 -0.0178 RR 2,11 0.13 6041.5151 6041.5449 -0.0298 RR 2,12 0.06 6042.1210 6042.1523 -0.0313 RR 2,13 0.50 6042.7509 6042.7594 -0.0085 RR 2,14 1.00 6043.3478 6043.3662 -0.0184					
RR 2, 4 0.25 6037.2531 6037.2822 -0.0291 RR 2, 5 1.00 6037.8745 6037.8925 -0.0180 RR 2, 6 0.50 6038.4989 6038.5024 -0.0035 RR 2, 7 1.00 6039.1064 6039.1118 -0.0054 RR 2, 8 0.00 6039.7390 6039.7207 0.0183 RR 2, 9 1.00 6040.3117 6040.3292 -0.0175 RR 2,10 1.00 6040.9194 6040.9372 -0.0178 RR 2,11 0.13 6041.5151 6041.5449 -0.0298 RR 2,12 0.06 6042.1210 6042.1523 -0.0313 RR 2,13 0.50 6042.7509 6042.7594 -0.0085 RR 2,14 1.00 6043.3478 6043.3662 -0.0184					
RR 2, 5 1.00 6037.8745 6037.8925 -0.0180 RR 2, 6 0.50 6038.4989 6038.5024 -0.0035 RR 2, 7 1.00 6039.1064 6039.1118 -0.0054 RR 2, 8 0.00 6039.7390 6039.7207 0.0183 RR 2, 9 1.00 6040.3117 6040.3292 -0.0175 RR 2,10 1.00 6040.9194 6040.9372 -0.0178 RR 2,11 0.13 6041.5151 6041.5449 -0.0298 RR 2,12 0.06 6042.1210 6042.1523 -0.0313 RR 2,13 0.50 6042.7509 6042.7594 -0.0085 RR 2,14 1.00 6043.3478 6043.3662 -0.0184	•				
RR 2, 6 0.50 6038.4989 6038.5024 -0.0035 RR 2, 7 1.00 6039.1064 6039.1118 -0.0054 RR 2, 8 0.00 6039.7390 6039.7207 0.0183 RR 2, 9 1.00 6040.3117 6040.3292 -0.0175 RR 2,10 1.00 6040.9194 6040.9372 -0.0178 RR 2,11 0.13 6041.5151 6041.5449 -0.0298 RR 2,12 0.06 6042.1210 6042.1523 -0.0313 RR 2,13 0.50 6042.7509 6042.7594 -0.0085 RR 2,14 1.00 6043.3478 6043.3662 -0.0184	•				
RR 2, 7 1.00 6039.1064 6039.1118 -0.0054 RR 2, 8 0.00 6039.7390 6039.7207 0.0183 RR 2, 9 1.00 6040.3117 6040.3292 -0.0175 RR 2,10 1.00 6040.9194 6040.9372 -0.0178 RR 2,11 0.13 6041.5151 6041.5449 -0.0298 RR 2,12 0.06 6042.1210 6042.1523 -0.0313 RR 2,13 0.50 6042.7509 6042.7594 -0.0085 RR 2,14 1.00 6043.3478 6043.3662 -0.0184	•				
RR 2, 8 0.00 6039.7390 6039.7207 0.0183 RR 2, 9 1.00 6040.3117 6040.3292 -0.0175 RR 2,10 1.00 6040.9194 6040.9372 -0.0178 RR 2,11 0.13 6041.5151 6041.5449 -0.0298 RR 2,12 0.06 6042.1210 6042.1523 -0.0313 RR 2,13 0.50 6042.7509 6042.7594 -0.0085 RR 2,14 1.00 6043.3478 6043.3662 -0.0184	-				
RR 2, 9 1.00 6040.3117 6040.3292 -0.0175 RR 2,10 1.00 6040.9194 6040.9372 -0.0178 RR 2,11 0.13 6041.5151 6041.5449 -0.0298 RR 2,12 0.06 6042.1210 6042.1523 -0.0313 RR 2,13 0.50 6042.7509 6042.7594 -0.0085 RR 2,14 1.00 6043.3478 6043.3662 -0.0184	· · · · · · · · · · · · · · · · · · ·				
RR 2,10 1.00 6040.9194 6040.9372 -0.0178 RR 2,11 0.13 6041.5151 6041.5449 -0.0298 RR 2,12 0.06 6042.1210 6042.1523 -0.0313 RR 2,13 0.50 6042.7509 6042.7594 -0.0085 RR 2,14 1.00 6043.3478 6043.3662 -0.0184	•				
RR 2,11 0.13 6041.5151 6041.5449 -0.0298 RR 2,12 0.06 6042.1210 6042.1523 -0.0313 RR 2,13 0.50 6042.7509 6042.7594 -0.0085 RR 2,14 1.00 6043.3478 6043.3662 -0.0184					
RR 2,12 0.06 6042.1210 6042.1523 -0.0313 RR 2,13 0.50 6042.7509 6042.7594 -0.0085 RR 2,14 1.00 6043.3478 6043.3662 -0.0184					
RR 2,13 0.50 6042.7509 6042.7594 -0.0085 RR 2,14 1.00 6043.3478 6043.3662 -0.0184	•				
RR 2,14 1.00 6043.3478 6043.3662 -0.0184					
	RR 2,18	1.00	6045.7660		

1	K J	WI	OBS FREQ	CALC FREQ	OBS-CALC
RR :	2,19	0.25	6046.4010	6046.3984	0.0026
	2,20		6047.0051	6047.0048	0.0003
	2,21		6047.5951	6047.6114	-0.0163
	2,22		6048.2572	6048.2182	0.0390
	2,23		6048.7462	6048.8253	-0.0791
	2,24		6049.4792	6049.4327	0.0465
	3,10			6038.5192	
	3, 9			6039.1375	
	3, 8		6039.7810	6039.7554	0.0256
	3, 7		6040.3660	6040.3728	-0.0068
	3, 6			6040.9897	
	3, 5			6041.6061	
	3, 4			6042.2219	
	3, 3			6042.8372	
	3, 3		6047.1371	6047.1282	0.0089
	3, 4		6047.7341	6047.7389	-0.0048
	3, 5		6048.3581	6048.3491	0.0090
	3, 6		6048.9771	6048.9587	0.0184
	3, 7		6049.5762	6049.5678	0.0084
	3, 8		6050.1532	6050.1764	-0.0232
	3, 9		6050.8262	6050.7846	0.0416
	3,10		6051.4081	6051.3923	0.0158
	3,11		6051.9901	6051.9996	-0.0095
	3,12		6052.6611	6052.6066	0.0545
	3,13		6053.2110	6053.2132	-0.0022
	3,14		6053.8170	6053.8196	-0.0026
	3,15		6054.4359	6054.4257	0.0102
	3,16		6055.0629	6055.0317	0.0312
	3,18		6056.2447	6056.2433	0.0014
	3,19		6056.9407	6056.8490	0.0917
	3,20		6057.4726	6057.4549	0.0177
	3,21		6058.0765	6058.0608	0.0157
	3,22		6058.7274	6058.6669	0.0605
	3,23		6059.3063	6059.2733	0.0330
	3,24		6059.9352	6059.8801	0.0551
	3,25		6060.5251	6060.4872	0.0379
	3,26		6061.1109	6061.0949	0.0160
	3,27		6061.7058	6061.7032	0.0026
	3,28		6062.3247	6062.3121	0.0126
	3,29		6063.0145	6062.9218	0.0927
	4,-1			6055.0387	3332
_	4, 4		6058.7274	6058.0971	0.6303
	4, 5		6059.4023	6058.7069	0.6954
	4, 6			6059.3163	
	4, 7		6060.6121	6059.9251	0.6870
	4, 8			6060.5333	
	4, 9		6061.8128	6061.1411	0.6717
	4,10		6062.4416	6061.7484	0.6932

RR 4,11	K J	WI	OBS FREQ	CALC FREQ	OBS-CALC
RR 4,12	RR 4.11	0.00	6063.0145	6062.3553	0.6592
RR 4,13					
RR 4,14					
RR 4,15	-		6064,8830		0.7092
RR 4,16	-				
RR 4,17	•				
RQ 5,-1 0.00 6065.2993 RR 5, 5 0.00 6068.4737 6068.9662 RR 5, 6 0.00 6069.0228 6070.1836 -1.1608 RR 5, 8 0.00 6069.0228 6070.7915 -1.0996 RR 5, 9 0.00 6070.2740 6071.3988 -1.1248 RR 5, 10 0.00 6070.8551 6072.0057 -1.1506 RR 5, 11 0.00 6071.5152 6072.6121 -1.0969 RR 5, 12 0.00 6072.1373 6073.2181 -1.0808 RR 5, 13 0.00 6072.7394 6073.8237 -1.0843 RR 5, 15 0.00 6073.3575 6074.4289 -1.0714 RR 5, 15 0.00 6073.3575 6074.4289 -1.0714 RR 5, 15 0.00 6073.3575 6074.4289 -1.0714 RR 5, 15 0.00 6073.3575 6075.0339 -1.0783 RR 5, 19 0.00 6076.3929 6077.4519 -1.0590 RR 5, 20 0.00 6077.0179 6078.0562 -1.0383 RR 5, 21 0.00 6077.0179 6078.0562 -1.0383 RR 5, 21 0.00 6077.0390 6078.6606 -1.0216 RR 5, 22 0.00 6078.2071 6079.2651 -1.0580 RP 6, 26 0.00 6059.4023 6059.3622 0.0401 RP 6, 20 0.00 6065.0009 6064.9555 0.0454 RP 6, 11 0.00 6065.0009 6064.9555 0.0454 RP 6, 12 0.00 6066.8610 6066.8192 0.0418 RP 6, 10 0.00 6068.6488 6068.6798 -0.0310 RP 6, 9 0.50 6069.9300 6069.9180 0.0120 RP 6, 8 0.00 6071.7780 6071.7713 0.0067 RR 6, 6 0.50 6079.7213 6079.7349 -0.0136 RR 6, 7 0.00 6080.3404 6080.3429 -0.0025 RR 6, 8 2.00 6080.9574 6080.9503 0.0071 RR 6, 9 0.50 6080.9574 6080.9503 0.0071 RR 6, 9 0.50 6081.5474 6081.5572 -0.0098 RR 6, 11 0.25 6082.7844 6082.7694 0.0150 RR 6, 12 2.00 6083.3684 6083.3748 -0.0064 RR 6, 13 0.13 6083.9574 6083.9797 -0.0223 RR 6, 14 0.13 6084.6094 6084.5843 0.0251 RR 6, 15 2.00 6085.8174 6085.1886 -0.0012 RR 6, 16 0.13 6085.8124 6085.7926 0.0198 RR 6, 17 0.50 6086.3874 6086.3964 -0.0090	•				
RR 5, 5 0.00 6068.4737 6069.5752 -1.1015 RR 5, 6 0.00 6068.4737 6069.5752 -1.1015 RR 5, 7 0.00 6069.0228 6070.1836 -1.1608 RR 5, 8 0.00 6069.6919 6070.7915 -1.0996 RR 5, 9 0.00 6070.2740 6071.3988 -1.1248 RR 5,10 0.00 6070.8551 6072.0057 -1.1506 RR 5,11 0.00 6071.5152 6072.6121 -1.0969 RR 5,12 0.00 6072.1373 6073.2181 -1.0808 RR 5,13 0.00 6072.7394 6073.8237 -1.0843 RR 5,14 0.00 6073.3575 6074.4289 -1.0714 RR 5,15 0.00 6073.3575 6074.4289 -1.0714 RR 5,15 0.00 6076.3929 6077.4519 -1.0590 RR 5,20 0.00 6077.0179 6078.0562 -1.0383 RR 5,21 0.00 6077.6390 6078.6606 -1.0216 RR 5,22 0.00 6077.6390 6078.6606 -1.0216 RR 5,22 0.00 6078.2071 6079.2651 -1.0580 RP 6,26 0.00 6059.4023 6059.3622 0.0401 RP 6,21 0.00 6065.0009 6064.9555 0.0454 RP 6,17 0.00 6068.0150 6068.0600 -0.0450 RP 6,11 0.00 6068.0150 6068.0600 -0.0450 RP 6,11 0.00 6068.0150 6068.0600 -0.0450 RP 6,11 0.00 6068.0150 6068.0600 -0.0450 RP 6,10 0.00 6068.0150 6068.0600 -0.0450 RP 6, 8 0.00 6079.7213 6079.7349 -0.00136 RR 6, 7 0.00 6069.9300 6079.7349 -0.00136 RR 6, 7 8.00 6080.9574 6080.9503 0.0071 RR 6, 9 0.50 6080.9574 6080.9503 0.0071 RR 6, 9 0.50 6081.5474 6081.5572 -0.0098 RR 6,11 0.25 6082.7844 6082.7694 0.00120 RR 6,12 2.00 6083.3684 6083.3748 -0.0064 RR 6,13 0.13 6083.9574 6082.1635 -0.0041 RR 6,11 0.25 6082.7844 6082.7694 0.00150 RR 6,12 2.00 6083.3684 6083.3748 -0.0064 RR 6,13 0.13 6083.9574 6082.1635 -0.0041 RR 6,14 0.13 6084.6094 6084.5843 0.0251 RR 6,15 2.00 6085.8174 6085.1886 -0.00122 RR 6,16 0.13 6085.8124 6085.7925 0.0198 RR 6,17 0.50 6085.8174 6085.1886 -0.0012	•		000010301		01/001
RR 5, 6 0.00 6068.4737 6069.5752 -1.1015 RR 5, 7 0.00 6069.0228 6070.1836 -1.1608 RR 5, 8 0.00 6069.6919 6070.7915 -1.0996 RR 5, 9 0.00 6070.2740 6071.3988 -1.1248 RR 5,10 0.00 6070.8551 6072.0057 -1.1506 RR 5,11 0.00 6071.5152 6072.6121 -1.0969 RR 5,12 0.00 6072.1373 6073.2181 -1.0808 RR 5,13 0.00 6072.7394 6073.8237 -1.0843 RR 5,14 0.00 6073.3575 6074.4289 -1.0714 RR 5,15 0.00 6073.9556 6075.0339 -1.0783 RR 5,19 0.00 6076.3929 6077.4519 -1.0590 RR 5,20 0.00 6077.0179 6078.0562 -1.0383 RR 5,21 0.00 6077.0390 6078.6606 -1.0216 RR 5,22 0.00 6077.6390 6078.6606 -1.0216 RR 5,22 0.00 6078.2071 6079.2651 -1.0580 RP 6,26 0.00 6059.4023 6059.3622 0.0401 RP 6,26 0.00 6062.5606 6062.4685 0.0921 RP 6,20 0.00 6065.0009 6064.9555 0.0454 RP 6,14 0.00 6065.0009 6064.9555 0.0454 RP 6,14 0.00 6066.8610 6066.8192 0.0418 RP 6,12 0.00 6068.0150 6068.0600 -0.0450 RP 6, 9 0.50 6069.9300 6079.2992 RP 6, 9 0.50 6069.9300 6079.7349 -0.0310 RP 6, 8 0.00 6071.7780 6071.1741 RR 6, 6 0.50 6079.7213 6079.7349 -0.0310 RR 6, 7 8.00 6080.3404 6080.3429 -0.0025 RR 6, 8 2.00 6080.3404 6080.3579 -0.0031 RR 6, 9 0.50 6081.5474 6082.7694 0.0150 RR 6, 11 0.25 6082.7844 6082.7694 0.0150 RR 6, 12 2.00 6083.3684 6083.3748 -0.0064 RR 6, 13 0.13 6083.3684 6083.3748 -0.0064 RR 6, 14 0.13 6084.6094 6084.3846 -0.0012 RR 6, 15 2.00 6085.1874 6085.1886 -0.0012 RR 6, 16 0.13 6085.8124 6085.7926 0.0198 RR 6, 17 0.50 6086.3874 6085.3964 -0.0090					
RR 5, 7			6068.4737		-1.1015
RR 5, 8					
RR 5, 9	-				
RR 5,10 0.00 6070.8551 6072.0057 -1.1506 RR 5,11 0.00 6071.5152 6072.6121 -1.0969 RR 5,12 0.00 6072.1373 6073.2181 -1.0808 RR 5,13 0.00 6072.7394 6073.8237 -1.0843 RR 5,14 0.00 6073.3575 6074.4289 -1.0714 RR 5,15 0.00 6073.9556 6075.0339 -1.0783 RR 5,19 0.00 6076.3929 6077.4519 -1.0590 RR 5,20 0.00 6077.0179 6078.0562 -1.0383 RR 5,21 0.00 6077.6390 6078.6606 -1.0216 RR 5,22 0.00 6078.2071 6079.2651 -1.0580 RP 6,26 0.00 6059.4023 6059.3622 0.0401 RP 6,21 0.00 6062.5606 6062.4685 0.0921 RP 6,20 0.00 6063.1755 6063.0903 0.0852 RP 6,17 0.00 6065.0009 6064.9555 0.0454 RP 6,14 0.00 6066.8610 6066.8192 0.0418 RP 6,11 0.00 6066.8610 6066.8192 0.0418 RP 6,11 0.00 6068.0150 6069.2992 RP 6, 9 0.50 6069.9300 6069.9180 0.0120 RP 6, 8 0.00 6071.1541 RP 6, 6 0.00 6077.7780 6077.7713 0.0067 RR 6, 6 0.50 6079.7213 6079.7349 -0.0136 RR 6, 7 8.00 6080.3404 6080.3429 -0.00125 RR 6, 8 2.00 6080.9574 6080.9503 0.0071 RR 6, 9 0.50 6081.5474 6081.5572 -0.0098 RR 6, 10 4.00 6082.1594 6082.1635 -0.0041 RR 6,11 0.25 6082.7844 6082.7694 0.0150 RR 6,12 2.00 6083.3684 6083.3748 -0.0064 RR 6,13 0.13 6083.9574 6083.9797 -0.0223 RR 6,14 0.13 6084.6094 6084.5843 0.0251 RR 6,15 2.00 6085.8124 6085.7926 0.0198 RR 6,17 0.50 6086.3874 6086.3964 -0.0090	•				
RR 5,11 0.00 6071.5152 6072.6121 -1.0969 RR 5,12 0.00 6072.1373 6073.2181 -1.0808 RR 5,13 0.00 6072.7394 6073.8237 -1.0843 RR 5,14 0.00 6073.3575 6074.4289 -1.0714 RR 5,15 0.00 6073.9556 6075.0339 -1.0718 RR 5,19 0.00 6076.3929 6077.4519 -1.0590 RR 5,20 0.00 6077.0179 6078.0562 -1.0383 RR 5,21 0.00 6077.6390 6078.6606 -1.0216 RR 5,22 0.00 6078.2071 6079.2651 -1.0580 RP 6,26 0.00 6059.4023 6059.3622 0.0401 RP 6,21 0.00 6062.5606 6062.4685 0.0921 RP 6,20 0.00 6063.1755 6063.0903 0.0852 RP 6,17 0.00 6065.0009 6064.9555 0.0454 RP 6,14 0.00 6066.8610 6066.8192 0.0418 RP 6,12 0.00 6068.6100 6066.8192 0.0418 RP 6,12 0.00 6068.6488 6066.6798 -0.0310 RP 6, 9 0.50 6069.9300 6069.9180 0.0120 RP 6, 8 0.00 6071.7780 6071.7713 0.0067 RR 6, 6 0.50 6079.7213 6079.7349 -0.0136 RR 6, 7 0.00 6080.3404 6080.3429 -0.0021 RR 6, 7 8.00 6080.3404 6080.3429 -0.0021 RR 6, 8 2.00 6080.3404 6080.3429 -0.0021 RR 6, 9 0.50 6080.3404 6080.3429 -0.0025 RR 6, 8 2.00 6080.3404 6080.3429 -0.0025 RR 6, 8 2.00 6080.3404 6080.3429 -0.0025 RR 6, 8 2.00 6080.3404 6080.3429 -0.0025 RR 6, 10 4.00 6082.1594 6082.1635 -0.0041 RR 6,11 0.25 6082.7844 6082.7694 0.0150 RR 6,12 2.00 6083.3684 6083.3748 -0.0064 RR 6,13 0.13 6083.9574 6083.9797 -0.0223 RR 6,14 0.13 6084.6094 6084.5843 0.0251 RR 6,15 2.00 6085.1874 6085.7926 0.0198 RR 6,17 0.50 6086.3874 6086.3964 -0.0090					
RR 5,12	•				
RR 5,13	•				
RR 5,14 0.00 6073.3575 6074.4289 -1.0714 RR 5,15 0.00 6073.9556 6075.0339 -1.0783 RR 5,19 0.00 6076.3929 6077.4519 -1.0590 RR 5,20 0.00 6077.0179 6078.0562 -1.0383 RR 5,21 0.00 6077.6390 6078.6606 -1.0216 RR 5,22 0.00 6078.2071 6079.2651 -1.0580 RP 6,26 0.00 6059.4023 6059.3622 0.0401 RP 6,21 0.00 6062.5606 6062.4685 0.0921 RP 6,20 0.00 6063.1755 6063.0903 0.0852 RP 6,17 0.00 6065.0009 6064.9555 0.0454 RP 6,12 0.00 6066.8610 6066.8192 0.0418 RP 6,12 0.00 6068.0150 6068.0600 -0.0450 RP 6,11 0.00 6068.6488 6068.6798 -0.0310 RP 6,10 0.00 6068.6488 6068.6798 RP 6,7 0.00 6070.5364 RP 6,7 0.00 6071.7780 6071.1541 RP 6, 6 0.00 6071.7780 6071.7713 0.0067 RR 6, 6 0.50 6079.7213 6079.7349 -0.0136 RR 6, 7 8.00 6080.3404 6080.3429 -0.00126 RR 6, 8 2.00 6080.3404 6080.3429 -0.0025 RR 6, 8 2.00 6080.9574 6080.9503 0.0071 RR 6, 9 0.50 6081.5474 6081.5572 -0.0098 RR 6,10 4.00 6082.1594 6082.1635 -0.0041 RR 6,11 0.25 6082.7844 6082.7694 0.0150 RR 6,12 2.00 6083.3684 6083.3748 -0.0064 RR 6,13 0.13 6083.9574 6083.9797 -0.0223 RR 6,14 0.13 6083.9574 6083.9797 -0.0223 RR 6,14 0.13 6084.6094 6084.5843 0.0251 RR 6,15 2.00 6085.8124 6085.7926 0.0198 RR 6,17 0.50 6086.3874 6086.3964 -0.0090	•				
RR 5,15					
RR 5,19					
RR 5,20 0.00 6077.0179 6078.0562 -1.0383 RR 5,21 0.00 6077.6390 6078.6606 -1.0216 RR 5,22 0.00 6078.2071 6079.2651 -1.0580 RP 6,26 0.00 6059.4023 6059.3622 0.0401 RP 6,21 0.00 6062.5606 6062.4685 0.0921 RP 6,20 0.00 6063.1755 6063.0903 0.0852 RP 6,17 0.00 6065.0009 6064.9555 0.0454 RP 6,14 0.00 6066.8610 6066.8192 0.0418 RP 6,12 0.00 6068.0150 6068.0600 -0.0450 RP 6,11 0.00 6068.6488 6068.6798 -0.0310 RP 6,10 0.00 6068.6488 6068.6798 -0.0310 RP 6, 9 0.50 6069.9300 6069.9180 0.0120 RP 6, 8 0.00 6071.7780 6071.7713 0.0067 RR 6, 6 0.50 6079.7213 6079.7349 -0.0136 RR 6, 7 8.00 6080.3404 6080.3429 -0.0025 RR 6, 8 2.00 6080.9574 6080.9503 0.0071 RR 6, 9 0.50 6081.5474 6081.5572 -0.0098 RR 6,11 0.25 6082.1594 6082.1635 -0.0041 RR 6,11 0.25 6082.1594 6082.1635 -0.0041 RR 6,11 0.25 6082.7844 6082.7694 0.0150 RR 6,12 2.00 6083.3684 6083.3748 -0.0064 RR 6,13 0.13 6083.9574 6083.9797 -0.0223 RR 6,14 0.13 6084.6094 6084.5843 0.0251 RR 6,15 2.00 6085.8124 6085.7926 0.0198 RR 6,17 0.50 6086.3874 6086.3964 -0.0090					
RR 5,21 0.00 6077.6390 6078.6606 -1.0216 RR 5,22 0.00 6078.2071 6079.2651 -1.0580 RP 6,26 0.00 6059.4023 6059.3622 0.0401 RP 6,21 0.00 6062.5606 6062.4685 0.0921 RP 6,20 0.00 6063.1755 6063.0903 0.0852 RP 6,17 0.00 6065.0009 6064.9555 0.0454 RP 6,14 0.00 6066.8610 6066.8192 0.0418 RP 6,12 0.00 6068.0150 6068.0600 -0.0450 RP 6,11 0.00 6068.6488 6068.6798 -0.0310 RP 6,10 0.00 6069.2992 RP 6, 9 0.50 6069.9300 6069.9180 0.0120 RP 6, 8 0.00 6071.1541 RP 6, 6 0.00 6071.7780 6071.1541 RP 6, 6 0.50 6079.7213 6079.7349 -0.0136 RR 6, 7 8.00 6080.3404 6080.3429 -0.0025 RR 6, 8 2.00 6080.9574 6080.9503 0.0071 RR 6, 9 0.50 6081.5474 6081.5572 -0.0098 RR 6,10 4.00 6082.1594 6082.1635 -0.0041 RR 6,11 0.25 6082.7844 6082.7694 0.0150 RR 6,12 2.00 6083.3684 6083.3748 -0.0064 RR 6,13 0.13 6083.9574 6083.9797 -0.0223 RR 6,14 0.13 6084.6094 6084.5843 0.0251 RR 6,15 2.00 6085.8124 6085.7926 0.0198 RR 6,17 0.50 6085.8124 6085.3964 -0.0090	•				
RR 5,22 0.00 6078.2071 6079.2651 -1.0580 RP 6,26 0.00 6059.4023 6059.3622 0.0401 RP 6,21 0.00 6062.5606 6062.4685 0.0921 RP 6,20 0.00 6063.1755 6063.0903 0.0852 RP 6,17 0.00 6065.0009 6064.9555 0.0454 RP 6,14 0.00 6066.8610 6066.8192 0.0418 RP 6,12 0.00 6068.0150 6068.0600 -0.0450 RP 6,11 0.00 6068.6488 6068.6798 -0.0310 RP 6,10 0.00 6069.9300 6069.2992 RP 6, 9 0.50 6069.9300 6069.9180 0.0120 RP 6, 8 0.00 6071.7780 6071.1541 RP 6, 6 0.50 6079.7213 6079.7349 -0.0136 RR 6, 7 8.00 6080.3404 6080.3429 -0.0025 RR 6, 8 2.00 6080.9574 6080.3429 -0.0025 RR 6, 8 2.00 6080.9574 6080.9503 0.0071 RR 6, 9 0.50 6081.5474 6081.5572 -0.0098 RR 6,10 4.00 6082.1594 6082.1635 -0.0041 RR 6,11 0.25 6082.7844 6082.7694 0.0150 RR 6,12 2.00 6083.3684 6083.3748 -0.0064 RR 6,13 0.13 6083.9574 6083.9797 -0.0223 RR 6,14 0.13 6084.6094 6084.5843 0.0251 RR 6,15 2.00 6085.8124 6085.7926 0.0198 RR 6,17 0.50 6086.3874 6086.3964 -0.0090					
RP 6,26 0.00 6059.4023 6059.3622 0.0401 RP 6,21 0.00 6062.5606 6062.4685 0.0921 RP 6,20 0.00 6063.1755 6063.0903 0.0852 RP 6,17 0.00 6065.0009 6064.9555 0.0454 RP 6,14 0.00 6066.8610 6066.8192 0.0418 RP 6,12 0.00 6068.0150 6068.0600 -0.0450 RP 6,11 0.00 6068.6488 6068.6798 -0.0310 RP 6,10 0.00 6069.9300 6069.9920 RP 6, 9 0.50 6069.9300 6069.9180 0.0120 RP 6, 8 0.00 6071.7780 6071.7541 RP 6, 6 0.50 6079.7213 6079.7349 -0.0136 RR 6, 7 8.00 6080.3404 6080.3429 -0.0025 RR 6, 8 2.00 6080.9574 6080.9503 0.0071 RR 6, 9 0.50 6081.5474 6081.5572 -0.0098 RR 6,10 4.00 6082.1594 6082.1635 -0.0041 RR 6,11 0.25 6082.7844 6082.7694 0.0150 RR 6,12 2.00 6083.3684 6083.3748 -0.0064 RR 6,13 0.13 6083.9574 6083.9797 -0.0223 RR 6,14 0.13 6084.6094 6084.5843 0.0251 RR 6,15 2.00 6085.8124 6085.7926 0.0198 RR 6,16 0.13 6085.8124 6085.7926 0.0198 RR 6,17 0.50 6086.3874 6086.3964 -0.0090	•				
RP 6,21 0.00 6062.5606 6062.4685 0.0921 RP 6,20 0.00 6063.1755 6063.0903 0.0852 RP 6,17 0.00 6065.0009 6064.9555 0.0454 RP 6,14 0.00 6066.8610 6066.8192 0.0418 RP 6,12 0.00 6068.0150 6068.0600 -0.0450 RP 6,11 0.00 6068.6488 6068.6798 -0.0310 RP 6,10 0.00 6069.9300 6069.9180 0.0120 RP 6, 8 0.00 6071.7780 6071.1541 RP 6, 6 0.00 6071.7780 6071.7713 0.0067 RR 6, 6 0.50 6079.7213 6079.7349 -0.0136 RR 6, 7 8.00 6080.3404 6080.3429 -0.0025 RR 6, 8 2.00 6080.9574 6080.9503 0.0071 RR 6, 9 0.50 6081.5474 6081.5572 -0.0098 RR 6,10 4.00 6082.1594 6082.1635 -0.0041 RR 6,11 0.25 6082.7844 6082.7694 0.0150 RR 6,12 2.00 6083.3684 6083.3748 -0.0064 RR 6,13 0.13 6083.9574 6083.9797 -0.0223 RR 6,14 0.13 6084.6094 6084.5843 0.0251 RR 6,15 2.00 6085.1874 6085.1886 -0.0012 RR 6,16 0.13 6085.8124 6085.7926 0.0198 RR 6,17 0.50 6086.3874 6086.3964 -0.0090	-				
RP 6,20 0.00 6063.1755 6063.0903 0.0852 RP 6,17 0.00 6065.0009 6064.9555 0.0454 RP 6,14 0.00 6066.8610 6066.8192 0.0418 RP 6,12 0.00 6068.0150 6068.0600 -0.0450 RP 6,11 0.00 6068.6488 6068.6798 -0.0310 RP 6,10 0.00 6069.9300 6069.9922 RP 6, 9 0.50 6069.9300 6069.9180 0.0120 RP 6, 8 0.00 6071.7780 6071.1541 RP 6, 6 0.00 6071.7780 6071.7713 0.0067 RR 6, 6 0.50 6079.7213 6079.7349 -0.0136 RR 6, 7 8.00 6080.3404 6080.3429 -0.0025 RR 6, 8 2.00 6080.9574 6080.9503 0.0071 RR 6, 9 0.50 6081.5474 6081.5572 -0.0098 RR 6,10 4.00 6082.1594 6082.1635 -0.0041 RR 6,11 0.25 6082.7844 6082.7694 0.0150 RR 6,12 2.00 6083.3684 6083.3748 -0.0064 RR 6,13 0.13 6083.9574 6083.9797 -0.0223 RR 6,14 0.13 6084.6094 6084.5843 0.0251 RR 6,15 2.00 6085.1874 6085.1886 -0.0012 RR 6,16 0.13 6085.8124 6085.7926 0.0198 RR 6,17 0.50 6086.3874 6086.3964 -0.0090	•				
RP 6,17 0.00 6065.0009 6064.9555 0.0454 RP 6,14 0.00 6066.8610 6066.8192 0.0418 RP 6,12 0.00 6068.0150 6068.0600 -0.0450 RP 6,11 0.00 6068.6488 6068.6798 -0.0310 RP 6,10 0.00 6069.9300 6069.9180 0.0120 RP 6, 9 0.50 6069.9300 6070.5364 RP 6, 7 0.00 6071.7780 6071.7713 0.0067 RR 6, 6 0.50 6079.7213 6079.7349 -0.0136 RR 6, 7 8.00 6080.3404 6080.3429 -0.0025 RR 6, 8 2.00 6080.9574 6080.9503 0.0071 RR 6, 9 0.50 6081.5474 6081.5572 -0.0098 RR 6,10 4.00 6082.1594 6082.1635 -0.0041 RR 6,11 0.25 6082.7844 6082.7694 0.0150 RR 6,12 2.00 6083.3684 6083.3748 -0.0064 RR 6,13 0.13 6083.9574 6083.9797 -0.0223 RR 6,14 0.13 6084.6094 6084.5843 0.0251 RR 6,15 2.00 6085.1874 6085.1886 -0.0012 RR 6,16 0.13 6085.8124 6085.7926 0.0198 RR 6,17 0.50 6086.3874 6086.3964 -0.0090	•				
RP 6,14 0.00 6066.8610 6066.8192 0.0418 RP 6,12 0.00 6068.0150 6068.0600 -0.0450 RP 6,11 0.00 6068.6488 6068.6798 -0.0310 RP 6,10 0.00 6069.9300 6069.2992 RP 6, 9 0.50 6069.9300 6069.9180 0.0120 RP 6, 8 0.00 6071.7780 6071.1541 RP 6, 6 0.00 6071.7780 6071.7713 0.0067 RR 6, 6 0.50 6079.7213 6079.7349 -0.0136 RR 6, 7 8.00 6080.3404 6080.3429 -0.0025 RR 6, 8 2.00 6080.9574 6080.9503 0.0071 RR 6, 9 0.50 6081.5474 6081.5572 -0.0098 RR 6,10 4.00 6082.1594 6082.1635 -0.0041 RR 6,11 0.25 6082.7844 6082.7694 0.0150 RR 6,12 2.00 6083.3684 6083.3748 -0.0064 RR 6,13 0.13 6083.9574 6083.9797 -0.0223 RR 6,14 0.13 6084.6094 6084.5843 0.0251 RR 6,15 2.00 6085.1874 6085.1886 -0.0012 RR 6,16 0.13 6085.8124 6085.7926 0.0198 RR 6,17 0.50 6086.3874 6086.3964 -0.0090	-				
RP 6,12 0.00 6068.0150 6068.0600 -0.0450 RP 6,11 0.00 6068.6488 6068.6798 -0.0310 RP 6,10 0.00 6069.2992 RP 6, 9 0.50 6069.9300 6069.9180 0.0120 RP 6, 8 0.00 6071.7780 6071.1541 RP 6, 6 0.00 6071.7780 6071.7713 0.0067 RR 6, 6 0.50 6079.7213 6079.7349 -0.0136 RR 6, 7 8.00 6080.3404 6080.3429 -0.0025 RR 6, 8 2.00 6080.9574 6080.9503 0.0071 RR 6, 9 0.50 6081.5474 6081.5572 -0.0098 RR 6,10 4.00 6082.1594 6082.1635 -0.0041 RR 6,11 0.25 6082.7844 6082.7694 0.0150 RR 6,12 2.00 6083.3684 6083.3748 -0.0064 RR 6,13 0.13 6083.9574 6083.9797 -0.0223 RR 6,14 0.13 6084.6094 6084.5843 0.0251 RR 6,15 2.00 6085.1874 6085.1886 -0.0012 RR 6,16 0.13 6085.8124 6085.7926 0.0198 RR 6,17 0.50 6086.3874 6086.3964 -0.0090	•				
RP 6,11 0.00 6068.6488 6068.6798 -0.0310 RP 6,10 0.00 6069.2992 RP 6, 9 0.50 6069.9300 6069.9180 0.0120 RP 6, 8 0.00 6070.5364 RP 6, 7 0.00 6071.7780 6071.7713 0.0067 RR 6, 6 0.50 6079.7213 6079.7349 -0.0136 RR 6, 7 8.00 6080.3404 6080.3429 -0.0025 RR 6, 8 2.00 6080.9574 6080.9503 0.0071 RR 6, 9 0.50 6081.5474 6081.5572 -0.0098 RR 6,10 4.00 6082.1594 6082.1635 -0.0041 RR 6,11 0.25 6082.7844 6082.7694 0.0150 RR 6,12 2.00 6083.3684 6083.3748 -0.0064 RR 6,13 0.13 6083.9574 6083.9797 -0.0223 RR 6,14 0.13 6084.6094 6084.5843 0.0251 RR 6,15 2.00 6085.1874 6085.1886 -0.0012 RR 6,16 0.13 6085.8124 6085.7926 0.0198 RR 6,17 0.50 6086.3874 6086.3964 -0.0090	-				
RP 6,10 0.00 6069.9300 6069.9180 0.0120 RP 6, 8 0.00 6070.5364 RP 6, 7 0.00 6071.1541 RP 6, 6 0.50 6079.7213 6079.7349 -0.0136 RR 6, 7 8.00 6080.3404 6080.3429 -0.0025 RR 6, 8 2.00 6080.9574 6080.9503 0.0071 RR 6, 9 0.50 6081.5474 6081.5572 -0.0098 RR 6,10 4.00 6082.1594 6082.1635 -0.0041 RR 6,11 0.25 6082.7844 6082.7694 0.0150 RR 6,12 2.00 6083.3684 6083.3748 -0.0064 RR 6,13 0.13 6083.9574 6083.9797 -0.0223 RR 6,14 0.13 6084.6094 6084.5843 0.0251 RR 6,15 2.00 6085.1874 6085.1886 -0.0012 RR 6,16 0.13 6085.8124 6085.7926 0.0198 RR 6,17 0.50 6086.3874 6086.3964 -0.0090					
RP 6, 9 0.50 6069.9300 6069.9180 0.0120 RP 6, 8 0.00 6070.5364 RP 6, 7 0.00 6071.1541 RP 6, 6 0.50 6079.7213 6079.7349 -0.0136 RR 6, 7 8.00 6080.3404 6080.3429 -0.0025 RR 6, 8 2.00 6080.9574 6080.9503 0.0071 RR 6, 9 0.50 6081.5474 6081.5572 -0.0098 RR 6,10 4.00 6082.1594 6082.1635 -0.0041 RR 6,11 0.25 6082.7844 6082.7694 0.0150 RR 6,12 2.00 6083.3684 6083.3748 -0.0064 RR 6,13 0.13 6083.9574 6083.9797 -0.0223 RR 6,14 0.13 6084.6094 6084.5843 0.0251 RR 6,15 2.00 6085.1874 6085.1886 -0.0012 RR 6,16 0.13 6085.8124 6085.7926 0.0198 RR 6,17 0.50 6086.3874 6086.3964 -0.0090	•				
RP 6, 8 0.00 6071.1541 RP 6, 7 0.00 6071.7780 6071.7713 0.0067 RR 6, 6 0.50 6079.7213 6079.7349 -0.0136 RR 6, 7 8.00 6080.3404 6080.3429 -0.0025 RR 6, 8 2.00 6080.9574 6080.9503 0.0071 RR 6, 9 0.50 6081.5474 6081.5572 -0.0098 RR 6,10 4.00 6082.1594 6082.1635 -0.0041 RR 6,11 0.25 6082.7844 6082.7694 0.0150 RR 6,12 2.00 6083.3684 6083.3748 -0.0064 RR 6,13 0.13 6083.9574 6083.9797 -0.0223 RR 6,14 0.13 6084.6094 6084.5843 0.0251 RR 6,15 2.00 6085.1874 6085.1886 -0.0012 RR 6,16 0.13 6085.8124 6085.7926 0.0198 RR 6,17 0.50 6086.3874 6086.3964 -0.0090			6069,9300		0.0120
RP 6, 7 0.00 6071.7780 6071.7713 0.0067 RR 6, 6 0.50 6079.7213 6079.7349 -0.0136 RR 6, 7 8.00 6080.3404 6080.3429 -0.0025 RR 6, 8 2.00 6080.9574 6080.9503 0.0071 RR 6, 9 0.50 6081.5474 6081.5572 -0.0098 RR 6,10 4.00 6082.1594 6082.1635 -0.0041 RR 6,11 0.25 6082.7844 6082.7694 0.0150 RR 6,12 2.00 6083.3684 6083.3748 -0.0064 RR 6,13 0.13 6083.9574 6083.9797 -0.0223 RR 6,14 0.13 6084.6094 6084.5843 0.0251 RR 6,15 2.00 6085.1874 6085.1886 -0.0012 RR 6,16 0.13 6085.8124 6085.7926 0.0198 RR 6,17 0.50 6086.3874 6086.3964 -0.0090					
RP 6, 6 0.00 6071.7780 6071.7713 0.0067 RR 6, 6 0.50 6079.7213 6079.7349 -0.0136 RR 6, 7 8.00 6080.3404 6080.3429 -0.0025 RR 6, 8 2.00 6080.9574 6080.9503 0.0071 RR 6, 9 0.50 6081.5474 6081.5572 -0.0098 RR 6,10 4.00 6082.1594 6082.1635 -0.0041 RR 6,11 0.25 6082.7844 6082.7694 0.0150 RR 6,12 2.00 6083.3684 6083.3748 -0.0064 RR 6,13 0.13 6083.9574 6083.9797 -0.0223 RR 6,14 0.13 6084.6094 6084.5843 0.0251 RR 6,15 2.00 6085.1874 6085.1886 -0.0012 RR 6,16 0.13 6085.8124 6085.7926 0.0198 RR 6,17 0.50 6086.3874 6086.3964 -0.0090					
RR 6, 6 0.50 6079.7213 6079.7349 -0.0136 RR 6, 7 8.00 6080.3404 6080.3429 -0.0025 RR 6, 8 2.00 6080.9574 6080.9503 0.0071 RR 6, 9 0.50 6081.5474 6081.5572 -0.0098 RR 6,10 4.00 6082.1594 6082.1635 -0.0041 RR 6,11 0.25 6082.7844 6082.7694 0.0150 RR 6,12 2.00 6083.3684 6083.3748 -0.0064 RR 6,13 0.13 6083.9574 6083.9797 -0.0223 RR 6,14 0.13 6084.6094 6084.5843 0.0251 RR 6,15 2.00 6085.1874 6085.1886 -0.0012 RR 6,16 0.13 6085.8124 6085.7926 0.0198 RR 6,17 0.50 6086.3874 6086.3964 -0.0090			6071.7780		0.0067
RR 6, 7 8.00 6080.3404 6080.3429 -0.0025 RR 6, 8 2.00 6080.9574 6080.9503 0.0071 RR 6, 9 0.50 6081.5474 6081.5572 -0.0098 RR 6,10 4.00 6082.1594 6082.1635 -0.0041 RR 6,11 0.25 6082.7844 6082.7694 0.0150 RR 6,12 2.00 6083.3684 6083.3748 -0.0064 RR 6,13 0.13 6083.9574 6083.9797 -0.0223 RR 6,14 0.13 6084.6094 6084.5843 0.0251 RR 6,15 2.00 6085.1874 6085.1886 -0.0012 RR 6,16 0.13 6085.8124 6085.7926 0.0198 RR 6,17 0.50 6086.3874 6086.3964 -0.0090	-				
RR 6, 8 2.00 6080.9574 6080.9503 0.0071 RR 6, 9 0.50 6081.5474 6081.5572 -0.0098 RR 6,10 4.00 6082.1594 6082.1635 -0.0041 RR 6,11 0.25 6082.7844 6082.7694 0.0150 RR 6,12 2.00 6083.3684 6083.3748 -0.0064 RR 6,13 0.13 6083.9574 6083.9797 -0.0223 RR 6,14 0.13 6084.6094 6084.5843 0.0251 RR 6,15 2.00 6085.1874 6085.1886 -0.0012 RR 6,16 0.13 6085.8124 6085.7926 0.0198 RR 6,17 0.50 6086.3874 6086.3964 -0.0090	•				
RR 6, 9 0.50 6081.5474 6081.5572 -0.0098 RR 6,10 4.00 6082.1594 6082.1635 -0.0041 RR 6,11 0.25 6082.7844 6082.7694 0.0150 RR 6,12 2.00 6083.3684 6083.3748 -0.0064 RR 6,13 0.13 6083.9574 6083.9797 -0.0223 RR 6,14 0.13 6084.6094 6084.5843 0.0251 RR 6,15 2.00 6085.1874 6085.1886 -0.0012 RR 6,16 0.13 6085.8124 6085.7926 0.0198 RR 6,17 0.50 6086.3874 6086.3964 -0.0090					
RR 6,10 4.00 6082.1594 6082.1635 -0.0041 RR 6,11 0.25 6082.7844 6082.7694 0.0150 RR 6,12 2.00 6083.3684 6083.3748 -0.0064 RR 6,13 0.13 6083.9574 6083.9797 -0.0223 RR 6,14 0.13 6084.6094 6084.5843 0.0251 RR 6,15 2.00 6085.1874 6085.1886 -0.0012 RR 6,16 0.13 6085.8124 6085.7926 0.0198 RR 6,17 0.50 6086.3874 6086.3964 -0.0090					
RR 6,11 0.25 6082.7844 6082.7694 0.0150 RR 6,12 2.00 6083.3684 6083.3748 -0.0064 RR 6,13 0.13 6083.9574 6083.9797 -0.0223 RR 6,14 0.13 6084.6094 6084.5843 0.0251 RR 6,15 2.00 6085.1874 6085.1886 -0.0012 RR 6,16 0.13 6085.8124 6085.7926 0.0198 RR 6,17 0.50 6086.3874 6086.3964 -0.0090					
RR 6,12 2.00 6083.3684 6083.3748 -0.0064 RR 6,13 0.13 6083.9574 6083.9797 -0.0223 RR 6,14 0.13 6084.6094 6084.5843 0.0251 RR 6,15 2.00 6085.1874 6085.1886 -0.0012 RR 6,16 0.13 6085.8124 6085.7926 0.0198 RR 6,17 0.50 6086.3874 6086.3964 -0.0090	•				
RR 6,13 0.13 6083.9574 6083.9797 -0.0223 RR 6,14 0.13 6084.6094 6084.5843 0.0251 RR 6,15 2.00 6085.1874 6085.1886 -0.0012 RR 6,16 0.13 6085.8124 6085.7926 0.0198 RR 6,17 0.50 6086.3874 6086.3964 -0.0090	•				
RR 6,14 0.13 6084.6094 6084.5843 0.0251 RR 6,15 2.00 6085.1874 6085.1886 -0.0012 RR 6,16 0.13 6085.8124 6085.7926 0.0198 RR 6,17 0.50 6086.3874 6086.3964 -0.0090	•				
RR 6,15 2.00 6085.1874 6085.1886 -0.0012 RR 6,16 0.13 6085.8124 6085.7926 0.0198 RR 6,17 0.50 6086.3874 6086.3964 -0.0090					
RR 6,16 0.13 6085.8124 6085.7926 0.0198 RR 6,17 0.50 6086.3874 6086.3964 -0.0090					
RR 6,17 0.50 6086.3874 6086.3964 -0.0090					
	-				
	RR 6,20	0.06	6088.2373	6088.2070	

RR 6,21	K J	WI	OBS FREQ	CALC FREQ	OBS-CALC
RR 6,22 0.00 6089.4933 6089.4141 0.0792 RR 6,23 0.25 6090.0283 6090.0178 0.0105 RR 6,24 2.00 6090.6242 6090.6218 0.0024 RR 6,25 0.13 6091.2022 6091.2262 -0.0240 RR 7,7 0.00 6091.8580 6090.4023 1.4557 RR 7, 8 0.00 6092.4550 6091.0092 1.4458 RR 7, 9 0.00 6093.0731 6091.6156 1.4575 RR 7,10 0.00 6093.6542 6092.2213 1.4329 RR 7,11 0.00 6094.2813 6092.8266 1.4547 RR 7,12 0.00 6094.2833 6092.8266 1.4547 RR 7,13 0.00 6094.8964 6093.4313 1.4651 RR 7,14 0.00 6096.1348 6094.6395 1.4953 RR 7,15 0.00 6096.7450 6095.2430 1.5020 RR 7,16 0.00 6097.9585 6096.4491 1.5094 RQ 8,-1 0.00 6097.9585 6096.4491 1.5094 RQ 8,-1 0.00 6109.0861 6101.5739 7.5122 RR 8, 8 0.00 6109.0861 6101.5739 7.5122 RR 8,10 0.00 6109.0861 6101.5739 7.5122 RR 8,11 0.00 6110.3626 6102.7836 7.5790 RR 8,12 0.00 6111.0113 6103.3876 7.6237 RR 8,13 0.00 6112.8428 6105.1970 7.5179 RR 8,11 0.00 6112.8428 6105.1970 7.5458 RR 9,10 0.00 6112.8428 6105.1970 7.5458 RR 9,10 0.00 612.870 6113.2448 6.9340 RR 9,11 0.00 612.870 6113.8476 6.9794 RR 9,11 0.00 6120.870 6113.8476 6.9794 RR 9,11 0.00 6120.870 6113.8476 6.9794 RR 9,11 0.00 6120.870 6113.8476 6.9794 RR 9,12 0.00 6121.3731 6114.4498 6.9233 RR 9,17 0.00 6124.4644 6117.4553 7.0091 RR 9,18 0.00 6124.9787 6118.0557 6.9230 RR 9,24 0.00 6125.6130 6118.6560 6.9570 RR 9,22 0.00 6124.9787 6118.0557 6.9230 RR 9,23 0.00 6124.9787 6118.0557 6.9230 RR 9,24 0.00 6124.9787 6118.0557 6.9230 RR 9,24 0.00 6124.9787 6118.0557 6.9230 RR 9,24 0.00 6124.9987 6118.0557 6.9230 RR 9,24 0.00 6125.6130 6118.6560 6.9570 RR 9,24 0.00 6125.6130 6118.6560 6.9570 RR 9,24 0.00 6127.4913 6120.4570 7.0343 RR 9,27 0.00 6120.2364 6119.2562 6.9802 RR 9,24 0.00 6120.7299 6121.8001 7.9298 RR10,11 0.00 6130.35366 6122.4032 7.9504 RR10,11 0.00 6130.35366 6122.4032 7.9504 RR10,10 0.00 6132.7955 6124.8097 7.9868 RR10,15 0.00 6133.4253 6125.4101 8.0152	RR 6.21	1.00	6088.8173	6088.8105	0.0068
RR 6,23					
RR 6,24					
RR 6,25	•				
RQ 7,-1 0.00 6091.8580 6090.4023 1.4557 RR 7, 7 0.00 6092.4550 6091.0092 1.4458 RR 7, 9 0.00 6093.0731 6091.6156 1.4575 RR 7,10 0.00 6093.6542 6092.2213 1.4329 RR 7,11 0.00 6094.8964 6093.4313 1.4651 RR 7,12 0.00 6094.8964 6093.4313 1.4651 RR 7,13 0.00 6094.8964 6093.4313 1.4651 RR 7,13 0.00 6095.4397 6094.0356 1.4041 RR 7,14 0.00 6096.7450 6095.8452 RR 7,15 0.00 6096.7450 6095.8462 RR 7,17 0.00 6096.7450 6095.8462 RR 7,17 0.00 6096.7450 6095.8462 RR 7,17 0.00 6096.7450 6095.8462 RR 8, 8 0.00 6108.4105 6100.9681 7.4424 RR 8, 9 0.00 6109.0861 6101.5739 7.5122 RR 8,10 0.00 6109.0861 6101.5739 7.5122 RR 8,10 0.00 6109.0861 6101.5739 7.5122 RR 8,11 0.00 6110.3626 6102.7836 7.5790 RR 8,12 0.00 6111.0113 6103.3876 7.6237 RR 8,13 0.00 6111.5882 6103.9912 7.5970 RR 8,13 0.00 6112.8428 6105.1970 7.6458 RR 9,10 0.00 6112.8428 6105.1970 7.6458 RR 9,10 0.00 6112.8428 6105.1970 7.6458 RR 9,10 0.00 6120.3786 6112.0377 6.9179 RR 9,11 0.00 6120.1788 6113.2448 6.9340 RR 9,10 0.00 6120.1788 6113.2448 6.9340 RR 9,11 0.00 6120.1788 6113.2448 6.9340 RR 9,12 0.00 6121.3731 6114.4498 6.9233 RR 9,17 0.00 6120.8270 6113.8476 6.9794 RR 9,14 0.00 6120.1788 6113.2448 6.9340 RR 9,15 0.00 6120.8270 6113.8476 6.9794 RR 9,14 0.00 6120.1788 6113.2448 6.9340 RR 9,17 0.00 6120.8270 6113.8476 6.9794 RR 9,18 0.00 6120.8270 6113.8476 6.9794 RR 9,19 0.00 6120.8270 6113.8476 6.9794 RR 9,19 0.00 6120.8270 6113.8476 6.9794 RR 9,20 0.00 6124.4644 6117.4553 7.0091 RR 9,20 0.00 6126.2364 6119.2562 6.9802 RR 9,23 0.00 6126.2364 6119.2562 6.9802 RR 9,24 0.00 6127.4913 6120.4570 7.0343 RR 9,20 0.00 6126.2364 6119.2562 6.9802 RR 9,23 0.00 6126.2364 6119.2562 6.9802 RR 9,24 0.00 6127.4913 6120.0577 7.9877 RR 0,015 0.00 6130.3536 6122.4032 7.9504 RR 0,015 0.00 6130.3536 6122.4032 7.9504					
RR 7, 7 0.00 6091.8580 6090.4023 1.4557 RR 7, 8 0.00 6092.4550 6091.0092 1.4458 RR 7, 9 0.00 6093.0731 6091.6156 1.4575 RR 7,10 0.00 6093.6542 6092.2213 1.4329 RR 7,11 0.00 6094.2813 6092.8266 1.4547 RR 7,12 0.00 6094.8964 6093.4313 1.4651 RR 7,13 0.00 6095.4397 6094.0356 1.4041 RR 7,14 0.00 6095.1348 6094.6395 1.4953 RR 7,15 0.00 6095.1348 6094.6395 1.4953 RR 7,16 0.00 6095.7450 6095.2430 1.5020 RR 7,16 0.00 6097.9585 6096.4491 1.5094 RQ 8,-1 0.00 6097.9585 6096.4491 1.5094 RR 8, 8 0.00 6108.4105 6100.9681 7.4424 RR 8, 9 0.00 6109.0961 6101.5739 7.5122 RR 8, 8 0.00 6109.0961 6101.5739 7.5122 RR 8,11 0.00 6110.3626 6102.7836 7.5790 RR 8,12 0.00 6111.0113 6103.3876 7.6237 RR 8,13 0.00 6111.5882 6103.9912 7.5970 RR 8,15 0.00 6112.8428 6105.1970 7.6458 RR 9,10 0.00 6113.3967 6105.7993 7.5974 RQ 9,-1 0.00 6113.3967 6105.7993 7.5974 RQ 9,-1 0.00 6118.9556 6112.0377 6.9179 RR 9,11 0.00 6120.1788 6113.2448 6.9340 RR 9,13 0.00 6120.1788 6113.2448 6.9340 RR 9,14 0.00 6120.1788 6113.2448 6.9340 RR 9,15 0.00 6120.1788 6113.2448 6.9340 RR 9,16 0.00 6120.8270 6113.8476 6.9979 RR 9,17 0.00 6120.1788 6113.2448 6.9340 RR 9,18 0.00 6122.3731 6114.4498 6.9233 RR 9,19 0.00 6124.9787 6112.6416 6.9794 RR 9,18 0.00 6122.56130 6118.6550 6.9802 RR 9,22 0.00 6126.2364 6119.2562 6.9802 RR 9,23 0.00 6127.4913 6120.4570 7.0343 RR 9,22 0.00 6125.6130 6118.6560 6.9570 RR 9,22 0.00 6125.6130 6118.0557 6.9230 RR 9,22 0.00 6126.2364 6119.2562 6.9802 RR 9,23 0.00 6127.4913 6120.4570 7.0343 RR 9,24 0.00 6127.4913 6120.4570 7.0343 RR 0,25 0.00 6127.4913 6120.4570 7.0343 RR 0,15 0.00 6130.3536 6122.4032 7.9504 RR10,10 0.00 6130.9934 6123.0057 7.9867 RR10,11 0.00 6133.4253 6125.4101 8.0152	•		0000000		00000
RR 7, 8	•		6091.8580	•	1.4557
RR 7, 9 0.00 6093.0731 6091.6156 1.4575 RR 7,10 0.00 6093.6542 6092.2213 1.4329 RR 7,11 0.00 6094.2813 6092.8266 1.4547 RR 7,12 0.00 6094.8836 6093.4313 1.4651 RR 7,13 0.00 6095.4397 6094.0356 1.4041 RR 7,14 0.00 6095.4397 6094.0356 1.4953 RR 7,15 0.00 6096.7450 6095.2430 1.5020 RR 7,16 0.00 6096.7450 6095.8462 RR 7,17 0.00 6097.9585 6096.4491 1.5094 RQ 8,-1 0.00 6108.4105 6100.9681 7.4424 RR 8, 9 0.00 6109.0861 6101.5739 7.5122 RR 8,10 0.00 6109.6969 6102.1790 7.5179 RR 8,11 0.00 6110.3626 6102.7836 7.5790 RR 8,12 0.00 6111.0113 6103.3876 7.6237 RR 8,13 0.00 6111.5882 6103.9912 7.5970 RR 8,15 0.00 6112.8428 6105.1970 7.6458 RR 8,16 0.00 6113.3967 6105.7993 7.5974 RQ 9,-1 0.00 6112.8428 6105.1970 7.6458 RR 9,10 0.00 6120.788 6112.0377 6.9179 RR 9,11 0.00 6120.788 6112.0377 6.9179 RR 9,11 0.00 6120.8270 6133.8476 6.9794 RR 9,13 0.00 6121.3731 6114.4498 6.9233 RR 9,17 0.00 6124.4644 6117.4553 7.0091 RR 9,18 0.00 6124.4644 6117.4553 7.0091 RR 9,18 0.00 6125.6130 6118.6560 6.9570 RR 9,22 0.00 6125.6130 6118.6560 6.9570 RR 9,22 0.00 6125.62364 6119.2562 6.9802 RR 9,23 0.00 6125.6330 6121.0576 7.0343 RR 9,27 0.00 6127.4913 6120.4570 7.0343 RR 9,27 0.00 6125.6336 6122.4032 7.9504 RR 9,28 0.00 6130.9344 6123.0057 7.9877 RR10,10 0.00 6130.934 6123.0057 7.9877 RR10,11 0.00 6130.934 6123.0057 7.9877 RR10,15 0.00 6132.7965 6124.8097 7.9868 RR10,16 0.00 6133.4253 6125.4101 8.0152	•				
RR 7,10 0.00 6093.6542 6092.2213 1.4329 RR 7,11 0.00 6094.2813 6092.8266 1.4547 RR 7,12 0.00 6094.8964 6093.4313 1.4651 RR 7,13 0.00 6095.4397 6094.0356 1.4041 RR 7,14 0.00 6095.1348 6094.6395 1.4953 RR 7,15 0.00 6096.7450 6095.2430 1.5020 RR 7,16 0.00 6097.9585 6096.4491 1.5094 RQ 8,-1 0.00 6097.9585 6096.4491 1.5094 RQ 8,-1 0.00 6097.9585 6096.4491 7.4424 RR 8, 9 0.00 6108.4105 6100.9681 7.4424 RR 8, 9 0.00 6109.0861 6101.5739 7.5122 RR 8,11 0.00 6100.3626 6102.7730 7.5179 RR 8,11 0.00 6110.3626 6102.7836 7.5790 RR 8,12 0.00 6111.0113 6103.3876 7.6237 RR 8,13 0.00 6111.5882 6103.9912 7.5970 RR 8,15 0.00 6112.8428 6105.1970 7.6458 RR 9,10 0.00 6112.8428 6105.1970 7.6458 RR 9,10 0.00 6119.5577 6112.6416 6.9161 RR 9,12 0.00 6120.8730 6113.2448 6.9340 RR 9,11 0.00 6120.8270 6113.8476 6.9794 RR 9,14 0.00 6120.8770 6113.8476 6.9794 RR 9,18 0.00 6124.4644 6117.4553 7.0091 RR 9,19 0.00 6124.4644 6117.4553 7.0091 RR 9,22 0.00 6124.4644 6117.4553 7.0091 RR 9,22 0.00 6122.8270 6113.8476 6.9794 RR 9,19 0.00 6125.6130 6118.6560 6.9570 RR 9,22 0.00 6124.4644 6117.4553 7.0091 RR 9,22 0.00 6122.8270 6113.8476 6.9233 RR 9,17 0.00 6124.4644 6117.4553 7.0091 RR 9,22 0.00 6124.4644 6117.4553 7.0091 RR 9,22 0.00 6122.8270 6113.8476 6.9794 RR 9,18 0.00 6123.8270 6118.0557 6.9230 RR 9,21 0.00 6124.4644 6117.4553 7.0091 RR 9,22 0.00 6125.6130 6118.6560 6.9570 RR 9,23 0.00 6127.4913 6120.4570 7.0343 RR 9,25 0.00 6120.8799 6121.8001 7.9298 RR10,11 0.00 6130.9934 6123.0057 7.9877 RR10,15 0.00 6132.7965 6124.8097 7.9868 RR10,16 0.00 6133.4253 6125.4101 8.0152	•				
RR 7,11 0.00 6094.2813 6092.8266 1.4547 RR 7,12 0.00 6094.8364 6093.4313 1.4651 RR 7,13 0.00 6095.4397 6094.0356 1.4041 RR 7,14 0.00 6096.1348 6094.6395 1.4953 RR 7,15 0.00 6096.7450 6095.2430 1.5020 RR 7,16 0.00 6097.9585 6095.4491 1.5094 RQ 8,-1 0.00 6097.9585 6095.4491 1.5094 RR 8, 8 0.00 6108.4105 6100.9661 7.4424 RR 8, 9 0.00 6109.0861 6101.5739 7.5122 RR 8,10 0.00 6109.6969 6102.1790 7.5179 RR 8,11 0.00 6110.3626 6102.7836 7.5790 RR 8,12 0.00 6111.0113 6103.3876 7.5230 RR 8,13 0.00 6111.5882 6103.9912 7.5970 RR 8,15 0.00 6112.8428 6105.1970 7.6458 RR 8,16 0.00 6113.3967 6105.7993 7.5974 RQ 9,-1 0.00 6119.5577 6112.6416 6.9161 RR 9,12 0.00 6120.8270 6113.8476 6.9794 RR 9,13 0.00 6120.8270 6113.8476 6.9233 RR 9,17 0.00 6124.4644 6117.4553 7.0091 RR 9,18 0.00 6124.4644 6117.4553 7.0091 RR 9,20 0.00 6124.4644 6117.4553 7.0091 RR 9,22 0.00 6124.4644 6117.4553 7.0091 RR 9,22 0.00 6125.6130 6118.6560 6.9570 RR 9,22 0.00 6125.6130 6118.6560 6.9570 RR 9,22 0.00 6125.6130 6118.6560 6.9570 RR 9,22 0.00 6126.2364 6119.2562 6.9802 RR 9,23 0.00 6127.4913 6122.0576 RQ10,-1 0.00 6130.9934 6122.0057 7.9878 RR10,10 0.00 6130.9934 6122.0057 7.9878 RR10,15 0.00 6133.4253 6125.4101 8.0152	•				
RR 7,12	-				
RR 7,13	-				1.4651
RR 7,14	-				1.4041
RR 7,15 0.00 6096.7450 6095.2430 1.5020 RR 7,16 0.00 6097.9585 6096.4491 1.5094 RQ 8,-1 0.00 6097.9585 6096.4491 1.5094 RQ 8,-1 0.00 6108.4105 6100.9681 7.4424 RR 8, 9 0.00 6109.0861 6101.5739 7.5122 RR 8,10 0.00 6109.6969 6102.1790 7.5179 RR 8,11 0.00 6110.3626 6102.7836 7.5790 RR 8,12 0.00 6111.0113 6103.3876 7.6237 RR 8,13 0.00 6111.5882 6103.9912 7.5970 RR 8,15 0.00 6112.8428 6105.1970 7.6458 RR 8,16 0.00 6113.3967 6105.7993 7.5974 RQ 9,-1 0.00 6118.9556 6112.0377 6.9179 RR 9,11 0.00 6120.1788 6113.2448 6.9340 RR 9,12 0.00 6120.1788 6113.2448 6.9340 RR 9,13 0.00 6120.8270 6113.8476 6.9794 RR 9,14 0.00 6121.3731 6114.4498 6.9233 RR 9,17 0.00 6124.4644 6117.4553 7.0091 RR 9,18 0.00 6124.9787 6118.0557 6.9230 RR 9,20 0.00 6125.6130 6118.0557 6.9230 RR 9,22 0.00 6126.2364 6119.2562 6.9802 RR 9,23 0.00 6127.4913 6120.4570 7.0343 RR 9,25 0.00 6129.7299 6121.8001 7.9298 RR10,10 0.00 6133.3536 6122.4032 7.9504 RR10,11 0.00 6130.3536 6122.4032 7.9504 RR10,12 0.00 6132.7965 6124.8097 7.9868 RR10,15 0.00 6133.4253 6125.4101 8.0152	-			6094.6395	1.4953
RR 7,16 0.00 6097.9585 6096.4491 1.5094 RQ 8,-1 0.00 6097.9585 6096.4491 1.5094 RQ 8,-1 0.00 6108.4105 6100.9681 7.4424 RR 8, 8 0.00 6109.0861 6101.5739 7.5122 RR 8,10 0.00 6109.6969 6102.1790 7.5179 RR 8,11 0.00 6110.3626 6102.7836 7.5790 RR 8,12 0.00 6111.0113 6103.3876 7.6237 RR 8,13 0.00 6112.8428 6103.9912 7.5970 RR 8,15 0.00 6112.8428 6105.1970 7.6458 RR 8,16 0.00 6113.3967 6105.7993 7.5974 RQ 9,-1 0.00 6118.9556 6112.0377 6.9179 RR 9,11 0.00 6120.8270 6113.2448 6.9340 RR 9,13 0.00 6120.8270 6113.8476 6.9794 RR 9,14 0.00 6121.3731 6114.4498 6.9233 RR 9,17 0.00 6124.4644 6117.4553 7.0091 RR 9,18 0.00 6124.9787 6118.0557 6.9230 RR 9,20 0.00 6124.9787 6118.0557 6.9230 RR 9,21 0.00 6125.6130 6116.2540 RR 9,22 0.00 6126.2364 6119.2562 6.9802 RR 9,23 0.00 6126.2364 6119.2562 6.9802 RR 9,24 0.00 6127.4913 6120.4570 7.0343 RR 9,25 0.00 6120.7299 6121.8001 7.9298 RR10,10 0.00 6133.934 6123.0057 7.9877 RR10,15 0.00 6132.7965 6124.8097 7.9868 RR10,16 0.00 6133.4253 6125.4101 8.0152	•				1.5020
RR 7,17 0.00 6097.9585 6096.4491 1.5094 RQ 8,-1 0.00 6095.4852 RR 8, 8 0.00 6108.4105 6100.9681 7.4424 RR 8, 9 0.00 6109.0861 6101.5739 7.5122 RR 8,10 0.00 6109.6969 6102.1790 7.5179 RR 8,11 0.00 6110.3626 6102.7836 7.5790 RR 8,12 0.00 6111.0113 6103.3876 7.6237 RR 8,13 0.00 6111.5882 6103.9912 7.5970 RR 8,15 0.00 6112.8428 6105.1970 7.6458 RR 8,16 0.00 6113.3967 6105.7993 7.5974 RQ 9,-1 0.00 6118.9556 6112.0377 6.9179 RR 9,11 0.00 6119.5577 6112.6416 6.9161 RR 9,12 0.00 6120.8270 6113.8476 6.9794 RR 9,13 0.00 6120.8270 6113.8476 6.9794 RR 9,14 0.00 6121.3731 6114.4498 6.9233 RR 9,17 0.00 6124.4644 6117.4553 7.0091 RR 9,20 0.00 6124.9787 6118.0557 6.9230 RR 9,21 0.00 6125.6130 6118.6560 6.9570 RR 9,22 0.00 6125.6130 6118.6560 6.9570 RR 9,23 0.00 6126.2364 6119.2562 6.9802 RR 9,23 0.00 6127.4913 6120.4570 7.0343 RR 9,25 0.00 6129.7299 6121.8001 7.9298 RR10,10 0.00 6130.3536 6122.4032 7.9504 RR10,11 0.00 6130.3536 6122.4032 7.9504 RR10,12 0.00 6130.3536 6122.4032 7.9504 RR10,15 0.00 6133.4253 6125.4101 8.0152	-				
RQ 8,-1 0.00 6108.4105 6100.9681 7.4424 RR 8, 9 0.00 6109.0861 6101.5739 7.5122 RR 8,10 0.00 6109.6969 6102.1790 7.5179 RR 8,11 0.00 6110.3626 6102.7836 7.5790 RR 8,12 0.00 6111.0113 6103.3876 7.6237 RR 8,15 0.00 6111.5882 6103.9912 7.5970 RR 8,15 0.00 6112.8428 6105.1970 7.6458 RR 8,16 0.00 6113.3967 6105.7993 7.5974 RQ 9,-1 0.00 6113.3967 6105.7993 7.5974 RQ 9,-1 0.00 6118.9556 6112.0377 6.9179 RR 9,11 0.00 6119.5577 6112.6416 6.9161 RR 9,12 0.00 6120.1788 6113.2448 6.9340 RR 9,13 0.00 6120.8270 6113.8476 6.9794 RR 9,14 0.00 6121.3731 6114.4498 6.9233 RR 9,17 0.00 6124.4644 6117.4553 7.0091 RR 9,18 0.00 6124.4644 6117.4553 7.0091 RR 9,20 0.00 6124.9787 6118.0557 6.9230 RR 9,21 0.00 6125.6130 6118.6560 6.9570 RR 9,22 0.00 6125.6130 6118.6560 6.9570 RR 9,23 0.00 6126.2364 6119.2562 6.9802 RR 9,24 0.00 6127.4913 6120.4570 7.0343 RR 9,25 0.00 6127.4913 6120.4570 7.0343 RR 9,25 0.00 6129.7299 6121.8001 7.9298 RR10,10 0.00 6130.3536 6122.4032 7.9504 RR10,12 0.00 6130.3934 6123.0057 7.9877 RR10,15 0.00 6133.4253 6125.4101 8.0152			6097.9585		1.5094
RR 8, 8 0.00 6108.4105 6100.9681 7.4424 RR 8, 9 0.00 6109.0861 6101.5739 7.5122 RR 8,10 0.00 6109.6969 6102.1790 7.5179 RR 8,11 0.00 6110.3626 6102.7836 7.5790 RR 8,12 0.00 6111.0113 6103.3876 7.6237 RR 8,13 0.00 6111.5882 6103.9912 7.5970 RR 8,15 0.00 6112.8428 6105.1970 7.6458 RR 8,16 0.00 6113.3967 6105.7993 7.5974 RQ 9,-1 0.00 6105.3489 RR 9,10 0.00 6118.9556 6112.0377 6.9179 RR 9,11 0.00 6119.5577 6112.6416 6.9161 RR 9,12 0.00 6120.1788 6113.2448 6.9340 RR 9,13 0.00 6120.8270 6113.8476 6.9794 RR 9,14 0.00 6121.3731 6114.4498 6.9233 RR 9,17 0.00 RR 9,18 0.00 6124.4644 6117.4553 7.0091 RR 9,20 0.00 6124.9787 6118.0557 6.9230 RR 9,21 0.00 6125.6130 6118.6560 6.9570 RR 9,22 0.00 6126.2364 6119.2562 6.9802 RR 9,23 0.00 6127.4913 6120.4570 7.0343 RR 9,25 0.00 6127.4913 6122.4032 7.9504 RR10,10 0.00 6130.3536 6122.4032 7.9504 RR10,11 0.00 6130.3536 6122.4032 7.9504 RR10,15 0.00 6132.7965 6124.8097 7.9868 RR10,16 0.00 6133.4253 6125.4101 8.0152	•				
RR 8, 9 0.00 6109.0861 6101.5739 7.5122 RR 8,10 0.00 6109.6969 6102.1790 7.5179 RR 8,11 0.00 6110.3626 6102.7836 7.5790 RR 8,12 0.00 6111.0113 6103.3876 7.6237 RR 8,13 0.00 6111.5882 6103.9912 7.5970 RR 8,15 0.00 6112.8428 6105.1970 7.6458 RR 8,16 0.00 6113.3967 6105.7993 7.5974 RQ 9,-1 0.00 6118.9556 6112.0377 6.9179 RR 9,10 0.00 6118.9556 6112.0377 6.9179 RR 9,11 0.00 6120.1788 6113.2448 6.9340 RR 9,13 0.00 6120.8270 6113.8476 6.9794 RR 9,14 0.00 6121.3731 6114.4498 6.9233 RR 9,17 0.00 6124.4644 6117.4553 7.0091 RR 9,18 0.00 6124.4644 6117.4553 7.0091 RR 9,20 0.00 6124.9787 6118.0557 6.9230 RR 9,21 0.00 6125.6130 6118.6560 6.9570 RR 9,22 0.00 6126.2364 6119.2562 6.9802 RR 9,23 0.00 6127.4913 6120.4570 7.0343 RR 9,25 0.00 6127.4913 6120.4570 7.0343 RR 9,26 0.00 6129.7299 6121.8001 7.9298 RR10,11 0.00 6130.3536 6122.4032 7.9504 RR10,12 0.00 6130.9934 6123.0057 7.9877 RR10,15 0.00 6132.7965 6124.8097 7.9868 RR10,16 0.00 6133.4253 6125.4101 8.0152			6108.4105		7.4424
RR 8,10 0.00 6109.6969 6102.1790 7.5179 RR 8,11 0.00 6110.3626 6102.7836 7.5790 RR 8,12 0.00 6111.0113 6103.3876 7.6237 RR 8,13 0.00 6111.5882 6103.9912 7.5970 RR 8,15 0.00 6112.8428 6105.1970 7.6458 RR 8,16 0.00 6113.3967 6105.7993 7.5974 RQ 9,-1 0.00 6118.9556 6112.0377 6.9179 RR 9,11 0.00 6119.5577 6112.6416 6.9161 RR 9,12 0.00 6120.1788 6113.2448 6.9340 RR 9,13 0.00 6120.1788 6113.2448 6.9340 RR 9,14 0.00 6121.3731 6114.4498 6.9233 RR 9,17 0.00 6124.4644 6117.4553 7.0091 RR 9,18 0.00 6124.9787 6118.0557 6.9230 RR 9,21 0.00 6124.9787 6118.0557 6.9230 RR 9,22 0.00 6125.6130 6118.6560 6.9570 RR 9,23 0.00 6126.2364 6119.2562 6.9802 RR 9,23 0.00 6127.4913 6120.4570 7.0343 RR 9,24 0.00 6127.4913 6120.4570 7.0343 RR 9,25 0.00 6127.4913 6120.4570 7.0343 RR 9,25 0.00 6127.4913 6120.4570 7.0343 RR 9,25 0.00 6127.4913 6120.4570 7.0343 RR 9,26 0.00 6129.7299 6121.8001 7.9298 RR10,11 0.00 6130.3536 6122.4032 7.9504 RR10,12 0.00 6130.3536 6122.4032 7.9504 RR10,15 0.00 6132.7965 6124.8097 7.9868 RR10,16 0.00 6133.4253 6125.4101 8.0152					7.5122
RR 8,11 0.00 6110.3626 6102.7836 7.5790 RR 8,12 0.00 6111.0113 6103.3876 7.6237 RR 8,13 0.00 6111.5882 6103.9912 7.5970 RR 8,15 0.00 6112.8428 6105.1970 7.6458 RR 8,16 0.00 6113.3967 6105.7993 7.5974 RQ 9,-1 0.00 6105.3489 RR 9,10 0.00 6118.9556 6112.0377 6.9179 RR 9,11 0.00 6119.5577 6112.6416 6.9161 RR 9,12 0.00 6120.1788 6113.2448 6.9340 RR 9,13 0.00 6120.8270 6113.8476 6.9794 RR 9,14 0.00 6121.3731 6114.4498 6.9233 RR 9,17 0.00 6124.4644 6117.4553 7.0091 RR 9,18 0.00 6124.4644 6117.4553 7.0091 RR 9,20 0.00 6124.9787 6118.0557 6.9230 RR 9,21 0.00 6125.6130 6118.6560 6.9570 RR 9,22 0.00 6125.6130 6118.6560 6.9570 RR 9,23 0.00 6125.6130 6118.6560 6.9570 RR 9,24 0.00 6125.6130 6118.6560 6.9570 RR 9,25 0.00 6126.2364 6119.2562 6.9802 RR 9,27 0.00 6126.2364 6119.2562 6.9802 RR 9,28 0.00 6127.4913 6120.4570 7.0343 RR 9,29 0.00 6129.7299 6121.8001 7.9298 RR10,10 0.00 6130.3536 6122.4032 7.9504 RR10,12 0.00 6130.9934 6123.0057 7.9877 RR10,15 0.00 6132.7965 6124.8097 7.9868 RR10,16 0.00 6133.4253 6125.4101 8.0152			6109.6969	6102.1790	
RR 8,12 0.00 6111.0113 6103.3876 7.6237 RR 8,13 0.00 6111.5882 6103.9912 7.5970 RR 8,15 0.00 6112.8428 6105.1970 7.6458 RR 8,16 0.00 6113.3967 6105.7993 7.5974 RQ 9,-1 0.00 6118.9556 6112.0377 6.9179 RR 9,10 0.00 6119.5577 6112.6416 6.9161 RR 9,12 0.00 6120.1788 6113.2448 6.9340 RR 9,13 0.00 6120.8270 6113.8476 6.9794 RR 9,14 0.00 6121.3731 6114.4498 6.9233 RR 9,17 0.00 6124.4644 6117.4553 7.0091 RR 9,18 0.00 6124.9787 6118.0557 6.9230 RR 9,20 0.00 6124.9787 6118.0557 6.9230 RR 9,21 0.00 6125.6130 6118.6560 6.9570 RR 9,22 0.00 6126.2364 6119.2562 6.9802 RR 9,23 0.00 6126.2364 6119.2562 6.9802 RR 9,24 0.00 6127.4913 6120.4570 7.0343 RR 9,25 0.00 6129.7299 6121.8001 7.9298 RR10,10 0.00 6130.3536 6122.4032 7.9504 RR10,12 0.00 6132.7965 6124.8097 7.9868 RR10,15 0.00 6133.4253 6125.4101 8.0152	•				
RR 8,13	•		6111.0113	6103.3876	7.6237
RR 8,15					
RR 8,16 0.00 6113.3967 6105.7993 7.5974 RQ 9,-1 0.00 6105.3489 RR 9,10 0.00 6118.9556 6112.0377 6.9179 RR 9,11 0.00 6119.5577 6112.6416 6.9161 RR 9,12 0.00 6120.1788 6113.2448 6.9340 RR 9,13 0.00 6120.8270 6113.8476 6.9794 RR 9,14 0.00 6121.3731 6114.4498 6.9233 RR 9,17 0.00 6121.3731 6116.2540 RR 9,18 0.00 6124.4644 6117.4553 7.0091 RR 9,20 0.00 6124.9787 6118.0557 6.9230 RR 9,21 0.00 6125.6130 6118.6560 6.9570 RR 9,22 0.00 6125.6130 6118.6560 6.9570 RR 9,23 0.00 6126.2364 6119.2562 6.9802 RR 9,24 0.00 6127.4913 6120.4570 7.0343 RR 9,25 0.00 6127.4913 6120.4570 7.0343 RR 9,25 0.00 6129.7299 6121.8001 7.9298 RR10,10 0.00 6130.3536 6122.4032 7.9504 RR10,12 0.00 6130.9934 6123.0057 7.9877 RR10,15 0.00 6132.7965 6124.8097 7.9868 RR10,16 0.00 6133.4253 6125.4101 8.0152					7.6458
RQ 9,-1 0.00 6118.9556 6112.0377 6.9179 RR 9,11 0.00 6119.5577 6112.6416 6.9161 RR 9,12 0.00 6120.1788 6113.2448 6.9340 RR 9,13 0.00 6120.8270 6113.8476 6.9794 RR 9,14 0.00 6121.3731 6114.4498 6.9233 RR 9,17 0.00 6121.3731 6114.4498 6.9233 RR 9,18 0.00 6116.2540 RR 9,18 0.00 6124.4644 6117.4553 7.0091 RR 9,20 0.00 6124.9787 6118.0557 6.9230 RR 9,21 0.00 6125.6130 6118.6560 6.9570 RR 9,22 0.00 6125.6130 6118.6560 6.9570 RR 9,23 0.00 6126.2364 6119.2562 6.9802 RR 9,24 0.00 6127.4913 6120.4570 7.0343 RR 9,25 0.00 6127.4913 6120.4570 7.0343 RR 9,26 0.00 6129.7299 6121.8001 7.9298 RR10,10 0.00 6130.3536 6122.4032 7.9504 RR10,12 0.00 6130.9934 6123.0057 7.9877 RR10,15 0.00 6132.7965 6124.8097 7.9868 RR10,16 0.00 6133.4253 6125.4101 8.0152					
RR 9,10 0.00 6118.9556 6112.0377 6.9179 RR 9,11 0.00 6119.5577 6112.6416 6.9161 RR 9,12 0.00 6120.1788 6113.2448 6.9340 RR 9,13 0.00 6120.8270 6113.8476 6.9794 RR 9,14 0.00 6121.3731 6114.4498 6.9233 RR 9,17 0.00 6116.2540 RR 9,18 0.00 6116.8548 RR 9,19 0.00 6124.4644 6117.4553 7.0091 RR 9,20 0.00 6124.9787 6118.0557 6.9230 RR 9,21 0.00 6125.6130 6118.6560 6.9570 RR 9,22 0.00 6125.6130 6118.6560 6.9570 RR 9,23 0.00 6126.2364 6119.2562 6.9802 RR 9,24 0.00 6127.4913 6120.4570 7.0343 RR 9,25 0.00 6127.4913 6120.4570 7.0343 RR 9,26 0.00 6129.7299 6121.8001 7.9298 RR10,10 0.00 6130.3536 6122.4032 7.9504 RR10,12 0.00 6130.9934 6123.0057 7.9877 RR10,15 0.00 6133.4253 6125.4101 8.0152					
RR 9,11 0.00 6119.5577 6112.6416 6.9161 RR 9,12 0.00 6120.1788 6113.2448 6.9340 RR 9,13 0.00 6120.8270 6113.8476 6.9794 RR 9,14 0.00 6121.3731 6114.4498 6.9233 RR 9,17 0.00 6116.2540 RR 9,18 0.00 6124.4644 6117.4553 7.0091 RR 9,20 0.00 6124.9787 6118.0557 6.9230 RR 9,21 0.00 6125.6130 6118.6560 6.9570 RR 9,22 0.00 6126.2364 6119.2562 6.9802 RR 9,23 0.00 6127.4913 6120.4570 7.0343 RR 9,25 0.00 6127.4913 6120.4570 7.0343 RR 9,25 0.00 6129.7299 6121.8001 7.9298 RR10,10 0.00 6130.3536 6122.4032 7.9504 RR10,12 0.00 6130.9934 6123.0057 7.9877 RR10,15 0.00 6132.7965 6124.8097 7.9868 RR10,16 0.00 6133.4253 6125.4101 8.0152			6118.9556		6.9179
RR 9,12 0.00 6120.1788 6113.2448 6.9340 RR 9,13 0.00 6120.8270 6113.8476 6.9794 RR 9,14 0.00 6121.3731 6114.4498 6.9233 RR 9,17 0.00 6116.2540 RR 9,18 0.00 6116.8548 RR 9,19 0.00 6124.4644 6117.4553 7.0091 RR 9,20 0.00 6124.9787 6118.0557 6.9230 RR 9,21 0.00 6125.6130 6118.6560 6.9570 RR 9,22 0.00 6126.2364 6119.2562 6.9802 RR 9,23 0.00 6127.4913 6120.4570 7.0343 RR 9,24 0.00 6127.4913 6120.4570 7.0343 RR 9,25 0.00 6127.4913 6120.4570 7.0343 RR 9,26 0.00 6129.7299 6121.8001 7.9298 RR10,10 0.00 6130.3536 6122.4032 7.9504 RR10,12 0.00 6130.9934 6123.0057 7.9877 RR10,15 0.00 6132.7965 6124.8097 7.9868 RR10,16 0.00 6133.4253 6125.4101 8.0152					
RR 9,13 0.00 6120.8270 6113.8476 6.9794 RR 9,14 0.00 6121.3731 6114.4498 6.9233 RR 9,17 0.00 6116.2540 RR 9,18 0.00 6116.8548 RR 9,19 0.00 6124.4644 6117.4553 7.0091 RR 9,20 0.00 6124.9787 6118.0557 6.9230 RR 9,21 0.00 6125.6130 6118.6560 6.9570 RR 9,22 0.00 6126.2364 6119.2562 6.9802 RR 9,23 0.00 6127.4913 6120.4570 7.0343 RR 9,24 0.00 6127.4913 6120.4570 7.0343 RR 9,25 0.00 6127.4913 6120.4570 7.0343 RR 9,26 0.00 6129.7299 6121.8001 7.9298 RR10,10 0.00 6130.3536 6122.4032 7.9504 RR10,12 0.00 6130.9934 6123.0057 7.9877 RR10,15 0.00 6132.7965 6124.8097 7.9868 RR10,16 0.00 6133.4253 6125.4101 8.0152	•				6.9340
RR 9,14 0.00 6121.3731 6114.4498 6.9233 RR 9,17 0.00 6116.2540 RR 9,18 0.00 6116.8548 RR 9,19 0.00 6124.4644 6117.4553 7.0091 RR 9,20 0.00 6124.9787 6118.0557 6.9230 RR 9,21 0.00 6125.6130 6118.6560 6.9570 RR 9,22 0.00 6126.2364 6119.2562 6.9802 RR 9,23 0.00 6127.4913 6120.4570 7.0343 RR 9,25 0.00 6127.4913 6120.4570 7.0343 RR 9,25 0.00 6129.7299 6121.8001 7.9298 RR10,10 0.00 6130.3536 6122.4032 7.9504 RR10,12 0.00 6130.9934 6123.0057 7.9877 RR10,15 0.00 6133.4253 6125.4101 8.0152	•				6.9794
RR 9,17 0.00 6116.2540 RR 9,18 0.00 6116.8548 RR 9,19 0.00 6124.4644 6117.4553 7.0091 RR 9,20 0.00 6124.9787 6118.0557 6.9230 RR 9,21 0.00 6125.6130 6118.6560 6.9570 RR 9,22 0.00 6126.2364 6119.2562 6.9802 RR 9,23 0.00 6127.4913 6120.4570 7.0343 RR 9,25 0.00 6127.4913 6120.4570 7.0343 RR 9,25 0.00 6129.7299 6121.8001 7.9298 RR10,10 0.00 6130.3536 6122.4032 7.9504 RR10,12 0.00 6130.9934 6123.0057 7.9877 RR10,15 0.00 6132.7965 6124.8097 7.9868 RR10,16 0.00 6133.4253 6125.4101 8.0152	•				
RR 9,18 0.00 6124.4644 6117.4553 7.0091 RR 9,20 0.00 6124.9787 6118.0557 6.9230 RR 9,21 0.00 6125.6130 6118.6560 6.9570 RR 9,22 0.00 6126.2364 6119.2562 6.9802 RR 9,23 0.00 6127.4913 6120.4570 7.0343 RR 9,24 0.00 6127.4913 6120.4570 7.0343 RR 9,25 0.00 6127.4913 6121.0576 RQ10,-1 0.00 6129.7299 6121.8001 7.9298 RR10,10 0.00 6130.3536 6122.4032 7.9504 RR10,12 0.00 6130.9934 6123.0057 7.9877 RR10,15 0.00 6132.7965 6124.8097 7.9868 RR10,16 0.00 6133.4253 6125.4101 8.0152					
RR 9,19 0.00 6124.4644 6117.4553 7.0091 RR 9,20 0.00 6124.9787 6118.0557 6.9230 RR 9,21 0.00 6125.6130 6118.6560 6.9570 RR 9,22 0.00 6126.2364 6119.2562 6.9802 RR 9,23 0.00 6127.4913 6120.4570 7.0343 RR 9,25 0.00 6127.4913 6120.4570 7.0343 RR 9,25 0.00 6129.7299 6121.8001 7.9298 RR10,10 0.00 6130.3536 6122.4032 7.9504 RR10,12 0.00 6130.9934 6123.0057 7.9877 RR10,15 0.00 6132.7965 6124.8097 7.9868 RR10,16 0.00 6133.4253 6125.4101 8.0152				6116.8548	
RR 9,20 0.00 6124.9787 6118.0557 6.9230 RR 9,21 0.00 6125.6130 6118.6560 6.9570 RR 9,22 0.00 6126.2364 6119.2562 6.9802 RR 9,23 0.00 6127.4913 6120.4570 7.0343 RR 9,25 0.00 6127.4913 6120.4570 7.0343 RR 9,25 0.00 6121.0576 RQ10,-1 0.00 6129.7299 6121.8001 7.9298 RR10,10 0.00 6130.3536 6122.4032 7.9504 RR10,12 0.00 6130.9934 6123.0057 7.9877 RR10,15 0.00 6132.7965 6124.8097 7.9868 RR10,16 0.00 6133.4253 6125.4101 8.0152			6124.4644		7.0091
RR 9,21 0.00 6125.6130 6118.6560 6.9570 RR 9,22 0.00 6126.2364 6119.2562 6.9802 RR 9,23 0.00 6119.8565 RR 9,24 0.00 6127.4913 6120.4570 7.0343 RR 9,25 0.00 6121.0576 RQ10,-1 0.00 6129.7299 6121.8001 7.9298 RR10,10 0.00 6130.3536 6122.4032 7.9504 RR10,12 0.00 6130.9934 6123.0057 7.9877 RR10,15 0.00 6132.7965 6124.8097 7.9868 RR10,16 0.00 6133.4253 6125.4101 8.0152					
RR 9,22 0.00 6126.2364 6119.2562 6.9802 RR 9,23 0.00 6119.8565 RR 9,24 0.00 6127.4913 6120.4570 7.0343 RR 9,25 0.00 6121.0576 RQ10,-1 0.00 6115.1169 RR10,10 0.00 6129.7299 6121.8001 7.9298 RR10,11 0.00 6130.3536 6122.4032 7.9504 RR10,12 0.00 6130.9934 6123.0057 7.9877 RR10,15 0.00 6132.7965 6124.8097 7.9868 RR10,16 0.00 6133.4253 6125.4101 8.0152	•				
RR 9,23 0.00 6119.8565 RR 9,24 0.00 6127.4913 6120.4570 7.0343 RR 9,25 0.00 6121.0576 RQ10,-1 0.00 6115.1169 RR10,10 0.00 6129.7299 6121.8001 7.9298 RR10,11 0.00 6130.3536 6122.4032 7.9504 RR10,12 0.00 6130.9934 6123.0057 7.9877 RR10,15 0.00 6132.7965 6124.8097 7.9868 RR10,16 0.00 6133.4253 6125.4101 8.0152	•		6126.2364		
RR 9,24 0.00 6127.4913 6120.4570 7.0343 RR 9,25 0.00 6121.0576 RQ10,-1 0.00 6115.1169 RR10,10 0.00 6129.7299 6121.8001 7.9298 RR10,11 0.00 6130.3536 6122.4032 7.9504 RR10,12 0.00 6130.9934 6123.0057 7.9877 RR10,15 0.00 6132.7965 6124.8097 7.9868 RR10,16 0.00 6133.4253 6125.4101 8.0152					
RR 9,25 0.00 6121.0576 RQ10,-1 0.00 6115.1169 RR10,10 0.00 6129.7299 6121.8001 7.9298 RR10,11 0.00 6130.3536 6122.4032 7.9504 RR10,12 0.00 6130.9934 6123.0057 7.9877 RR10,15 0.00 6132.7965 6124.8097 7.9868 RR10,16 0.00 6133.4253 6125.4101 8.0152	-		6127.4913		7.0343
RQ10,-1 0.00 6115.1169 RR10,10 0.00 6129.7299 6121.8001 7.9298 RR10,11 0.00 6130.3536 6122.4032 7.9504 RR10,12 0.00 6130.9934 6123.0057 7.9877 RR10,15 0.00 6132.7965 6124.8097 7.9868 RR10,16 0.00 6133.4253 6125.4101 8.0152	-				
RR10,10 0.00 6129.7299 6121.8001 7.9298 RR10,11 0.00 6130.3536 6122.4032 7.9504 RR10,12 0.00 6130.9934 6123.0057 7.9877 RR10,15 0.00 6132.7965 6124.8097 7.9868 RR10,16 0.00 6133.4253 6125.4101 8.0152	-				
RR10,11 0.00 6130.3536 6122.4032 7.9504 RR10,12 0.00 6130.9934 6123.0057 7.9877 RR10,15 0.00 6132.7965 6124.8097 7.9868 RR10,16 0.00 6133.4253 6125.4101 8.0152			6129.7299		7.9298
RR10,12 0.00 6130.9934 6123.0057 7.9877 RR10,15 0.00 6132.7965 6124.8097 7.9868 RR10,16 0.00 6133.4253 6125.4101 8.0152	•				
RR10,15 0.00 6132.7965 6124.8097 7.9868 RR10,16 0.00 6133.4253 6125.4101 8.0152	•				
RR10,16 0.00 6133.4253 6125.4101 8.0152					
• .					

K	J	WI	OBS FREQ	CALC FREQ	OBS-CALC
RR10,	19	0.00	6135.2988	6127.2091	8.0897
RR10,		0.00	6136.4955	6128.4073	8.0882
RR10,	23	0.00	6137.7362	6129.6052	8.1310
RR10,	24	0.00	6138.3071	6130.2043	8.1028
RQ11,	-1	0.00		6124.7941	
RR11,	11	0.00	6140.2340	6132.0736	8.1604
RR11,		0.00	6142.0799	6133.8764	8.2035
RR11,		0.00	6142.7160	6134.4762	8.2398
RR11,		0.00	6143.3320	6135.0755	8.2565
RR11,		0.00	6143.9110	6135.6744	8.2366
RR11,		0.00	6144.5391	6136.2728	8 .2 663
RR11,		0.00	6145.1411	6136.8710	8.2701
RR11,		0.00	6145.7883	6137.4689	8.3194
RR11,		0.00	6146.9805	6138.6642	8.3163
RQ12,		0.00		6134.3884	
RR12,		0.00		6142.2612	
RR12,		0.00		6142.8611	
RR12,		0.00		6143.4604	
RR12,		0.00		6144.0591	
RR12,		0.00		6144.6573	
RR12,		0.00		6145.2549	
RR12,		0.00		6145.8521	
RR12,		0.00		6146.4490	
RQ13,		0.00		6143.9112	
RR13,		0.00		6152.3740	
RR13,		0.00	•	6152.9722	
RR13,		0.00		6153.5697	
RR13,		0.00		6154.1666	
RR13,	1/	0.00		6154.7630	



LIST OF REFERENCES

- 1. C. Di Lauro and I. M. Mills, J. Mol. Spectrosc. 21, 386 (1966).
- 2. H. Matsuura, T. Nakagawa, and J. Overend, J. Chem. Phys. 59, 1449 (1973).
- 3. P. Connes, Air Force Cambridge Research Laboratories, Special Report Number 114, Aspen International Conference on Fourier Spectroscopy, 1970, Vanasse, Stair, and Baker, editors, p. 121.
- 4. S. C. Hurlock and J. R. Hanratty, Appl. Spectrosc. 28, 362 (1974).
- 5. P. D. Willson and T. H. Edwards, Sampling and Smoothing of Spectra, Applied Spectroscopy Reviews, 12(1) (Marcell Dekker, Inc.), (1976), p. 1.
- P. A. Jansson, R. H. Hunt, and E. K. Plyler, J. Opt. Soc. Am. <u>60</u>, 596 (1970).
- 7. P. D. Willson, Ph.D. dissertation, Michigan State University, 1973.
- 8. G. Halsey and W. E. Blass, Appl. Optics 16, 286 (1977).
- 9. R. W. Peterson and T. H. Edwards, J. Mol. Spectrosc. $\underline{41}$, 137 (1972).
- 10. T. L. Barnett and T. H. Edwards, J. Mol. Spectrosc. <u>20</u>, 347 (1966).
- 11. R. W. Peterson and T. H. Edwards, J. Mol. Spectrosc. 38, 1 (1971).
- 12. T. L. Barnett and T. H. Edwards, J. Mol. Spectrosc. 20, 352 (1966).
- 13. T. L. Barnett and T. H. Edwards, J. Mol. Spectrosc. 23, 302 (1967).
- 14. R. W. Peterson and T. H. Edwards, J. Mol. Spectrosc. <u>38</u>, 524 (1971).

- 15. B. Podolsky, Phys. Rev. 32, 812 (1928).
- 16. E. B. Wilson, Jr. and J. B. Howard, J. Chem. Phys. $\underline{4}$, 260 (1936).
- 17. B. T. Darling and D. M. Dennison, Phys. Rev. <u>57</u>, 128 (1940).
- 18. W. H. Shaffer, H. H. Nielsen, and L. H. Thomas, Phys. Rev. <u>56</u>, 895 (1939).
- 19. M. Goldsmith, G. Amat, and H. H. Nielsen, J. Chem. Phys. 24, 1178 (1956).
- 20. M. Goldsmith, G. Amat, and H. H. Nielsen, J. Chem. Phys. <u>27</u>, 838 (1957).
- 21. G. Amat, and H. H. Nielsen, J. Chem. Phys. 27, 845 (1957).
- 22. G. Amat, and H. H. Nielsen, J. Chem. Phys. 29, 665 (1958).
- 23. G. Amat, and H. H. Nielsen, J. Chem. Phys. <u>36</u>, 1869 (1962).
- 24. M. L. Grenier-Besson, G. Amat, and H. H. Nielsen, J. Chem. Phys. <u>36</u>, 3454 (1962).
- 25. M. L. Grenier-Besson, J. Physique Rad. 21, 555 (1960).
- 26. G. J. Cartwright and I. M. Mills, J. Mol. Spectrosc. $\underline{34}$, 415 (1970).
- 27. D. R. Anderson and J. Overend, Spectrochimica Acta 28A, 1231 (1972).
- 28. R. W. Peterson, Ph.D. dissertation, Michigan State University, 1969.
- 29. R. R. Ernst. Rev. Sci. Instrum. 36, 1689 (1965).
- 30. K. N. Rao, C. J. Humphreys, and D. H. Rank, Wavelength Standards in the Infrared, Academic Press, New York, (1966), p. 160.
- 31. C. Amiot and G. Guelachvilli, J. Mol. Spectrosc. <u>59</u>, 171 (1976).
- 32. J. L. Aubel, Ph.D. dissertation, Michigan State University, 1964.
- 33. D. B. Keck, Ph.D. dissertation, Michigan State University, 1967.

- 34. T. L. Barnett, Ph.D. dissertation, Michigan State University, 1967.
- 35. J. R. Gillis, Ph.D. dissertation, Michigan State University, 1979.
- 36. Michigan State University High Resolution Infrared Lab Software Package.
- 37. Reference unknown.
- 38. W. E. Blass and G. W. Halsey, Deconvolution of Absorption Spectra, Academic Press, 1981.
- 39. J. Pliva, A. S. Pine, and P. D. Willson, Applied Optics 19, 1833 (1980).
- 40. P. M. Wilt, F. W. Hecker, J. D. Fehribach, Dale E. Bardin, and T. H. Edwards, J. Mol. Spectrosc. 90, 33 (1981).
- 41. P. Venkateswarlu, J. Chem. Phys. 19, 293 (1951).
- 42. F. W. Parker, A. H. Nielsen and W. H. Fletcher, J. Mol. Spectrosc. 1, 107 (1957).
- 43. J. L. Duncan, D. C. McKean, F. Tullini, G. D. Nivellini, and J. Perez Pena, J. Mol. Spectrosc. 69, 123 (1978).
- 44. G. Herzberg, Molecular Spectra and Molecular Structure II: Infrared and Raman Spectra of Polyatomic Molecules, Van Nostrand, New York, (1945), p. 425.
- 45. D. Boucher, J. Burie, J. Demaison, A. Dubrulle, J. Legand, and B. Segard, J. Mol. Spectrosc. 64, 290 (1977).
- 46. John W. Boyd, Ph.D. dissertation, Michigan State University, 1963.

MICHIGAN STATE UNIV. LIBRARIES
31293106148921